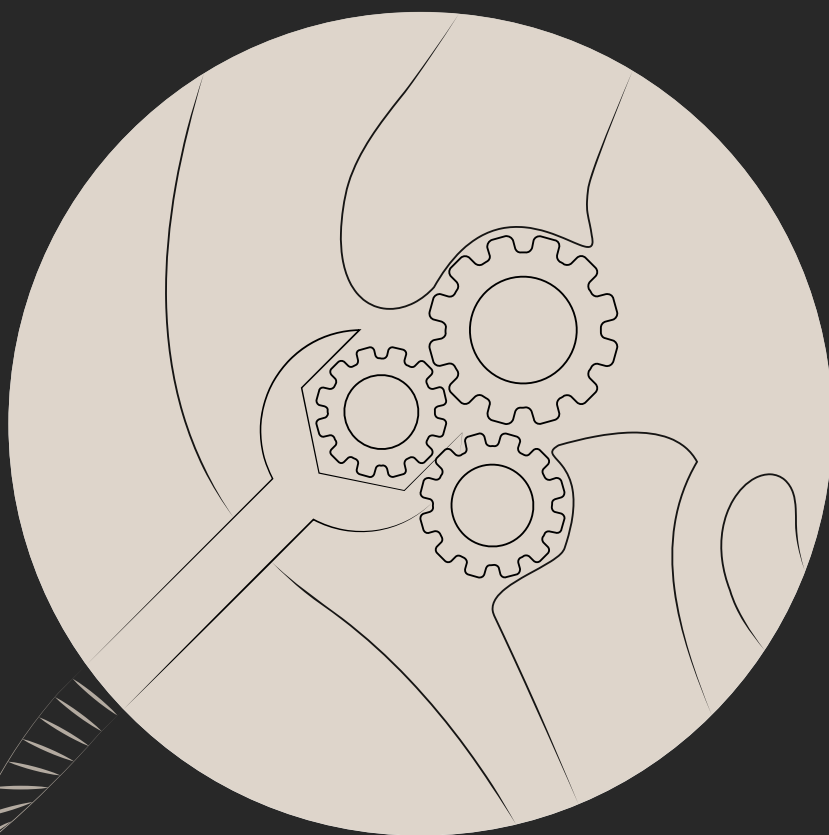


TOOLS AND TECHNOLOGIES FOR CARTILAGE REPAIR



JOÃO PEDRO MARQUES GARCIA



TOOLS AND TECHNOLOGIES FOR CATILAGE REPAIR

João Pedro Marques Garcia

Author: João Pedro Marques Garcia
ISBN: 978-94-92597-48-9

Cover design: Luís Garcia
Layout: Luís Garcia
Printing: PrintSupport4U

Financial support for the printing of this thesis was generously provided by the Netherlands Society for Biomaterials and Tissue Engineering (NBTE) and Anna FondsINOREF.

Copyright © João Garcia, the Netherlands, 2020. All rights reserved. No part of this thesis may be reproduced, distributed, stored in a retrieval system of any nature, or transmitted in any form or by any means without the written permission of the author or, when appropriate, the publisher of the publications.

TOOLS AND TECHNOLOGIES FOR CATILAGE REPAIR

Instrumenten en Technologieën voor Kraakbeenherstel
(met een samenvatting in het Nederlands)

Proefschrift

ter verkrijging van de graad van doctor aan de
Universiteit Utrecht
op gezag van de
rector magnificus, prof.dr. H.R.B.M. Kummeling,
ingevolge het besluit van het college voor promoties
in het openbaar te verdedigen op

donderdag 3 september 2020 des ochtends te 9.15 uur

door

João Pedro Marques Garcia

geboren op 5 september 1992
te Viana do Castelo, Portugal

Promotoren:

Prof. dr. F.C. Oner

Prof. dr. M.A. Tryfonidou

Copromotor:

Dr. L.B. Creemers

Dit proefschrift werd mogelijk gemaakt met financiële steun van:
European Union's Horizon 2020 research and innovation programme under the Marie
Sklodowska-Curie grant agreement No 642414 (TargetCaRe)

Dedicated to
Avô Marques and *Avô Zeca*, the finest story-tellers

Chapter 1	8
Introduction and Thesis Outline	
Chapter 2	20
Drug Delivery in Intervertebral Disc Degeneration and Osteoarthritis: Selecting the Optimal Platform for the Delivery of Disease-Modifying Agents	
Chapter 3	42
Fibrin-Hyaluronic Acid Hydrogel-Based Delivery of Antisense Oligonucleotides for ADAMTS5 Inhibition in Co-Delivered and Resident Joint Cells in Osteoarthritis	
Chapter 4	68
In Vitro Tissue Penetration and Inhibitory Activity of Modified Antisense Oligonucleotide Against ADAMTS5 in Osteoarthritic Cartilage	
Chapter 5	80
Association Between Oncostatin M Expression and Inflammatory Phenotype in Experimental Arthritis Models and Osteoarthritis Patients	
Chapter 6	102
Contrast Enhanced Computed Tomography for Real-Time Quantification of Glycosaminoglycans in Cartilage Tissue Engineered Constructs	
Chapter 7	124
Summary and Discussion	
Appendices	140
References	142
Nederlandse Samenvatting	164
Abbreviation List	168
Acknowledgments	172
Publication List	178
Curriculum Vitae	180



CHAPTER 1

INTRODUCTION AND THESIS OUTLINE



1. Burden of Osteoarthritis

Osteoarthritis (OA) is a chronic and degenerative disease affecting synovial joints, and a leading cause of disability worldwide¹. OA is among the most prevalent musculoskeletal disorders and the most common form of arthritis, affecting roughly 9 and 18% of men and women above the age of 60, respectively^{2,3}. These percentages are predicted to increase in the coming years due to aging of the population and an ever-increasing prevalence of obesity worldwide^{2,4}.

Currently, no disease-modifying therapies are available, with treatment being limited to physiotherapy, diet, pain management, and surgical joint replacement at an end-stage^{5,6}. Subsequently, OA constitutes a major socio-economic burden affecting both health and social care systems³, with an estimated cost of 8500 euros per patient per year on surgical interventions, pain medication and indirect costs related to productivity loss⁷. Considering that OA is a heterogeneous disease and patients display different phenotypes, therapy efficiency is further limited by their use on unselected patient populations⁸. Hence, improved patient stratification based on disease phenotype and biomarker profiles will be a crucial step towards elucidating OA pathology, and guiding patient selection and treatment optimization⁸⁻¹⁰.

Additionally, there is an unmet need for the development of new drugs and treatment schemes that not only treat the symptomatic disease, but also slow down the progressive and chronic degenerative processes^{5,6}. Even though there were some promising preclinical candidates, including growth factors, anti-inflammatory drugs or enzyme inhibitors, so far none has been approved by regulatory agencies due to their lack of efficiency in humans^{5,6}. Therapeutic efficiency is often hampered by the limited availability of the drugs within the joint environment, therefore improved therapy outcomes could potentially be achieved through the development of platforms for controlled and targeted drug release^{11,12}.

It is evident that many obstacles need to be overcome before efficient therapies reach the clinic. First, patient populations need to be defined based on their OA phenotype and specific dysregulated pathways. Secondly, the development of new therapeutics targeting the aforementioned OA-specific mechanisms will be pivotal. Likely, treatment strategies will benefit from the incorporation of the new therapeutics into drug delivery platforms aiming at prolonged drug retention and targeting in the diseased joint. Last but not least, new *in vitro* and preclinical multimodal monitoring tools need to be developed to better measure and screen treatment outcomes at preclinical stages. In this thesis, it is postulated that OA research is multifaceted, and that by combining patient stratification, target discovery and drug development, and the use of preclinical monitoring tools more efficient OA therapies can be developed.

2. The joint in health and disease

2.1 Joint structure and anatomy

Synovial joints are crucial components of the musculoskeletal system as they represent the anatomical structure that connects bones and allow for body movement. Articular cartilage (AC) is located at the surface of bones in the joint, and due to its unique mechanical and load-bearing properties, it allows for smooth and frictionless movements¹³. Lining the inner part of the synovial capsule is a thin membrane of connective tissue, or synovium, that is responsible for producing synovial fluid, which plays a crucial role in joint biomechanics, lubrication and cartilage homeostasis¹⁴. AC is an avascular tissue, hence nutrition is largely dependent on solute diffusion from the synovial fluid^{13,15}. On the other hand, the synovium contains both blood and lymphatic vessels, in addition to nerve fibers¹⁴. The meniscus is a cartilaginous structure located between articular cartilage surfaces, functioning as shock absorbing and load distribution component. Finally, the ligaments and muscles around the joint are largely responsible for holding the joint together.

Articular cartilage is composed of a dense and tightly packed extracellular matrix (ECM), which, in turn, has two major macromolecules: collagens and proteoglycans¹³. Collagen molecules, mostly collagen type II, account for around 70% of the total dry weight of cartilage and they form a fibril network where the proteoglycans are contained^{13,16}. Proteoglycans are composed by an aggrecan core unit and glycosaminoglycan (GAG) chains, and, in cartilage, they form large complexes with hyaluronic acid¹³. Proteoglycans represent 30% of the cartilage dry weight, and due to their fixed negative charge, water molecules are attracted to the collagen-proteoglycan network¹³. In fact, water is the most abundant component in AC, representing around 70% of the wet weight¹³. The high water content, together with the osmotic pressure generated by the negative charge of proteoglycans, provides cartilage matrix with its essential shock absorption and load dissipation properties¹³. Additionally, other macromolecules are present within the AC at lower percentages, i.e. collagen type IV, III and XI, and elastin^{13,16}.

AC can be divided into 4 regions: the superficial, medial, deep and calcified layer. While collagen density is higher in the superficial when compared to deeper layers, proteoglycans and water distribution displays an opposite gradient, with higher amounts in the deep zone¹³. Likewise, articular chondrocytes, the only resident cell type in AC, display an anisotropic organization, with an elongated morphology in superficial layers and a rounder shape in deeper areas. Chondrocytes are relatively quiescent cells with low metabolic activity and reduced regenerative capacity. These cells are also responsible for ECM production and remodeling, through synthesis of matrix components, enzymes (i.e., metalloproteinases and aggrecanases), and inflammatory mediators^{13,17}.

2.2 Osteoarthritis and joint damage

Even though OA is known to be a complex disease with multiple etiologies, it is widely accepted that biomechanical (i.e., trauma, instability) and biochemical factors

act on the chondrocytes, altering their phenotype and gene expression patterns¹⁷. In OA, chondrocytes enter a proliferative state while simultaneously synthesizing matrix components, in an attempt to repair matrix damage¹⁷⁻¹⁹. However, the production of matrix-degrading proteinases and inflammatory cytokines is also increased, which leads to progressive loss of collagen type II and aggrecan¹⁷. Metalloproteinases (MMPs), and in particular MMP-13, are mainly responsible for the breakdown of collagen molecules^{20,21}, while the ADAMTS (A Disintegrin And Metalloproteinase with Thrombospondin motifs) family, namely ADAMTS-4 and 5, are the key players in aggrecan degradation²⁰⁻²².

Degradation products of both collagen and aggrecan, among other matrix components, further stimulate cartilage degradation and inflammatory responses. In addition, structural organization of collagen fibrils is altered, affecting the three-dimensional (3D) architecture of the cartilage matrix and rendering it less resistant to mechanical stress²³.

Besides cartilage, bone is also affected in OA. During OA, there is a thickening of the subchondral plate, together with formation of bone spurs at the cartilage edges (osteophytes), and bone cysts in the subchondral bone²⁴. Subchondral bone thickening results from an increased vascularization and enhanced cartilage calcification²⁵. Lately, it has been suggested that subchondral bone has more than a passive role in OA pathogenesis, with compelling evidence showing subchondral changes associating with, or even preceding, cartilage damage^{10,26-28}. This phenomenon is likely to occur through the local production of soluble mediators in the subchondral bone that contribute to defective cartilage remodeling and hence degradation^{29,30}. The diffusion of soluble mediators is thought to be enhanced due to increased porosity of subchondral bone during OA³⁰.

Contrary to other types of arthritis, such as rheumatoid and psoriatic arthritis, OA is not clinically regarded as an inflammatory disease^{10,31}. Nevertheless, inflammation of the synovium, also known as synovitis, is associated with clinical symptoms of OA, disease progression and worsening of cartilage degradation through the production of soluble mediators³¹⁻³³. Synovitis is thought to occur in response to injury and degradation of cartilage matrix, and it is characterized by cell infiltration (macrophages, B cells and T-lymphocytes) and production of inflammatory mediators³². Upon release of matrix degradation products, an inflammatory cascade is initiated through production of cytokines and chemokines that further activates chondrocytes and induce matrix degradation. In a vicious cycle, this will lead to additional cytokine and enzyme production by the synovial and cartilage cells, perpetuating cartilage degradation^{31,32}. Also upon traumatic injury, such as meniscus tears or ligament injuries, patients display signs of synovial inflammation and distinct cytokine profiles in the synovial fluid³⁴⁻⁴⁰ and traumatic injuries are known to be a risk factor for the development of OA^{33,41,42}.

Pro-inflammatory mediators such as interleukin-1 (IL-1), tumor necrosis factor alpha (TNF- α), prostaglandins and nitric oxide (NO) have been proposed to be associated with cartilage degradation through up-regulation of MMPs and ADAMTSs^{31,43,44}, although their clear involvement in OA pathology has not been proven. Other cytokines such as IL-6, oncostatin M (OSM) and IL-17 have also been associated with synovial inflammation and

cartilage damage^{31,32}. The inflammatory cascade also affects the NF- κ B signaling pathway, which was shown to be abnormally up-regulated in osteoarthritic chondrocytes and to induce expression of MMPs and ADAMTSs⁴⁵⁻⁴⁷. Furthermore, inflammatory pathways are tightly related with symptomatic pain in OA, through the increase of local levels of nerve growth factor (NGF) and subsequent activation of peripheral nociceptors³¹.

The increasing prevalence of OA has been paralleled with the completion of numerous clinical trials that have failed to show significant therapeutic effects of a wide-range of drugs. In the following subchapters, a summary of the motives leading to clinical trial failure is done, together with potential strategies that can improve OA treatment in the future setting the scene for this thesis.

3. Current treatments, limitations and future directions

Current clinical approaches for OA mainly aim at symptom management and relief. Although not very efficient, physical therapy and weight loss aim at restoring and strengthen muscle and joint function, while reducing the mechanical stress. On the other hand, pharmacological therapy resorting to analgesics or non-steroidal anti-inflammatory drugs (NSAIDs) leads to effective but short-lived pain relief. Additionally, these strategies do not target the pathological mechanisms underlying OA, hence cartilage degradation progresses up to a stage where surgical replacement of the joint may be indicated.

In the last years, many biological therapies have been tested in clinical trials, yet with rather disappointing results^{6,8}. Ranging from growth factors to anti-inflammatory drugs and enzyme inhibitors, the different classes of therapeutics have failed to demonstrate significant disease-reverting effects after successful and promising preclinical testing. In brief, negative results can be divided in lack of efficiency in reverting the pathological process and the occurrence of severe side effects and toxicity. In Chapter 2, an extensive review on each drug category is included, together with a summary of the clinical trials involving these, and the reasons leading to unsuccessful trials and negative results.

OA, as a multifactorial disease, involves the action of different effector molecules, hence therapies might benefit from the development of different drug types, which can target pathways or molecules that are otherwise “undruggable”. Emerging drug categories such as ribonucleic acid (RNA) therapeutics have triggered substantial interest by academia and industry due their high targeting specificity and tailorability. Additionally, it has been proposed that intra-articular controlled delivery of disease-modifying agents might increase the benefit:risk ratio of such molecules by, on one hand, increasing the local concentrations of the drug and, on the other, decreasing systemic exposure^{8,11,12}.

OA is not only a disease with multiple etiologies, but it can also be manifested with different phenotypes. While in some patients cartilage might be the most active component in the pathological process, some other subgroups might have higher degrees of inflammation. The degree of synovitis and the inflammatory profiles are different among patients, and even in the same patient throughout the course of the disease^{48,49}.

Thus, therapy efficiency in specific phenotypes of OA can be overshadowed by testing in unselected patient populations. Hence, there is a need to define patient populations and phenotypes, providing a more personalized approach in OA treatment^{49,50,51}.

3.1 RNA therapeutics and drug delivery

Over the past years, RNA therapeutics have emerged as potential drug candidates to target and treat diseases at the RNA level^{52,53}. These molecules act on the translation mechanisms, namely at the messenger RNA (mRNA) level, hence modifying gene expression and protein production. Contrary to small molecule drugs or inhibitors that act at the protein level, by intervening at the translational level, RNA therapeutics produce a faster and longer lasting effect^{52,53}. More importantly, they can be designed to virtually target any mRNA, expanding the range of “druggable” targets without significantly altering the characteristics of the drug (e.g., pharmacokinetics and pharmacodynamics).

These therapeutics can be roughly divided into two main categories: double stranded small interfering RNAs (siRNAs) or single stranded antisense oligonucleotides (ASOs)^{52,53}. While their mechanism of action is different, both strategies generally result in the degradation of the target mRNA or inhibition of the translation processes, which ultimately results in a reduction of the protein expression^{52,54}. siRNAs will bind to their target mRNA, and consequently activate a group of cytoplasmic enzymes that will cut the mRNA strand. On the other hand, ASOs are smaller oligonucleotides composed by RNA or DNA nucleotides and bind to their target mRNA sequence through Watson-Crick base pairing. Additionally, ASOs can bind to micro RNAs (miRNAs) and pre-mRNAs (in the nucleus). Once bound to their target, they can act by inducing target degradation, translation arrest or by modulating mRNA splicing.

Despite the initial promises and enormous potential of these molecules, *in vivo* instability, off-target effects and the low cellular uptake constituted a major challenge before they could be clinically applied. Recently, chemical modification of siRNAs and ASOs have rendered them more resistant to endonuclease degradation and conferred them with higher binding affinity and specificity. Nonetheless, cellular uptake and endosomal escape still constitute a major challenge, namely for siRNAs that generally require the use of delivery systems, such as liposomes, nanoparticles or viral vectors^{52,55}. ASOs, however, due to their smaller size and chemical modifications, are taken up by the cells and are able to escape the endosome without the aid of any carrier, in a process denominated *gymnosis*⁵⁵⁻⁵⁹. The substitution of one oxygen by a sulfur atom in the phosphate group of the nucleotides originated the phosphorothioate backbone modification^{60,61}. Furthermore, nucleotide modifications such as 2'-O-methyl (2'-OMe), 2'-O-methoxyethyl (2'-OMOE), and Locked Nucleic Acids (LNAs) have been used⁵⁵. These modifications gave ASOs an improved stability and higher hydrophobicity that is essential for interacting and crossing the lipid bilayers of cell membranes and endosomes^{54,62-64}. Importantly, these modifications do not impair ASO interaction with its target or degradation machinery. On the other hand, siRNA is more sensitive to chemical

modifications as they can impair RNA interference mechanisms⁶⁵⁻⁶⁸, hence very limited modifications are possible^{55,67}. Due to their high therapeutic potential, ASOs are being explored as therapies for cancer^{69,70}, neurological disorders⁷¹, immunodeficiencies⁷², and cardiovascular and metabolic diseases^{73,74}. In OA, several matrix-degrading enzymes and pro-inflammatory molecules are up-regulated and their *in vivo* inhibition has been shown to delay cartilage degradation. In this regard, ASOs can potentially be developed for the knockdown of one, or perhaps, several targets simultaneously.

For drugs targeting tissues and cells in the joint, local administration offers many advantages as compared to other forms of administration, such as systemic or oral routes^{11,12}. Contrary to systemic applications, local drug delivery provides higher drug bioavailability in the joint and reduced systemic side effects. Additionally, as opposed to other forms of arthritis, OA affects usually a single joint and, therefore, the localized nature of the disease makes it suitable for intra-articular drug delivery¹¹.

The rationale behind intra-articular drug delivery is that the drug is incorporated in a delivery platform (i.e., hydrogels, micro- or nanoparticles), which are subsequently injected intra-articularly. Depending on the type and properties of the delivery platform, it can act as i) a simple drug depot that will release the drug in a controlled manner over time or ii) actively target specific cells and tissues within the joint environment, such as chondrocytes, synoviocytes or macrophages. By providing a controlled and prolonged drug retention within the joint, delivery systems also diminish patient discomfort and infection risk by decreasing the number of necessary injections^{11,12}. The recent advances in intra-articular drug delivery systems are extensively reviewed in Chapter 2 and elsewhere^{11,75}.

3.2 Target discovery, drug development and patient stratification

Although OA is generally limited to a single joint, there is a considerable range of heterogeneity in disease features and phenotypes, which results from distinct biochemical and molecular processes^{9,10}. As mentioned before, this has been proposed as a major cause of failed clinical trials, as these are generally carried out in unselected patient populations, potentially camouflaging significant therapeutic effects in specific OA subgroups⁸. Currently, it is postulated that there are three main subpopulations in OA, namely i) mechanically-driven, ii) inflammation-driven, and iii) bone-driven^{8,50,76}. Yet, these phenotypes are not static, but rather dynamic and interchangeable as the tissues communicate with each other^{50,77}. Moreover, interaction with a variety of environmental/risk factors such as genetics, metabolism and hormonal dysregulation will define disease progression rate and phenotype⁵⁰. Nowadays, OA diagnosis is performed with a combination of clinical manifestations and radiographic imaging, nevertheless both symptoms and radiographic OA are generally significant and visible at later disease stages. Hence, the development and validation of novel technologies (e.g., imaging) and biomarkers will be crucial for early diagnostics, differentiation between OA phenotypes, monitoring of disease activity and progression^{9,78}. Additionally, this will elucidate the

pathogenesis behind the different phenotypes, provide potential targets for drug development, and guide patient selection for clinical trials^{8-10,50,51}.

Currently, conventional radiography is the gold standard in diagnosis and evaluation of OA⁷⁹. Additionally, joint space narrowing is the only FDA-approved structural and endpoint marker to assess the efficacy of disease-modifying drugs⁸⁰. However, radiography reduces the joint environment to 2D images, and more importantly, it lacks the sensitivity to show and monitor relevant disease-associated changes in soft tissues, namely cartilage, synovium, and meniscus⁷⁹. More recently, techniques such as magnetic resonance imaging (MRI) and ultrasound (US) have been applied in OA research for their unique characteristics in imaging soft-tissue structure and morphology^{79,81,82}. Both MRI and US have been shown to be sensitive at imaging inflammation⁸³⁻⁸⁶, bone changes⁸⁷⁻⁸⁹, and cartilage degradation^{90,91}. Furthermore, these techniques allow imaging of the joint as a whole organ.

Different animal models of OA are reported in literature and are nowadays used for both pathogenesis studies and preclinical testing of different therapeutics⁹². While some are naturally occurring, the most widely used models OA is induced as disease progression is usually faster, hence shortening the duration of the studies. Additionally, induced OA models usually only recapitulate specific processes and phenotypes OA, and therefore lack the complexity of OA observed in humans^{92,93}. Therefore, careful selection of preclinical models is necessary for the study the different OA processes, as well as to assess the efficacy of therapeutics targeting phenotypic-specific pathways.

Further insight into the mechanisms of disease and tissue involvement, together with implementation of novel and more complete imaging technologies, will shed light on which effectors are important in the pathologic process of the different OA phenotypes^{78,94}. Combined efforts between imaging, and discovery of new targets and effector molecules will allow patient stratification and patient-specific drug development.

3.3 Pre-clinical imaging and monitoring tools in cartilage engineering and OA research

As mentioned above, the development of novel imaging modalities will be detrimental for the early detection of OA and differentiation between disease phenotypes. Equally important is the development of monitoring tools for in vitro and pre-clinical assessment of therapeutic efficacy of novel approaches.

Tissue engineering and regenerative medicine are currently one of the most promising therapeutic approaches for OA^{5,95,96}. These strategies involve the use of cells, biomaterial scaffolds, and/or stimulatory factors (e.g., mechanical stimuli and growth factors) aiming at production of cartilage-like tissue in an attempt to repair damaged cartilage^{95,96}. However, in vitro research carried out in OA and cartilage repair is limited to destructive and invasive methods to assess tissue and matrix quality^{97,98}. Immunohistochemistry and biochemical assays at mid- or endpoints provide limited spatiotemporal information on the constructs and tissues being studied. Therefore, there is an undeniable necessity for

the development of techniques that enable non-destructive and longitudinal monitoring of engineered (cartilage) constructs⁹⁷⁻⁹⁹. Some of these techniques encompass imaging modalities such as computed tomography (CT)^{100,101}, MRI¹⁰²⁻¹⁰⁵, US¹⁰⁶⁻¹⁰⁸, and optical imaging, as well as advanced toolkits for measuring cellular activity and matrix production¹⁰⁹.

The implementation of these techniques will provide non-destructive monitoring of engineered (cartilage) constructs, allowing the same samples to be followed overtime and avoiding erroneous extrapolations among samples. Ideally, these techniques will also deliver detailed information on the 3D architecture and structural organization of such constructs and their matrix components. Importantly, these modalities could potentially serve as a screening tool for optimal sample selection prior to implantation in animal models and, perhaps, in human patients.

4. Aim and thesis outline

The main aim of this thesis is to explore the current status of cartilage repair, and to show proof-of-concept of new technologies that can be used to advance and potentiate OA treatment. OA is a multifactorial condition affecting the synovial joints and, to date, no disease-modifying treatment is available. This comes after a plethora of failed and unsuccessful clinical trials. The negative outcomes are usually a result of: i) targeting the wrong effector molecules or lack of drug specificity, ii) route of administration, iii) testing of therapies in unselected patient populations. Hence in this thesis it is postulated that a “paradigm-shift” is necessary to advance OA treatment. Research is warranted on the mechanisms underlying the different disease phenotypes, definition of biomarkers, and on the development of biomarker-targeted drugs. Likely, efficiency of therapeutic strategies will potentially be higher in targeted OA phenotypes, rather than general populations.

Firstly, in chapter 2, the currently available treatments for OA are overviewed, together with a review on the clinical trials carried out so far. Additional focus is given to preclinical developments in bioactives against OA, as well as to recent developments in drug delivery systems. Moreover, a head-to-head comparison is made between OA and intervertebral disc degeneration, from pathology to treatment strategies, as both clinical entities may profit from advances in the drug delivery field.

In chapter 3, we investigate the suitability of using a hydrogel platform for the delivery of modified ASOs targeting ADAMTS5 as an approach for sustained intra-articular gene silencing of OA-related genes. Furthermore, in chapter 4, we explore the applicability of such antisense drugs on human cartilage explants. ASOs are known for their capacity for unassisted internalization, yet, cartilage matrix is very compact and drug diffusion has been shown to be extremely difficult. Hence, in this chapter, we study the diffusion properties of modified ASOs in cartilage explants, as well as their ability to transfect chondrocytes in situ and promote efficient and functional gene knockdown.

As mentioned previously, OA patients can display different phenotypes, which represent different mechanisms underlying the active disease. Hence, therapy efficiency will likely benefit of targeting the right patient population. In chapter 5, we map the expression of OSM in two animal models of OA, and explore its correlation with prevalence of hallmarks of arthritis, namely cartilage damage, inflammation and osteophytes. Furthermore, we explore the correlation of OSM with other inflammatory cytokines measure in the synovial fluid of OA patients.

In chapter 6, we describe the development of a quantitative and imaging method for monitoring of cartilage tissue engineered constructs *in vitro*. Cartilage tissue engineering research is currently limited to destructive analytical methods such as histology and biochemical assays. In this chapter, we introduce a novel method that allows for non-destructive and longitudinal quantification of proteoglycans and 3D imaging of tissue-engineered constructs.



CHAPTER 2

DRUG DELIVERY IN INTERVERTEBRAL DISC DEGENERATION AND OSTEOARTHRITIS: SELECTING THE OPTIMAL PLATFORM FOR THE DELIVERY OF DISEASE-MODIFYING AGENTS

João Pedro Garcia, Fabio Colella, Marco Sorbona, Andrea Lolli,
Bernardo Antunes, Domenico D'Atri, Florian P.Y. Barré, Jacopo Oieni,
Letizia Vainieri, Luana Zerrillo, Serdar Capar, Sonja Haeckel,
Yunpeng Cai, Laura B. Creemers

João Pedro Garcia, Fabio Colella, and Marco Sorbona contributed equally.

Under revision.



Abstract

Osteoarthritis (OA) and intervertebral disc degeneration (IVDD) as major cause of chronic low back pain represents the most common degenerative joint pathologies and are leading causes of pain and disability in adults. Articular cartilage (AC) and intervertebral discs are cartilaginous tissues with a similar biochemical composition and pathophysiological aspects of degeneration. Although treatments directed at reversing these conditions are yet to be developed, many promising disease-modifying drug candidates are currently under investigation. Given the localized nature of these chronic diseases, drug delivery systems have the potential to enhance therapeutic outcomes by providing controlled and targeted release of bioactives, minimizing the number of injections needed and increasing drug concentration in the affected areas. This review provides a comprehensive overview of the currently most promising disease-modifying drugs as well as potential drug delivery systems for OA and IVDD therapy.

1. Introduction

Musculoskeletal diseases are a major cause of disability and morbidity worldwide^{2,3}. Osteoarthritis (OA) and low back pain (LBP) associated with chronic and progressive degeneration of articular cartilage and intervertebral discs (IVDs), respectively, account for more than 50% of patients with musculoskeletal diseases³. For early stages, current treatments are generally focused on pain management, while surgical intervention is often needed for late-stage disease. Despite the extensive and compelling preclinical evidence on the efficacy of different therapeutic molecules (i.e. growth factors and cytokine inhibitors), to date, no disease-modifying treatments aiming at tissue repair and regeneration are available^{5,6}. The clinical trials carried out so far have shown disappointing results, as the drugs showed only short-lived to no beneficial effects⁶. This is mainly attributed to the heterogeneous and multifactorial profile of the diseases, as different tissues and different pathways, from inflammation to degeneration, are involved in their pathophysiology^{5,6,10}. Equally important, the short half-life of the bioactives within the joint and the disc limits the duration of their therapeutic activity, hence decreasing efficacy^{6,12,11}. In this regard, drug delivery systems might play a crucial role as part of novel therapeutic strategies due to their capacity to incorporate different types of drugs, tunable release profiles and targeting ability. By concentrating and prolonging the presence of the drugs in the tissues, these systems might contribute to improved drug efficacy and therapeutic effect^{12,11}.

This review focuses on state-of-the-art bioactives targeting joint degeneration, and current developments on drug delivery systems that can be used to enhance their efficacy

2. Synovial joints and intervertebral discs: histological, biochemical and physio-pathological features

Synovial joints and IVDs are crucial tissues for body movement and shock absorption due to their unique properties of load distribution, gliding and wear resistance. Articular cartilage is located at the end of long bones in synovial joints, which in turn are together by ligaments and a dense fibrous connective tissue forming the articular capsule^{13,12}. Lining the inner part of the synovial capsule is the synovial membrane, which is crucial for maintaining joint homeostasis¹⁴. The intervertebral discs (IVDs) are composed by two different tissue types: an outer lamellar structure called annulus fibrosus (AF) enclosing an inner gelatinous structure called nucleus pulposus (NP) which acts as a shock absorber. At their upper and lower side, IVDs are limited by cartilaginous endplates and the vertebral bodies^{13,14}. In the AC, chondrocytes can assume different morphologies whether they are located in the superficial, middle, deep or calcified layer of the cartilage^{13,12}. In the IVDs, the fibrocartilaginous AF contains fibroblast-like and spindle-shaped cells, whereas the NP contains rounded chondrocyte-like cells¹⁴.

In the AC, collagen type II represents 90-95% of total collagen fibers and provides resistance to tensile loads. In addition, the collagen network also contains collagen types I, III, IV, V, VI, IX, XI^{13,23}. Proteoglycans are also a key component of cartilage matrix due to their highly-charged nature, which attracts and retains water within cartilage (65-80% wet weight), enabling resistance against compressive forces and mechanical loading^{13,115}. Cartilage matrix also contains a small amount of other non-collagenous proteins such as lubricin and elastin, which are necessary to reduce friction during load-bearing articulating activities and provide elasticity to the matrix, respectively^{13,112}. In IVDs, the external part of the AF is rich in collagen type I, while collagen type II and proteoglycans are found in the inner NP tissue. Both articular cartilage and IVDs are characterized by an absence of vascular, neural and lymphatic networks, except for the outer AF which contains a limited number of blood vessels and nerves^{13,110}. Cartilage nutrition depends on the diffusion of nutrients present in the synovial fluid and basal subchondral bone (bone marrow) and on compression and relaxation cycles of the tissue^{13,116}, whereas IVDs rely mainly on diffusion through the cartilaginous endplate^{117,118}. The lack of vascular networks contributes to the lack of regenerative capacity of these tissues, and additionally makes them less accessible to systemically administered drugs.

Not only the risk factors for OA or intervertebral disc degeneration (IVDD) are similar (i.e. trauma, aging, obesity, and abnormal mechanical stress)¹¹⁰, but also the pathological evolution of both diseases share common aspects. During the development of disease, the cells undergo a phenotypic switch which leads to disruption of tissue homeostasis and impaired extracellular matrix (ECM) turnover¹¹⁷, accompanied by low grade inflammation^{31,119} (Figure 1). Cells form clusters, their balance in collagen production switches from collagen II to collagen I, concomitant with the upregulation of matrix-degrading proteinases (i.e. metalloproteinases and aggrecanases) and inflammatory cytokines^{113,120}. Hypertrophic differentiation is observed at later stages and, ultimately, cells undergo apoptosis^{112,121}. This abnormal response results in a decreased amount of proteoglycans, and collagen type II, increased collagen I, and loss of water. Macroscopically, fibrillation of the cartilage surface and fibrotic changes in the NP are observed. In the AF, the shear stress caused by tissue degeneration stimulates fibrosis and production of nitric oxide by resident cells¹²². The perpetuation of such pathological changes and the progression of degeneration lead to inflammation, stiffness and pain¹¹⁰. In IVDD, pain is likely induced by neovascularization and spreading of sensory nerves into the endplate and inner annulus¹²³⁻¹²⁵. With disease progression, increased tissue calcification occurs. Although in OA vascular penetration into the decalcified layer is seen¹¹³, in the degenerating IVD the number of capillary buds in the endplate is reduced¹²⁶. Additionally, cellular senescence has been proposed as a mechanism involved in both OA and IVDD^{121,127}. Senescence, which is a stress-response mechanism, is characterized by cell cycle arrest, resistance to apoptosis and a pro-inflammatory phenotype^{127,128}. Senescent cells have been found to be more prevalent in OA cartilage and IVDD than in healthy tissue¹²⁹. Additionally, in the joint, senescent cells can also be found in other tissues such as the synovium, a structure that plays a major role in OA development and progression^{127,128}.

In sum, OA and IVDDs involve cell phenotype changes that, by promoting inflammation and matrix degradation, drive tissue and joint degeneration. Therefore, there is an urgent need for the development of novel therapeutic strategies aimed at blocking disease progression and/or promoting tissue regeneration.

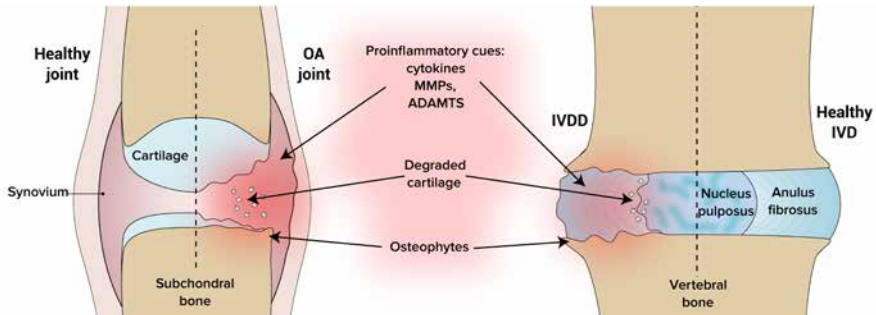


Figure 1: Schematic representation of a diarthrodial joint and intervertebral disc and the main pathological and morphological changes in OA and IVDD including cartilage degradation, osteophytes formation and synovial inflammation.

3. Current clinical approaches for OA and IVDD

First-line therapies for OA and IVDD generally aim at relieving pain and improving function, with a combination of analgesic pharmacological and non-pharmacological treatments. Non-pharmacological approaches include exercise and physiotherapy¹³⁰⁻¹³². Pharmacological therapy for OA or IVDD is largely represented by analgesics, non-steroidal anti-inflammatory drugs (NSAIDs), and opioids¹³¹⁻¹³³. The administration of oral analgesics, such as paracetamol, represents the first therapeutic solution to control mild pain^{133,134}. However, paracetamol is often not effective, leading physicians to prescribe NSAIDs (e.g. ibuprofen) at the lowest effective dose and for a limited time, due to the risk of side effects in the gastrointestinal (GI) tract and antiplatelet activity¹³⁵⁻¹³⁷. Alternatively, in OA, cyclooxygenase (COX)-2 selective NSAIDs were shown to have the anti-inflammatory and analgesic efficacy of traditional non-selective NSAIDs, with significantly reduced GI-related side effects¹³⁸. However, concerns on the cardiovascular effects of COX-2 inhibitors have been raised^{139,140}. In disc degeneration and low back pain, muscle relaxants are sometimes used to control non-specific musculoskeletal pain¹⁴¹⁻¹⁴³. Opioids are used as an alternative to NSAIDs for both OA and IVDD related back pain^{10,133,134}, yet this carries a significant risk of side-effects and addiction^{135,144}. Local injection of steroids and corticosteroids has also been used in the clinic for pain management of moderate-to-severe pain, although much more frequently in OA^{137,145-147}. Also here, adverse reactions such as tissue injury by repeated injections, infections and stimulation of inflammation by crystallized corticosteroids can occur¹³⁶.

Intra-articular hyaluronic acid (HA) injections are frequently used for symptom relief

in OA in an attempt to restore the viscoelasticity of the synovial fluid^{11,136}. The alleged analgesic effect of HA has been shown to be dependent on its molecular weight, with higher molecular weight possibly producing more effective and durable effects¹⁴⁸. Platelet-rich Plasma (PRP) injection is another intra-articular therapy recently introduced as an experimental treatment for OA^{149,150}. PRP is a preparation of concentrated blood plasma with increased platelet concentration, growth factors and other mediators¹⁴⁹. It has been suggested to have anti-inflammatory effects, and may reduce pain (105) and efficiency has been suggested to be higher and more uniform than HA^{150,151}. However, the Osteoarthritis Research Society International has recently officially recommended against the use of PRP “because the evidence in support of these treatments is of extremely low quality” and “formulations themselves have not yet been standardized”¹⁵². The latter is related to the myriad of procedures to prepare PRP^{149,152}.

When pain management is no longer effective, invasive surgical interventions are necessary, such as end-stage total joint replacement for OA¹³² and spinal fusion for disc degeneration¹⁵³. Unfortunately, prostheses have a limited lifetime and revision surgeries have a much higher risk of failure, posing problems for younger patients. Additionally, analogous to the treatment of traumatic cartilage defects¹⁵⁴, autologous chondrocyte implantation (ACI) was tested in patients with knee OA, with a significant clinical improvement after a 5-year evaluation period¹⁵⁵. However, this technique would be only applicable to patients with small sized and limited number of lesions. Additionally, the population followed in this study was relatively young¹⁵⁵. Altogether, even though these surgical approaches are effective at reducing pain, their efficacy is often suboptimal in terms of stability and integration, thus failing to restore function¹⁵⁶.

The increasing prevalence of both OA and IVDD as well as the lack of optimal treatment represents a major socio-economic burden worldwide, and therefore strongly calls for more effective therapeutic solutions. In the coming years, the identification of new therapeutic targets followed by the development of disease-modifying drugs for OA (DMOADs) and IVDD aiming at restoring tissue quality and function will be crucial.

3.1 Drugs: the old and the new

The abovementioned treatments focus mainly on symptom treatment rather than on reducing, halting or even reversing disease progression^{5,157}. An ideal disease-modifying agent should focus on either inhibiting catabolic pathways or stimulating repair and regeneration^{158,159}. However, and despite their enormous potential, to date no disease-modifying agents have been approved for OA or IVDD, owing to their side effects when administered systemically, short half-life in the tissue when injected locally, and ultimately, their lack of efficacy^{11,160}. Some of the DMOADs and disease-modifying drugs for IVDD being tested in clinical trials are summarized in Table 1 and Figure 2 and described in the next sub-chapters.

Class	Name/Description	Disease	Phase	Main Results	References / Clinical trial no
Anti-cytokine therapy	Intravenous administration of Tanezumab (Anti-NGF antibody)	OA	Phase II (completed)	Pain reduction and function improvement	NCT00394563 NCT00399490 ^{66,67}
	Intravenous and subcutaneous administration of Tanezumab (Anti-NGF antibody)	OA	Phase III (halted)	Study terminated due to adverse side effects such as worsening of OA and bone necrosis	NCT00994890 NCT01089725 ⁶⁸
	Subcutaneous administration of Tanezumab (Anti-NGF antibody)	OA	Phase III (completed)	Pain and function improvement in patients with moderate to severe OA, together with a higher prevalence of adverse events	NCT02697773 ⁶⁹
	Intra-articular injection of Anakinra (IL-1R receptor antagonist)	OA	Phase II (completed)	Anakinra was well tolerated however no improvements were observed compared to placebo group	NCT00110916 ⁷⁰
	Intravenous or subcutaneous administration of AMG 108 (anti-IL-1 receptor antibody)	OA	Phase II (completed)	Safety profile of AMG 108 was comparable to placebo, however no statistically significant improvements were observed	NCT00110942 ⁷¹
	Subcutaneous administration of Lukituzumab (antibody against IL-1a and IL-1 β)	OA	Phase II (completed)	No significant changes were observed in pain scores, synovitis and cartilage thickness	NCT02087904 ⁷²
	Subcutaneous administration of Lukituzumab (antibody against IL-1a and IL-1 β)	Hand OA	Phase IIa (completed)	No improvements were observed in pain and imaging outcomes when compared to placebo	NCT02384538 ⁷³
Growth factors	Epidural injection of Eterncept (TNF- α inhibitor)	IVDD – herniated disc	Phase II (completed)	Decrease of back and leg pain, and function improvement	NCT00364572 ⁷⁴
	Intra-articular administration of BMP-7	OA	Phase I (completed)	BMP-7 was shown to have a safe profile, and a trend for symptomatic improvement was observed	NCT00456157 ⁷⁵
	Intra-articular injection of FGF-18 (sprifermin)	OA	Phase I (completed)	FGF-18 was shown to be safe and non-toxic, but no significant improvement in cartilage thickness was observed. Pain reduction was higher in placebo group.	NCT01033994 ⁷⁶
	Single or double intradiscal injection of rhGDF-5	IVDD	Phase I and II (completed)	No results available	NCT01158924 NCT01182337 NCT01124006 NCT00813813

Table 1: Pre-clinical disease modifying drugs for OA and IVDD (continuation).

Class	Name/Description	Disease	Phase	Main Results	References / Clinical trial no
Enzyme inhibitors	Oral administration of doxycycline, broad-spectrum MMP inhibitor	OA	Phase II (completed)	No effect on symptomatic OA; Increased risk of adverse events	NTR1111 ⁷⁷
	Oral administration of PG-116800, broad-spectrum MMP inhibitor	OA	Phase II (completed)	No function or pain improvement; Increased musculoskeletal toxicity	NCT00041756 ⁷⁸
	M6495, anti-ADAMTS-5 nanobody	OA	Phase I (completed)	No results available	NCT03224702 NCT03583346
	Oral administration of GLPG1972, ADAMTS-5 inhibitor	OA	Phase I (completed) and Phase II (undergoing)	No results available	NCT03311009 NCT03595618
	Oral administration of SD-6010, a selective iNOS inhibitor	OA	Phase II (completed)	The compound was well tolerated, yet no clinical benefit was obtained when compared to placebo	NCT00565812 ⁷⁹
	Single local injection of SD-6010, a selective iNOS inhibitor	OA	Phase III (recruiting)	No results available	NCT03928184
	Oral administration of doxycycline, broad-spectrum MMP inhibitor	OA	Phase II (completed)	No effect on symptomatic OA; Increased risk of adverse events	NTR1111 ⁷⁷
	Oral administration of PG-116800, broad-spectrum MMP inhibitor	OA	Phase II (completed)	No function or pain improvement; Increased musculoskeletal toxicity	NCT00041756 ⁷⁸
Others	Single local injection of SM04690, a Wnt pathway inhibitor	IVDD	Phase I (terminated)	No results available	NCT03246399
	Single local injection of SM04690, a Wnt pathway inhibitor	OA	Phase I (completed)	SM04690 displayed a safe profile, without evidence of systemic exposure	NCT02095548 ⁸⁰
	Single local injection of SM04690, a Wnt pathway inhibitor	OA	Phase II (completed)	SM04690 yielded improvement in pain and function measurements	NCT02536833 ⁸¹
	Single local injection of SM04690, a Wnt pathway inhibitor	OA	Phase III (recruiting)	No results available	NCT03928184
	Intra-articular injection of UBX0101, a senolytic drug	OA	Phase I (completed)	No results available	NCT03513016
	Oral administration of calcitonin	OA	Phase III	No beneficial effects observed	NCT00486434 NCT00704847 ⁸²

3.1.1 Antibodies and cytokine inhibitors

Therapies using monoclonal antibodies and cytokine inhibitors have been the most tested strategies so far. A monoclonal antibody raised against nerve growth factor (NGF), called Tanezumab, was shown to be effective in reducing pain in hip and knee OA¹⁶¹. However, serious adverse events were noted, including knee osteonecrosis, rapid progression of OA, and increased incidence of total joint replacement. Although side effects were mainly observed when combined with NSAIDs, some clinical trials have come to a halt¹⁶¹⁻¹⁶³. Another similar clinical trial administering Tanezumab subcutaneously showed significant function and pain improvements in patients with moderate to severe hip or knee OA, yet more adverse events and total joint replacements were observed¹⁶⁴. Conflicting results were also obtained with TNF α inhibition. Intra-articular administration

of Adalimumab, an antibody against TNF- α , was shown to improve pain and function scores in a trial in knee OA¹⁷⁸, but did not have any therapeutic effect in erosive hand OA¹⁷⁹. Similarly, use of anti-cytokine therapy for low back pain has been investigated, yet the majority of trials concerned patients with sciatica associated with disc herniation, without any reference to disc degeneration¹⁸⁰. Also here, the results of the trials are conflicting amongst each other. Several studies reported improvements in back and leg pain and function upon subcutaneous or epidural injection of Etanercept, a TNF- α selective inhibitor^{169,181}. Yet, in two other studies Etanercept did not lead to improved primary outcomes, leg pain and disability index, when compared to placebo or steroid-treated groups^{182,183}. Whether these treatments are also able to promote disc regeneration remains unclear. IL-1 has also been targeted in joint degeneration. Anakinra, a IL-1 receptor antagonist (IL-1Ra), did not lead to symptomatic improvements compared to placebo in a 3-month follow up clinical study for OA¹⁶⁵. Likewise, in a study where AMG 108, an antibody against IL-1 receptor 1, was administered IV or subcutaneously in OA patients, no beneficial clinical effects were observed when compared to the placebo group at a 3-month follow-up¹⁶⁶. Interestingly, in a pre-clinical study conducted in arthritic mice, combined antibody-mediated inhibition of IL-17 and TNF- α showed improved cartilage protection when compared with single inhibition, showcasing the beneficial therapeutic effect of multi-target blockade¹⁸⁴. Similarly, combined inhibition of IL-1 α and IL-1 β showed improved cartilage protection when compared to single inhibition in a mouse model of OA¹⁸⁵. Nevertheless, in a clinical trial where patients with knee OA were bi-weekly treated subcutaneously with Lutikizumab, a bispecific antibody for IL-1 ν and IL-1 α , no beneficial effects were observed in pain scores, synovitis or cartilage thickness over a 50-week period¹⁶⁷. Similar results were observed in a clinical trial testing bi-weekly subcutaneous administration of Lutikizumab for the treatment of erosive hand OA¹⁶⁸. Despite a decrease in serum levels of inflammatory markers, no significant pain or function improvements were observed when compared to placebo group¹⁶⁸.

3.1.2 Enzyme inhibitors

Another class of agents that has been proposed as therapeutics for degenerative joint diseases is the enzyme inhibitors, namely MMPs inhibitors¹⁸⁶. These inhibitors are synthetic agents that mimic the role of endogenous tissue inhibitors of metalloproteinases (TIMPs). Yet, despite promising preclinical data showing chondroprotective effects in OA¹⁸⁶⁻¹⁸⁸, clinical trials have failed to show efficacy of these agents in humans so far and an association with severe side effects^{5,172,173,189}. Oral administration of doxycycline, a general MMP inhibitor, did not have any effect on symptom reduction and was associated with more severe side effects in patients with OA¹⁷². Similar results were observed for oral administration of PG-116800, another broad-range MMP inhibitor¹⁷³. No changes were observed in pain and function scores when compared to placebo group, yet there was an increased occurrence of musculoskeletal toxicity¹⁷³. The side effects are likely associated with the broad spectrum of inhibition of such molecules and the variety of roles MMPs play in several tissues throughout the body, together with the fact that the

drugs have been mainly administered orally or systemically for long periods⁶.

Currently, efforts are focused on the development of more specific MMP inhibitors, in particular for MMP-13, which is thought to be the most important MMP in OA cartilage^{6,190-193}. Likewise, the ADAMTS enzyme family has an important role in cartilage degradation. M6495, a nanobody against ADAMTS-5 previously shown to be chondroprotective^{194,195}, is currently being tested in clinical trials for its safety, tolerability and pharmacokinetics upon subcutaneous injection (NCT03224702, NCT03583346). Additionally, the safety and efficiency of the small molecule inhibitor GLPG1972 targeting ADAMTS5 are being currently evaluated in Phase I and II clinical trials (NCT03311009, NCT03595618)

iNOS has been linked to progressive degeneration in OA¹⁹⁶, and its inhibition led to decreased levels of catabolic effectors in a OA dog model¹⁹⁷. An iNOS inhibitor has also entered a phase II clinical trial for treatment of knee OA, however, no functional benefit or pain decrease were observed when compared to the placebo group upon oral administration¹⁷⁴. Calcitonin, a small peptide that was shown to have protective effects on cartilage and bone in preclinical studies¹⁹⁸⁻²⁰⁰, also failed to improve treatment outcomes in two phase III clinical trials carried out in OA patients¹⁷⁷. In this study, the authors hypothesized the lack of efficacy could be derived, among others, from the low exposure to the compound¹⁷⁷.

3.1.3 Growth factors

Growth factors have also been proposed for treatment of knee OA. In a randomized, double-blind, placebo-controlled trial, BMP-7 was intra-articularly administered to knee OA patients, showing good tolerability and safety profiles²⁰¹. Even though a symptomatic improvement was observed, no follow-up studies have been carried out so far. Based on preclinical studies in rabbit models of IVDD showing the potential of growth and differentiation factor-5 (GDF-5)²⁰² and BMP-7^{203,204} to restore disc height and structure, phase I and II clinical trials have been carried out testing the safety and efficacy of intradiscal injection of recombinant human GDF-5 and BMP-7. However, these trials have been discontinued for unknown reasons. In a placebo-controlled trial, FGF-18 (or sprifermin) was injected intra-articularly to knee OA patients in single or multiple doses over a 3-week period¹⁷¹. FGF-18 has been previously reported to exert anabolic effects on chondrocytes and cartilage^{205,206}. After 1 year follow-up, while lower cartilage volume loss and increased joint width in the lateral compartment was reported in patients treated with FGF-18, higher pain relief was observed in the placebo group.

3.1.4 Gene and oligonucleotide therapy

Gene therapy offers unprecedented tools for the modulation of gene products involved in pathological and repair pathways^{207,208}. As the exact causes behind OA remain unknown, gene therapy for OA focuses on either up-regulating therapeutic genes or down-regulating disease-associated genes using plasmid DNA, mRNA or short oligonucleotides, such as small interfering RNA (siRNA) and antisense oligonucleotides²⁰⁸. Together, these strategies have the common goal to halt degeneration while improving

local repair and regeneration²⁰⁸. Both strategies can be employed by means of non-viral or viral transfection, and theoretically be performed *ex vivo*, where cells are transfected prior to transplantation into the joint, or *in vivo*, upon direct gene transfer to joint tissues^{207,208}. While viral gene delivery strategies for OA have been already tested in clinical trials^{209,210}, non-viral gene delivery is still in its infancy. The main limitation of non-viral strategies is the low efficiency of gene transfer and subsequently low levels of transgene expression, and the transient effects, as opposed to viral approaches²¹¹. For IVDD-associated chronic low back pain, clinical trials using either non-viral or viral gene therapy have not been carried out so far²¹². While the preclinical potential of gene therapy to treat degenerative joint diseases is established^{213,214}, more preclinical and clinical trials need to be carried out to assess the safety and efficacy of such strategies.

The investigation of epigenetic changes during OA development also offers the potential to discover novel therapeutic targets. Recent studies showed that a wide range of microRNAs (miRNAs) plays important roles in the maintenance of cartilage homeostasis, and consequently in the pathological processes preceding or sustaining OA and cartilage degradation²¹⁵⁻²²². MiRNA-140 was shown to exert a crucial role in cartilage development and homeostasis^{223,224}. Intra-articular injections of miRNA 140 led to anti-inflammatory effects, cartilage matrix production and slower OA progression in both mice²²⁵ and rat²²⁶ models of OA. Recent preclinical studies showed the feasibility of antisense oligonucleotide-mediated silencing of microRNA-181a-5p²²⁷, a microRNA found to be increased in OA cartilage²²⁰. Intra-articular injections of a modified antisense oligonucleotide led to attenuation of cartilage degradation and reduction of catabolic molecules in two rodent models of OA²²⁷. Likewise, evidence is being gathered on the involvement of miRNAs in disc degeneration²²⁸⁻²³⁰. Modified antisense oligonucleotides may in addition be potential alternatives to small molecules for the inhibition of other OA-associated proteins²³¹⁻²³³. More recently, other epigenetic regulators such as long noncoding RNAs and circulating miRNAs have been investigated for their roles in the pathophysiology of OA and, therefore, their potential use as biomarkers and therapeutic targets²³⁴⁻²³⁶. Although there is substantial *in vitro* evidence supporting the potential of these molecules or their inhibitors as therapeutics for both OA or IVDD, a better understanding of their spatiotemporal expression is necessary to avoid cytotoxicity and off-target effects^{212,237,238}. Moreover, efficient and targeted delivery of miRNAs or their inhibitors for therapeutic purposes should be carefully evaluated due to potential degradation by RNases and Toll-like receptor-mediated immune system activation^{221,230,239}.

3.1.5 Others

The Wnt signaling pathway is known to be not only a key regulator of joint and disc development and function, but also a relevant component involved in joint and disc pathology and hence degeneration⁵. Hence, the Wnt pathway has been a studied therapeutic target for OA and IVDD. Phase I and II clinical trials have been carried out testing the safety and efficacy of SM04690, as treatment for OA^{175,176}. In these clinical trials, SM04690 improved pain and function according to the WOMAC score^{175,176}. A follow-up

phase III clinical trial is currently underway (NCT03928184). The same drug was also proposed as therapeutic for IVDD, following a preclinical study where matrix production and disc height were observed in a rodent-model of disc degeneration²⁴⁰. The molecule has since then entered a phase I clinical trial for treatment of disc degeneration, yet the study was halted for business reasons (NCT03246399).

Lately, a new class of drugs targeting senescence mechanisms is emerging as a new therapeutic approach for OA²⁴¹. UBX101, a drug that increases p53 activity and hence inducing apoptosis in senescent cells, entered a phase clinical trial to evaluate safety and tolerability in OA patients²⁴². This drug was previously shown to be effective in eliminating senescent cells and in slowing down disease progression in a mouse model of OA¹²⁸. While senescence has been pinned out as a hallmark of IVDD, the development senolytic drugs for disc degeneration is still in its infancy²⁴³.

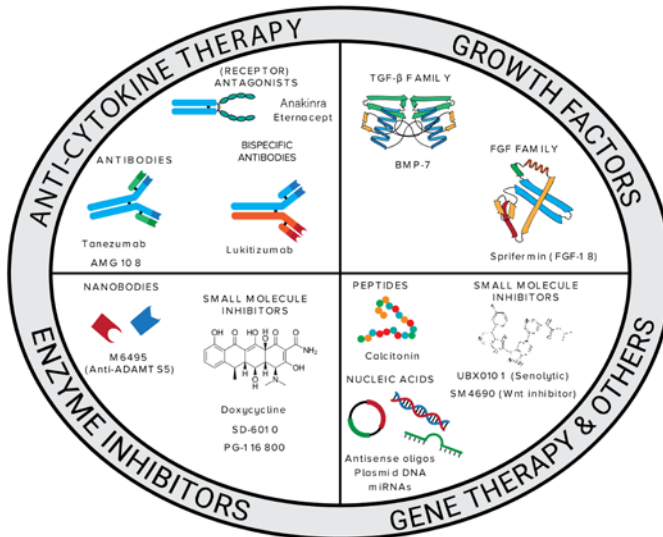


Figure 2: Pre-clinical drugs that are currently in testing as disease-modifying agents for OA and IVDD therapy, ranging from cytokine/enzyme inhibitors to promoters of anabolic pathways.

All in all, most of the novel pharmacological treatments for OA and IVDD show little to no efficiency in cartilage repair in clinical studies, although being promising in pre-clinical research. Most of the drawbacks of the previously tested drugs are related with either prolonged systemic overexposure and subsequent off-target side effects such as for the enzyme inhibitors, but also short bioavailability in the target tissue leading to a lack of efficacy, especially for small molecule drugs are likely to have played a role. Additionally, and specially for IVD, due to the avascularity, presence of endplates and

absence of a synovial space, systemically-administered drugs have limited bioavailability within the local tissue¹¹. Therefore, improved therapeutic outcomes are likely to be obtained through local injections in drug delivery platforms. These systems can be tailored to provide local and a sustained drug release, as well as targeting of specific cell/tissue types.

4. Drug delivery systems

Several approaches have been taken towards the application of biocompatible and safe drug delivery platforms for the improvement of therapeutic outcomes (Table 2 and Figure 3). Among these strategies, microparticles and hydrogels are used as drug depot for local extracellular drug release. Continuous drug release over time or upon endogenous (e.g. enzymatic activity, temperature, pH) or external stimuli (e.g. ultrasound) can be tailored to achieve drug concentrations within the therapeutic window for prolonged periods of time¹². On the other hand, since OA and IVDD involve different tissues with varied roles during pathogenesis, drug delivery using targeting moieties may facilitate and improve drug delivery to specific cells and tissues.

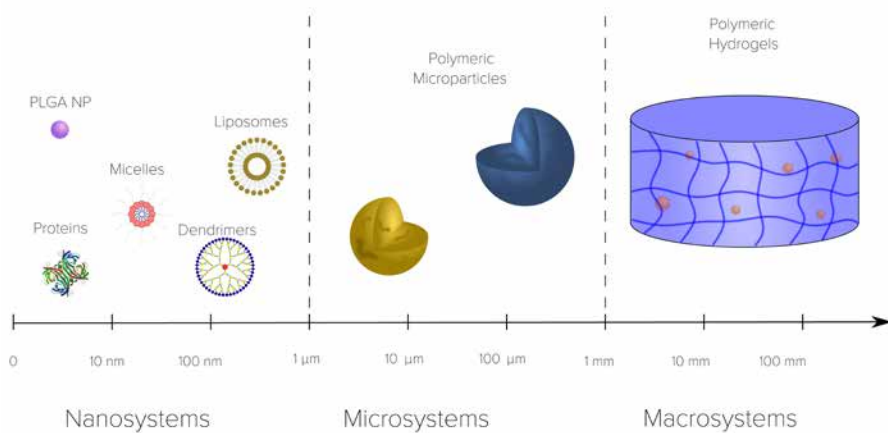


Figure 3: Schematic representation of the different drug delivery platforms according to their size, from nano to macrosystems.

4.1 Microparticles

Microparticles are micron size particulate systems. Due to their size, ranging from one to hundreds of microns, injected microparticles can be well retained within the joint cavity, escaping the main mechanisms of clearance: vasculature and the lymphatic system¹². Microparticles can be designed to encapsulate a variety of drug candidates, ranging from small hydrophobic drugs such as corticosteroids and non-steroidal anti-

inflammatory drugs (NSAIDs) to large macromolecules such as enzymes and antibodies and therefore offering the possibility to encapsulate drug-modifying OA drugs (DMOADs). To tune their degradability and hence their release profile, microparticles can be formulated using different biomaterials.

Up until now, only one microparticle-based drug delivery system has reached the clinic. This product is based on triamcinolone acetonide-loaded poly(lactic-co-glycolic acid) (PLGA) microspheres and commercialized under the name of Zilretta® / FX006²⁴⁴. In OA patients, the system showed improved joint retention and prolonged anti-inflammatory effects compared to the injection of bolus TAA (Kenalog 40®)²⁴⁵. However, in a phase-3 clinical trial, FX006 failed to outperform the standard of care bolus suspension of microcrystalline TAA in the primary outcome parameter. Nevertheless, the novel formulation did show significantly better results in several secondary outcome parameters²⁴⁶. A new clinical trial is ongoing to evaluate the effect of FX006 on synovial inflammation in OA patients²⁴⁷.

Other microparticle formulations, ranging from synthetic to natural polymers have been used in preclinical studies. Microspheres derived from the synthetic polyester amide (PEA) polymer and loaded with triamcinolone acetonide (TAA), were tested in several models of joint pathology²⁴⁸. In collagenase-induced OA rats, the TAA-PEA microparticles showed a retention time of over two months and reduction of inflammation²⁴⁸. In addition, the TAA-PEA formulation was also shown to be superior to TAA-loaded PLGA microparticles in reducing pain, swelling, lameness and synovitis in a rat model of acute arthritis²⁴⁹. In a trauma-induced OA model, reduction of PGE2 levels, synovial inflammation, osteophyte formation and subchondral bone sclerosis were observed using celecoxib-loaded PEA microspheres, whereas extended exposure to TAA enhanced degeneration^{250,251}. In a canine model of IVDD, celecoxib-loaded PEA microspheres inhibited osteophyte formation and sclerosis similarly to the rat OA model, and even prevented further degeneration. However, TAA delivery in the same model only reduced the expression of a pain marker^{252,253}. In contrast, in a rat model of IVD trauma, prevention of IVD degeneration was observed after delivery of corticosterone using tricalcium phosphate (TCP) microcapsules²⁵⁴. A new drug formulation, combining synthetic poly(lactic) acid (PLA) nano- and microparticles, encapsulating drug nanocrystals of a few hundred nanometers, allowed an extended release profile of the encapsulated drugs, specifically kartogenin and p38 β /MAPK inhibitor^{255,256}. Using these drug formulations, a protective effect on cartilage integrity and reduction of disease markers were observed in an OA mouse model^{255,256}. Microparticles of silk fibroin, a natural polymer, also increased the retention of a fluorescent dye within the joint cavity after intra-articular injection²⁵⁷. By exploiting their biodegradability and biocompatibility, PRP-containing gelatin hydrogel microspheres were shown to significantly delay OA and IVDD progression in ACLT and degenerated IVD rabbit models²⁵⁸⁻²⁶⁰.

Another approach towards controlling drug release dynamics and avoid the typical drug burst release of microparticles was reported in a study where ibuprofen was chemically functionalized to the backbone of a polymer chain instead of loaded

into the particles²⁶¹. Here, a methacrylic derivative of ibuprofen was co-polymerized with an oligo(ethylene-glycol) methacrylate and poly(PLGA-PEG) dimethacrylate, and used to form microparticles of 40-100 μm . The release of regenerated ibuprofen was obtained by hydrolysis of the ester bond, allowing a gradual release of 13% over a three month period²⁶¹.

Sustained delivery of IL-1ra-loaded PLGA microspheres in IVDD led to attenuation of NP degeneration in in vitro human IVD tissue culture²⁶². Regenerative factors have been formulated in microparticle drug delivery systems to a much lesser extent. Only in one study PLGA microparticles loaded with dexamethasone and FGF-2-embedded heparin/poly(L-lysine) nanoparticles were shown to promote rat MSC proliferation and differentiation into NP cells in vitro²⁶³ and induce partial tissue regeneration in a rat model of disc degeneration²⁶⁴.

4.2 Nanoparticles

Nanoparticles can be either exploited to increase drug retention time or to target specific areas within the joint, as their smaller size allows for efficient use of targeting moieties and facilitates penetration and diffusion within the dense cartilage matrix. Using different nanoparticle formulations and production methods, size and surface properties can be modulated, allowing loading of a large range of drugs. However, the resulting drug release profile depends on several factors such as pH, temperature, nanoparticle degradation, drug diffusion and loss of binding interactions. Different types of nanoparticles have been widely used for OA and IVDD treatment in preclinical animal models, including polymeric nanoparticle, micelles and liposomes.

4.2.1 Polymeric nanoparticles

Polymeric nanoparticles can be derived from several biocompatible and biodegradable polymers, allowing tuning of their drug loading and release properties. In addition, due to their small size and flexibility, polymeric nanoparticles can be functionalized to allow targeted delivery to specific tissues or cells by the addition of extracellular matrix- or cell-binding ligands. For instance, using the collagen II $\beta 1$ -binding peptide (WYRGRL) nanoparticles retention was increased 72-fold within the articular cartilage of murine knee joints, exploiting the tissue as a drug reservoir²⁶⁵. Targeting can also be achieved by making use of electrostatic interaction. Avidin is a positively charged protein with an isoelectric point of ~ 8 in physiological conditions and with a hydrodynamic radius of 7 nm which makes it small enough to diffuse through the dense cartilage matrix²⁶⁶. Due to its positive charge, avidin has a strong affinity to the negatively charged cartilage matrix, and this facilitates a faster penetration and longer retention of the protein carrier within cartilage²⁶⁶⁻²⁶⁸. Drugs like dexamethasone and insulin-like growth factor 1 (IGF-1) were conjugated to avidin nanoparticles through a biotin linker allowing the loading of the carrier with potentially four different molecules²⁶⁶⁻²⁶⁸. Avidin nanoparticles showed full thickness penetration into the articular cartilage of rat knee joints, a half-life of 29 hours and retention time within the joint of 7 days²⁶⁷. This study

shows how the engineering of nanoparticles can improve the delivery of therapeutics to specific cell types or areas. Amine terminal polyamidoamine (PAMAM) dendrimers were functionalized with poly(ethylene glycol) (PEG) and utilized to deliver insulin-like growth factor 1 (IGF-1) for the regeneration of articular cartilage in a rat model of OA²⁶⁹. The electrostatic interaction between the positively charged dendrimer and the negatively charged cartilage matrix allowed a 10-times higher nanoparticle retention up to thirty days. The subsequent *in vivo* study in an OA rat model demonstrated improved cartilage repair when using IGF-1 conjugated to dendrimers as opposed to injection of free IGF-1²⁶⁹. Altogether, these studies highlight the beneficial effect of using positively charged nanoparticles and their interaction with the negatively charged matrix for OA treatment.

An example of nanoparticles used for IVDD therapy are albumin/heparin nanoparticles which were used for the release of stromal cell-derived factor-1 α (SDF-1 α) and the recruitment of bone marrow resident mesenchymal stem cells (MSCs)²⁷⁰. Using this strategy, regeneration of the damaged disc compared to the delivery SDF-1 α without delivery system was reported.

4.2.2. Micelles

Micelles are supramolecular self-assembled nanoparticles that spontaneously form upon hydration of amphiphiles. Amphiphiles are molecules which contain a hydrophilic and a hydrophobic part. When hydrated in aqueous solution, amphiphiles reorganize themselves to form nanoparticles containing a hydrophobic core and a hydrophilic external shell facing the water media. These vesicles are formed in aqueous solution when the amphiphilic molecule reaches a certain concentration threshold known as critical micelle concentration (CMC). These particles allow the encapsulation of poorly soluble hydrophobic drugs within the hydrophobic core²⁷¹. Expectably, incorporation of hydrophilic molecules is rather difficult and dependent on covalent conjugation to the external hydrophilic shell of the micelles²⁷². The vesicle diameter usually ranges between 10 to 100 nm, depending on the ratio between the hydrophilic and hydrophobic part of the amphiphilic molecule. Size can also vary depending of the nature of the encapsulated drug. Advances in polymer chemistry, and the use of block copolymers with lower CMC for the preparation of polymeric micelles has been yielding vesicles with higher *in vivo* stability, which makes them suitable candidates for drug delivery²⁷¹. Several micelle formulations have been investigated for OA therapy. Rapamycin-loaded micelles delivered intra-articularly in a gelatin hydrogel were shown to delay OA progression in arthritic mice²⁷³. In a similar approach, PEGylated kartogenin-based micelles delivered in a HA hydrogel were used to prevent OA progression in an anterior cruciate ligament transection (ACLT) rat model²⁷⁴. PEGylation is a common strategy to provide particles with stealth properties and allow longer circulation time and retention *in vivo*. Several other micelle formulations have been tested for the treatment of inflammatory arthritis by delivering dexamethasone²⁷⁵⁻²⁷⁸, cyclosporin-A²⁷⁹, and indomethacin²⁸⁰. The covalent entrapment of dexamethasone in core-crosslinked polymeric micelles composed by poly(ethylene glycol) (PEG) and poly(N-(2-hydroxypropyl)methacrylamide-lactate)

(pHPMAmLac_n) rendered particles with controllable and tunable release kinetics. Once injected in two animal models of rheumatoid arthritis, the micelles induced improvements in arthritic scores²⁷⁵. Also folic acid-functionalized polysialic acid/cholesterol micelles loaded with dexamethasone demonstrated improved arthritic scores when compared to non-targeted micelles and dexamethasone alone²⁸¹.

Micelle polyplexes composed of polyethylene glycol-polyamino acid block copolymers and loaded with an anabolic mRNA were also used for IVDD therapy in a rat model of disc degeneration²⁸². The strategy led to maintenance of disc integrity and prevention of inflammation induced by administration of naked mRNA. MiR-29a-loaded micelle polyplexes encapsulated into hydrogels were also used for IVDD treatment in animal models²⁸³. The polymers of both hydrogel and particles were MMP-responsive, causing the release of micelles from the gel. Subsequent removal of the PEG shell from particles, enhanced their cellular uptake and endosomal escape. The strategy led to reduced MMP-2 levels and attenuation of IVD fibrosis in vivo²⁸³.

4.2.3 Liposomes

Liposomes, which were the first nanoparticles to be translated to clinical applications, are synthetic vesicles made of phospholipid bilayer(s) and structurally arranged as a cellular membrane²⁸⁴⁻²⁸⁶. Phospholipids are natural amphiphiles which contain a hydrophobic apolar tail and a hydrophilic polar head. The size of the liposomes can range from 50 nm to 5 μ m, depending on the number of bilayers constituting the liposome. As opposed to micelles, liposomes contain a hydrophilic core and a hydrophobic lipid outer bilayer which allows the encapsulation of hydrophilic and hydrophobic drugs, respectively^{284,287}. Among the different attractive properties of liposomes, particular attention is given to their elevated degree of biocompatibility, the possibility of encapsulating drugs of different nature, and their wide range of functionalization possibilities²⁸⁴. Similarly, to micelles, liposomes have highly versatile physical and chemical properties that can be tailored according to the intended use. Different components can be added to the lipid bilayer to achieve longer circulation times, targeting of specific tissues and controlled release profiles.

The use of liposomes for treatment of joint diseases has been explored in the last decades. For instance, a study demonstrated the feasibility of targeted liposomal-based delivery of plasmid DNA to chondrocytes²⁸⁸. Efficient *in vivo* gene transfer and expression in chondrocytes was observed upon intra-articular injection in rats. Expression of the exogenous gene was limited to chondrocytes located in both superficial and middle layer. The limited penetration and transfection of the 200 nm vesicles again draws attention to the importance of the particle size for efficient full depth diffusion, and therefore efficacy. Multilamellar liposomes were used for intra-articular controlled delivery of dexamethasone and diclofenac²⁸⁹. The liposomes were composed of soybean phosphatidylcholine and dipalmitoyl phosphatidylethanolamine, and further functionalized with HA and collagen to increase their bioadhesive properties and affinity for extracellular matrix^{289,290}. Single or combined delivery of dexamethasone

and diclofenac reduced knee-joint inflammation in a MIA-induced rat model of OA over a time span of 17 days²⁸⁹. Furthermore, HA-coated liposomes were shown to have a greater effect when compared to the collagen-coated counterpart, which was attributed to higher cartilage binding affinity^{289,290}. Similarly, liposomes formulated from soybean phosphatidylcholine and cholesterol for encapsulation and delivery of celecoxib and embedded within a HA gel protected cartilage from degeneration as compared to the free celecoxib in a rabbit model of OA²⁹¹. However, as the effect of the liposome alone was not evaluated, the beneficial effect cannot be attributed with certainty to the controlled and sustained release of celecoxib, especially as liposomes are known to increase joint lubrication^{292,293}. Nevertheless, this dual treatment modality of liposomes does increase their attractiveness as a therapeutic strategy in degenerative joint disease.

The use of liposomes for IVDD treatment has been minimally investigated so far, but a study optimized lipofectamine for the transfection of a human telomerase reverse transcriptase (hTERT) construct in cultured NP cells²⁹⁴. Liposomal siRNA could also downregulate Caspase 3 and ADAMT5 levels in a rabbit model of disc degeneration, showing beneficial effects compared to saline control²⁹⁵.

In the past years, also drug delivery systems derived from cell membranes have been a subject of research as, due to their autologous nature, they can reduce adverse effects observed with exogenous liposomes. One example of cell-derived particles are nanoghosts, MSC-derived nanoparticles obtained after removal of the cell content and subsequent extrusion²⁹⁶. Nanoghosts have been recently applied for drug delivery in mouse models of cancer, leading to significant results in terms of tumor regression and mouse survival²⁹⁶. In addition, because of the possibility to produce these nanoparticles in larger scale, they also offer a significant advantage in comparison with exosomes, which lack satisfactory scalable production methods²⁹⁷.

4.3 Hydrogels

Similarly to microparticles, hydrogel can be used as drug delivery systems for small and big molecules, acting as a localized drug depot. Hydrogels are 3D water-containing structures formed by crosslinked natural or synthetic polymers. Importantly, their physical properties such as density and porosity can be tuned by adjusting polymer composition and concentration, therefore allowing for optimal drug incorporation and release^{298,299}. While the high water content gives the hydrogel a biocompatible profile, the polymer mesh provides adjustable mechanical properties^{298,299}. Moreover, drug release profiles can be further modified by adjusting polymer crosslinking and degradability. Hence, many hydrogel formulations have been explored for intra-articular and intra-discal drug delivery, ranging from natural-derived (alginate, chitosan, collagen, gellan gum, hyaluronic acid) to synthetic materials (Polyethylene glycol, poly-N-isopropylacrylamide, polyvinyl alcohol, polyvinylpyrrolidone).

For OA treatment, HA-hydrogels represent the most frequently used formulation because of the improvement of joint function through slow release of HA and the possible loading of several drugs. For instance, a HA-doxycycline hydrogel was demonstrated

to have improved pharmacokinetic and therapeutic profiles over HA or doxycycline alone³⁰⁰. Upon partial meniscectomy and unilateral fibular ligament transection in rabbits, the proposed system displayed decreased occurrence of fibrillation and osteophyte formation. Importantly, lower degrees of pain were observed for rabbits treated with the HA-doxycycline formulation. A HA-based hydrogel was also shown to improve SDF-1 delivery and recruitment of MSCs in an ex vivo model of nucleotomy³⁰¹.

Stimuli-responsive hydrogels have also attracted great interest due to their ability to release the drug after chemical or physical stimuli. A thermoresponsive hydrogel composed by PCL-PEG-PCL triblock copolymer loaded with celecoxib was demonstrated to have a sustained drug release of about 4-8 weeks upon intra-articular injection in rats³⁰². In addition, hydrogel systems in which the release of therapeutics is triggered by the overexpression of tissue remodeling enzymes have been developed³⁰³. Using this strategy, TAA-loaded hydrogel disassembly and drug release were demonstrated to be specifically triggered by synovial MMP levels in vitro, and dependent on arthritis flares in vivo³⁰³. In a canine model of IVD degeneration, a thermoresponsive poly-N-isopropylacrylamide MgFe-layered double hydroxide hydrogel was used for celecoxib delivery³⁰⁴. Despite the excellent in vivo biocompatibility, the strategy only led to a limited reduction of prostaglandin levels in a canine model of mild IVD degeneration, requiring further investigation in models with a more severe phenotype³⁰⁴.

Hydrogels represent a very versatile drug delivery systems which has also been applied for gene therapy such as modulation of disease-causing genes or anti-chondrogenic factors through the delivery of siRNA, antisense oligonucleotides and anti-miR drugs^{232,233,305,306}.

In a large animal model of disc degeneration, BMP-2 and BMP-2/7 heterodimers were conjugated to a HA hydrogel and intradiscally injected³⁰⁷. Even though conjugation was shown to be effective, no improved disc regeneration was observed, in what the authors hypothesized to be related to low dosage and low release from the hydrogel.

Table 2: Main drug delivery systems for OA and IVDD.

Category	Size	Removal mechanism	Modifications	Advantages	Disadvantages
Microparticles	1-1000 μm	Foreign body response. Biodegradation	Different sizes. Tuneable drug loading and release dynamic. Surface coating for controlled drug release. Retention within the joint.	Sustained or controlled drug release. Minimisation of injections needed.	Inflammatory response. Particle solvent might cause toxicity
Nanoparticles (polymeric, liposomes, micelles)	Diameter of 1-1000 nm in at least one dimension and a diameter of 1-100 nm	Foreign body response. Cell internalization. Biodegradation.	Different sizes. Surface modifications for modulation of charge, size and matrix/cell interactions. Antibody or peptide functionalisation for targeted delivery. Matrix penetration/diffusion	Penetration of biological membranes. Targeted drug delivery. Enhancement of solubility of hydrophobic drugs. Enhanced drug stability.	Nanoparticles aggregation. Immunogenicity. Particle solvent might cause toxicity
Hydrogels	Mesh size of 5-100 nm	Biodegradation	Modification of mesh size and degradation profile for controlled drug release. Cell homing properties. Local drug delivery.	Sustained or controlled drug release. Tunability. High biocompatibility due to the high water content.	Hydrophobic drugs are not ideal to be encapsulated. Difficult to handle. Not-adherent.

5. Conclusions and Future Perspectives

The articular cartilage and intervertebral disc are tissues with similar structural and biochemical properties. There is an unmet clinical need for new therapeutic molecules that can act on the effector pathways that lead to degeneration, aiming at repair and regeneration. Different disease modifying drugs have been proposed and extensively tested *in vitro* and in pre-clinical models. However, the undesired side effects and limited efficacy observed in clinical trials have delayed their clinical approval. One of the factors greatly affecting therapeutic efficacy lies on the short-term retention of many drugs within joints and limited targeting to specific tissues. Thus, the combination of an effective disease-modifying drug with a safe delivery strategy is a crucial step forward towards regeneration.

In terms of drug delivery strategies applied in OA and IVDD, microparticles and hydrogels are currently being used as site-specific drug depots. Both systems can derive from different synthetic or natural polymers and, depending on the production methods, degradation and drug release profiles can be tuned according with the application and target tissue. Besides the enhanced bioavailability and prolonged therapeutic periods, these systems reduce the need for multiple injections and systemic drug exposure. In addition, hydrogels can also be applied for cell delivery or recruitment and differentiation of endogenous MSCs. On the other hand, the selective targeting of different cell/tissue types in different disease stages using functionalized nanoparticles could allow a more selective and patient-specific therapeutic strategy. Positive outcomes have been obtained in preclinical models using either polymeric nanoparticles, liposomes or micelles. For cartilage targeting, small size and positive charge are ideal requirements for drug delivery within the matrix. Nanoparticle functionalized with cartilage-binding peptides and liposomes are also attractive platforms due to their ability to favor drug accumulation in specific areas and intrinsic lubricative properties, respectively. IVDD therapy have been less explored so far. Microparticles demonstrated how enhanced therapeutic outcomes can be obtained through sustained delivery of off-the-shelf drugs. Hydrogels have still only been largely explored for cell homing or delivery properties, yet more drug delivery applications in preclinical models are needed. Since the ideal strategy should adapt the drug delivery to the actual disease stage, enzyme-responsive hydrogels are an exciting option which was proven effective. Furthermore, since the NP is more prone to degeneration, more attention has been paid to the regeneration of this tissue. However, future therapies should aim at restoration of both NP and AF.

Importantly, also the choice of drug is a crucial step towards the design of an efficient therapy. Current disease modifying disease drugs for OA and IVDD allow wide intervention on many aspects of the diseases, ranging from blockage of matrix-degradative enzymes, inflammation and bone resorption to stimulation of new ECM synthesis. Selecting the best drug and intervention time goes in parallel with the necessity of the identification of novel disease biomarkers. It is also conceivable that multiple drugs at different disease stages might be more effective, favoring the parallel development of multiscale-drug

delivery platforms.

A final consideration for the development of any drug delivery approach regards their biocompatibility and cytotoxicity. In the future, a larger focus on studies of specific methods to identify local and systemic off-target effects might facilitate the screening and translation of safe and effective drug delivery systems into clinical practice.

To sum up, ongoing studies on the pathophysiology of OA and IVDD, the development of therapeutic aimed at blocking disease progression or inducing a regenerative response, and the optimization of drug delivery strategies have the potential to meet the current necessities for curative therapies.



3

CHAPTER 3

FIBRIN-HYALURONIC ACID HYDROGEL-BASED DELIVERY OF ANTISENSE OLIGONUCLEOTIDES FOR ADAMTS5 INHIBITION IN CO-DELIVERED AND RESIDENT JOINT CELLS IN OSTEOARTHRITIS

João Pedro Garcia, Jeroen Stein, Yunpeng Cai, Frank Riemers,
Ezequiel Wexselblatt, Jesper Wengel, Marianna Tryfonidou,
Avner Yayon, Kenneth A. Howard, Laura B. Creemers

Published in Journal of Controlled Release

Abstract

To date no disease-modifying drugs for osteoarthritis (OA) are available, with treatment limited to the use of pain killers and prosthetic replacement. The ADAMTS (A Disintegrin and Metallo Proteinase with Thrombospondin Motifs) enzyme family is thought to be instrumental in the loss of proteoglycans during cartilage degeneration in OA, and their inhibition was shown to reverse osteoarthritic cartilage degeneration. Locked Nucleic Acid (LNA)-modified antisense oligonucleotides (gapmers) released from biomaterial scaffolds for specific and prolonged ADAMTS inhibition in co-delivered and resident chondrocytes, is an attractive therapeutic strategy. Here, a gapmer sequence identified from a gapmer screen showed 90% ADAMTS5 silencing in a monolayer culture of human OA chondrocytes. Incorporation of the gapmer in a fibrin-hyaluronic acid hydrogel exhibited a sustained release profile up to 14 days. Gapmers loaded in hydrogels were able to transfect both co-embedded chondrocytes and chondrocytes in a neighboring gapmer-free hydrogel, as demonstrated by flow cytometry and confocal microscopy. Efficient knockdown of ADAMTS5 was shown up to 14 days in both cell populations, i.e. the gapmer loaded and gapmer-free hydrogel. This work demonstrates the use applicability of a hydrogel as a platform for combined local delivery of chondrocytes and an ADAMTS-targeting gapmer for catabolic gene modulation in OA.

1. Introduction

Osteoarthritis (OA) is the most common joint disorder in the aged population, and a leading cause of morbidity worldwide due to functional impairment and pain¹. Defined as a chronic and progressive disease of the whole joint, OA is predominantly characterized by cartilage degeneration, subchondral sclerosis, osteophyte formation, and inflammation of the synovial capsule^{1,308}. At the cellular level, OA is marked by an increased production of catabolic molecules leading to progressive and irreversible loss of collagen and aggrecan¹⁷. To date, disease modifying therapies remain unavailable, and OA treatment is limited to corticosteroid administration for pain relief and prosthetic replacement of the affected joints at an end stage^{1,3,5}. One feature correlated with pain and radiographic stage in OA patients is the presence of cartilage lesions of variable size³⁰⁹⁻³¹¹. These are generally a result of weakening of the joint and a factor highly associated with disease progression³¹². Such lesions may be a viable target for regenerative approaches. Autologous chondrocyte implantation (ACI), or MACI (matrix-assisted ACI) have shown to be effective in repair of focal lesion of the cartilage after joint trauma, but such approach will not be viable in the OA joint, as long as both the transplanted cells and those in the neighboring tissue are in a permanently catabolic state³¹³.

Among the major catabolic factors in OA, the matrix degrading ADAMTS (a disintegrin and metallo proteinase with thrombospondin motifs) family, in particular ADAMTS4 and ADAMTS5, were shown to be instrumental in the degenerative events that lead to OA^{314,315}. These enzymes are known to be synthesized not only by chondrocytes but also other joint tissues, such as the synovium³¹⁶. Inhibition of these proteases prevented degradation both in human cartilage explants^{315,317,318} and in animal models of OA, even reversing cartilage degeneration³¹⁹⁻³²¹. Hence, their inhibition is a promising therapeutic approach in OA. Nevertheless, non-specific small molecule drugs can cause side effects upon systemic administration and are, even if administered locally, rapidly cleared resulting in reduced duration of action¹¹.

Gene silencing strategies have shown great potential in overcoming these setbacks⁵⁵. However, the efficiency of small interfering RNAs is dependent on viral or non-viral vectors for cellular internalization, which can pose additional issues regarding toxicity^{55,322}. In this regard, locked nucleic acid (LNA)-modified gapmers are a particularly attractive alternative. Gapmers are single stranded antisense oligonucleotides (ASOs) composed by a central block of DNA flanked by modified nucleotides⁶². Once inside the cell, gapmers arrest protein translation by activation of RNase H1-mediated messenger RNA (mRNA) cleavage or steric hindrance of the splicing or translational machinery⁵⁴. The presence of LNAs together with phosphorothioate (PS) backbone modifications confer improved stability and resistance to endonuclease degradation, hence improving the pharmacokinetic profiles^{62,63}. Together with the smaller size of the molecule, these modifications are thought to promote unassisted cellular internalization by a process denominated "gymnosis"^{56-59,323}.

Even though chemical modifications of ASOs have been shown to enhance silencing

potency and pharmacokinetic profiles with concomitant prolongation of effects⁵⁴, rapid systemic clearance may still reduce longevity of therapeutic efficacy. Additionally, intravenous administration might further limit drug bioavailability in avascular tissues such as cartilage. Hence, direct intra-articular administration in controlled release systems can minimize systemic side-effects while allowing for a higher and prolonged bioavailability of the therapeutics in the joint environment^{11,324}. Biomaterial carriers, such as hydrogels, are ideally suited as local sustained release reservoir for drugs^{11,324-326}.

We hypothesize that the combination of chondrocytes and ASOs in a hydrogel scaffold for re-surfacing and treatment of focal lesions in OA joints will provide prolonged inhibition of ADAMTS expression both in transplanted chondrocytes and surrounding joint tissue cells. Ultimately, this treatment strategy targets OA by sustained silencing of OA-related genes in combination with cell therapy for regeneration. Here, we show proof of principle for this approach by using a fibrin (F) and hyaluronic acid (HA) hydrogel (F:HA) as a platform for combined delivery of cells and an ADAMTS5-targeting ASO in a novel in vitro system mimicking chondrocyte delivery for cartilage resurfacing and its interaction with surrounding native joint tissues exposed to a pro-inflammatory environment.

2. Materials and methods

2.1 Materials

The F:HA hydrogel at a ratio of 3.2:1 was manufactured and provided by ProCore Bio-med Inc. (Israel), at final concentrations of 6.21 and 1.94 mg/mL of fibrinogen and HA, respectively. ASOs sequences were designed by JW and YC and purchased from Eurogentec (Netherlands).

All ASOs were synthesized as all-phosphorothioate linked sequences except for the Cy5-labeled gapmer, which was synthesized as an all-phosphorodiester sequence (Table 1). The golden standard siRNA was used as a control. Previously described siRNA sequences targeting ADAMTS5 and β -catenin interacting protein 1 (CTNNBIP1) were purchased from Eurogentec (Table 1)^{315,327}. CTNNBIP1 was shown to be a potential off-target of ASO3.

Table 1. ASOs and siRNA sequences

ASO ID	Nucleotide sequence	Length
ASO 1 (non-targeting)	5'-IT ⁺ IA ⁺ IG ⁺ dC ⁺ dC ⁺ dT ⁺ dG ⁺ dT ⁺ dC ⁺ dA ⁺ dC ⁺ dT ⁺ dT ⁺ IC ⁺ IT ⁺ IC ⁺ 3'	16
ASO 2	5'-IA ⁺ C ⁺ IT ⁺ T ⁺ dT ⁺ dT ⁺ dA ⁺ dT ⁺ dG ⁺ dT ⁺ dG ⁺ dG ⁺ dG ⁺ IT ⁺ IT ⁺ IG ⁺ IC ⁺ 3'	17
ASO 3	5'-C ⁺ IT ⁺ IT ⁺ dT ⁺ dT ⁺ dA ⁺ dT ⁺ dG ⁺ dT ⁺ dG ⁺ dG ⁺ dG ⁺ IT ⁺ IT ⁺ IG ⁺ 3'	15
ASO 4	5'-IG ⁺ IA ⁺ IG ⁺ dA ⁺ dG ⁺ dA ⁺ dA ⁺ dA ⁺ dG ⁺ dT ⁺ dA ⁺ dG ⁺ aT ⁺ aT ⁺ IG ⁺ 3'	15
Cy5-ASO	5'-Cy5-ICITITdTdTdAdTdGdTdGdGdGITTIG 3'	15
Anti-ADAMTS5 siRNA	Sense strand 5'-AAGAUAGCGCUAAUGUCUU 3' Anti-sense strand 5'-AAGACAUUAGCGCUUUCUU 3'	21
Anti-CTNNBIP1 siRNA	Sense strand 5'-GALUGGAUCAACCGUGACA 3' Anti-sense strand 5'-JGUCAGGUUGAUCCCAUC 3'	19

I⁺ denotes for locked nucleotide bases. T⁺ denotes for phosphorothioated DNA bases. "d" denotes for DNA nucleotides.

2.2 Cell isolation and culture

Human articular chondrocytes were isolated from articular cartilage from patients with OA undergoing total knee arthroplasty. The anonymous use of redundant tissue for research purposes is part of the standard treatment agreement with patients in the University Medical Center Utrecht and was carried out under protocol n° 15-092 of the UMCU's Review Board of the BioBank. Chondrocytes were isolated by mincing and subsequently digesting the cartilage overnight at 37°C in Dulbecco's Modified Eagle's Medium Glutamax (DMEM, Thermo Fischer Scientific) supplemented with 0.15% (w/v) type II collagenase (Worthington Biochemical Corporation), 10% (v/v) Fetal Bovine Serum (FBS, Biowest) and 100 U/mL penicillin and streptomycin (Gibco).

Undigested debris were removed using a 70 µm cell strainer followed by a PBS wash. Cells were subsequently plated and grown in a humidified incubator at 37°C with expansion medium consisting of DMEM supplemented with 10% FBS, 0.2 nM ascorbic-2-phosphate (Sigma-Aldrich), 100 U/mL penicillin and streptomycin and 10 ng/mL basic fibroblast growth factor (bFGF, R&D Systems). Medium was renewed every 3 days. Cells were expanded until passage one and either frozen or further expanded and used for experiments at passage 2.

2.3 Gene knockdown in monolayer

The four different ASOs were tested in order to choose the most potent one resulting in sufficient silencing of ADAMTS5. Human articular chondrocytes were plated at a density of 1×10^5 cells per well in 24-well plates and grown in DMEM containing 100 mg/mL of penicillin and streptomycin, 0.2 nM Ascorbic-2-Phosphate, 1x Insulin-Transferrin-Selenium-Ethanolamine (ITS-X, Thermo Fischer Scientific) and 50 ng/mL L-proline (Sigma-Aldrich) for 24h in a humidified incubator at 37°C and 5% CO₂. Gappers were diluted in medium and added to the cells at a final concentration of 1 µM. Cells were cultured for an additional 72h and expression levels of ADAMTS5 were determined by Real-Time PCR (qPCR). Fold-change in gene expression was evaluated compared to non-treated cells as described in section 2.10. For screening experiments, the housekeeping gene 18S was used for normalization of ADAMTS5 expression.

Cytotoxicity of the gappers was determined by measuring cellular lactate dehydrogenase (LDH) release using the Cytotoxicity Detection KitPLUS (Roche) according to the manufacturer's instructions. Culture media were collected 24h after adding the ASOs to the cells. The LDH activity in culture supernatant was measured at 490 nm and 680 nm with a Benchmark Microplate reader (Bio-Rad). Viability of cells transfected with ASOs was calculated according to the manufacturer's instructions.

A similar experiment was set up to evaluate the effect of siRNA-mediated CTNNBIP1 silencing on ADAMTS5 expression. Cells were cultured as described above, transfected with anti-CTNNBIP1 siRNA (20 nM) and Lipofectamine RNAiMAX (Thermo Fischer Scientific) and further cultured for 72h. Gene expression analysis of ADAMTS5 and CTNNBIP1 was performed as described above.

2.4 Dose response of gapmer-mediated ADAMTS5 silencing in TNF- α /OSM-stimulated OA chondrocytes

Human articular chondrocytes were plated at a density of 1×10^5 cells per well in 24-well plates and grown in DMEM medium containing 100 U/mL of penicillin and streptomycin, 0.2 nM ascorbic-2-phosphate, 50 ng/mL L-proline in a humidified incubator at 37°C, 5% CO₂. After 24h tumor necrosis factor alpha (TNF- α) (10 ng/mL) and oncostatin M (OSM) (1 ng/mL) were added to the cells at concentrations of 10 and 1 ng/mL, respectively, to provide pro-inflammatory stimuli and thereby mimic a catabolic environment and enhancing ADAMTS5 expression.

Gapmer 3 was added to the cells at concentrations of 100, 250, 500 and 1000 nM. As a positive control, anti-ADAMTS5 siRNA (20 nM) was added to the cells using Lipofectamine RNAiMAX according to the manufacturer's instructions. The non-targeting sequence ASO 1 was added at a concentration of 1000 nM as a negative control. Cells were cultured for an additional 72h and expression levels of ADAMTS5 and 18S (housekeeping gene) were determined by qPCR. Fold-change in gene expression was evaluated relatively to non-treated cells.

2.5 Release profiles

To investigate the loading efficiency of the F:HA hydrogel and assess the gapmer-release profiles, Cy5-labeled gapmer was incorporated in 150 and 300 μ l of F:HA hydrogel at concentrations of 1 and 5 μ M. After mixing the hydrogel and gapmer solutions, 10 μ l of human thrombin (50 U/mL) in 1M CaCl₂ were added, followed by a 40-minute incubation at 37°C in a 5% CO₂ humidified incubator to allow polymerization. Hydrogels were then washed with DMEM medium and fluorescence was measured using Fluoroskan Ascent FL fluorometer (Thermo Fischer Scientific) with an emission/excitation pair of 620/670 nm. DMEM medium was used as release buffer. After t₀, hydrogels were incubated in 1 mL release buffer at 37°C in 5% CO₂ humidified incubator. At every timepoint, release buffer was completely removed, and new buffer added. Fluorescence in the medium was measured immediately after collection at the different timepoints up to 14 days. Loading efficiency of the gapmer on the hydrogels was calculated based on the initial amount of gapmer mixed in the hydrogel minus the non-incorporated gapmer removed during washing. The incorporated amount was then considered as 100% for the subsequent release measurements.

Release was calculated based on a standard curve (10 nM to 1000 nM) of Cy5-gapmer prepared at t₀. The series of samples composing the standard curve were incubated together with the hydrogels for the whole experiment, and samples were taken at every timepoint to account for decrease of fluorescence of the Cy5 label over time.

One hydrogel was harvested at day 3 and processed for analysis of gapmer distribution. The hydrogel was fixed in 4% formalin for 10 min followed by 5% PBS-BSA blocking for 30 min. Subsequently, the hydrogel was incubated for 1h at room temperature with 2 μ g/ml anti-fibrinogen antibody (DAKO). Then, Alexa Fluor® 488-labeled secondary

antibody rabbit anti-goat (Thermo Fischer) was added at a concentration of 8 $\mu\text{g/ml}$ and incubated for 1h at room temperature. Between each step, the samples were washed three times with PBS containing 0.05% Tween. Samples were imaged with a Leica SP8X (Leica) confocal microscope. Image processing and analysis was performed using Fiji (National Institutes of Health, Bethesda, USA) software version 1.50³²⁸.

2.6 Gapmer delivery in hydrogel culture

A 3D in vitro model composed of two separate hydrogel constructs was established (Figure 1): the top hydrogel containing OA chondrocytes (mimicking therapeutically “delivered cells”) and gapmers, and the bottom hydrogel containing OA chondrocytes only to represent “resident cells”. The top hydrogel was prepared by mixing 150 μl of F:HA hydrogel, 10 μl of cell suspension (2.5×10^5 cells) and 7.5 μl of ASO solution (final concentration 0.1 to 5 μM) in a 2 mL Eppendorf tube, whereas the bottom hydrogel was prepared by mixing the same hydrogel volume with 10 μl of cell suspension (2.5×10^5 cells) in a 48-well plate. For polymerization, thrombin (50 U/mL) was added to the hydrogels followed by incubation at 37°C for 30 min. After polymerization the top hydrogel was transferred to the 48-well plate upon addition of 1 mL of culture medium. This set-up was used for subsequent experiments.

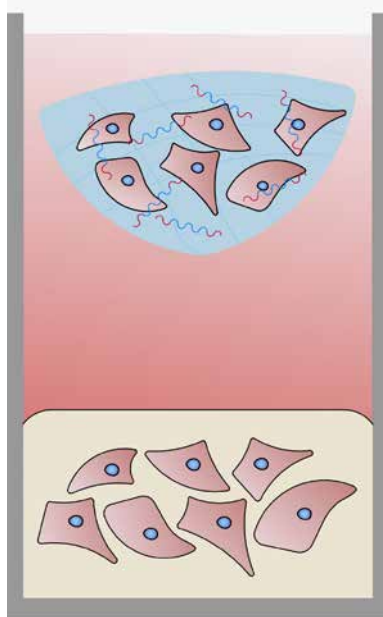


Figure 1. Scheme of two-hydrogel in vitro model. Top hydrogel containing ASOs and OA chondrocytes (mimicking therapeutically “delivered cells”). Bottom hydrogel containing OA chondrocytes only (“resident cells”)

2.7 Diffusion and transfection studies

For quantitative assessment of gapmer-cell association, the in vitro model described above was cultured for 3 days with 0.1 and 1 μM Cy5-labeled gapmer in the top hydrogel. Upon harvesting the hydrogels were digested separately and processed for flow cytometry analysis. Digestion was carried out at 37°C for 20 min using 0.25% (w/v) trypsin (25200056, Thermo Fischer Scientific), followed by filtration through 0.22 μm filters (Merck) to remove hydrogel debris. The cell suspension was centrifuged and resuspended (2 \times) in ice-cold PBS and stained with 100 ng/mL DAPI for 5 min, staining debris, and apoptotic and dead cells as an additional parameter for population gating. DAPI excess was removed by washing the cells in ice-cold PBS. Finally, cells were resuspended in a flow cytometry buffer (2% BSA, 2 mM EDTA, and 25 mM HEPES) and analyzed using a FACSCanto II (BD Biosciences) flow cytometer for DAPI (FL1 channel: 405 nm excitation laser, 450/40 BP filter) and Cy5 (FL2 channel: 633 nm excitation laser; 620/20 BP filter). Cell doublets and debris were gated out based on forward (FSC) and side (SSC) scatters. DAPI-negative cells were then analyzed for their Cy5 intensity. Ten thousand events were acquired, and data were further analyzed using FlowJo (TreeStar) software version 10.0. Experiment was performed in triplicate (n=3).

Furthermore, confocal microscopy was performed to assess gapmer diffusion to the bottom hydrogel and transfection of embedded cells. The experimental set up was the same as described above. At the endpoint the hydrogels were washed twice with PBS and fixed in formalin for 1h, followed by DAPI stain (100 ng/mL) for 1h to ensure full thickness staining. Samples were imaged axially with a Leica SP8X (Leica) confocal microscope and a 20x objective. Image processing and analysis was performed using Fiji (National Institutes of Health, Bethesda, USA) software version 1.50³²⁸.

2.8 Subcellular localization of gapmers

To assess subcellular localization of the gapmers, the in vitro model was used with a gapmer concentration of 1 μM in the top hydrogel and cultured for 3 days. At the endpoint, digestion of the hydrogels was carried out at 37°C for 20 min using trypsin, as described previously. Subsequently, the cells were plated in Cellview™ dishes (Greiner Bio-one) and cultured for 24h to allow cell attachment.

Cells were fixed in 4% formalin for 10 min, followed by permeabilization with 0.2% PBS-Triton for 20 min. Blocking was performed using 5% PBS-BSA for 30 min followed by 1h incubation at room temperature with 1.25 $\mu\text{g}/\text{ml}$ anti-EEA1 (610456, BD Biosciences) or 1.5 $\mu\text{g}/\text{mL}$ anti-LAMP1 (H4A3, DSHB) antibodies targeting early endosomes and lysosomes, respectively. Subsequently, Alexa Fluor® 488-labeled secondary antibody goat anti-mouse (Thermo Fischer) was added at a concentration of 8 $\mu\text{g}/\text{ml}$ and incubated for 1h at room temperature. Cells were counterstained with 2.5 $\mu\text{g}/\text{mL}$ Phalloidin-TRITC (Sigma-Aldrich) and 100 ng/mL DAPI for 1 hour. Between each step, cells were washed three times with 0.05% PBS-Tween. Images were acquired using a Leica SP8X confocal microscope (Leica) and 63 \times /1.4 oil-immersion objective. Image processing and analysis was performed using Fiji (National Institutes of Health, Bethesda, USA) software version 1.50³²⁸.

2.9 ADAMTS5 silencing in TNF- α /OSM-stimulated OA chondrocytes

To evaluate the silencing efficiency of the gapmer, the in vitro model was cultured for 7 and 14 days. ASO 1, 3 or anti-ADAMTS5 siRNA were embedded in the top hydrogel at concentrations of 5 (7 and 14 days) and 10 μ M (14 days). After polymerization, the hydrogels were incubated with DMEM supplemented with 5 μ M ϵ -aminocaproic acid (Sigma-Aldrich) to delay fibrin degradation³²⁹, 10 ng/mL recombinant human TNF- α and 1 ng/mL OSM. Medium was replaced twice a week and hydrogels were harvested for downstream analysis at days 7 and 14. The expression of ADAMTS5 and the housekeeping genes GAPDH, RPL19 and SDHA were measured by qPCR. ADAMTS4 expression was analyzed as a control for off target effects. Cells embedded in top and bottom hydrogels were analyzed individually.

2.10 RNA isolation and qPCR

Total RNA was isolated in TRIzol Reagent (Invitrogen) according to the manufacturer's instructions. RNA was dissolved in DNase/RNase-Free water (Qiagen). Total RNA (200 ng-500 ng) was converted to cDNA by High Capacity cDNA Reverse Transcription Kit (Thermo Fischer Scientific) using an iCycler Thermal Cycler (Bio-Rad) according with the manufacturer's instructions. Real-time PCR reactions were performed using the iTAQ SYBR Green Reaction Mix Kit Mastermix (Bio-Rad) reaction kit according to the manufacturer's instructions in an iCycler CFX384 Touch thermal cycler (Bio-Rad). Reactions were prepared in 10 μ l total volume with 0.92 μ l PCR-H₂O, 0.04 μ l forward primer (0.4 μ M), 0.04 μ l reverse primer (0.4 μ M) and 5 μ l iTAQ SYBR Green Reaction Mix (BioRad) to which 4 μ l of fifty times diluted cDNA was added as template. Expression of ADAMTS5, ADAMTS4, CTNBP1 and the housekeeping genes glyceraldehyde 3-phosphate dehydrogenase (GAPDH), ribosomal protein L19 (RPL19) and succinate dehydrogenase complex subunit A (SDHA) were analyzed by a three-step amplification qPCR. As mentioned above, for screening experiments, 18S was used as housekeeping gene. Data analysis and Cq values were obtained with a Bio-Rad CFX Manager 3.1 (Bio-Rad). Details of primers used in real-time PCR are listed in Table S1. The amplified PCR fragment extended over at least one exon border. In order to generate relative gene expression, the Pfaffl method was used to account for differences in primer efficiencies³³⁰.

2.11 Statistical analysis

All data were analyzed using IBM® SPSS® Statistics version 21. Data were all normally distributed but violated the assumption of homogeneity of variances. One-way analysis of variance (One-way ANOVA) was used together with Welch test for the equality of the means. Post-hoc comparisons across groups were carried out using the Games-Howell post-hoc test. All the biological experiments were performed in three different donors (n=3). For every condition 4 biological replicates were used.

3. Results

3.1 Selection of anti-ADAMTS5 ASO sequences in 2D chondrocyte culture

A set of 3 gapmers (ASOs 2, 3 and 4) targeting human ADAMTS5 were designed and screened for ADAMTS5 silencing. At 1000 nM, gene silencing was shown to be higher for all donors with ASO 3, with above 10-fold (>90%) knockdown (Figure 2a). In contrast, ASOs 2 and 4 did not mediate significant ADAMTS5 silencing in comparison with non-treated cells. A non-targeting gapmer was used as a negative control (ASO 1) and did not significantly affect the expression of ADAMTS5. Based on this preliminary screening, ASO 3 was selected for subsequent experiments with ASO 1 used as a negative non-targeting control.

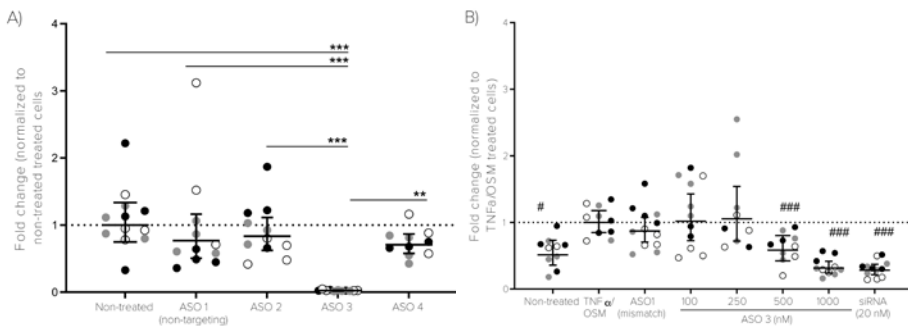


Figure 2. ASO-mediated ADAMTS5 silencing in primary human OA chondrocytes. a) ASO sequence validation. ADAMTS5 expression levels in primary human OA chondrocytes 72h after treatment with 1000 nM of different ADAMTS5-targeting ASO sequences. b) Dose response to different concentrations of ASO 3. ADAMTS5 expression levels in TNF- α /OSM-stimulated primary human OA chondrocytes 72h after treatment with different concentrations of the “best-performing” sequence (ASO 3). ASO 1 (non-targeting) and anti-ADAMTS5 siRNA were used as negative and positive controls, respectively. Data are presented geometric mean (mid-line) and 95% confidence interval (CI). Black: Donor 1; White: Donor 2; Gray: Donor 3. * represents statistically significant differences as depicted; # represents statistically significant differences to the TNF- α /OSM group; (*p < 0.05, **p < 0.01 and ***p < 0.001)

Gapmer-mediated silencing of TNF- α /OSM-stimulated ADAMTS5 expression by OA chondrocytes was then investigated. Similar to siRNA, the gapmer sequence was shown to promote a 4-fold decrease in ADAMTS5 at a concentration of 1000 nM. (Figure 2b). Silencing was also observed at a concentration of 500 nM. The non-targeting gapmer ASO 1 did not alter ADAMTS5 expression. Additionally, none of the concentrations were shown to be cytotoxic as measured by LDH release (Figure S1).

3.2 Release kinetics

Gapmer incorporation efficiency, measured immediately after polymerization and washing, was shown to be around 93% for all conditions (Figure 3a, Table S1). All formulations displayed similar release profiles, characterized by a burst release of 50% of the cargo within the first 24h, followed by a gradual and sustained release until day 14.

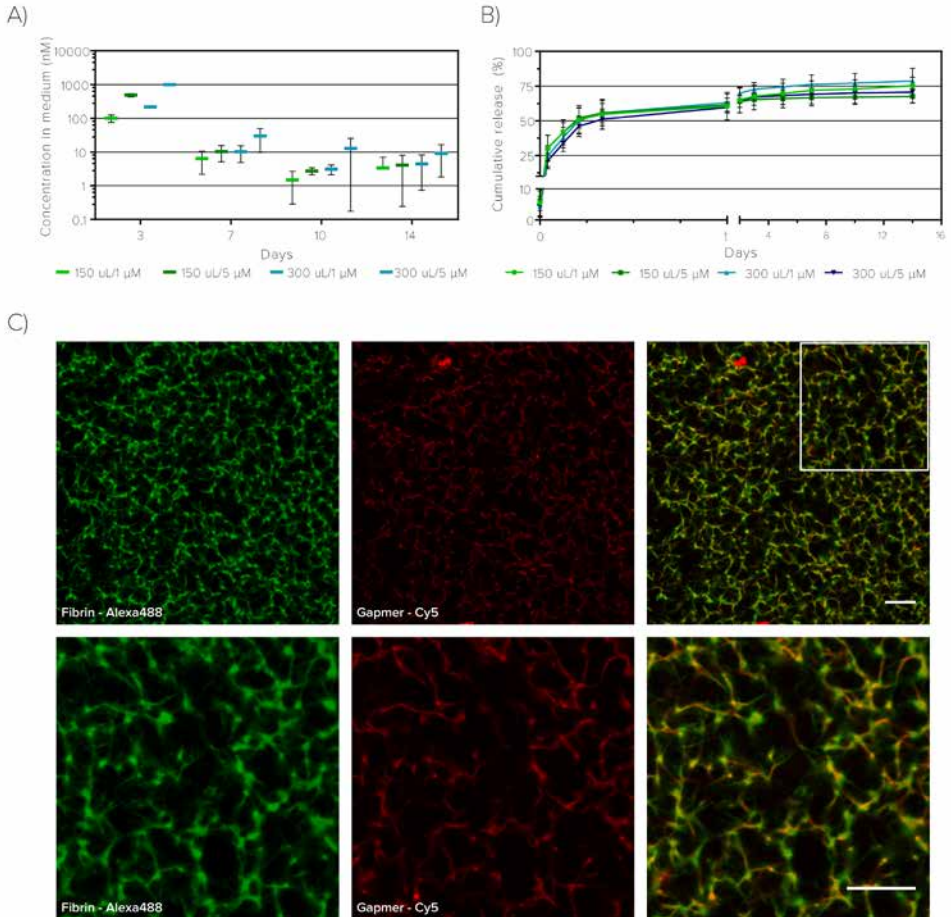


Figure 3. Gapmer release profiles. a) Cumulative release profiles of different hydrogel/gapmer formulations. b) Gapmer concentration in the medium. Different concentrations of Cy5-labeled ASO (1 and 5 μ M) were incorporated into different F:HA hydrogel volumes (150 and 300 μ l). c) Co-localization of fibrin strands with gapmers. Fibrin was detected using an anti-fibrin antibody and an Alexa Fluor® 488-labeled secondary antibody. Hydrogels were imaged using a confocal microscope. Bottom row represents a zoomed in picture of top row (white square). Scale bar: 10 μ m.

At day 14, 25-30% of the gapmer was still incorporated for all the tested formulations. The release during the first three days, gave rise to concentrations in the media of 100, 500, 200 and 1000 nM for the 150 μ l/1 μ M, 150 μ l/5 μ M, 300 μ l/1 μ M and 300 μ l/5 μ M hydrogel/gapmer formulations, respectively (Figure 3b). Confocal imaging of the hydrogel/gapmer system at day 3 showed co-localization of the gapmer with the fibrin fibers, indicating possible interaction between the two molecules (Figure 3c). This may explain the prolonged retention of the remaining 25-30% of gapmer inside the hydrogels. For subsequent 3D cell construct experiments, the formulations with 150 μ l of hydrogel were used.

3.3 Gapmer diffusion and transfection of chondrocytes in 3D structures

To evaluate gapmer diffusion from the hydrogel and subsequent entry into neighboring structures, a Cy5-gapmer-loaded hydrogel with chondrocytes was co-cultured for 3 days together with another hydrogel containing only chondrocytes. At day 3, the gapmer had diffused and penetrated into the adjacent hydrogel as shown by confocal microscopy (Figure 4a). Co-localization was observed for DAPI and Cy5 signals, suggesting partial cellular accumulation of the released gapmer. Line-scan analysis further corroborated these findings. Histograms of the intensity profiles for DAPI and Cy5 confirmed the peak overlap for both signals (Figure 4b).

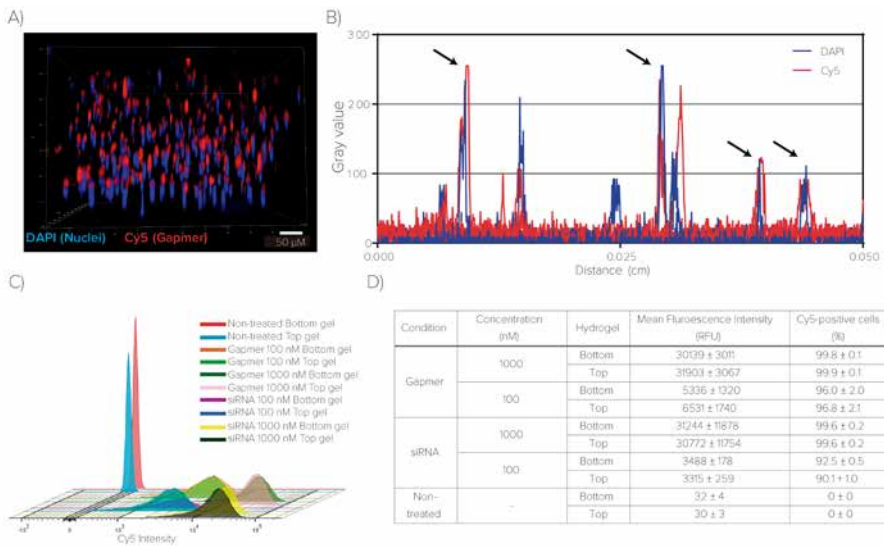


Figure 4. Gapmer diffusion and cellular association. a) 3D reconstruction of 350 μm of the bottom hydrogel 72h after culture with Cy5-labeled gapmer in the top hydrogel. Blue: DAPI, Red: Cy5. b) Line-scan analysis of intensity profiles for DAPI and Cy5. c) Representative flow cytometric analysis of OA chondrocytes cultured in the bottom and top hydrogels in the presence of 100 and 1000 nM gapmer or siRNA. d) Mean Fluorescence intensity and percentage of Cy5-positive cells.

For a more quantitative assay, a similar experimental set up was used at two different concentrations of Cy5 labeled gapmer (100 and 1000 nM). After 3 days of culture, hydrogels were digested and cells were processed for flow cytometry. As a control, hydrogels loaded with equal concentration of Cy5 labeled siRNA were taken along. The percentage of Cy5-positive cells was above 95% for all the ASO conditions and did not change significantly with gapmer concentration (Figures 4c and 4d). A ten-fold increase in the mean fluorescence intensity is observed with the 1000 nM concentration compared with the 100 nM condition. Hydrogels containing siRNA showed similar patterns of fluorescence intensity and Cy5-positive cells.

3.4 Subcellular localization

As flow cytometry does not discriminate between association with the cell membrane or intracellular location, both hydrogels were digested, followed by plating of the cells in monolayer. Confocal imaging of the cells showed that the gapmer was located intracellularly and co-localized with lysosomes in cells from both top and bottom hydrogels (Figure 5). No intracellular co-localization was found for siRNA, indicating the positivity observed in flow cytometric analysis was likely due to membrane association rather than internalization. The gapmer did not co-localize with early endosomes as shown by using a marker for early endosomes (EEA1) (Figure S2). Gapmer accumulation in other vesicular structures other than lysosomes was suggested by punctate staining in structures negative for EEA1. Although intra-cellular trafficking may have been affected by the presence of PS modifications, co-localization using a PS ASO-Cy5 sequence was shown to be the same as the colocalization of the phosphodiester sequence (Figure S3)

3.5 Gapmer-mediated silencing of ADAMTS5 in 3D cell constructs

Silencing of ADAMTS5 in primary human OA chondrocytes upon TNF- α /OSM stimulation was assessed in the two-gel system. After day 7, ASO treatment induced a 2.5- (60%) and 3.3-fold (70%) decrease in ADAMTS5 expression levels in the bottom and top hydrogels, respectively ($p < 0.001$, Figures 6a and 6b).

At day 14, inhibition of ADAMTS5 was also observed. A 35% reduction in ADAMTS5 expression was observed in the bottom hydrogel (Figure 6c), whereas a 45% silencing was observed for the top hydrogel ($p < 0.01$, Figure 6d). Additionally, at a gapmer concentration of 10 μM , silencing appeared to increase to 50 and 55% in the bottom ($p < 0.05$) and top ($p < 0.001$) hydrogels, respectively. Both ASO 1 (non-targeting) and siRNA showed no knockdown of ADAMTS5 expression at any of the studied timepoints. None of the tested sequences affected the levels of ADAMTS4 gene expression (Figure S4). However, a trend was noted towards a knockdown of CTNBP1 by ASO 3 (Figure 7) at day 7, which was lost at day 14. Regardless, gapmer effect on ADAMTS5 expression was shown to be direct and not mediated through CTNBP1 activity, as was shown by siRNA-mediated silencing of the latter gene. (Figure S5).

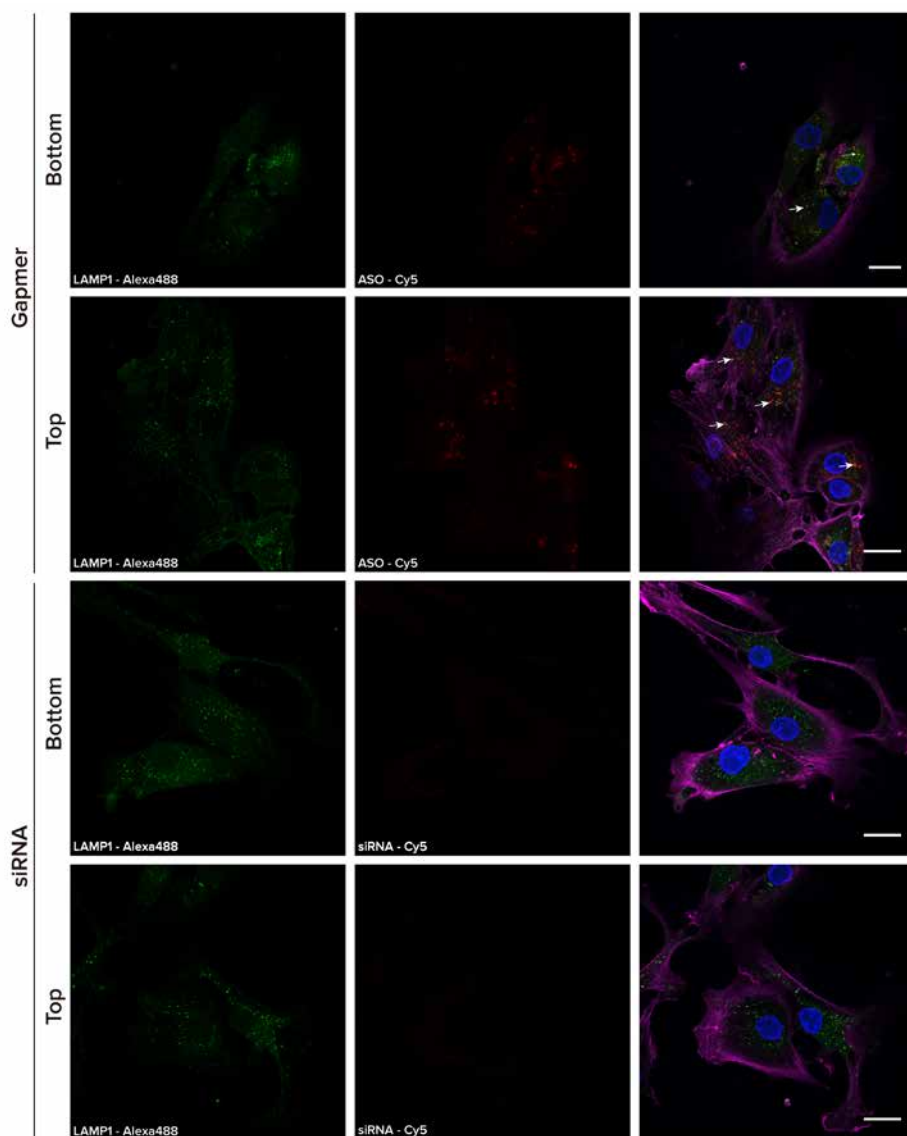


Figure 5. Co-localization of ASOs and siRNA. OA chondrocytes were harvested from both bottom and top F:HA hydrogels after 3 days of culture and plated in monolayer for 24h. Lysosomal staining was performed using an anti-LAMP1 primary antibody and an Alexa Fluor® 488-labeled secondary antibody. Cells were counterstained with DAPI and Phalloidin-TRITC. Green: LAMP1 (Lysosomes); Red: Cy5-gapmer/Cy5-siRNA; Blue: Nuclei; Purple: F-actin. White arrows indicate lysosomal co-localization. Scale bar: 20 μ m.

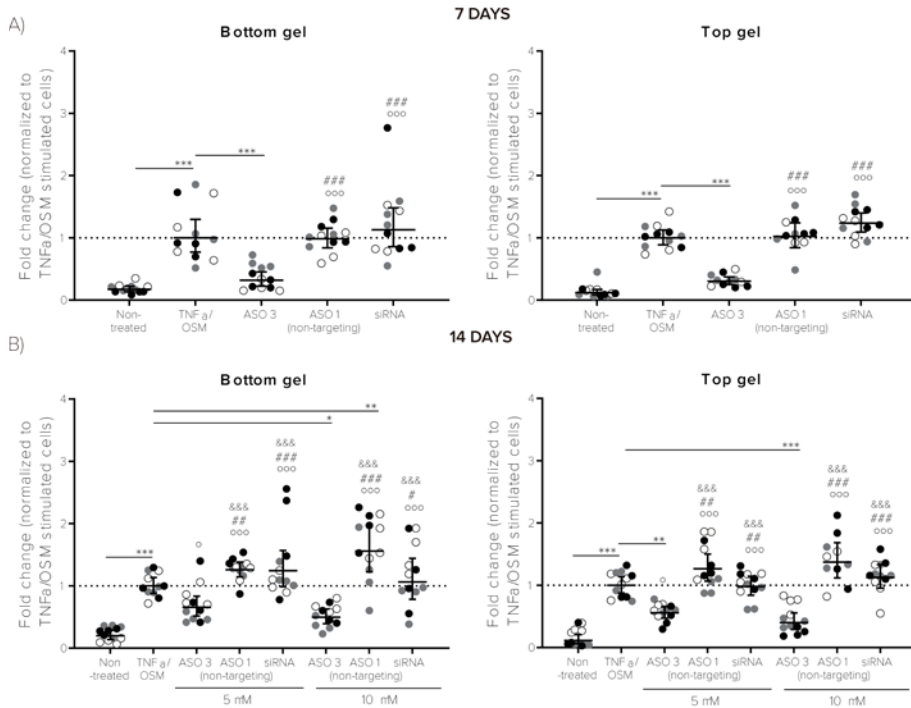


Figure 6. Long-term gapmer-mediated ADAMTS5 knockdown in 3D cell constructs. Fold change in ADAMTS5 gene expression in both top and bottom F:HA hydrogels after 7 (a) and 14 (b) days of culture. ASO and siRNA sequences were incorporated in the F:HA hydrogel together with human OA chondrocytes and co-cultured with a secondary F:HA hydrogel containing cells only. Data presented are geometric mean (mid-line) and 95% confidence interval (CI). Experiment was performed in 3 biological replicates. Individual data points are represented in the graphs. Black: Donor 1; White: Donor 2; Gray: Donor 3. * represents statistically significant differences to the TNF- α /OSM group; ° represents statistically significant differences to the non-treated group. (*p < 0.05, **p < 0.01 and ***p < 0.001)

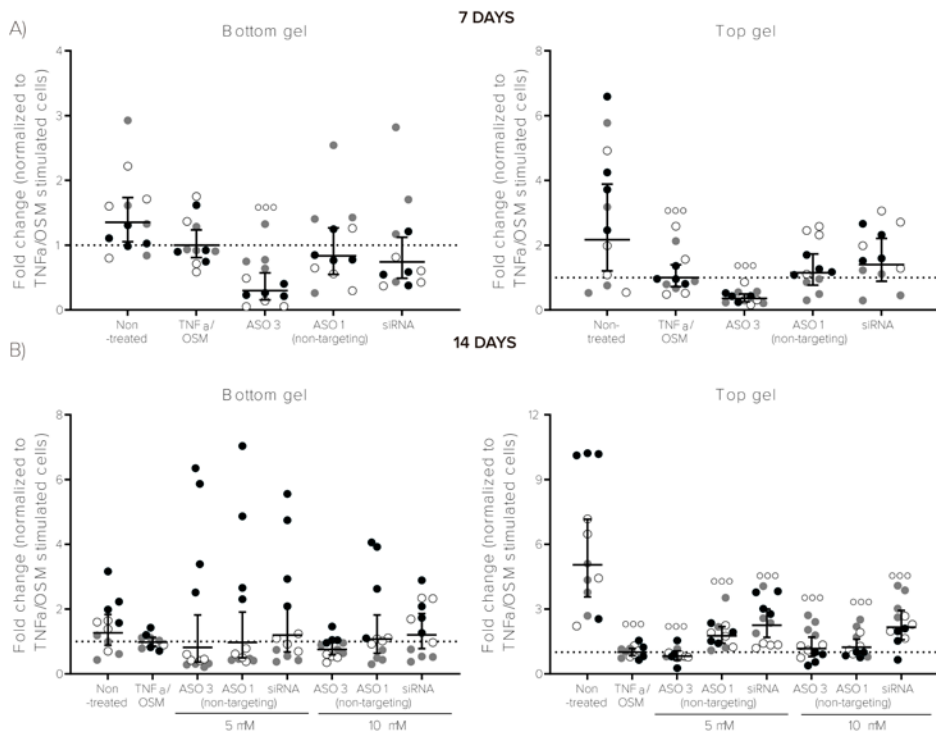


Figure 7. CTNNBIP1 expression. Fold change in CTNNBIP1 expression in both top and bottom F:HA hydrogels after 7 (a) and 14 (b) days of culture. ASO and siRNA sequences were incorporated in the F:HA hydrogel together with human OA chondrocytes and co-cultured with a secondary F:HA hydrogel containing cells only. Data presented are geometric mean (mid-line) and 95% confidence interval (CI). Experiment was performed in 3 biological replicates. Individual data points are represented in the graph. Black: Donor 1; White: Donor 2; Gray: Donor 3. ° represents statistically significant differences to the non-treated cells; (° $p < 0.05$, °° $p < 0.01$ and °°° $p < 0.001$)

4. Discussion

The ADAMTS enzyme family, in particular ADAMTS4 and ADAMTS5, play pivotal roles in proteoglycan degradation in OA, and inhibition of these molecules have proved to be beneficial for cartilage repair³¹⁴. Antisense technologies offer unprecedented advantages when compared to other small molecule drugs, due to their higher target specificity and duration of action associated with arrest or interference with translation. Modified ASO gapmers are especially attractive due to their enhanced stability and capacity for unassisted internalization that offers gene silencing without the necessity for a transfection agent, which may simplify clinical translation.

In this study, we show proof-of-concept for the feasibility of hydrogel-based delivery of cells and gapmers for long-term silencing of OA-related genes. For this purpose, we

established a culture model composed of two F:HA hydrogel constructs, one containing gapmers and OA chondrocytes mimicking a clinically implanted scaffold, and another one containing only OA chondrocytes mimicking resident joint cells. A sustained release for up to 14 days was found, with \approx 25% of the gapmer retained at day 14, most likely associated with fibrin binding. Similar release profiles were observed across all the formulations, suggesting the system is not yet saturated, and higher gapmer concentrations can further be incorporated. Furthermore, efficient ADAMTS5 knockdown in 3D constructs of OA chondrocytes was observed at days 7 and 14 for gapmer concentrations of 5 and 10 μ M.

The two other ASO sequences, although sharing the same targeting moiety, display significant differences in silencing activities. The differences are likely due to varying lengths and LNA composition, since one is 17-nucleotide long and has four flanking LNAs in comparison with the other 15-nucleotide ASO 3 contained three flanking LNAs. Even though counterintuitive, it has previously been shown that shorter ASOs with lower affinity can potentially perform better than longer ASOs with higher affinity for the same targeting site³³¹⁻³³³. This is attributed to diminished accessibility to the target region for the larger ASOs, or by an increased probability for the formation of secondary structures⁶³. Clearly, there is a trade-off reduction of off target effects by increasing gapmer length while maintaining its binding affinity to the target region (i.e. by lowering LNA content) might due to increased mismatched basepairs with the off-target region⁶³. Additionally, the number and type of chemical modifications to the backbone of the ASOs were also shown to play a role in silencing efficiencies^{331,333}. Altogether, these parameters are thought to affect the internalization capability of the ASOs, intracellular trafficking³³³, coupling and uncoupling to target mRNA before and after RNase H1 cleavage, as well as RNase H1 recruitment³³⁴. Hence, these findings show ASO design and respective modifications are crucial steps for an efficient antisense activity⁵⁶.

Additional validation of the most active gapmer was performed in TNF- α /OSM-stimulated OA chondrocytes mimicking thereby the inflammatory joint environment. The selected sequence was shown to produce efficient silencing at concentrations above 500 nM and to yield ADAMTS5 knockdown levels comparable to lipofectamine/siRNA control. The gapmer concentrations used in this study were efficient in the low micromolar range, as reported in other studies^{56,57,62,231}, in contrast to the 50-times lower concentrations required for siRNA. Yet the absence of transfection agents shows superiority of the gapmers over siRNAs, which corroborates previous studies on limited unassisted internalization of siRNAs³³⁵.

From a clinical perspective it is important that sustained local release of the therapeutic molecule is achieved^{11,324}. The F:HA hydrogel selected as a model system is currently being tested in clinical trials and fibrin and hyaluronic acid are already clinically used as cell carrier in surgical procedures^{336,337}, and in intra-articular injections for joint lubrication³³⁸, respectively. The combination of ASOs with delivery platforms allows for sustained and prolonged silencing of their target genes, decreasing matrix degradation rate and enhancing repair and regeneration of the damaged tissue by both transplanted and endogenous cells.

Upon incorporation in the F:HA hydrogel, a 14-day long release was observed and, at the endpoint, 25% of the gapmer remained within the hydrogel. It is worth noting that release experiments were performed in the absence of cells. The presence of cells within the hydrogel may have led to faster release profiles, due to higher degradation and contraction of the construct. However, upon implantation of the hydrogel within an articular focal lesion, diffusion would be limited mainly to the area exposed to synovial fluid, therefore, decreasing the surface-to-volume ratio, and theoretically, promoting a slower release. Gapmer retention at day 14 is likely due to electrostatic and/or hydrophobic interactions with fibrin strands, as previously demonstrated³³⁹. Hence, these results suggest that by varying fibrin and hyaluronic acid content, release kinetics can be further tuned.

The mechanisms by which gapmers are internalized are not fully understood yet, however some studies have proposed a two-step mechanism initiated by adsorption to the cell membrane, and subsequent internalization through multiple endocytic pathways^{57-59,323}. Here, LNA-based ASOs were shown to be able to penetrate into a secondary three-dimensional cell construct and transfect “resident” cells upon release from the delivery platform. High cellular association rates were observed for both ASO and siRNA sequences, yet confocal imaging confirmed that only ASOs were able to enter cells as seen by cytoplasmic localization and lysosomal co-localization. Gapmer accumulation upon “gymnotic” delivery was also observed in vesicular structures other than lysosomes, which may have represented the so-called P-bodies^{56,58,59}, perinuclear structures⁵⁸, or others as reported in previous studies.

To what extent the gapmers in the lysosomes and the unspecified cytoplasmic aggregates found were active is not completely clear. Additionally, RNase H1 is known to be present and mediate ASO-induced mRNA cleavage in both in cytoplasm and nuclei^{59,340}. Accordingly, the silencing and imaging results from the current study corroborate previous findings that nuclear localization is not required for effective ASO-mediated silencing^{56,58,59}. Additionally, the possibility of diffuse cytoplasmic distribution cannot be discarded.

After 1 week, effective silencing was found in both hydrogel constructs, suggesting proof of principle of delivery to adjacent tissues *in vivo*. Yet, relatively lower silencing was found after a longer period of time. Most likely, hydrogel loading and hence silencing can be optimized further, as was suggested by the effects of the higher loading. At the current release profiles, the highest loading applied would correspond to a maximum concentration in the lower range of non-toxic concentrations previously reported^{56,57,231}. In addition, TNF- α and OSM levels in synovial fluid of OA patients were shown to be within in the pg/ml range, hence at least 100-times lower than used in this study²⁴¹⁻³⁴³. Therefore, the 5-6 fold increase of ADAMTS5 expression observed in this study, which was shown to be only 2.4-fold in damaged cartilage area compared to healthy cartilage³⁴⁴, may have been more difficult to silence.

Upon checking for off target effects, ADAMTS4 was not silenced by the gapmer sequence used, but CTNBP1 expression did appear to be inhibited at day 7, although

statistical significance was not reached. CTNNBIP1 is a protein that negatively regulates the β -catenin/Wnt pathway by preventing interaction between β -catenin and transcription factor 4³⁴⁵. The ADAMTS5 silencing was not mediated by CTNNBIP1, as shown by the lack of effect on ADAMTS expression upon siRNA-mediated silencing of CTNNBIP1. To what extent the limited effects on CTNNBIP1 found here will affect cartilage metabolism is unclear, as little is known about the role of this gene in this tissue. However, the notion that overexpression of this gene in mice caused disorders in cartilage development³⁴⁶, may even suggest silencing may be beneficial.

Although the initially envisaged clinical application of the current system is cartilage resurfacing in OA joints, gapmer delivery can be extended towards other orthopedic applications. Acute and traumatic injuries to the knee such as meniscus tears, anterior cruciate ligament injury or cartilage defects are known to be major risk factors for the development of post-traumatic OA⁴¹, which is most likely related to the increased production of several MMPs, aggrecanases and pro-inflammatory cytokines^{34,35,347,348}. Indeed, ADAMTS4 activity was found to be a major predictor of postoperative outcome following (M)ACI for focal cartilage defect repair³⁴⁹. The use of the current hydrogel-gapmer construct may therefore also enhance the treatment outcome of joint traumas such as cartilage defects, either as add on to (M)ACI, or as cell free system in microfracture for smaller sized defects^{350,351}. Similarly, novel cell-based approaches towards meniscus repair could be enhanced using the current approach³⁵². Importantly, the use of gapmers allows for further tailoring of treatment by mere selection of the target to be silenced. For example, we previously showed the feasibility of an anti-COX2 gapmer-loaded chitosan/hyaluronic acid hydrogel as a strategy for targeted knockdown of the inflammatory enzyme COX2, in OA chondrocytes²³¹. Given the fact that OA is a very heterogeneous and multi-factorial disease, one can hypothesize that ASOs can be tailored in a patient-specific manner to target the most relevant genes.

Although the sequence described here may also affect CTNNBIP1, from a technological point of view this does not underplay the general applicability of this approach. From a clinical point of view the sequence used may even be more effective for this reason, although from a regulatory perspective a sequence targeting ADAMTS5 only may be preferable.

In this work, we successfully introduce the strategy of combined delivery of cells and LNA-modified ASOs in a hydrogel-based scaffold for long-term knockdown of OA-related genes. The long-term release and prolonged silencing renders the proposed system an attractive strategy for intra-articular delivery of both cells and ASOs. As the hydrogel has already been approved for the treatment of OA, it likely is an ideal candidate for use in combination with drug delivery.

5. Conclusion

In this study, we show proof-of-concept for the combined delivery of cells and ASOs in hydrogel-based scaffold as a potential therapeutic strategy for cartilage re-surfacing and silencing of OA-related genes. The F:HA hydrogel platform displayed a 14-days sustained release of the incorporated ASO, and allowed for ASO uptake by primary human OA chondrocytes after diffusion into the hydrogel. Moreover, efficient ADAMTS5 knockdown was found. Future studies will be focused on ex vivo evaluation of the potential of LNA-based ASOs as new therapeutic agents for modulation of OA-related genes.

Gene	Primer Sequence		Annealing Temperature (°C)	Product Size (bp)
ADAMTS5	Forward	5' GCCAGCGGATGTGTCAAGC 3'	63	130
	Reverse	5' ACACCTCCCGGACGCAGA 3'		
ADAMTS4	Forward	5' TCATCACTGACTTCTTGACAA 3'	61.5	83
	Reverse	5' GAAAGTCACAGGCAGATGCA 3'		
18S	Forward	5' GTAACCCGTTGAACCCATT 3'	57	151
	Reverse	5' CCATCCAATCGGTAGTAGCG 3'		
GAPDH	Forward	5' TGCACCACCAACTGCTTAGC 3'	62	87
	Reverse	5' GGCATGGACTGTGGTCATGAG 3'		
RPL9	Forward	5' ATGAGTATGCTCAGGCTTCAG 3'	64	150
	Reverse	5' GATCAGCCCATCTTTGATGAG 3'		
SDHA	Forward	5' TGGGAACAAGAGGGCATCTG 3'	58	86
	Reverse	5' CCACCACTGCATCAAATTCATG 3'		
CTNBP1	Forward	5' GTGCTGCTCATGCTCGGAA 3'	66	137
	Reverse	5' ACGTCCTCTGCACCCCTGGTC 3'		

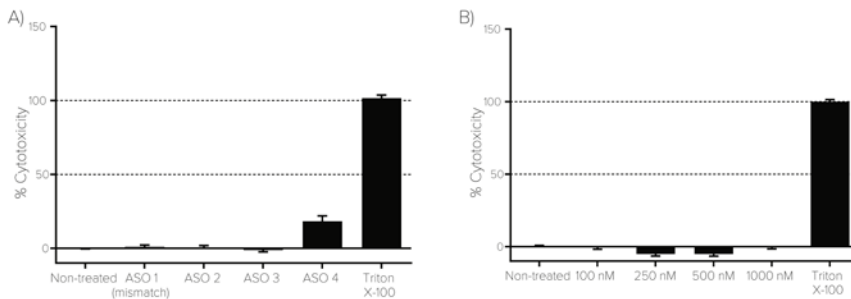


Fig. S1. ASOs cytocompatibility. LDH activity and release were measured upon 3 days incubation of OA chondrocytes with the gapmer sequences. Lysis buffer (0.2 % Triton X-100) was added as positive control for total cell death. a) Cytotoxicity of the different gapmer sequences at a concentration of 1 μ M. b) Cytotoxicity of the ASO 3 at different concentrations. Data are normalized to the non-treated group. Data are presented as mean \pm SD.

Table S2. Incorporation efficiency for gapmer-loaded hydrogels

Hydrogel formulation	Incorporation efficiency (%)
150 μ l/1 μ M	94.4 \pm 6.0
150 μ l/5 μ M	93.9 \pm 4.5
300 μ l/1 μ M	95.7 \pm 4.8
300 μ l/5 μ M	96.0 \pm 4.1

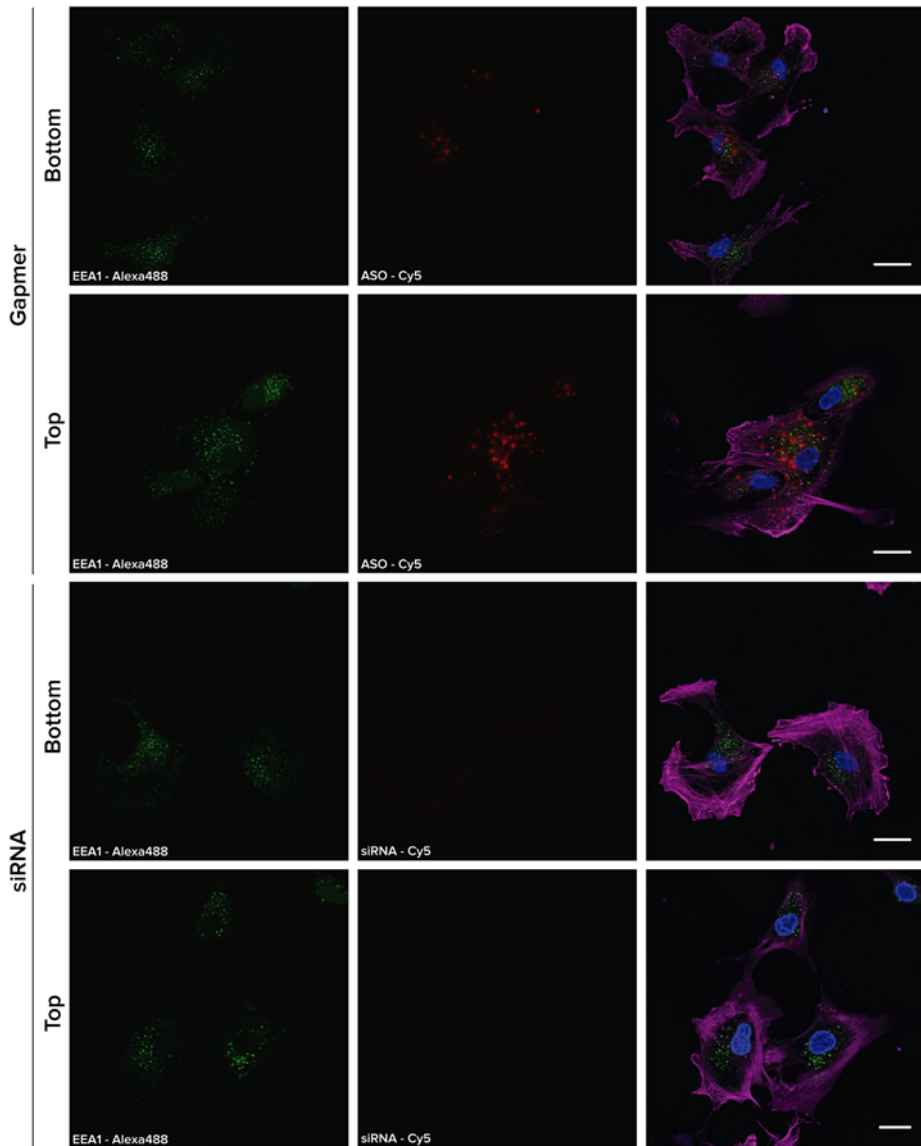


Fig. S2. Intra-cellular co-localization of ASOs and siRNA. OA chondrocytes were harvested from both bottom and top F:HA hydrogels after 3 days of culture and plated in monolayer for 24h. Endosomal staining was performed using an anti-EEA1 primary antibody and an Alexa488-conjugated secondary antibody. Cells were counterstained with DAPI and Phalloidin-TRITC. Green: EEA1 (Lysosomes); Red: Cy5-gapmer/Cy5-siRNA; Blue: Nuclei; Purple: F-actin. Scale bar: 20 μ m.

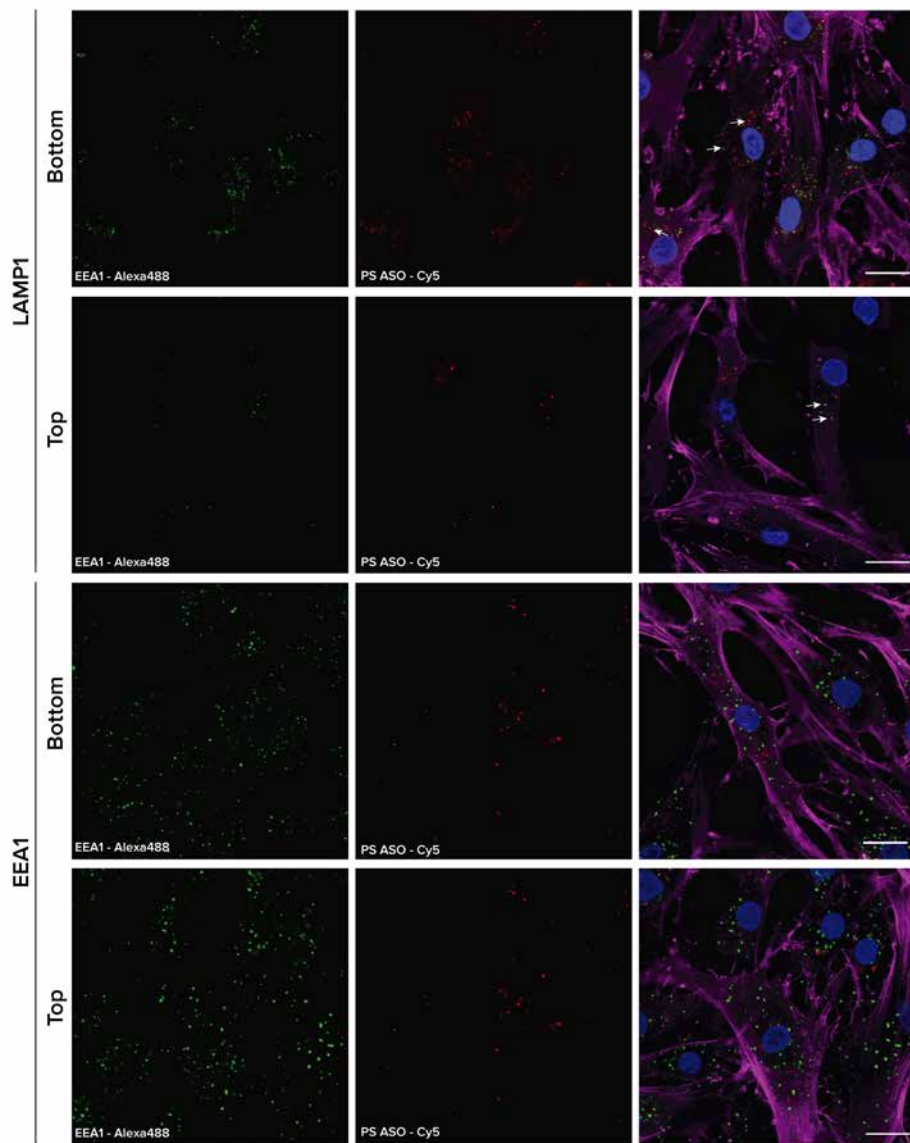


Fig. S2. Intra-cellular co-localization of ASOs and siRNA. OA chondrocytes were harvested from both bottom and top F:HA hydrogels after 3 days of culture and plated in monolayer for 24h. Endosomal staining was performed using an anti-EEA1 primary antibody and an Alexa488-conjugated secondary antibody. Cells were counterstained with DAPI and Phalloidin-TRITC. Green: EEA1 (Lysosomes); Red: Cy5-gapmer/Cy5-siRNA; Blue: Nuclei; Purple: F-actin. Scale bar: 20 μ m.

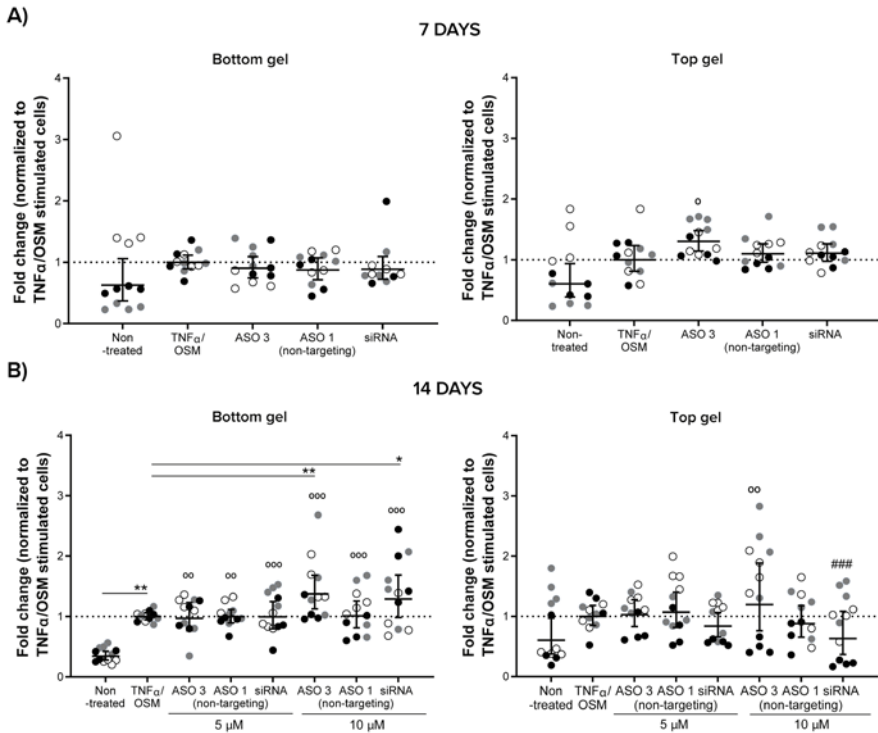


Fig. S4. ADAMTS4 expression. Fold change in ADAMTS4 expression in both top and bottom F:HA hydrogels after 7 (a and b) and 14 (c and d) days of culture. ASO and siRNA sequences were incorporated in the F:HA hydrogel together with Data presented are geometric mean (mid-line) and 95% confidence interval (CI). Experiment was performed in 3 biological replicates. Individual data points are represented in the graph. Black: Donor 1; White: Donor 2; Gray: Donor 3. * represents statistically significant differences to the TNF- β /OSM group; \circ represents statistically significant differences to the Non-treated group. (* $p < 0.05$, ** $p < 0.01$ and *** $p < 0.001$)

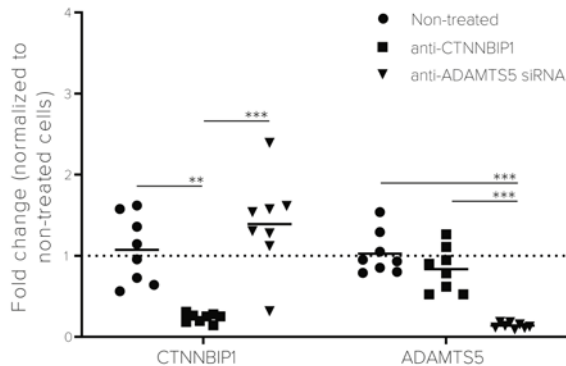


Fig. S5. CTNBNB1P1 and ADAMTS5 expression. Fold change in CTNBNB1P1 and ADAMTS5 expression in primary human OA chondrocytes upon 72h after treatment with anti-CTNBNB1P1 and anti-ADAMTS5 siRNAs (20 nM). (* $p < 0.05$, ** $p < 0.01$ and *** $p < 0.001$)

The image features a large, light brown circle in the center, containing the white number '4'. To the left of the circle is a stylized, curved leaf-like shape with a series of parallel lines radiating from its inner edge. A thin horizontal line extends from the right side of the circle towards the edge of the frame.

4

CHAPTER 4

IN VITRO TISSUE PENETRATION AND INHIBITORYACTIVITY OF A MODIFIED ANTISENSE OLIGONUCLEOTIDE AGAINST ADAMTS-5 IN OSTEOARTHRITIC CARTILAGE

João Pedro Garcia, Jesper Wengel, F. Cumhur Öner, Marianna A. Tryfonidou, Kenneth A.
Howard, Laura B. Creemers

Study in progress

Abstract

The ADAMTS enzyme family, in particular ADAMTS4 and ADAMTS5, are considered to be key players in cartilage degeneration, and their inhibition has shown beneficial effects. In this context, modified antisense oligonucleotides (ASO), or gapmers, are a promising tool for silencing of OA-related genes. Gapmers are composed by a central block of DNA flanked by locked nucleic acid nucleotides, which confers them improved stability and capacity for cellular internalization.

In this study, human cartilage explants were cultured in the presence of a previously validated gapmer sequence against ADAMTS5. The ASO was shown to efficiently diffuse into full-thickness human cartilage explants and to co-localize with resident chondrocytes. Importantly, efficient ASO-mediated ADAMTS5 silencing was shown after 15 days of culture in human cartilage explants cultured in the presence of pro-inflammatory stimuli (TNF- α and OSM). An ADAMTS5-targeting siRNA sequence without transfection reagent was used as control, and despite showing efficient diffusion into the explants did not produce gene knockdown.

Altogether, these findings on the applicability of ASO against ADAMTS5 highlight the potential of antisense therapies using gapmers as therapeutic strategy for the knockdown of OA-related genes.

1. Introduction

Osteoarthritis (OA) is one of the most prevalent musculoskeletal disorders worldwide, and involves structural changes and chronic low inflammation levels that ultimately cause pain and functional disability^{1,2,31}. OA is marked by a disruption of cartilage homeostasis and increased extracellular matrix (ECM) degradation. A major cause is an increased production of catabolic enzymes leading to progressive and irreversible loss of collagen type II and proteoglycans¹¹³. Phenotypic change, from quiescence to hypertrophy, and subsequent death of chondrocytes is an additional hallmark of OA that further contributes to and perpetuates cartilage degradation^{353,354}.

To date, OA treatment follows a “care but no cure” approach as no effective disease modifying drugs are available⁵. Hence, treatment is limited to pharmacological and physiotherapy approaches for pain management, and prosthetic replacement of the affected joints in end-stage OA. Hence, there is an unmet need for new therapeutic alternatives that not only aim at symptom relief, but also at stopping and, ideally, reverting the degenerative process^{6,355}. In this regard, the targeting of OA-related effectors have been focus of attention^{5,356,357}. The ADAMTS enzyme family, in particular ADAMTS4 and ADAMTS5, have been previously demonstrated to be key players in cartilage degradation together with matrix metalloproteinases (MMPs)^{314,315}. Inhibition of each or both proteases prevented matrix degradation both in human cartilage explants^{315,317} and in animal models of OA³¹⁹⁻³²¹.

In the last years, significant efforts have been put into development of disease-modifying OA drugs targeting key enzymes in OA^{172,173,189,191,317}, however, to date no effective inhibitors are clinically available⁶. Clinical trials using small molecule inhibitors have reported disappointing outcomes, namely the lack of efficacy and increased occurrence of side effects, likely owing to the broad spectrum of action of the molecules and prolonged systemic exposure^{6,173,189}. The lack of efficacy of disease-modifying drugs for OA may also relate to limited drug diffusion and penetration in cartilage matrix^{269,324}, which inherent to the avascularity of the cartilaginous matrix which is primarily nourished through solute transport by diffusion from the synovial fluid^{324,358,359}. Additionally, the high density and negative charge of cartilage matrix makes it almost impenetrable to large and negatively charged molecules^{266,269}.

RNA-based therapeutics are a particularly attractive strategy for gene silencing and enzyme inhibition due to their target specificity as compared to other drugs with more general effects such as small molecule inhibitors. By acting at the RNA level, such strategies often produce faster and longer lasting effects, as compared to small molecule drugs⁵³. Even though small interfering RNAs (siRNAs) are powerful silencing agents, they require delivery vehicles that promote cellular internalization, which generally are toxic for cells and tissues and constitute an additional obstacle for clinical translation⁵⁵. Contrary to siRNAs, gapmers have an intrinsic capacity for cellular internalization without aid of delivery platforms^{54,56,58}. Gapmers are antisense oligonucleotides (ASOs) composed by a central block of DNA with phosphonothioate backbone flanked by locked nucleic acids

subsequently digesting the cartilage overnight at 37°C in Dulbecco's Modified Eagle's Medium Glutamax (DMEM, Thermo Fischer Scientific) supplemented with 0.15% (w/v) type II collagenase (Worthington Biochemical Corporation), 10% (v/v) Fetal Bovine Serum (FBS, Biowest) and 100 U/mL penicillin and streptomycin (Gibco). Undigested debris were removed using a 70 µm cell strainer followed by a PBS wash. Cells were subsequently plated and grown in a humidified incubator at 37°C with expansion medium consisting of DMEM supplemented with 10% FBS, 0.2 nM ascorbic-2-phosphate (Sigma-Aldrich), 100 U/mL penicillin and streptomycin and 10 ng/mL basic fibroblast growth factor (bFGF, R&D Systems). Medium was renewed every 3 days. Cells were expanded until passage one and either frozen or further expanded and used for experiments at passage 2. Full depth human cartilage explants were isolated from articular cartilage using 4 mm diameter biopsy punches and cultured in DMEM as described above.

2.3 ASO diffusion

Cartilage explants were cultured in DMEM medium containing 100 U/mL of penicillin and streptomycin, 0.2 nM ascorbic-2-phosphate, 50 ng/mL L-proline in a humidified incubator at 37°C, 5% CO₂. Cy5-labeled ASO and siRNA were added to the explants at a concentration of 1 µM. Media was collected at 3, 6 and 24 hours and fluorescence was measured in a Fluoroskan Ascent FL fluorometer (Thermo Fischer Scientific) with an emission/excitation pair of 620/670 nm. Diffusion into the cartilage explants was calculated by subtracting the fluorescence in the media to the fluorescence of the initial amount of Cy5-gapmer (1 µM). After 24 of culture the explants were washed in PBS and subsequently snap frozen using liquid nitrogen. Using a cryotome, the explants were sectioned in 10 µm thick slices and subsequently imaged using a Leica SP8X (Leica) confocal microscope. Image processing and analysis was performed using Fiji (National Institutes of Health, Bethesda, USA) software version 1.50³²⁸.

2.4 Ex vivo ADAMTS5 silencing

Cartilage explants were cultured in the presence or absence of tumor necrosis factor alpha (TNF-α) (10 ng/mL) and oncostatin M (OSM) (1 ng/mL) to provide pro-inflammatory stimuli, and thereby mimicking a catabolic environment and enhancing ADAMTS5 expression. ADAMTS5 targeting ASO was added to the explants at a concentration of 5 µM. Anti-ADAMTS5 siRNA and non-targeting ASO at the same concentration were used as positive and negative control, respectively. Explants were cultured for 15 days, and media were collected and renewed biweekly. After 15 days of culture explants were processed for RNA isolation or papain digestion prior to biochemical analysis.

2.5 RNA isolation and real time PCR (qPCR)

Before RNA isolation, cartilage explants (n = 3) were frozen in liquid nitrogen and pulverized with a hammer. TRIzol Reagent (Invitrogen) was added to the cartilage and subsequently homogenized with a tissue homogenizer. Total RNA was isolated according to the manufacturer's instructions. RNA was dissolved in DNase/RNase-Free

water (Qiagen). Total RNA (300 ng) was converted to cDNA by the High Capacity cDNA Reverse Transcription Kit (Thermo Fischer Scientific) using an iCycler Thermal Cycler (Bio-Rad) according to the manufacturer's instructions. Real-time PCR reactions were performed using the iTAQ SYBR Green Reaction Mix Kit Mastermix (Bio-Rad) reaction kit according to the manufacturer's instructions in a Light Cycler 96 (Roche). Reactions were prepared in 20 μ l total volume with 7 μ l PCR- H_2O , 0.5 μ l forward primer (0.5 μ M), 0.5 μ l reverse primer (0.5 μ M) and 10 μ l iTAQ SYBR Green Reaction Mix (BioRad) to which 2 μ l of five times diluted cDNA was added as template. Expression of ADAMTS5 and the housekeeping genes glyceraldehyde 3-phosphate dehydrogenase (GAPDH), ribosomal protein L19 (RPL19) and succinate dehydrogenase complex subunit A (SDHA) were analyzed by a three-step amplification qPCR. Data analysis and Cq values were obtained with a LightCycler 96 Application software (Roche). The amplified PCR fragment extended over at least one exon border. In order to generate relative gene expression, the Pfaffl method was used to account for differences in primer efficiencies³³⁰. Details of primers used in real-time PCR are listed in Table 2.

Table 2. Primer details

Gene		Primer Sequence	Annealing Temperature (°C)	Product Size (bp)
ADAMTS5	Forward	5' GCCAGCGGATGTGTGCAAGC 3'	63	130
	Reverse	5' ACACTTCCCCGGACGCAGA 3'		
	Reverse	5' GAAAGTCACAGGCAGATGCA 3'		
GAPDH	Forward	5' TGCACCACCAACTGCTTAGC 3'	62	87
	Reverse	5' GGCATGGACTGTGGTCATGAG 3'		
RPL9	Forward	5' ATGAGTATGCTCAGGCTTCAG 3'	64	150
	Reverse	5' GATCAGCCCATCTTTGATGAG 3'		
SDHA	Forward	5' TGGGAACAAGAGGGCATCTG 3'	58	86
	Reverse	5' CCACCACTGCATCAAATTCATG 3'		

2.6 Papain digestion and glycosaminoglycan (GAG) quantification

Explants (n = 3) were lyophilized overnight and dry weight was measured. Subsequently, explants were digested with a papain solution overnight at 60 °C, and total GAG content was measured using the 1,9-dimethylmethylene blue (DMMB) assay³⁶⁰. GAGs release to the media were also quantified using DMMB assay.

2.7 Statistical analysis

All data were analyzed using IBM® SPSS® Statistics version 21. Silencing efficiency was analysed by univariate analysis of variance using a randomized block design, using treatment and donors as fixed factors. Assumption of normally distributed residuals was met. A post-hoc test with Bonferroni correction was applied for multiple comparisons between treatments (p value < 0.05). All experiments were performed in at least two different donors (n=2).

3. Results

3.1 ASOs and siRNA efficiently diffuse into full thickness cartilage explants

Cartilage explants were incubated with Cy5-labeled ASO and siRNA for 24 hours, and uptake was calculated by measuring residual fluorescence in medium using a standard curve of labelled ASO or siRNA. The ASO was shown to efficiently diffuse into the explant reaching around 90% penetration at 24 hours, while siRNA had an uptake limited to 60%, although the uptake at 3 hours was already 60% (Figure 1a). Confocal imaging of cartilage explants revealed that both ASO and siRNA colocalized with chondrocytes in the superficial and deep layers of cartilage (Figure 1b).

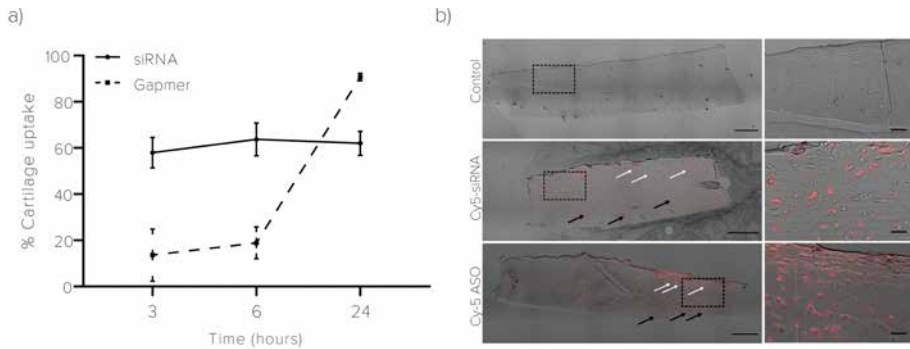


Figure 1. ASO and siRNA diffusion in human cartilage explants. a) Diffusion kinetics of Cy5-labeled ASO and siRNA in cartilage explants over 24 hours. b) Confocal imaging of full thickness cartilage explants cultured for 24 hours in the presence of 1 μM Cy5-labeled ASO and siRNA. Red: Cy5. White arrows: Positive cells in superficial layer; Black arrows: Positive cells in deep layer. Scale bar: 500 μm. Images on the right represent a zoomed in image of the images on the left (black dashed line). Scale bar: 100 μm.

Subsequently, a previously validated anti-ADAMTS5 ASO²³² was investigated for its ability to silence ADAMTS5 in cartilage explants stimulated with TNF- α /OSM. TNF- α /OSM was shown to increase ADAMTS5 expression when compared to non-treated control explants (Figure 2). The ADAMTS5-targeting ASO was shown to significantly silence ADAMTS5, with a mean knockdown of ~70 %. Both siRNA and the non-targeting ASO had no significant negating effect on ADAMTS5 expression.

Total GAG content and GAG released from the explants were measured at the end of culture period and over time, respectively. No statistically significant differences were found between conditions in total GAG content (Figure 3a). GAG release was increased at days 3, 8 and 12 in all conditions where explants were exposed to TNF- α /OSM (independent of the presence of siRNA/ASOs) compared to the non-treated explants.

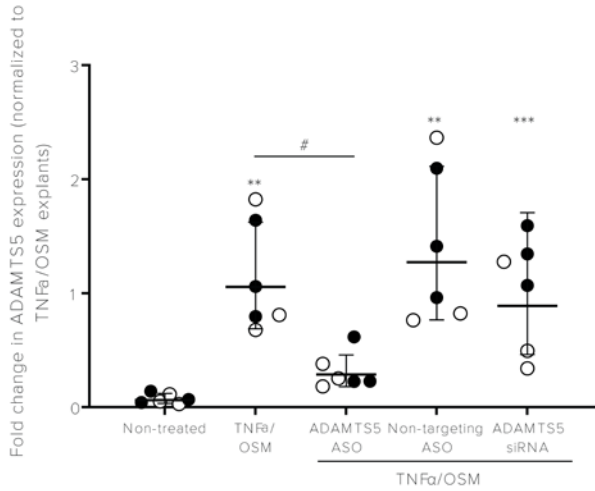


Figure 2. Efficient ADAMTS5 silencing after 15 days culture. Fold change in ADAMTS5 gene expression in human cartilage explants after 15 days of culture. Cartilage explants were cultured with and without TNF- α /OSM stimulation. The effect of 5 μ M ADAMTS5-targeting ASO was determined in explants cultured with TNF- α /OSM. An ADAMTS5 targeting siRNA and a non-targeting ASO were used as controls (5 μ M). Data presented are geometric mean (mid-line) and 95% confidence interval (CI). Experiment was performed in 2 biological replicates. Individual data points are represented in the graphs. White: Donor 1; Black: Donor 2; * $p < 0.05$, ** $p < 0.01$ and *** $p < 0.001$ represent statistically significant differences to the non-treated group; # represents statistically significant differences to the TNF- α /OSM group.

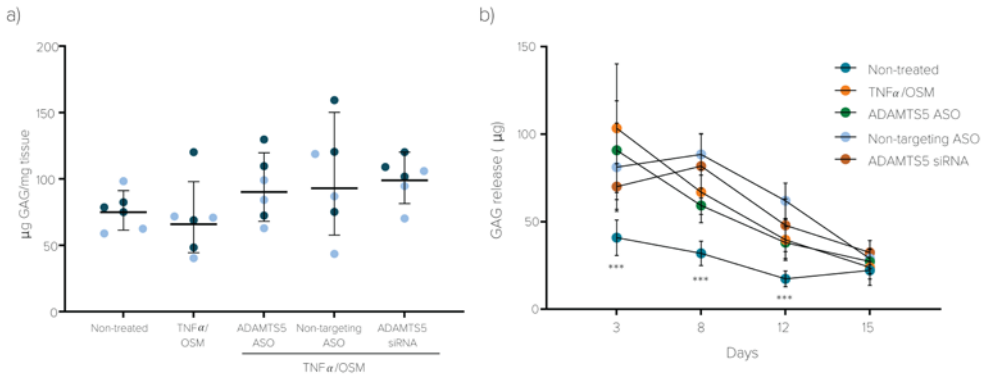


Figure 3. Explant GAG content and release after incubation with ADAMTS5 ASO and siRNA. a) GAG content per mg of tissue (dry weight) measured by DMMB after a 15-day culture period. Data presented are geometric mean (mid-line) and 95% CI. Experiment was performed in 2 biological replicates. Individual data points are represented in the graphs. Light Blue: Donor 1; Dark Blue: Donor 2; b) Explant GAG release measured over 15 days. Data are presented as geometric mean (mid-line) and 95% CI. * represents statistically significant differences between non-treated explants and explants in all other remaining conditions (*** $p < 0.001$).

4. Discussion

Cartilage degradation during OA is orchestrated by different matrix degrading enzymes such as MMPs and ADAMTS^{314,361}, and the inhibition of these catabolic molecules has since early been proposed as a therapeutic approach for OA. Modified antisense therapeutics are promising strategies for inhibition of such enzymes⁵⁴. Chemical modifications confer on these molecules a higher binding affinity and stability, which further reinforce their target specificity and efficiency^{62,63}. Importantly, modified ASOs have an intrinsic capacity for cellular internalization, and subsequent endosomal escape⁵⁸, outperforming other types of gene modulators. In this study we report the use of ASOs for the knockdown of ADAMTS5 in human osteoarthritic cartilage. A previously validated gapmer against ADAMTS5²³² showed efficient diffusion and penetration in full depth human cartilage explants, and co-localization with resident chondrocytes. Additionally, the ASO sequence promoted efficient ADAMTS5 silencing at the gene expression in cartilage explants after 15 days of culture, which was not achieved with siRNA.

A vast majority of the preclinical studies involving development and testing of novel drugs for OA are conducted in small animal models, where cartilage tissue is 15 to 20 times thinner than humans^{269,362}. For instance, insulin growth factor-1 was shown to fully penetrate rat cartilage after 2 days, while it took 6 days to penetrate 20 μm of bovine cartilage³⁵⁸. This addresses the necessity of performing drug diffusion tests in thicker cartilage samples when developing drugs for OA therapy. In this study, both gapmer and siRNA sequences were shown to diffuse into full thickness (~ 2 mm) human cartilage explants over a period of 24 hours and to co-localize with resident chondrocytes. Importantly, only the gapmer sequence was shown to produce significant ADAMTS5 silencing, highlighting the efficiency of this molecule over the gold-standard siRNA. In fact, the majority of the studies on siRNA-based approaches for cartilage repair generally use nanocarriers as a mean to increase transfection efficiency³⁶³⁻³⁶⁵. In these studies, siRNA was encapsulated in positively-charged carriers with a diameter size between 50 and 60 nm. However, while nanocarriers can potentially enhance the therapeutic efficacy of siRNAs, they often have cytotoxic effects^{55,322}, which can bring additional hurdles towards clinical translation corroborating thereby the advantages of employing ASOs that can penetrate the dense cartilage matrix and effectively silence their targets without the use of carriers.

Despite the silencing achieved, the ASO targeting ADAMTS5 did not prevent GAG release. The GAGs released upon treatment with TNF α /OSM in the media, which cumulatively ranged from 50-70% of the total GAG content of the explants, represent GAGs being produced by chondrocytes and GAGs being released from the matrix due to catabolic processes³⁶⁶. As such, while the former needs to be addressed by complementary techniques, TNF- α /OSM stimulation leads to upregulation of other matrix-degrading enzymes, such as ADAMTS4³¹⁵ and MMP-3³⁶⁷. Indeed, ADAMTS4 has been suggested to be the main enzyme responsible for proteoglycan degradation in human OA³⁶⁸. Therefore, a relevant chondroprotective effect of the ASO sequence targeting

ADAMTS5 might be masked by the activity of other enzymes. Functional assays to directly assess ADAMTS5 activity are necessary to confirm functional ASO-mediated silencing. These include enzymatic assays to measure ADAMTS5 activity or to quantify ADAMTS5-generated degradation products. Furthermore, histological and immunohistochemical evaluation of the explants treated with the ASO will provide additional information on individual components of the cartilage matrix, namely aggrecan.

To the best of our knowledge, so far only two other studies have reported *ex vivo* and/or preclinical testing of LNA-modified ASOs as therapeutic strategy for OA. Recently, chondroprotective effects of an LNA-based ASO targeting miR-RNA-181a were reported²²⁷. MiRNA-181a has been described as a key mediator of cartilage degeneration in facet joint (FJ) OA²²⁰. The reported ASO attenuated cartilage damage in two animal models of OA (FJ and knee) after 2 intra-articular injections, corroborating the ability of these molecules to diffuse into cartilage and produce efficient silencing. Importantly, in this study, the inhibition of cartilage damage was associated with a decreased expression of catabolic markers. One can hypothesize that human OA patients would benefit from administration of such bioactives in drug delivery platforms to minimize number of injections and to provide high local concentrations for longer time periods. The incorporation of an ASO against the anti-chondrogenic miR-221 in a hydrogel scaffold for regeneration of cartilage focal defects yielded efficient *in situ* gene silencing and endogenous cartilage repair in subcutaneously implanted osteochondral defects 4 weeks after surgery²³³. However, the authors did not report the use of free ASO as a control. Altogether these studies highlight the potential of LNA-modified ASOs as disease-modifying drugs for OA.

In conclusion, we demonstrated the applicability of highly specific and efficient modified ASOs for gene silencing in OA targeting ADAMTS5 as a proof-of-concept. ASOs can “virtually” be designed to target any mRNA or miRNA, making them unique platforms for drug development. Further studies will focus on the development of gapmers targeting other key players in OA, such as ADAMTS4. Likely, potential antisense-based OA therapies will benefit from the simultaneous targeting of multiple genes.



CHAPTER 5

ASSOCIATION BETWEEN ONCOSTATIN M EXPRESSION AND INFLAMMATORY PHENOTYPE IN EXPERIMENTAL ARTHRITIS MODELS AND OSTEOARTHRITIS PATIENTS

João Pedro Garcia, Lizette Utomo, Imke Rudnik-Jansen, Nicolaas P. A. Zuithoff, Anita Krouwels, Gerjo van Osch, Laura B. Creemers

Manuscript Submitted

Abstract

Pro-inflammatory cytokines play a major role in osteoarthritis (OA), yet so far, the specific cytokines involved in the pathology of OA have not been identified. Oncostatin M (OSM) has been shown to be elevated in synovial fluid of most rheumatoid arthritis patients, but only in a limited subset of OA patients. Furthermore, little is known about OSM expression in joint tissues during OA and how its expression correlates with hallmarks of disease.

In this study, we mapped OSM expression in the joint tissues of two rat models of arthritis: an acute inflammatory model and an instability-induced osteoarthritic model. Reanalysis of an existing dataset on cytokine profiling of OA synovial fluid was performed to assess pattern differences between patients positive and negative for OSM. In the inflammatory model, OSM expression correlated with synovitis and osteophyte formation but not with cartilage damage. In the instability model of OA, an increase in synovitis, cartilage damage, and osteophyte formation was observed without changes in OSM expression. Additionally, OA synovial fluid with detectable OSM contained higher levels of other inflammatory cytokines, namely IFN- α , IL-1 α and TNF- α , likely indicating a more inflammatory state.

Taken together these data indicate OSM might play a prominent role in inflammatory phenotypes of OA, and can potentially be used as biomarker or target for drug development in osteoarthritis.

1. Introduction

Osteoarthritis (OA) is the most prevalent musculoskeletal disorder and a leading cause of disability and morbidity worldwide^{1,3}. It is a chronic and degenerative joint disease not only characterized by progressive cartilage degradation, but also by changes in subchondral bone, ligaments, synovial lining, and joint muscles¹. Even though OA is known to be a complex disease with multiple etiologies, it is widely accepted that mechanical factors, together with both biochemical cues are the main key players in the disease pathogenesis^{1,31}. Chondrocytes and synovial cells are thought to jointly act as catalyst for the degeneration process by producing matrix-degrading enzymes, such as metalloproteinases (MMPs) and aggrecanases (or a disintegrin and metalloproteinase with thrombospondin motifs – ADAMTSs)¹. Contrary to rheumatoid arthritis (RA), OA is not clinically described as an inflammatory disease, although synovial inflammation, joint swelling and pain are common findings in OA patients^{10,31}. Tumor necrosis factor alpha (TNF- α) and interleukin 1 (IL-1) are two of the most studied mediators in OA. In vitro, they have been shown to increase production of matrix-degrading enzymes and other inflammatory mediators such as MMPs 1, 3, and 13, ADAMTSs 4 and 5, and IL-6 in chondrocytes³¹. However, growing evidence suggests that IL-1 and TNF- α do not play a major role in OA. Several clinical trials targeting these cytokines have shown no effect^{165,167,369}, contrasting the clear alleviation of symptoms in RA upon their inhibition. These observations may be in part explained by the fact that in the OA joint the levels of these mediators are lower than those of their natural inhibitors, such as IL-1 receptor antagonist and soluble TNF- α receptors^{370,371}.

Another cytokine that was shown to be associated with OA is oncostatin M (OSM). OSM, a cytokine from the IL-6 family, is known to be an important mediator of inflammation in RA, and has been found to be elevated in synovial fluid of RA patients^{372,373}. In RA, OSM is thought to promote cartilage degradation and bone erosion, and augment inflammation^{374,375}. Moreover, OSM has been shown to promote cartilage degradation both in vitro and in vivo, especially in combination with other cytokines such as IL-1 β and TNF- α ^{374,376-379}.

In OA, OSM levels were found to be detectable in synovial fluid in up to 30% of the patients^{341,372,380,381}. In vitro inhibition of OSM in OA synovial fluid promoted anabolic and repair processes in osteoarthritic cartilage³⁸⁰. OSM, as well as other cytokines from the IL-6 cytokine family, have been extensively described to also have important roles in bone development and formation³⁸². In fact, OSM was shown to mediate bone homeostasis, with studies showing increased periosteal bone apposition, and others reporting bone resorption upon intra-articular OSM overexpression^{375,378,379,383,384}. Accordingly, OSM has been found in osteoblasts and bone lining cells³⁸⁴. Additionally, OSM has been shown to be produced by macrophages³⁷³ and neutrophils³⁸⁵ both in vitro and in vivo, in in vitro-activated T lymphocytes³⁸⁶, and mast cells³⁸⁷. These cells are present in both the synovial lining and synovial fluid during inflammation in both OA and RA⁴³. However, to what extent other cells and tissues in the joint produce OSM, and how this expression correlates with

hallmarks of arthritis, such as cartilage damage, inflammation and osteophyte formation is still unclear.

The goal of this study was to map OSM expression in the joint in two different rat models: the peptidoglycan-polysaccharide-induced arthritis model (PGPS) and the anterior cruciate ligament transection and partial meniscectomy of the medial meniscus model (ACLT). While the first is an acute inflammation model, predominantly characterized by localized synovitis³⁸⁸, the latter is characterized by joint destabilization and subsequent development of OA³⁸⁹. We also evaluated whether OSM expression is associated with hallmarks of disease, such as cartilage damage, synovial inflammation and osteophyte formation in these models. Additionally, we analyzed the expression pattern of synovial cytokines in relation to expression of OSM in an existing dataset on cytokine expression in synovial fluid samples from OA patients.

2. Methods

2.1 Synovial fluid collection and cytokine measurements

Data of previously published cytokine profiles in synovial fluid of OA patients were re-analyzed³⁸¹. In brief, synovial fluid was collected from 27 OA patients (mean age = 70) undergoing total knee arthroplasty and according to the Medical Ethical regulations of the University Medical Centre Utrecht and the 'good use of redundant tissue for clinical research' guideline constructed by the Dutch Federation of Medical Research Societies on collection of redundant tissue for research. Cytokine measurements of OSM, IL-1 α , IL-1 β , IL-4, IL-6, IL-7, IL-8, IL-10, IL-13, TNF- α , IFN- α , and IL-1Ra were measured using a multiplex bead assay (Luminex, Luminex Corporation, Austin TX, USA) as described previously³⁸¹.

2.2 Animal Models

All animal experiments were carried out according to the ARRIVE guidelines and the approved protocols (AVD108002015282, WP#800-15-282-01-003 and WP#104970-2) of the Utrecht University Ethical Committee for Animal Care and Use, following the central commission of animal experiments guidelines for animal research in the Netherlands. 8-week-old female Sprague Dawley rats of approximately 230 grams (Charles River Laboratories, The Netherlands) were used for this study. Rats were allowed to acclimatize for 1 week and housed in groups of 3 to 4 rats per cage which included enrichment under a 12h light/dark cycle. Ad libitum food and water was provided.

In the PGPS model, 6 rats were randomly taken from their cages and local synovitis was induced by priming their left joint (experimental joint) by an intra-articular injection of 25 μ L PGPS (100 P fraction with 5 mg rhamnose/mL PGPS, Lee Laboratories) at a concentration of 0.17 mg/mL, under general isoflurane anesthesia (day -14)²⁴⁹. At days 0, 14, and 28 synovitis was reactivated in the experimental knee joints by intravenous injection of 500 μ L of PGPS (0.28 mg/mL PGPS) via the tail vein. Animals were euthanized after 6 weeks with CO₂. For the ACLT model, OA was induced unilaterally through anterior

cruciate ligament transection and partial medial meniscectomy in the left knee of six rats that were randomly taken from their cages, under general isoflurane anesthesia³⁹⁰. After 16 weeks, rats were euthanized with CO₂.

2.3 Histology

After euthanasia, all rat hind limbs were collected for histological analysis and joints were fixed in 4% formaldehyde solution (Klinipath BV, Netherlands) at room temperature for 1 week and subsequently decalcified at room temperature in 0.5 M ethylenediaminetetraacetic acid (EDTA; VWR international BV) solution for a total of 8 weeks. Re-fixation was performed for 3 days in 4% formaldehyde every 2 weeks. Then, samples were embedded in paraffin and cut into 5- μ m thick coronal knee joint sections. Sections were taken from the middle part of the joint. Samples from the ACLT model were not sufficiently decalcified and had to be deparaffinized, decalcified in EDTA for an additional 4 weeks and re-embedded in paraffin.

Sections were stained with safranin-O/fast green to evaluate cartilage damage using the Mankin score (0 complete healthy – 14 total cartilage destruction)³⁹¹. Hematoxylin/eosin staining was used to evaluate synovitis using the Krenn score³⁹². Scoring was done in a random order by two independent observers (JPG, IRJ) blinded for treatment, and scores were averaged.

Staining for tartrate-resistant acid phosphatase (TRAP) activity was performed to detect osteoclasts. Sections were deparaffinized in xylene, rehydrated, washed in running tap water for 5 min, and incubated with 0.2 M acetate buffer-tartaric acid for 20 min at 37°C. Subsequently, Naphtol AS-MX phosphate (0.5 mg/mL, Sigma-Aldrich) and Fast red TR salt (1.1 mg/mL, Sigma-Aldrich) were added to the samples and incubated for another 3 hours. Sections were counterstained with Mayer's hematoxylin. Osteoclasts were defined as multinucleated TRAP-positive cells in the periosteum, growth plate and subchondral bone of both tibia and femur. The number and brightness of stained osteoclasts were assessed and scored on a scale from 0 to 4 (0 = no staining, and 4 = numerous positive cells and bright staining). Scoring was done in a random order by two independent observers (JPG, AK) blinded for treatment, and scores were averaged.

2.4 OSM immunohistochemistry

Sections were deparaffinized in xylene, rehydrated, and subsequently blocked for nonspecific endogenous peroxidase by incubating with 0.3% H₂O₂ for 10 min. Due to the re-embedding step in the ACLT joints, antigen retrieval was performed for these samples by incubating them with 1 mg/mL pepsin (Sigma-Aldrich) for 2 hours at 37°C followed by incubation with 10 mg/mL hyaluronidase (Sigma-Aldrich) for 30 min at 37°C. Between each step, slides were washed three times with PBS containing 0.1% Tween-20 (PBS-T) for 5 min. We confirmed that antigen retrieval did not affect OSM staining in the PGPS model, nor was relative staining intensity between the tissues changed, suggesting staining patterns were not dependent on tissue processing or antigen retrieval in the two models (Table S1 and Figure S1). Then, sections were blocked in PBS containing 5%

BSA for 30 min followed by overnight incubation at 4 °C with the primary antibody (2 µg/mL mouse monoclonal OSM (B-6), sc-133229, Santa Cruz). Mouse IgG isotype at 2 µg/mL was used as negative control (Figure S2). The next day, sections were washed three times with PBS-T for 5 min, followed by incubation with the secondary antibody for 1 hr at room temperature (BrightVision poly-HRP-anti mouse, Dako). After washing with PBS-T, sections were incubated with DAB substrate for 5-10 min, briefly counterstained with Weigert's Hematoxylin and rinsed with running tap water for 10 min. Finally, sections were dehydrated with a series ethanol and xylene and permanently mounted with Depex mounting medium (Sigma-Aldrich).

For quantification purposes, the stained joint sections were ranked from 0 to 3 (0 = no staining; 3 = maximum staining) based on OSM staining intensity in the articular cartilage, periosteum, menisci, femorotibial synovium, and collateral ligaments. Cartilage, periosteum and menisci were further divided in individual compartments (Table S2). Scoring was done in a random order by two independent observers blinded for treatment (JPG, LU), and scores were averaged.

2.5 Micro-CT analysis

Directly after euthanasia, animals were imaged using a Quantum FX µ-CT scanner (PerkinElmer, Waltham, MA) with the following parameters: time = 3 min, isotropic voxel size = 30 µm³, tube voltage of 90 kV, tube current = 180 µA. Scans were reconstructed using the scanner's software (PerkinElmer, Waltham, MA, USA). ImageJ software was used for image analysis (ImageJ, 1.47v, NIH, Bethesda, USA). Serial 2D scans of the femur, tibia, and patella were evaluated for subchondral sclerosis and osteophyte volume.

2.6 Statistics

IBM SPSS 25.0 (IBM, New York, NY) was used for statistical analysis. The intra-class correlation coefficient (ICC) was used to calculate inter-rater variability for the OSM scoring system. A two-way mixed-effect model based on a mean-rating (k=2) and absolute agreement was used, as previously described³⁹³. ICC estimates and the 95% confidence intervals (CI) were reported.

Non-parametric Kruskal-Wallis tests were conducted to evaluate statistically significant differences between treatment groups (control vs. induced) and between compartments (i.e. femur vs. tibia, and lateral vs. medial). The correlation between cartilage damage, synovitis and OSM staining was evaluated with a non-parametric Spearman rho correlation test. P-values of <0.05 were considered statistically significant.

Fischer exact test was performed to examine the relation between frequency of osteophyte formation and induction of OA. Osteophyte presence was classified as Yes/No for each of the 4 analyzed compartments (lateral and medial femur condyles, and lateral and medial tibial plateaus) for a total of 24 compartments (4 compartments x 6 joints). Chi-square statistics are reported with degrees of freedom and sample size, the Pearson chi-square value and the significance level.

On the dataset of cytokine levels in synovial fluid of OA patients, spearman's

rank correlation was used to analyze the relationship between OSM expression and expression of the remaining cytokines in the human synovial fluid. To analyze differences in cytokine expression between patients with detectable and non-detectable levels of OSM (OSM+ and OSM-), and due to the small number of patients, a generalized linear model was used. The generalized linear model was performed with an unstructured (i.e. GEE type) residual covariance matrix to analyze multiple normally distributed outcomes. Since the distribution of cytokine concentration values were highly skewed, we used log transformed outcomes for the statistical analysis. We specifically choose this model to obtain a single likelihood ratio test for the hypothesis that the pattern of cytokine expressions differs between patient groups (OSM- vs OSM+). Additionally, the model estimated differences between patient groups for each cytokine separately. For ease of interpretation, these differences (with 95% CI) were transformed back to the original scale by taking the exponential and applying a smearing factor³⁹⁴. The p-values of the Wald tests for individual cytokine expressions were used to rank the differences between groups.

3. Results

3.1 Mapping and quantification of OSM expression in joint tissues

To map the presence of OSM in different phenotypes of joint diseases, OSM expression was evaluated by immunohistochemistry in two mouse models: inflammatory arthritis (PGPS model) and degenerative OA (ACLT) model. Specificity of the staining was confirmed by the absence of staining in the negative control, performed with IgG isotype (Figure S2). In the PGPS model, extracellular OSM staining was observed in articular cartilage, meniscus, periosteum, and synovium (Figure 1). Additionally, intracellular staining was observed in articular chondrocytes and meniscal fibrochondrocytes (Figure 2). In both tissue structures, OSM-positive cells were found in the superficial cell layers, while absent in deeper layers. In the synovium, intracellular OSM staining was prominent in the subintimal layers rather than the lining. In the ACLT model, extracellular OSM staining was found in the periosteum and synovium, but not in cartilage or meniscus (Figure 1). Even though synovial staining was less extensive, intracellular staining was observed in the lining (Figure 2). Similar to the PGPS model, intracellular staining was found in articular cartilage and menisci.

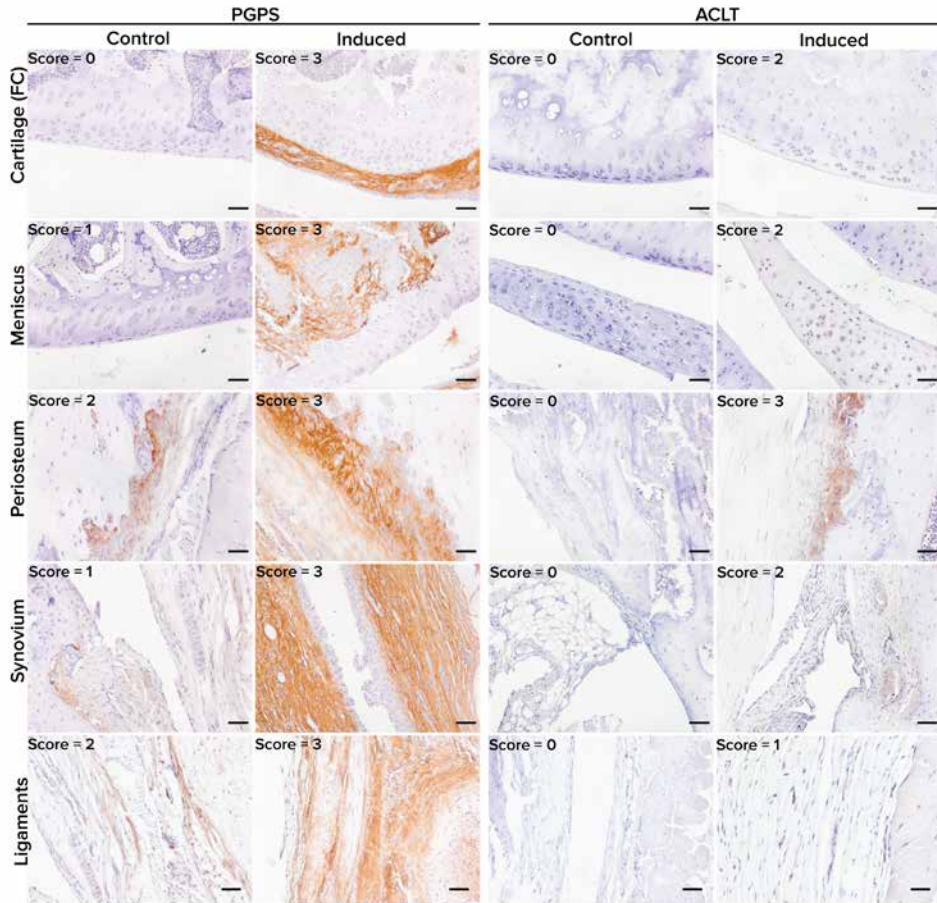


Figure 1. OSM expression pattern in acute arthritis and instability-induced OA. Representative pictures of OSM expression (brown staining) in different joint structures: Femur condyle (FC) cartilage, meniscus, periosteum and synovium. Acute arthritis in the PGPS model was induced by intra-articular injection of PGPS in the left knee. The ACLT model was induced unilaterally (left knee) through anterior cruciate ligament transection and partial medial meniscectomy. Individual scores for each structure are displayed in the top left corner of each picture. Scale bar: 50 μ m.

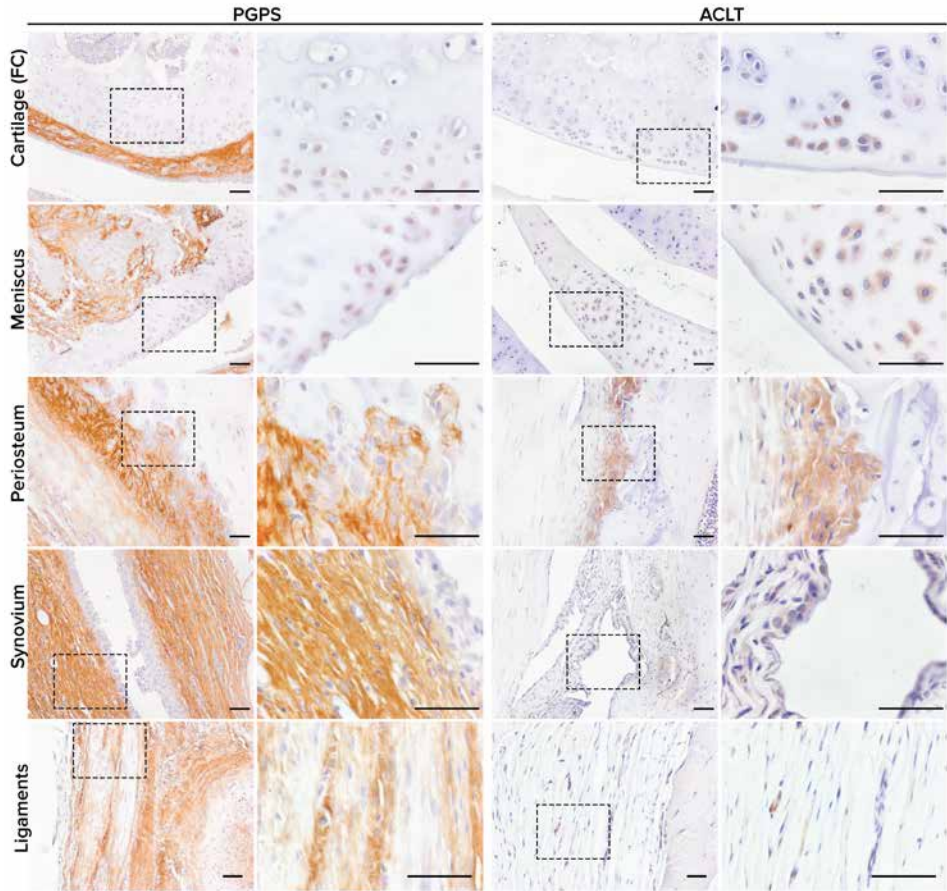


Figure 2. Intra and extracellular OSM expression patterns in acute arthritis and instability induced OA. Representative pictures of OSM expression in different joint structures: Femur condyle (FC) cartilage, meniscus, periosteum, synovium and ligaments. Scale bar: 50 μ m.

Expression of OSM was semi-quantified by scoring the knee tissues from 0 to 3 based on OSM staining intensity in the articular cartilage, periosteum, menisci, synovium, and ligaments. The ICC values for inter-rater variability were 0.828 [0.766-0.875] for the PGPS model and 0.827 [0.758-0.873] for the ACLT model, indicating a good reliability among the two independent scorers.

In the PGPS model, OSM staining was more predominant in cartilage of the lateral femoral condyle, and in both lateral and medial tibial plateau cartilages of the diseased knees as compared to control knees, but this was not the case in the ACLT model (Figure 3a). Regarding the femoral periosteum, OSM expression in lateral and medial compartments of diseased joints was higher than control joints in the PGPS model, but not in the ACLT model (Figure 3b).

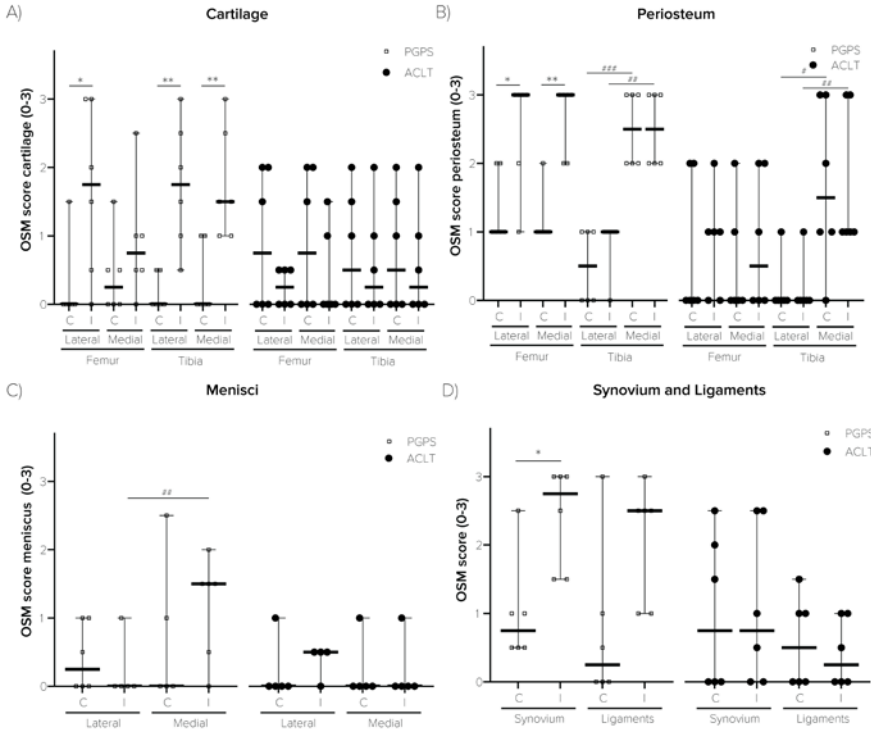


Figure 3. OSM expression in two rodent models of acute arthritis and instability induced OA. OSM score per anatomical structure: cartilage (a), periosteum (b), meniscus (c), synovium, and ligaments (d). Control (C), Induced (I). 0 = no staining, 1 = slight staining, 2 = moderate staining, 3 = extensive staining. Each individual data point represents a rat knee. Squared symbols (white) refer to the PGPS model. Circular symbols (black) refer to the ACLT model. Data are presented as median and 95 % CI. (*: $p < 0.05$, **: $p < 0.01$, and ***: $p < 0.001$).

Expression of OSM in the tibial periosteum was not affected by induction of arthritis in any of the models. No differences in OSM expression were observed in the lateral or medial meniscus in neither of the models (Figure 3c). Finally, expression was higher in the synovium of PGPS-injected joints than in the synovium of the control joints (Figure 3d). No differences in OSM expression were found in the ligaments in the PGPS knees, and in the synovium and ligaments in the ACLT joints.

Additionally, in both models, OSM expression in the tibial periosteum was significantly higher in the medial compartment compared to lateral, independently of induction of disease (Figure 3b). This was not observed for the femoral periosteum.

3.2. Expression of OSM correlates with synovitis in the PGPS model of acute arthritis

While the overall OSM score was shown to be significantly higher in PGPS-injected knees than in control knees ($p < 0.01$; Figure 4a), no differences were observed between OA or control knees in the ACLT model ($p = 0.873$).

In both models, induction of disease led to increased synovitis according to the Krenn score (Figure 4b), however cartilage damage was only observed in induced joints of the ACLT model ($p < 0.05$) (Figure 4c).

Furthermore, the total OSM score strongly correlated with synovitis in the PGPS model ($\rho = 0.848$, $p = 0.001$, Figure 4d), but not in the ACLT model ($\rho = 0.272$, $p = 0.387$, Figure 4d). No correlation was found between OSM expression and cartilage damage in either model (Figure 4e).

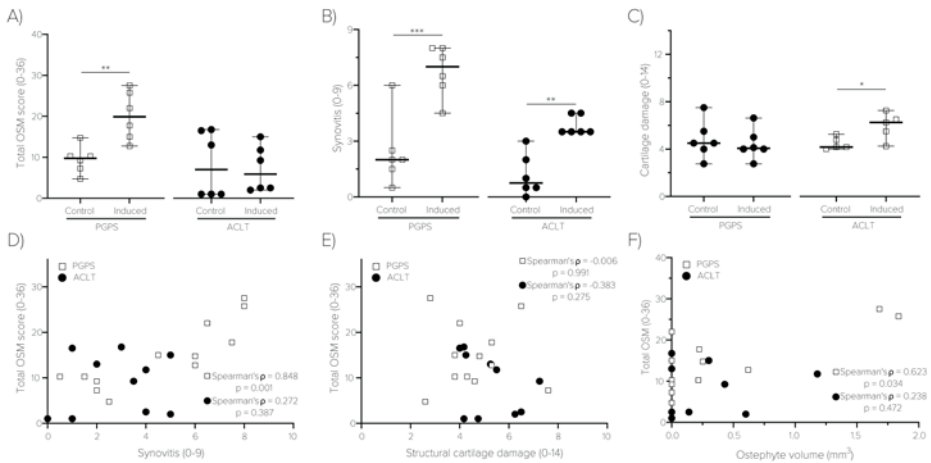


Figure 4. Total OSM expression and correlation with synovitis, cartilage damage and osteophyte volume. a) Total OSM score was calculated by adding up the individual scores for every compartment (min = 0; max = 32). b) Synovitis was scored according to the Krenn score. c) Cartilage damage was scored according to the Mankin score. Data are presented as median and 95% CI. Each individual data point represents a rat knee. (*: $p < 0.05$, **: $p < 0.01$ and ***: $p < 0.001$). d) Correlation scatterplot between total OSM staining and synovitis score in both PGPS and ACLT models. e) Correlation scatterplot between total OSM staining and articular cartilage damage in both PGPS and ACLT models. f) Correlation scatterplot between total OSM and osteophyte volume in both PGPS and ACLT models. Each individual data point represents a rat knee.

Finally, osteophyte volume was moderately correlated with the total OSM expression in the PGPS knees ($\rho = 0.623$, $p = 0.034$), but not in the ACLT knees ($\rho = 0.238$, $p = 0.472$) (Figures 4f). No differences in subchondral sclerosis were observed between induced and control joints in either model (Figure S3). Likewise, no differences in TRAP staining were found between induced and control joints in neither model (Figure S4 and S5).

3.3. Cytokine profile of osteoarthritis patients

OSM was detected in the synovial fluid of 6 out of 27 patients (OSM+), and was undetectable in 21 patients (OSM-). The concentration of OSM showed a positive and significant correlation with the concentration of other pro-inflammatory cytokines, namely IL-1 α ($r = 0.461$, $p = 0.016$), TNF- α ($r = 0.481$, $p = 0.011$), and IFN- α ($r = 0.573$, $p = 0.002$) (Table S3). A generalized linear mixed model was conducted with and without explanatory variables (OSM grouping) to assess differences in cytokine expression pattern between OSM+ and OSM- patients. A likelihood ratio test between the two models indicated significant difference in cytokine expression patterns between the two patient groups [$\chi^2(11) = 43.48$, $p < 0.0001$]. The lowest p values were observed for inflammatory cytokines (IFN- α , IL-1 α and TNF- α), likely indicating a more differential expression of these cytokines between OSM+ and OSM- patients, as compared to the remaining cytokines (Figure 5 and Table S4).

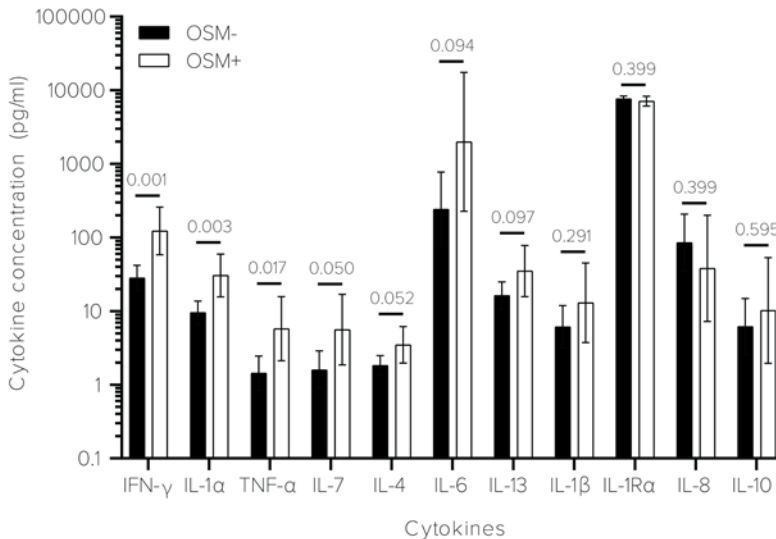


Figure 5. Cytokine concentration in synovial fluid of OA patients. Concentration values were back transformed to the original scale as described before³⁹⁴. Data are presented as median and 95 % CI, with the p-values of the Wald tests for the individual cytokines.

4. Discussion

In this study, we have for the first time mapped the presence of OSM in various joint tissues in two models of arthritis. OSM expression correlated with disease hallmarks in the acute inflammatory arthritis model, but not in the instability-induced osteoarthritis model, suggesting an association with a more inflammatory phenotype. This was in line with the reanalysis of previously obtained data in a patient cohort, where we observed that OSM concentration positively correlated with other inflammatory cytokines, namely IL-1 α , TNF- α and IFN- γ . Furthermore, generalized linear model analysis showed these cytokines to be the most likely cytokines to be differentially expressed among the patient group with and the patient group without OSM expression.

Extensive extracellular OSM expression was recognized in the synovial capsule, possibly derived from infiltrating inflammatory cells such as macrophages, neutrophils, and T-cells, as previously reported^{373,385,386}. These cell types are known to migrate to synovium during OA and RA, and to mediate inflammatory pathways⁴³. High neutrophil counts are detected in most RA patients compared to healthy controls³⁹⁵, while in OA patients, neutrophil presence is associated only with severe and late stages³⁹⁶. In line with this, cell infiltration, synovitis and synovial OSM staining were indeed seen to a greater extent in the inflammatory (PGPS) mouse model.

Intracellular OSM staining was observed in the most superficial layers in articular cartilage and meniscus. In human OA patients, OSM levels in cartilage tissue were previously shown to be even higher than in synovial fluid³⁸¹. However, to what extent chondrocytes contribute to the disease process is still unclear.

Interestingly, OSM staining was also found in the tibial and femoral periosteum. OSM has been previously detected in osteoblasts, bone-lining cells and osteocytes³⁸⁴. Intra-articular overexpression of OSM has been shown to promote periosteal bone formation and deposition^{383,384}, in a process that is thought to occur through inhibition of sclerostin^{384,397}, a negative regulator of bone formation. However, OSM has also been associated with bone erosion when simultaneously overexpressed with IL-1 α or TNF- α ^{375,378,379}. Here, the presence of OSM in the periosteum of both models indicates this cytokine may be part of the as yet enigmatic role of bone homeostasis and remodeling in OA³⁹⁸. Additionally, OSM expression was higher in the medial tibial periosteum than in the lateral, independent of induction of arthritis. Gait analysis in mice has shown weight is distributed more towards the medial side than the lateral, and mechanical loading has been shown to enhance OSM gene expression³⁹⁹⁻⁴⁰¹.

OSM expression correlated with osteophyte volume in the PGPS model, but not in the ACLT model. While the exact mechanisms leading to osteophyte formation are still unknown, osteophyte formation was shown to be associated with synovial inflammation and macrophage infiltration^{402,403}. Hence, one could hypothesize that OSM production by infiltrating cells could potentially contribute to osteophyte formation in the PGPS model in a direct or indirect manner.

Furthermore, OSM expression also correlated with the degree of inflammation in the

PGPS model, but not in the ACLT model despite increased synovitis. This might suggest OSM to play a more prominent role in inflammation of the PGPS model and to associate with a more inflammatory phenotype. These findings are supported by analysis of OA synovial fluid cytokines, that showed that OSM concentration correlated with other pro-inflammatory cytokines, in particular IFN- α , IL-1 α , and TNF- α . Additionally, these cytokines were shown to be elevated in OSM+ patients.

Synovial levels of OSM were shown to be higher in patients with cartilage defects than in healthy subjects³⁸¹. However, in this study, cartilage damage was only found in the ACLT model and not in the PGPS model. This may be due to the fact that in PGPS-induced arthritis animals were sacrificed after 6 weeks compared to 16 weeks in the ACLT model. Nevertheless, also in a long-term PGPS study after 12 weeks no cartilage damage was observed, despite increased synovitis⁴⁰⁴. Since no correlation was found between cartilage damage and OSM score in either of the models, it can be hypothesized that in late stage disease, damage is a cause rather than a consequence of inflammation. Possibly, inflammatory cytokines play a role in the early chain of events initiating rather than maintaining OA. TNF- α and IL-1 α , for instance, have been shown to be still elevated 12 weeks after ACLT in a rat model⁴⁰⁵. Additionally, it was shown before that synovial levels of IL-10 were up-regulated immediately upon ACL injury in humans and remained elevated more than 3 months after injury, while TNF- α levels progressively increased after injury³⁴. TNF- α and IL-1 α levels post trauma were also shown to be associated with severity of cartilage damage upon ACL injury in patients⁴⁰⁶, and blockade of IL-1R immediately after injury was suggested to improve joint integrity⁴⁰⁷.

Although we did not evaluate if other cytokines were elevated in the PGPS model, it is known that OSM alone at the concentrations found in the OA synovial fluid does not promote cartilage degradation *in vitro*, but may rather inhibit matrix production³⁸⁰. On the other hand, even though OSM expression was not elevated in the ACLT model 16 weeks post induction, it is still possible that low levels of OSM are a prerequisite to act in concert with other pro-inflammatory cytokines to promote cartilage damage. Additionally, we cannot exclude that OSM levels were elevated at earlier time points, as a consequence of the traumatic injury.

Despite the extensive *in vitro* and *in vivo* evidence on the role of inflammatory cytokines (e.g. IL-1 α , TNF- α) in OA and on their inhibition as a therapeutic approach, most of the clinical trials carried out so far have been presented with disappointing outcomes^{6,355}. The negative results have been attributed to a short lifetime of the inhibitor drugs within the joint, although they also have been suggested not to be the right effector molecules^{6,12}. Possibly, the disappointing results are related to the disease profile of the patients; The degree of synovitis and the inflammatory mediators involved may be different among patients, suggesting patient selection and stratification might improve trial outcomes and treatment efficacy^{8,51}.

One of the limitations of this study is the fact that OSM expression in the OA models was evaluated by immunohistochemistry at the endpoint of the experiment. Additionally, the study would benefit from having midpoint histological analysis to assess the presence

of OSM and the extent of cartilage damage and synovitis over time. Another limitation of the study is the small patient number available for analysis of cytokine expression in OA synovial fluid, as a higher number of patients would increase the power of the statistical analysis. Additionally, the study would benefit from information regarding the severity of OA (i.e. Kellgren-Lawrence score, Mankin score) and synovitis (i.e. Krenn score), and patient scores. Thus, a more complete comparison could be done between the clinical data and the data obtained with the experimental models.

In conclusion, in this study we have shown that OSM expression is associated with synovial inflammation and osteophyte formation, but not with cartilage damage in an acute arthritis model. On the other hand, although the ACLT model resulted in cartilage damage, synovial inflammation, and osteophytes, these parameters did not correlate with OSM expression. Additionally, in a cohort of OA patients, patients with detectable OSM had higher expression of other pro-inflammatory cytokines. Taken together, these data suggest that OSM might have a prominent role in inflammatory types of OA, and can potentially be used as a biomarker for patient stratification or as a target for future drug development. To further elucidate the role of OSM in OA, future studies should focus on in vivo inhibition of OSM upon induction of OA, and on the evaluation of the subsequent effect on cartilage damage, inflammation, and other hallmarks of arthritis.

Supplementary Information

Table S1. Reliability assessment between PGPS samples stained with and without antigen retrieval.

Structure	Intra-class correlation	Confidence Interval (95 %)	
		Lower limit	Upper limit
Cartilage	0.870	0.671	0.945
Periosteum	0.919	0.826	0.962
Synovium	0.922	0.536	0.987
Meniscus	0.893	0.584	0.973
Ligaments	0.975	0.805	0.996

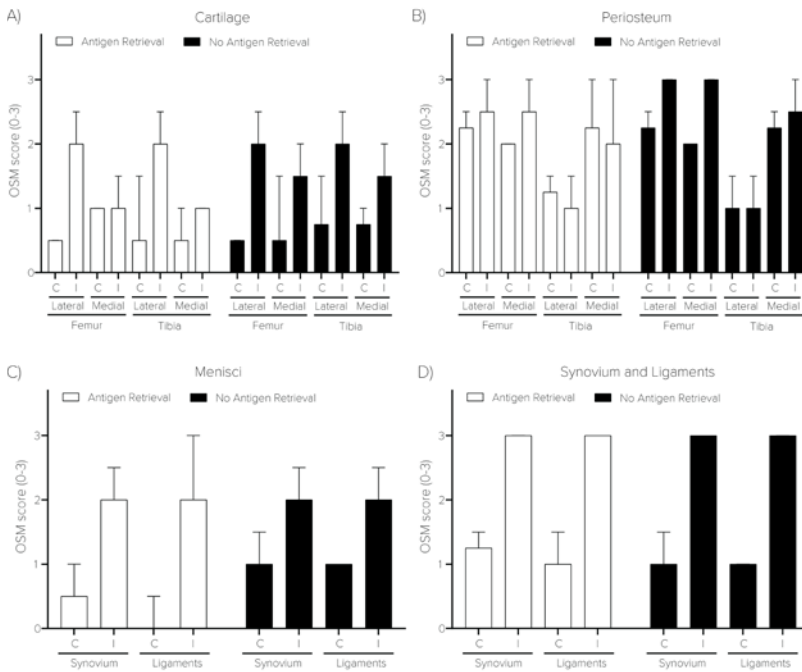


Figure S1. Effect of antigen retrieval on OSM scoring in the PGPS model samples. OSM score per anatomical structure: cartilage (a), periosteum (b), meniscus (c), synovium, and ligaments (d). Control (C), Induced (I). 0 = no staining, 1 = slight staining, 2 = moderate staining, 3 = extensive staining. Data are presented as median and 95 % CI.

Due to limited availability of samples, seven samples from the PGPS model were stained for OSM with and without antigen retrieval. OSM was scored as described before (0-3) for cartilage, periosteum, synovium, meniscus and ligaments. Scoring was done in a random order by two independent observers blinded for treatment and staining method, and scores were averaged.

The intra-class correlation coefficient (ICC) was used to calculate the agreement in OSM score between the two staining methods. A two-way mixed-effect model based on a mean-rating ($k=2$) and absolute agreement was used. ICC estimates and the 95% confidence intervals (CI) were reported. The ICC values are above 0.870 for all the joint structures, indicating that antigen retrieval does not affect the scoring for the PGPS model. Thus, the samples without antigen retrieval were used.

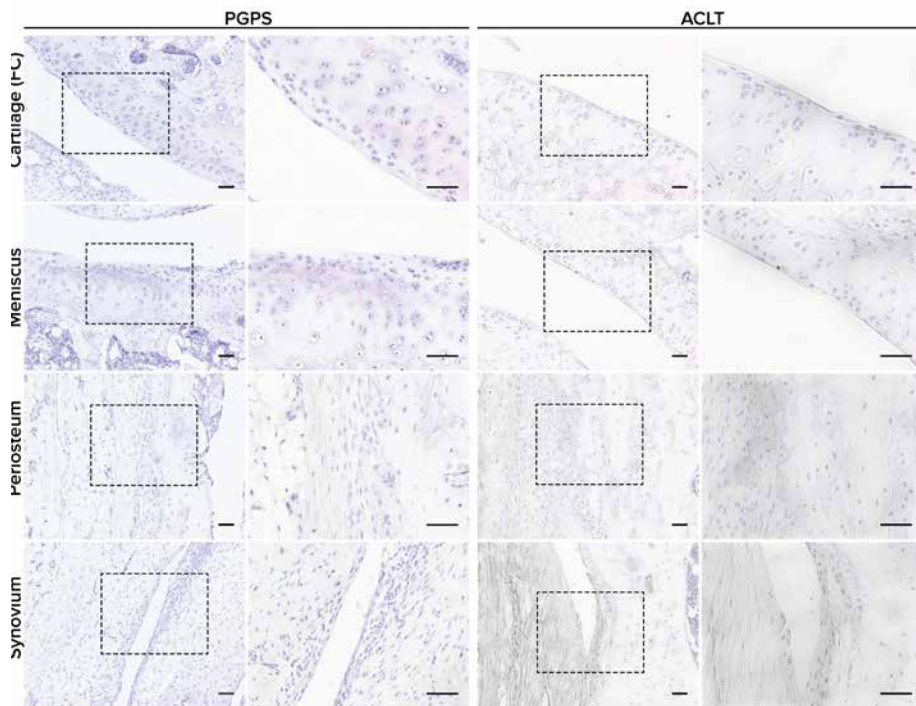


Figure S2. Negative control with mouse IgG isotype. Representative pictures of different joint structures: Femur condyle (FC) cartilage, meniscus, periosteum and synovium. Scale bar: 50 μ m.

Table S2. Joint compartments

Structure	Compartment
Cartilage	Lateral femoral condyle
	Medial femoral condyle
	Lateral tibia plateau
	Medial tibia plateau
Periosteum	Lateral femur
	Medial femur
	Lateral tibia
	Medial tibia
Meniscus	Lateral
	Medial
Synovium	Femorotibial synovium
Ligaments	Collateral ligaments

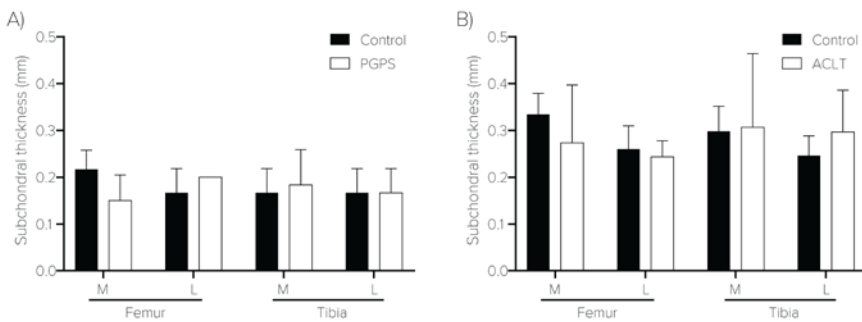


Figure S3. Subchondral bone sclerosis. Subchondral bone thickness measured by μ CT in the PGPS (a) and ACLT + pMMx (b) models. Subchondral bone thickness was measured in the medial and lateral compartments of both femur condyle and tibia plateau.

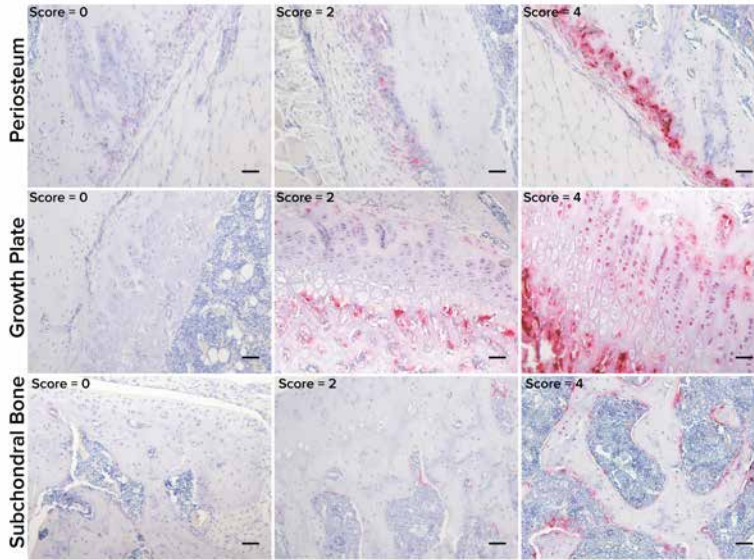


Figure S4. Trap staining. Representative pictures of different joint structures quantified for TRAP staining: periosteum, growth plate and subchondral bone.

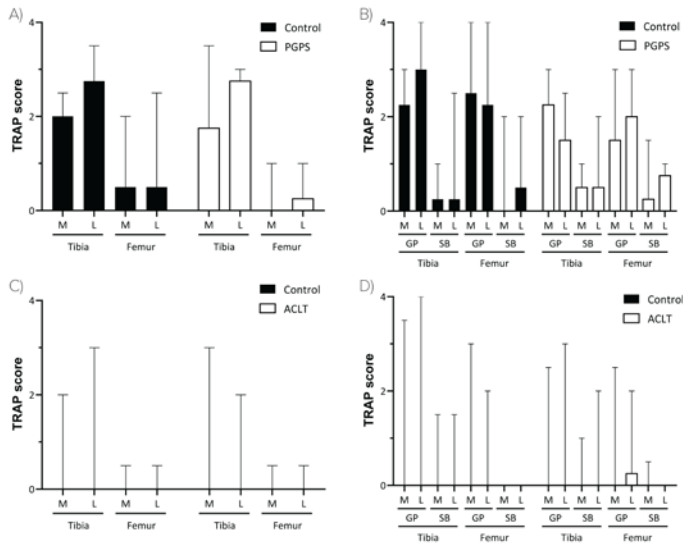


Figure S5. Quantification of TRAP staining. TRAP staining was performed in the knee sections of the PGPS (a and b), and ACLT + pMMx (c and d) models. TRAP staining was scored in periosteum (a and c), growth plate (GP) and subchondral bone (SB) (b and d) for tibia and femur in both medial (M) and lateral (L) compartments. Scoring was done in a random order by two independent observers blinded for treatment (JPG, AK), and scores were averaged. Data are presented as median and 95 % CI.

Table S3. Spearman's correlation between OSM and remaining cytokines

OSM		
Cytokines	Spearman's rho	p value
IL-1 α	0.461	0.016*
IL-1 β	0.193	0.335
IL-4	0.289	0.144
IL-6	0.350	0.074
IL-8	0.035	0.863
IL-7	0.450	0.019*
IL-10	0.106	0.599
IL-13	0.359	0.066
TNF- α	0.481	0.011*
IFN- γ	0.573	0.002*
IL-1Ra	0.038	0.852

Table S4. Differences in cytokine concentration between patient groups (OSM- - OSM+)

Cytokine	Difference	Sig.	95% Confidence Interval	
			Upper	Lower
IFN- γ	-94.90	0.001	-39.43	-217.65
IL-1 α	-20.91	0.003	-8.93	-45.78
TNF- α	-4.35	0.017	-1.28	-13.30
IL-7	-4.00	0.050	-0.97	-14.03
IL-4	-1.64	0.052	-0.61	-3.66
IL-6	-1743.25	0.094	-150.13	-16669.00
IL-13	-18.74	0.097	-5.13	-52.89
IL-1 β	-6.92	0.291	-0.62	-33.31
IL-1Ra	557.27	0.399	968.29	27.67
IL-8	47.28	0.399	27.90	7.05
IL-10	-4.05	0.595	0.59	-38.39



CHAPTER 6

CONTRAST ENHANCED COMPUTED TOMOGRAPHY FOR REAL-TIME QUANTIFICATION OF GLYCOSAMINOGLY- CANS IN CARTILAGE TISSUE ENGINEERED CONSTRUCTS

João Pedro Garcia, Alessia Longoni, Debby Gawlitta, Antoine J.W.P. Rosenberg, Mark W. Grinstaff, Juha Töyräs, Harrie Weinans, Laura B. Creemers, Behdad Pouran

Published in Acta Biomaterialia

Abstract

Tissue engineering and regenerative medicine are two therapeutic strategies to treat, and to potentially cure, diseases affecting cartilaginous tissues, such as osteoarthritis and cartilage defects. Insights into the processes occurring during regeneration are essential to steer and inform development of the envisaged regenerative strategy, however tools are needed for longitudinal and quantitative monitoring of cartilage matrix components. In this study, we introduce a contrast-enhanced computed tomography (CECT)-based method using a cationic iodinated contrast agent (CA4+) for longitudinal quantification of glycosaminoglycans (GAG) in cartilage-engineered constructs. CA4+ concentration and scanning protocols were first optimized to ensure no cytotoxicity and a facile procedure with minimal radiation dose. Chondrocyte and mesenchymal stem cell pellets, containing different GAG content were generated and exposed to CA4+. The CA4+ content in the pellets, as determined by micro computed tomography, was plotted against GAG content, as measured by 1,9-dimethylmethylene blue analysis, and showed a high linear correlation. The established equation was used for longitudinal measurements of GAG content over 28 days of pellet culture. Importantly, this method did not adversely affect cell viability or chondrogenesis. Additionally, the CA4+ distribution accurately matched safranin-O staining on histological sections. Hence, we show proof-of-concept for the application of CECT, utilizing a positively charged contrast agent, for longitudinal and quantitative imaging of GAG distribution in cartilage tissue-engineered constructs.

1. Introduction

Joint disorders are a major cause of morbidity and disability worldwide, and represent both significant healthcare and socio-economical burdens³. Osteoarthritis and joint trauma, which adversely affect articular cartilage, ultimately lead to its degradation over time^{1,41}. The extracellular matrix (ECM) of cartilage is mainly composed of proteoglycans, collagen II, and water¹. The pathogenesis of degeneration is still poorly understood, however degradation is accompanied by breakdown of proteoglycans, which inherently induces a reduction in the mechanical properties and poorer functional performance of the tissue¹. Currently, disease modifying therapies remain unavailable for OA and treatments are limited to pain relief and palliative care at early stages, and joint prosthesis at the end-stage¹⁵. Hence, there is a need for new treatment modalities that promote tissue repair and regeneration. In this context, tissue engineering and regenerative medicine are of interest as therapeutic approaches^{5,95}, which employ the use of cells, biomaterial scaffolds, and/or stimulatory factors to ultimately produce cartilaginous-like tissue⁹⁵. Currently, most of the available techniques to assess the effects of these factors on matrix production and tissue quality are destructive. Usually, engineered-tissues are harvested at mid or endpoints and subjected to biochemical assays such as the 1,9-dimethylmethylene blue (DMMB) and hydroxyproline assays for quantification of total glycosaminoglycans (GAGs) and collagen content, respectively^{360,408}. In addition, constructs are processed for histology and immunohistochemistry (IHC), which only provide a two-dimensional and qualitative assessment of matrix components and tissue quality^{98,409}. However, the detailed understanding of the regeneration process over time is of critical importance for achieving full regenerative potency *in vitro* and *in vivo*. Therefore, it is of significant importance to develop non-invasive and non-destructive imaging techniques for real-time, three-dimensional (3D), and quantitative monitoring of cartilage tissue-engineered constructs. Such techniques will enable monitoring of *in vitro* regeneration over time, evaluation of ECM components, optimization of chondrogenic activity, and, ultimately, screening to identify the best performing tissue constructs before implantation.

Efforts are ongoing to develop such tools and techniques. For example, ultrasound is used as a standalone procedure or in combination with fluorescence techniques to assess both matrix composition and mechanical properties in cartilage tissue-engineered constructs^{106-108,410,411}. More recently, a set of reporter genes is described for transfection of MSCs as a monitoring tool for real-time characterization of the chondrogenic differentiation process⁴¹². Also dielectric impedance spectroscopy was proposed as a label-free and non-destructive method to evaluate cellular viability and survival during and after biofabrication processes⁴¹³. Despite these recent advances, most of the described techniques are qualitative, do not quantify ECM components, or lack the resolution to assess the 3D distribution of the matrix components.

Contrast-enhanced computed tomographic (CECT) imaging is a rapid and readily available imaging modality used to study many different tissues⁴¹⁴, namely tissues with

low X-ray attenuation to include articular cartilage^{100,415-418}, meniscus⁴¹⁹⁻⁴²¹, intervertebral disc⁴²²⁻⁴²⁴, and xyphoid cartilage⁴²⁵. Due to the compositional differences among these tissues, contrast agent diffusion and flux will vary^{416,420}. While GAGs are mainly responsible for electrostatic interactions, collagen fibers will drive steric hindrance⁴²⁰. CECT provides unique high-resolution 3D information and quantification on composition and distribution of crucial constituents within articular cartilage. Charge-driven transport of negatively or positively charged iodinated contrast agents (i.e., ioxaglate and CA4+, respectively) provides more efficient imaging of GAGs with greater sensitivity⁴²⁶⁻⁴²⁹. Due to the anionic fixed charge of cartilage ECM, anionic contrast agents inversely correlate with GAG content, while positively-charged contrast agents display a positive correlation with GAG content with considerably higher sensitivity^{100,416,424,426,430-434}. Hence, we hypothesize that CA4+-based CECT will allow for longitudinal imaging and GAG quantification in cartilage tissue-engineered constructs. In this work, we propose a CECT-based approach as a high-resolution 3D “histology” technique for real-time spatiotemporal quantification of total GAG content in tissue-engineered constructs, which potentially replaces the currently available destructive assays.

2. Materials and methods

2.1. Cell isolation and culture

Human articular chondrocytes (ACs) were isolated from articular cartilage from patients with OA undergoing total knee arthroplasty. The anonymous use of redundant tissue for research purposes is part of the standard treatment agreement with patients in the University Medical Center Utrecht and was carried out under protocol n° 15-092 of the UMCU's Review Board of the BioBank. Chondrocytes were isolated by mincing and subsequently digesting the cartilage overnight at 37 °C in Dulbecco's Modified Eagle's Medium Glutamax (31966, DMEM, Gibco) supplemented with 0.15 % (w/v) type II collagenase (CLS-2, Worthington Biochemical Corporation), 10 % (v/v) Fetal Bovine Serum (FBS, S14068S1810, Biowest), and 100 U/mL penicillin and 100 mg/ml streptomycin (15140122, Gibco).

Undigested debris was removed using a 70 µm cell strainer followed by a PBS wash. Subsequently, cells were plated and grown in a humidified incubator at 37 °C and 5 % CO₂ with expansion medium consisting of DMEM supplemented with 10 % FBS, 0.2 mM ascorbic-2-phosphate (ASAP, A8960, Sigma-Aldrich), 100 U/mL penicillin, 100 mg/ml streptomycin and 10 ng/mL basic fibroblast growth factor (bFGF, 233-FB; R&D Systems). Medium was renewed every 3 days. Cells were expanded until passage one, frozen, stored, and subsequently thawed and used for experiments at passage 2.

Human mesenchymal stem cells (MSCs) were isolated from the bone marrow aspirate of a 20-year old female patient. The aspirate was taken after informed consent, according to a protocol approved by the local Medical Ethics Committee (TCBio-08-001-K University Medical Centre Utrecht, The Netherlands). The mononuclear fraction

was separated using Ficoll-paque (GE17-5446, Sigma-Aldrich) and selected based on their plastic adherence. MSCs were cultured in a humidified incubator at 37 °C and 5 % CO₂ with MSC expansion medium consisting of α -MEM (22561, Gibco) supplemented with 10 % FBS, 0.2 mM ASAP, 100 U/mL penicillin with 100 mg/mL streptomycin and 1 ng/ml bFGF. The medium was refreshed three times per week and MSCs were passaged at subconfluency. Subsequently, MSC multilineage potential was confirmed as previously described⁴³⁵. MSCs were used for experiments at passage 4.

For the experiments, ACs and MSCs were pelleted by centrifugation at 300 g for 6 min at a density of 2×10^5 and 2.5×10^5 cells per pellet, respectively. Subsequently, AC pellets were cultured in high glucose DMEM medium containing 100 U/mL penicillin and 100 mg/mL streptomycin, 0.2 mM ASAP, 1x insulin-transferrin-selenium-ethanolamine (ITS-X, 51500056, Gibco), and 50 μ g/mL L-proline (P0380, Sigma-Aldrich) in a humidified incubator at 37 °C and 5 % CO₂. MSCs were cultured in chondrogenic differentiation medium, consisting of high glucose DMEM supplemented with 1 % ITS premix (354352, Corning), 10^{-7} M dexamethasone (D8893, Sigma), 100 U/mL penicillin and 100 mg/mL streptomycin, and 0.2 mM ASAP. Pellets of ACs and MSCs were cultured for 14, 21 and 28 days in the presence or absence of 10 ng/ml of transforming growth factor beta 1 (TGF- β 1, 240-B, R&D Systems).

2.2. Cytotoxicity

The contrast agent CA4+ (MW = 1354 g/mol, q = +4) was synthesized and provided by the lab of Mark W. Grinstaff²⁶. Cytotoxicity of CA4+ was examined by measuring the activity of lactate dehydrogenase (LDH) and assessing metabolic activity of the cells by the Alamar Blue assay. At day 0, 12000 primary human OA chondrocytes were plated in ultra-low attachment 96-well plates and incubated for 24 hours in DMEM medium containing 100 U/mL penicillin and 100 mg/mL streptomycin, 0.2 mM ASAP, 1x ITS-X, and 50 μ g/mL L-proline. Subsequently, CA4+ was added to the cells at different concentrations of 2, 4, 8, 16 and 20 and 30 milligrams iodine per ml (mg/ml) followed by 3 or 24 hours incubation. Cells non-exposed to CA4+ were used as negative control. Upon incubation, conditioned medium was collected and analysed for LDH activity using the Cytotoxicity Detection KitPLUS (4744926001, Roche) following the manufacturer's instructions. Cytotoxicity was expressed as a percentage of the (maximum) toxicity in cells treated with 0.15 % Triton X-100, according to the manufacturer's instructions.

The medium was then changed to culture medium containing 10 % (v/v) Alamar Blue and incubated overnight. Fluorescence of the medium (ex = 544 nm, em = 620 nm) was measured in a microplate reader (Fluoroskan Ascent, ThermoFisher Scientific). The metabolic activity was expressed as a percentage of the viability of untreated cells. Experiments were repeated for three different donors.

2.3. CA4+ incubation and μ CT scanning

Pellets were incubated in a solution containing 4 mg/ml CA4+ in culture medium for 3 hours. After incubation, the medium was removed from the culture tube and μ CT

was performed at voxel size of $20 \mu\text{m}^3$ in four different protocols, namely I) 90 kV tube voltage with i) 3 minutes and ii) 26 seconds scan time, and II) 70 kV tube voltage with i) 3 minutes and ii) 26 seconds scan time, all under $200 \mu\text{A}$ tube current. The mentioned tube voltages were chosen to achieve a higher signal-to-noise ratio, and hence better resolution and sensitivity. The samples were scanned in 15 ml falcon tubes and, before imaging, medium was removed, however complete removal of the CA4+ solution was not observed. Scanning was performed using a micro-computed tomography scanner (μCT , Quantum FX, Perkin Elmer, USA). 3D reconstruction was carried out automatically after completion of each scan using the scanner's software (Quantum FX μCT software, Perkin Elmer, USA). A phantom series of CA4+ at increasing concentrations (0, 2.5, 5, 10, 20 and 40 mg/ml) was used to normalize the grey values measured within the pellets, and hence convert them to CA4+ concentrations. To this end, three regions of interest were taken for each pellet and average pixel value was converted to average CA4+ concentration, based on the phantom series. CA4+ content was calculated by multiplying average CA4+ concentration in the pellets by pellet volume (Equation 1) obtained by global segmentation upon applying a noise removal filter using Fiji (software version 1.50, National Institutes of Health, Bethesda, USA) and BoneJ plugin^{328,436}.

$$\text{CA4}^+ \text{ content} = \text{CA4}^+ \text{ concentration} \times \text{Pellet volume (1)}$$

After scanning, $300 \mu\text{l}$ of plain medium was added to the pellets overnight to promote washing out of the CA4+, thus preventing interference with DMMB. Upon washing, pellets were digested with papain and GAGs were measured using DMMB. DMMB was additionally performed on the washing media. Total GAGs were then plotted against CA4+ content. Experiment was performed in triplicate and samples were pooled for linear regression analysis. The equation obtained from the CA4+/GAG linear regression was used to obtain predicted GAG content values in subsequent experiments. For validation of the established equation, a different set of pellets was scanned upon culturing. After scanning, pellets were digested in papain followed by DMMB assay. The measured GAG values were plotted against predicted values obtained using the established equation.

X-ray doses of each scanning protocol were measured using RaySafe Solo (Ray Safe, Sweden) dosimeter.

2.4. Dynamic and longitudinal assessment of GAG content and distribution

Human ACs were pelleted and cultured as described in section 2.3. Pellets were cultured for a total of 31 days. Culture medium was collected and replaced twice a week. CA4+ incubation and μCT scanning were performed at days 14, 21 and 28. A day before scanning, medium was replaced by medium containing 10 % (v/v) Alamar Blue followed by overnight incubation. The day after, metabolic activity was evaluated by measuring fluorescence in the medium as mentioned in section 2.2. The pellets were then incubated with $300 \mu\text{l}$ of 4 mg/ml CA4+ for 3 hours and subsequently scanned at 70 kV tube voltage for 26 seconds. After scanning, pellets were washed twice in $600 \mu\text{l}$

of plain medium for 1 and 3 hours, respectively. The washing was performed to ensure faster and more efficient removal of CA4+ to decrease the probability of cytotoxic effects and interference with subsequent μ CT scans. Metabolic activity was again measured post-scanning. DMMB was performed in the collected medium every 3 or 4 days to quantify GAG release. At the end of the 32-day culture period, pellets were digested and processed for GAG and DNA analysis by DMMB and Pico Green, respectively. Non-treated (no scan and no CA4+) pellets as well as pellets exposed to scanning or CA4+ incubation alone were taken as controls to evaluate their individual effects on metabolic activity. A longitudinal scheme of the experiment is depicted in Fig. 4a.

2.5. Comparison between histology and μ CT imaging

Human ACs and MSCs were pelleted and cultured for 14 days as described above in the absence or presence of TGF- β . Additionally, as a more relevant tissue culture model, MSCs were cultured in collagen type I hydrogels. To fabricate the hydrogels, 1×10^6 MSCs (cell density of 20×10^6 cells/ml) were mixed with 50 μ l of a 4 mg/ml collagen type I solution (Corning, 354249), which was allowed to gel for one hour at 37 $^{\circ}$ C, 5 % CO₂. Upon gelation, hydrogels were cultured in chondrogenic medium in the presence of 10 ng/ml TGF- β for 28 days.

At the endpoint, the constructs were incubated with 4 mg/ml CA4+ for 3 hours. After incubation, the medium was removed and pellets were embedded in TissueTek (4593, Sakura) and snap frozen in cryomoulds (10 mm \times 10 mm \times 5 mm) using liquid nitrogen. The slab shape of the mold guaranteed that the constructs were scanned and sectioned in the same orientation and direction. Constructs were frozen in pairs to facilitate adjustments regarding the orientation after sectioning (by using one pellet as reference for relative position) as depicted in Fig. S1. μ CT was performed at voxel size of 20 μ m³ at a 70 kV tube voltage for both 26 seconds and 3 min under 200 μ A tube current. During scanning samples were kept frozen using dry ice.

After scanning, pellets were sectioned using a cryotome. Four sections of 10 μ m were collected every 100 μ m. Sectioning was performed according to the coordinates of the with μ CT slices.

Safranin-O/Fast-Green staining was performed to stain GAGs in the pellet sections with Mayer's hematoxylin counterstaining of nuclei. The sections were imaged with a light microscope (BX51, Olympus, The Netherlands). Images were acquired with a 1.25x magnification. Histological images were first aligned and then compared to their corresponding slices in the μ CT stacks using Fiji.

2.6. Statistical analysis

All data were analysed using IBM® SPSS® Statistics version 21. Cytotoxicity on monolayer was analysed by univariate analysis of variance using a randomized block design. A post-hoc test with Bonferroni correction was applied for multiple comparisons between treatments (p value < 0.05).

Linear regression analysis was applied to evaluate whether the CA4+ content

correlated with GAG content. The coefficient of determination (R^2) was used to assess the correlations. Significance level was set at p value < 0.05. The intra-class correlation coefficient (ICC) was used to calculate measurement reliability for the GAG prediction model. A two-way mixed-effect model based on mean-rating (k=2) and absolute agreement was used, as previously described³⁹³. ICC estimate and the 95 % confidence intervals (CI) were reported.

Data on longitudinal measurements of metabolic activity and GAG release were analysed using a linear mixed model, followed by pairwise comparison with Bonferroni adjustment (p value < 0.05). Model selection was based on the lowest Akaike Information Criterion. Donor served as random effect factor and condition, days and their interaction served as fixed effect factors. Regression coefficients were estimated by the maximum likelihood method.

Accuracy of the established equation was evaluated by Pearson's correlation. Additionally, relative error was calculated for each measurement, according with the following formula (Equation 2):

$$\text{Relative error} = \frac{|\text{Predicted value} - \text{Real value}|}{\text{Real value}} \times 100\%$$

Differences in total GAG content and GAG/DNA ratio between the treatment conditions were determined by univariate analysis of variance using a randomized block design. The data were first logarithmically transformed so the assumptions of normality of residuals and homogeneity of variances were met. A post-hoc test with Bonferroni correction was applied for multiple comparisons (p value < 0.05),

3. Results

3.1. Cytotoxicity

To determine the boundary concentration of CA4+ in terms of cytotoxicity, ACs were incubated with increasing concentrations of CA4+ (2 to 30 mg/ml) for 3 and 24 hours.

With concentrations up to 30 mg/ml and 3 hours incubation no cytotoxic effects were detected at metabolic activity and LDH activity levels, yet an increased metabolic activity was observed for concentrations up to 8 mg/ml (Fig. 1a and 1c). However, longer incubation times (24 hours) led to a decrease in metabolic activity at concentrations above 8 mg/ml (Fig. 1b). Furthermore, LDH activity increased above a CA4+ concentration of 20 mg/ml (Fig. 1d).

3.2. Correlation between CA4+ and GAG contents

AC pellets cultured in presence or absence of 10 ng/ml TGF- β for 14, 21 and 28 days were used to evaluate the relationship between CA4+ and GAG content. The CA4+ content within the pellets linearly related with the total GAG content as measured by DMMB (Fig.

2). Linear regression analysis showed R^2 values above 0.87 and p values < 0.0001 for all the scanning protocols (Table 1). The scanning protocol with a tube voltage of 70 kV and a scanning time of 26 seconds was as effective as the other protocols, and was shown to yield a lower X-ray dose (Table 1).

To validate the accuracy of the model, a different set of pellets was scanned after 3 hours of incubation with 4 mg/mL CA4+ and subsequently washed, digested and analyzed with DMMB. Predicted GAG content was calculated using equation 3 from table 1, and plotted against real GAG content as measured by DMMB (Fig. 3a). A significant correlation was observed (Pearson $r = 0.92$ $p = 0.0001$), and the mean relative error was shown to be 22 % (Fig. 3b). The relative error became negative with higher GAG contents, indicating an underestimation for these samples. The ICC value for inter-measurement reliability was 0.884, indicating a good agreement between the two predicted and measured GAGs.

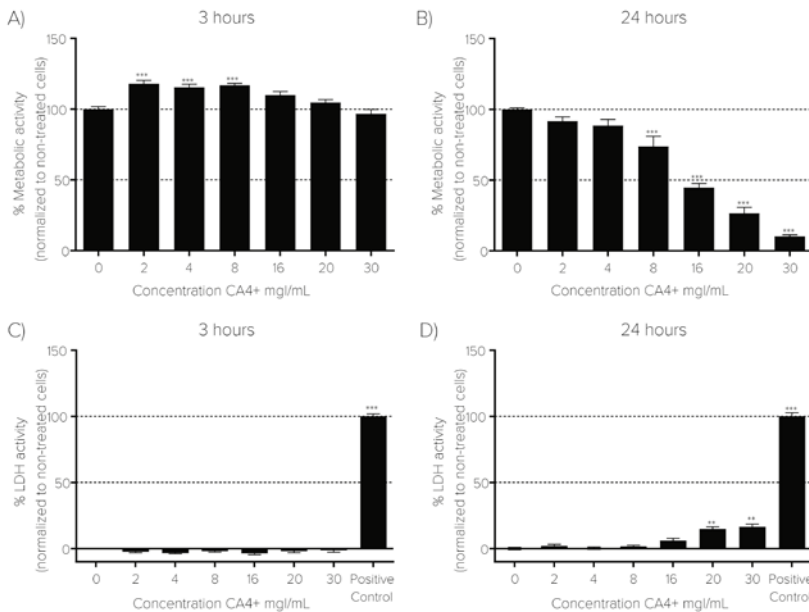


Figure 1. Effect of CA4+ on the viability of human chondrocytes. Metabolic activity and LDH activity measured after 3 (a and c) and 24 (b and d) hours incubation with CA4+ concentrations of 2, 4, 8, 16, 20 and 30 mg/mL. Cells without CA4+ were used as controls. A solution of 0.15 % Triton-X was used as positive control for complete cell lysis. Data are represented as mean \pm standard deviation (SD). Experiment was performed in three biological replicates ($n = 3$). * represents statistically significant differences compared to non-treated cells (0 mg/ml CA4+). (* $p < 0.05$, ** $p < 0.01$ and *** $p < 0.001$)

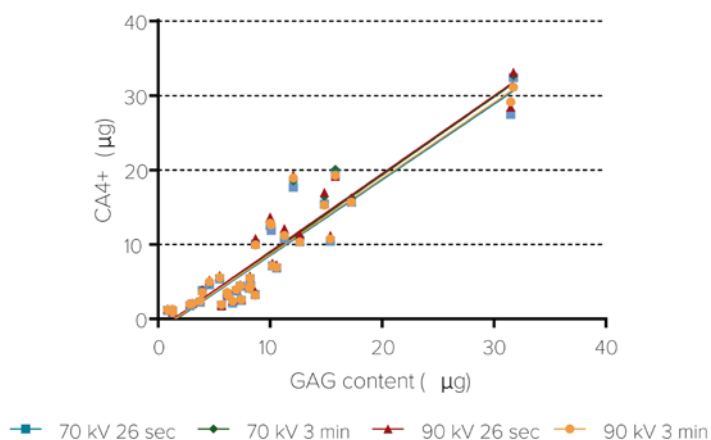


Figure 2. Correlation between CA4+ and total GAG contents upon 3 hours incubation. CA4+ and GAG contents of pellets were determined by μ CT and DMMB, respectively. CA4+ content values were plotted against total GAG content for each scanning protocol and data was fitted by linear regression. Colored lines represent linear regression for each scanning protocol. Data presented here were pooled from three independent experiments.

Additionally, pellet volume increased with GAG content (Fig. S2). Importantly, CA4+ incubation yielded a maximum concentration of 15 mg/l/mL CA4+ within the pellets (Fig. S3), which was shown to be cytocompatible. In subsequent experiments, 4 mg/l/mL CA4+ concentration and a scanning protocol of 70 kV 26 seconds were used, the latter to minimize radiation dose.

Table 1. Linear regression of CA4+ concentration with total GAG content.

Scanning Protocol (X-ray dose, mGy)	Equation	R ²	p value
70 kV 26 sec (29.50 mGy)	$GAGs = \frac{CA4^+ + 1.67}{1.01}$ (3)	0.88	<0.0001
70 kV 3 min (184.90 mGy)	$GAGs = \frac{CA4^+ + 1.70}{1.05}$ (4)	0.88	<0.0001
90 kV 26 sec (47.65 mGy)	$GAGs = \frac{CA4^+ + 1.42}{1.05}$ (5)	0.87	<0.0001
90 kV 3 min (431.50 mGy)	$GAGs = \frac{CA4^+ - 1.54}{1.02}$ (6)	0.87	<0.0001

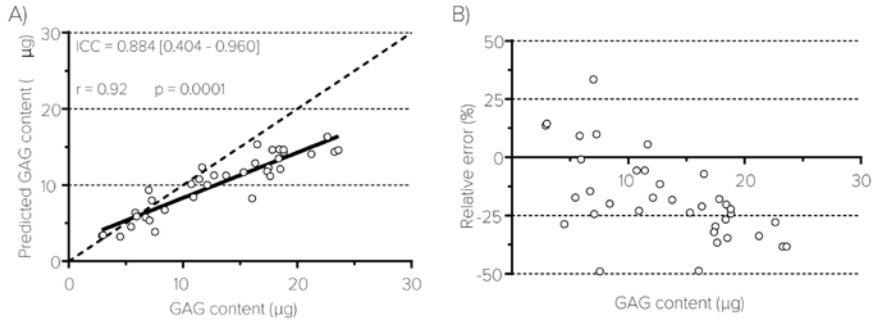


Figure 3. Validation of the prediction model. Pellets were scanned using 70 kV tube voltage and 26 sec acquisition time upon 3 hours incubation with 4 mg/ml CA4+. a) DMMB-determined GAG values were plotted against predicted values using equation 3 from table 1. Dashed line represents theoretical complete match between predicted and real values (). b) Relative error calculated based on real GAG content.

3.3. Longitudinal monitoring of chondrogenic pellets

To evaluate whether this method could be used for real-time and longitudinal measurements of GAG production, pellets were cultured for 31 days, and scanned at 14, 21 and 28 days.

The metabolic activity of the pellets was shown to be unaffected by both the μ CT scanning and the CA4+ incubation, when compared to control pellets (Fig. 4b). A statistically significant higher metabolic activity is observed between the pellets exposed only to the scanning procedure and the remaining conditions at days 21, 28 and 29 ($p < 0.05$).

GAG release into the media was shown to be unaffected by CA4+ incubation plus scanning when compared to control pellets, further suggesting the protocol does not affect GAG production (Fig. 4c). A significantly higher GAG release was observed for pellets only exposed to scanning in comparison with the remaining conditions from day 17 onwards. Despite these effects during culture, at the end of the culture period, neither GAG nor GAG/DNA levels were significantly different across the different conditions (Fig. 4d and 4e). Similarly, DNA levels were also not affected by CA4+ and/or scanning (Fig. S4). The washing protocol was shown to be effective for CA4+ removal, with most of the contrast agent being washed out of the pellets after 3 hours, and with X-ray absorption values returning to baseline after an overnight washing step (Fig. S5).

Finally, the X-ray absorption values were converted into CA4+ content (Fig. 4f) by multiplying the CA4+ concentration by the pellet volume. Subsequently, CA4+ content was used to predict total GAG content (Fig. 4g) using the previously established equation (Equation 3):

$$GAGs = \frac{CA4^+ + 1.67}{1.01} \quad (3)$$

As shown in Fig. 4f and 4g, there was a trend for increasing CA4+ content throughout the culture period, reflecting an increase in GAG content.

3.4. CA4+ spatial distribution vs. safranin-O histology

As seen in Fig. 5, CA4+ distribution via CECT matched with GAG distribution as determined by safranin-O staining. While chondrocyte pellets showed a more homogeneous GAG distribution, MSCs yielded pellets with more heterogenous GAG distribution. On the other hand, chondrocytes and MSCs that were not chondrogenically differentiated showed a very low CA4+ signal that matched the absence of safranin-O staining. The distribution of CA4+ matched safranin-O histology independently of scanning time, yet with a lower signal to noise ratio for the protocol using 26 seconds acquisition time (Fig. 5). Furthermore, CECT allowed for 3D reconstruction of the construct, providing information on 3D GAG distribution and construct volume. Also, tests on collagen hydrogels containing chondrogenically differentiated MSCs showed that CA4+ distribution matched the safranin-O staining pattern (Fig. 6, Supplementary Movie 1).

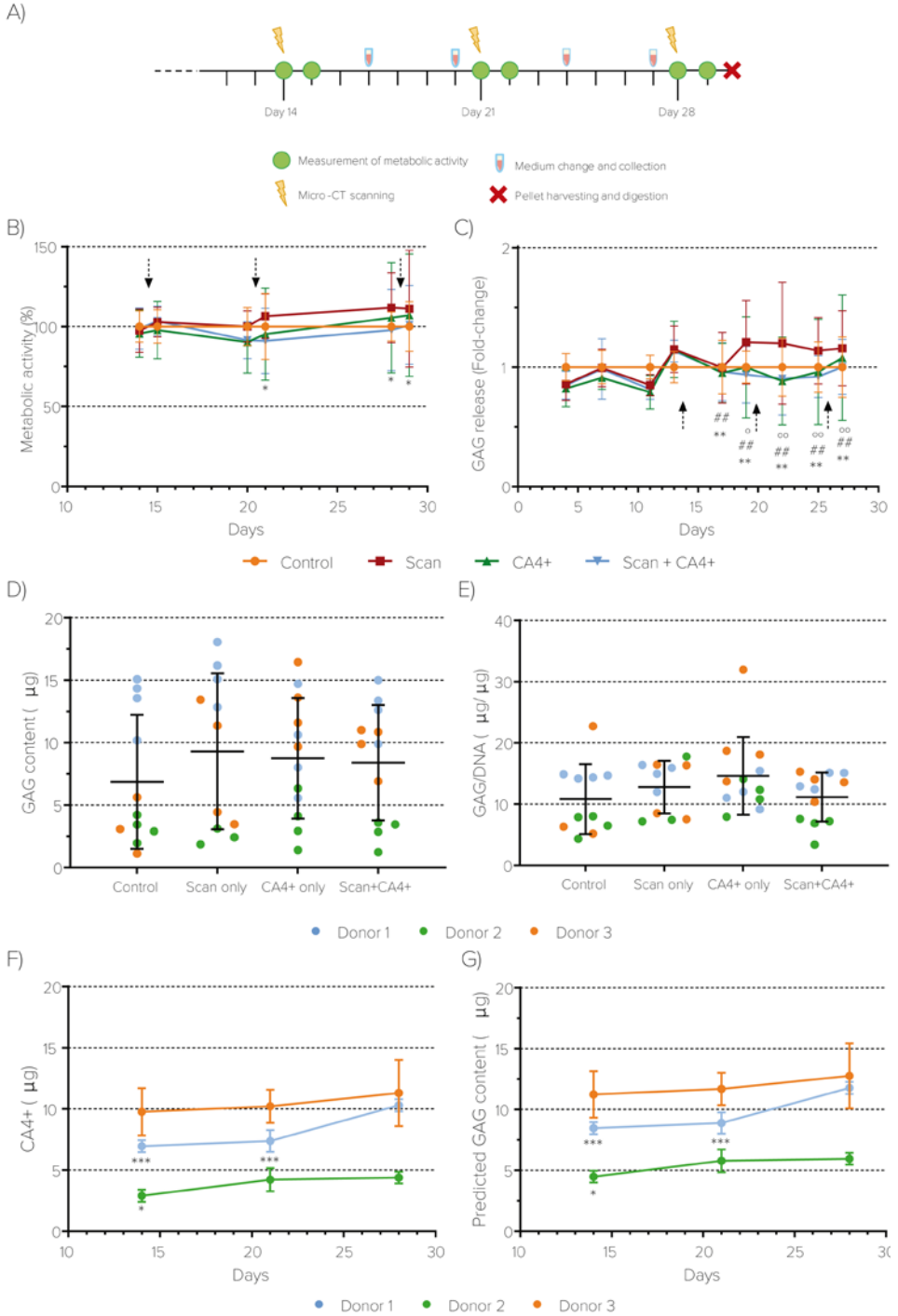


Figure 4. CECT-based longitudinal determination of total GAG content in chondrogenic pellets. a) Schematic representation of longitudinal monitoring of chondrogenic pellets. b) Metabolic activity of chondrogenic pellets measured before and after μ CT scanning and CA4+ incubation. Data are represented as percentage of metabolic activity of control pellets ($n = 3$). c) GAG release. Data are represented as fold-change compared to the untreated control pellets at the same time point ($n = 3$). Arrows represent timing of CA4+ incubation and/or scanning. * represents statistically significant differences between the "Scan" and "Scan + CA4+" pellets. # represents statistically significant difference between the "Scan" and "CA4+" pellets. ° represents statistically significant difference between the "Scan" and "Control" groups. (* $p < 0.05$, ** $p < 0.01$ and *** $p < 0.001$). d) Total GAG content measured by DMMB after a 30-day culture period. e) GAG/DNA content measured after a 30-day culture period. Data are presented by mean \pm SD. Note that colour legends differ between figures b, c and d, e, f and g. g) CA4+ content within pellets determined using tube voltage of 70 kV and acquisition time of 26 seconds. h) Predicted total GAG content calculated based on equation (3), describing the CA4+ vs. GAG correlation determined using tube voltage 70 kV and 26 seconds acquisition time. * represents statistically significant differences between days 14 or 21 and day 28. (* $p < 0.05$ and *** $p < 0.001$)

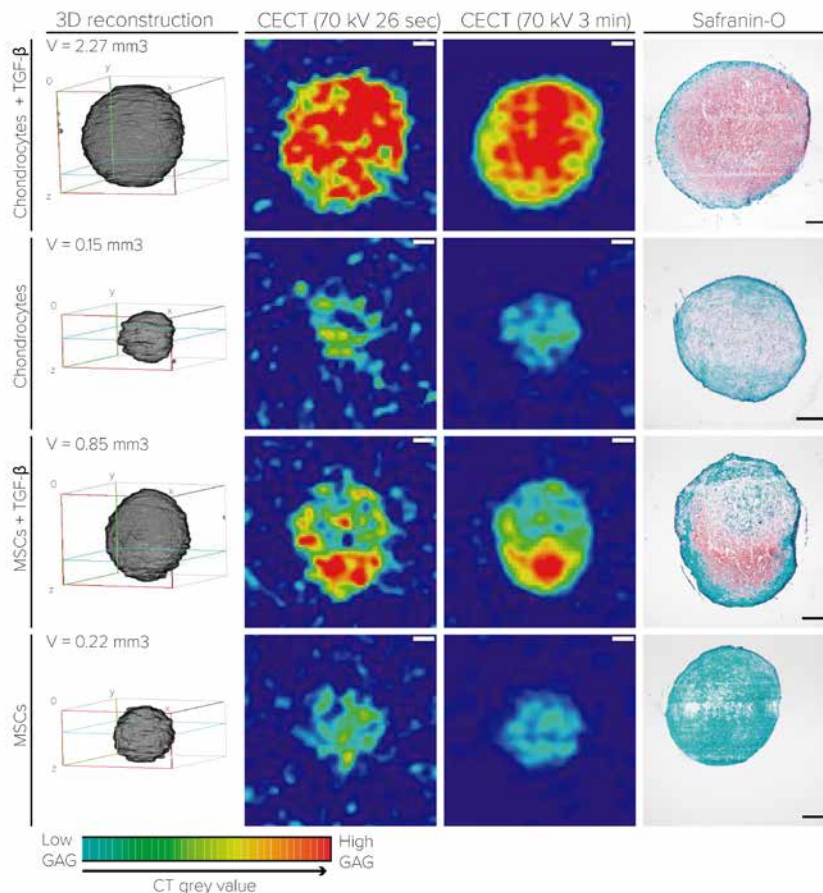


Figure 5. Comparison between CA4+ and GAG distributions. Pellets were scanned at 70 kV for i) 26 seconds and ii) 3 minutes upon 3 hours incubation with 4 mg/l/mL CA4+. Scale bar: 200 μ m.

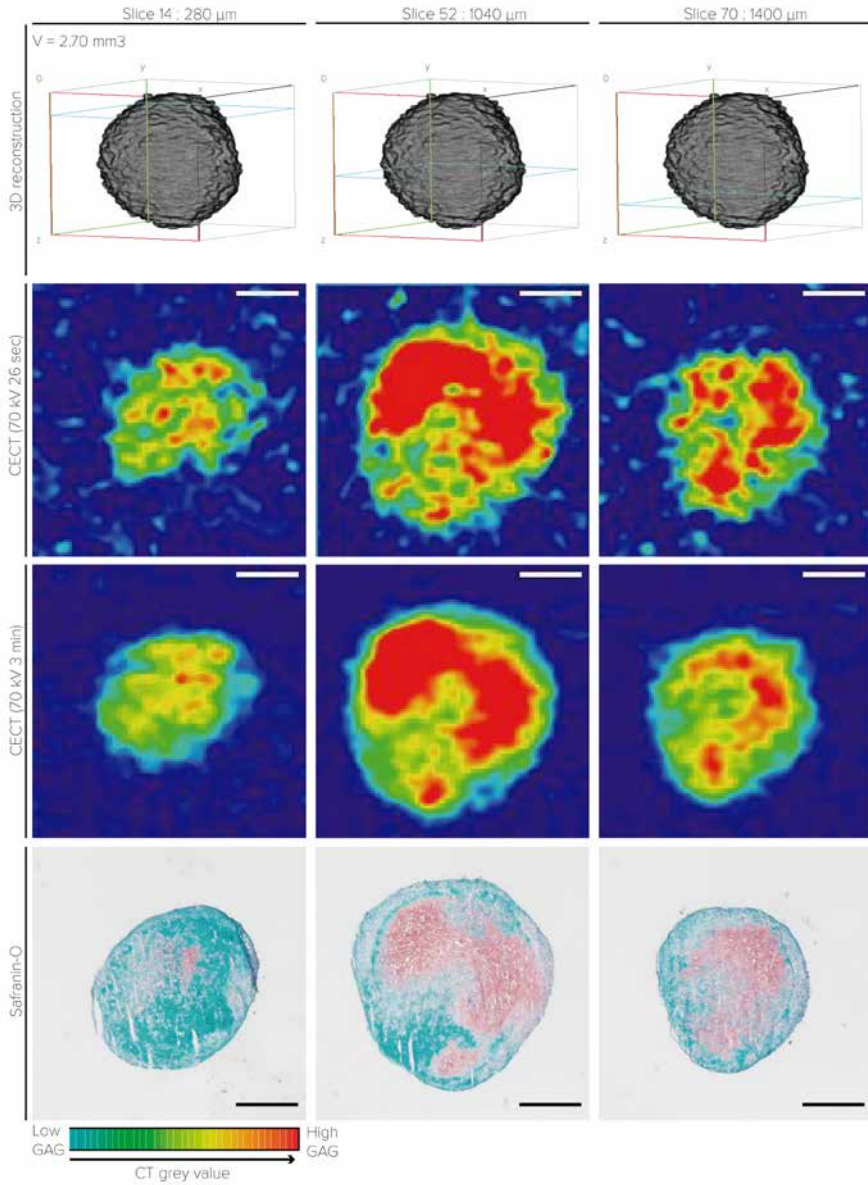


Figure 6. 3D reconstruction of CA4+ and GAG distribution in a collagen gel containing MSCs. Gels were scanned at 70 kV for i) 26 seconds and ii) 3 minutes upon 3 hours incubation with 4 mg/ml CA4+. Slice number indicates the distance from the upper part of the construct. Blue line (top row) identifies the slice corresponding to the CECT and safranin-O images. Scale bar: 500 μm.

3. Discussion

Musculoskeletal diseases such as OA or cartilage injuries are in need of new therapies, and tissue engineering and regenerative medicine strategies hold significant promise⁹⁵. However, for these strategies to rapidly progress to the clinic, additional quantitative techniques and tools are needed for the 3D and longitudinal monitoring of *in vitro* regeneration^{98,101,429}. To this end, we show proof-of-concept for the applicability of a CECT-based method, by demonstrating a correlation between CA4+ concentration and total GAG content, and its subsequently use to predict total GAG content at different timepoints. As mentioned previously, it is crucial for such method to be non-destructive and compatible with cell culture. Hence, we firstly looked at the effect of CA4+ exposure on cell viability. Concentrations above 8 mg/ml and an exposure of 24 hours led to significant negative effects on cell viability, which was likely caused by the cationic nature of the CA4+. In fact, cationic molecules and particles are known to promote cellular toxicity through interaction with and disruption of the cellular membrane⁴³⁷. Shortening the incubation time and lowering the concentration of CA4+ decreased the risk of over-exposure and hence reduced cytotoxicity. While *in vitro* toxicity of CA4+ has not been reported, previous studies on cartilage explants used incubation periods of up to 24 hours and CA4+ concentrations of 12 and 27 mg/ml^{431,432,434}. For the pellet systems in this study, 3 hours incubation with CA4+ at 4 mg/ml yielded positive and linear correlations between CA4+ and total GAG content for all evaluated scanning protocols.

For subsequent experiments, the scanning protocol with a tube voltage of 70 kV and 26 seconds, plus a CA4+ concentration of 4 mg/ml and 3 hours incubation were chosen. Validation of the technique with the previously described parameters and a different set of samples corroborated its suitability for the determination of total GAG content based on a CA4+ concentration of 4 mg/ml and 3 hours incubation. The ICC between predicted and measured GAG content was shown to be 0.884, indicating a good agreement and reliability between measurements³⁹³. However, the proposed technique is not free of error as we observed the average error for predicted GAG content to be 22 %. Likely, part of the error arises from discrepancies associated with pellet volume measurements using μ CT data with suboptimal spatial resolution. Hence, enhanced spatial resolution may improve pellet segmentation, which can help minimizing volume measurement error. Additionally, the differences in total GAG content distribution observed between the regression model and its validation can partially explain the obtained error. However, the increasing values of CA4+ content with developing chondrogenic pellets corroborates the robustness of the technique to predict GAG content longitudinally. For future studies, a higher number of constructs containing a wider range of GAG content should be used to reduce errors between regression and prediction experiments.

Subsequently, the feasibility of using such model for real-time measurements of GAG production in chondrogenic pellets was assessed. Optimization of scanning parameters and incubation protocols rendered the protocol non-toxic and harmless to chondrogenesis, as measured by GAG production. The proposed protocol was found to

be cytocompatible, with no deleterious effects on the metabolic activity of chondrogenic pellets after multiple exposures to X-rays and CA4+ (70 kV, 26 seconds/ 4 mg/ml CA4+, 3 hours). Most importantly, no significant changes were found at the endpoint on the total GAG and GAG/DNA content across conditions, proving that this method is compatible with chondrogenic culture and differentiation.

Additionally, the proposed technique allowed for quantitative and 3D imaging, not only in pellets but also in more complex and relevant tissue culture models such as hydrogels, offering insight on the 3D distribution and organization of GAGs. Comparison between CECT images and safranin-O staining on tissue sections showed that CA4+ distribution closely reflects GAG localization and distribution within the constructs, allowing for “3D histological” evaluation. Noteworthy, the proposed technique offers the unparalleled features of not only being non-destructive but also being time-efficient compared to conventional safranin-O histology which carries the risk of sectioning artifacts while being destructive and labor-intensive^{100,101,409}.

The scanning protocol yielded X-ray doses of approximately 30 mGy, which is below that reported to be cytotoxic and anti-chondrogenic for chondrocytes⁴³⁸⁻⁴⁴². A single dose of 2 or 10 Gy was reported to cause no deleterious effects on GAG synthesis or deposition in chondrocytes cultured in pellets⁴⁴¹. On the contrary, proliferation and DNA synthesis were halted temporarily and permanently with 2 and 10 Gy doses, respectively⁴⁴¹. In another study, even though MSC viability was shown to remain unaffected by a 2 Gy dose, there was a decreased expression of chondrogenic markers such as aggrecan and type II collagen⁴⁴². Importantly, most studies often report X-ray doses of 1 Gy and above, which are at least 30 times higher than the dose used in this study. Accordingly, we did not see any negative effects of μ CT imaging on cell viability or DNA content. However, we did observe an increased GAG release for scanned pellets without CA4+. Although final GAG content was not altered, it is still to be clarified whether lower X-ray doses can stimulate GAG production and/or release. Moreover, additional studies are needed to gain insight on the long-term effects of low X-ray and CA4+ exposures on cells within tissues. Such studies should address DNA damage or mutations, as well as the effects on chondrogenic markers and differentiation.

For the implementation of the proposed technique a few considerations should be considered. Firstly, validation and/or optimization of the method should be performed for every construct type, as diffusion is dependent on construct size and matrix composition^{266,443,444}. As shown before, diffusion time increases relatively to the square of the tissue thickness^{445,446}. Another important step in the protocol is the washout of CA4+, as accumulation within the construct may lead to toxicity and ultimately affect chondrogenesis, and preclude accurate real-time measurement of CA4+ and hence GAG content. Additionally, retention of the CA4+ within the construct might affect subsequent scans. A single solution of contrast agent should be prepared at the start of the experiment to avoid discrepancies in dilutions and between sequential measurements, which can potentially lead to differences in grey values and therefore negatively affect the GAG vs CA4+ correlation. Finally, automatization of image processing and analysis

will additionally render the protocol more sensitive and accurate.

Given our successful study with chondrocytes and MSCs based pellets, this method for monitoring GAG production is likely advantageous for other cartilage tissue-engineered constructs based on biomaterials such as hydrogels and bioprinted scaffolds. Additionally, future studies should examine its utility in other tissue-engineered tissues such as the cornea^{447,448}, intervertebral discs^{117,449}, and heart valves^{450,451}, where GAGs are known to play crucial morphological and physiological roles. The proposed method is also of potential use as a pre-implantation tool, where constructs are screened prior to implantation in an animal model. When implemented, this method may offer unprecedented insight on chondrogenic development within cartilage-engineered constructs and facilitate the advancement of such therapies to the clinic. In conclusion, CA4+-based CECT is a useful and non-destructive quantitative technique for 3D imaging and longitudinal assessment of GAG production and distribution in cartilage tissue engineering.

Supplementary Information

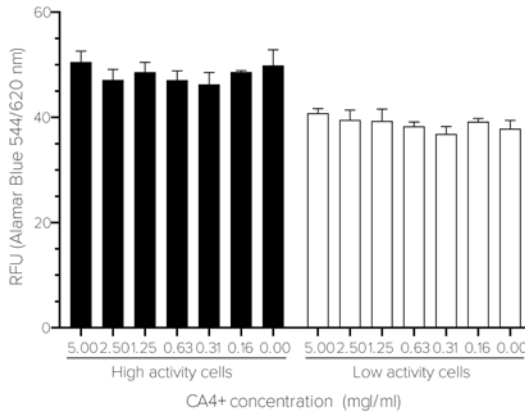


Figure S1. CA4+ does not interfere with the Alamar Blue assay. Chondrocytes were plated in monolayer i) with and ii) without TGF- β to obtain cell populations with high and low metabolic activity, respectively. One day after plating, media containing 10 % (w/v) Alamar Blue was added to the cells and incubated overnight. The media containing Alamar Blue was collected and mixed with increasing concentrations of CA4+ (0-5 mg/ml), followed by fluorescence measurements (ex = 544 nm, em = 620 nm). Raw fluorescence units (RFU). Univariate analysis of variance followed by Bonferroni post-hoc test was performed to evaluate differences in fluorescence across concentrations.

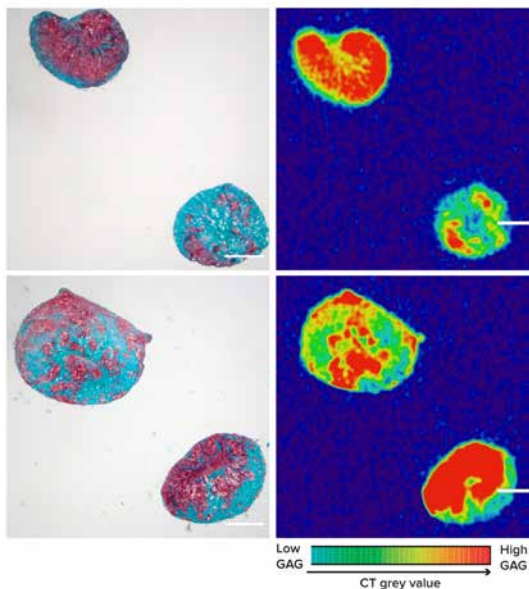


Figure S2. Representation of the alignment and comparison between histology and μ CT pictures. Scale bar: 1000 μ m.

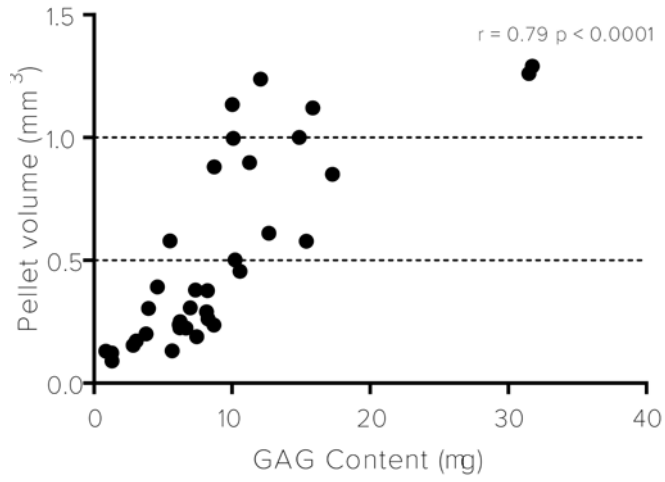


Figure S3. Pellet volume vs sGAG content. Pellet volume was measured using ImageJ and BoneJ. GAG content was measured by DMMB.

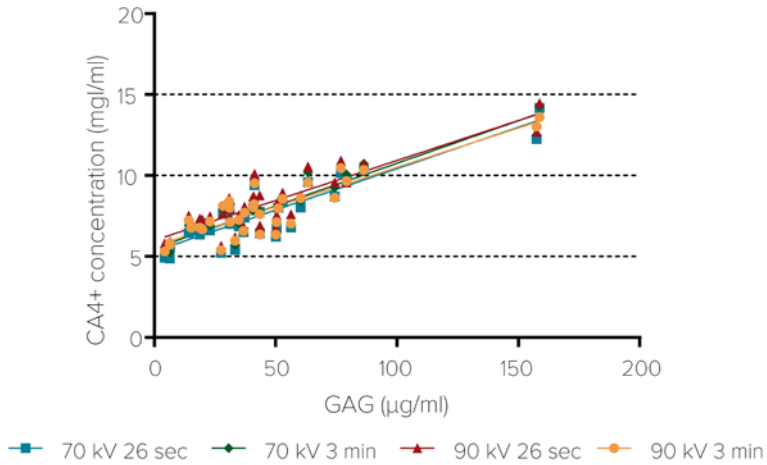


Figure S4. Correlation between CA4+ and GAG concentration upon 3 hours incubation (4 mg/ml).

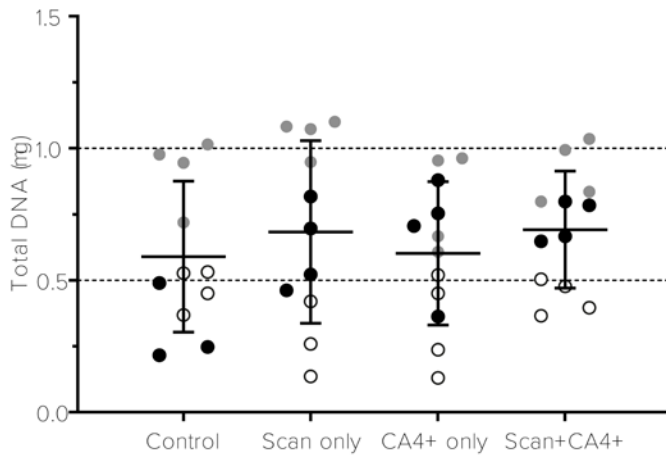


Figure S5. Total DNA content. DNA content measured after a 30-day culture period. Data are presented by mean \pm SD. Blue: Donor 1; Green: Donor 2; Orange: Donor 3.

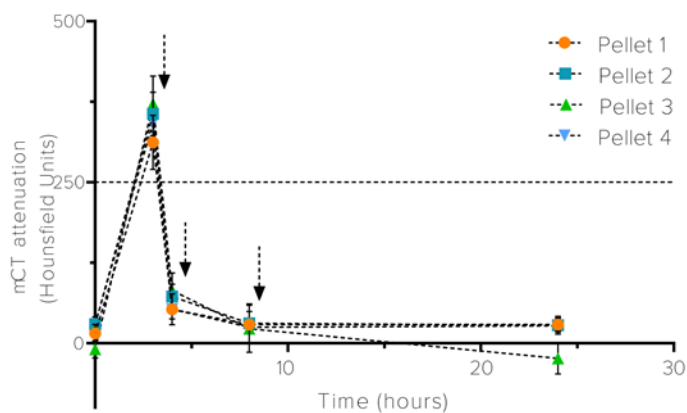


Figure S6. μ CT attenuation values of pellets upon incubation with CA4+ and washing out. Pellets were incubated with 4 mg/mL CA4+ for 3 hours. Arrows indicate medium changes. Attenuation values go back to baseline upon 4 hours wash.



7

CHAPTER 7

SUMMARY AND DISCUSSION



Summary

Osteoarthritis (OA) is one of the most predominant musculoskeletal diseases and the most common of arthritis, affecting about 15 % of the population worldwide. It is a highly debilitating condition that affects the patient's quality of life, and consequently it has a great impact on the social and healthcare systems. To date, no efficient therapy is available. Hence there is an unmet need for the development of therapeutic strategies that aim at stopping the degenerative processes additionally to the symptomatic treatment.

Over the last years, a wide number of clinical trials has been carried out testing different biological therapies for OA, however they were often presented with disappointing results. In brief, the negative results were derived from the lack of efficacy of the drugs being tested and the occurrence of severe side effects, which results from a short availability of the drugs within the joint and prolonged systemic exposure, respectively. Furthermore, most of the clinical trials reported up to now have been carried out on unselected patient populations, which could potentially have masked the efficiency of specific drugs on specific patient groups. Many obstacles are hampering the development of successful therapies for OA. Hence, in this thesis we have faced research in OA from different perspectives, and postulate that by combining target discovery and novel drug development, together with better preclinical screening tools, the development of efficient therapeutic strategies for OA will be possible.

In chapter 2, a summary of the current treatment approaches for OA is given, together with a review on the recent developments on drug delivery platforms for OA. Here, focus is given on how drug delivery systems can potentiate treatment efficiency by providing higher local drug concentration and prolonged exposure, while decreasing the probability of unwanted side effects due to systemic exposure. In line with this, in chapter 3 we show the applicability of a hydrogel platform for the delivery of locked nucleic acid (LNA)-modified antisense oligonucleotides (ASOs) targeting a cartilage degrading enzyme, ADAMTS5, as an approach for sustained intra-articular gene silencing of OA-related genes. Here we show that incorporation of the ASO in the gel yielded efficient gene knockdown up to 14-days of culture in OA chondrocytes. Following these results, we sought to evaluate the ability of this ASO sequence to silence ADAMTS5 in cartilage explants. Cartilage is an extremely dense tissue owing to its high contents of proteoglycans and collagen type II, hence drug diffusion and penetration constitutes one of the main challenges in cartilage drug delivery. Hence, in chapter 4 we explored the diffusion properties of LNA-modified ASOs in cartilage explants, as well as their ability to transfect chondrocytes in situ and promote efficient gene silencing. ASOs, as well as the gold standard siRNA, were able to diffuse into cartilage explants and co-localize

with chondrocytes. Nevertheless, only ASOs yielded significant silencing of ADAMTS5, showing the improved stability and transfection capacity of the antisense technology.

As previously mentioned, OA patients present with different symptomatic profiles, which represent different mechanisms underlying the active disease. Hence, therapy efficiency will likely benefit of targeting the right patient population. In chapter 5, we map the expression of OSM in two animal models of OA, an instability-induced model and an inflammatory model as a possible example of a protein that can both serve as a biomarker and target for a specific population. Here, we found that OSM correlates with hallmarks of arthritis in the inflammatory model but not in the instability-induced model. As a comparison with clinical data, OSM presence in the synovial fluid of OA patients associated with higher concentrations of other pro-inflammatory cytokines. Altogether, these data show that OSM associates with a more inflammatory type of OA, and could potentially be used both as a target for drug development and as a method for patient stratification.

Finally, in chapter 6, we describe the development of a quantitative and imaging method for monitoring of cartilage regeneration *in vitro*. Cartilage regeneration research is currently limited to destructive analytical methods such as histology and biochemical assays. In this chapter, we developed a computed tomography-based method that allows for non-destructive and longitudinal quantification of proteoglycans in cartilage-engineered constructs. Importantly, this technique allows for detailed 3D imaging of proteoglycan distribution, providing information that was impossible to obtain with traditional methods. The development and implementation of such techniques will be crucial for *in vitro* and preclinical screening and testing of newly developed therapies before they reach the clinic.

Discussion

Osteoarthritis (OA) is a degenerative and progressive disease of the synovial joints that affects a large part of the population worldwide¹. It is a highly impairing disease that affects the patient's quality of life, and has direct and indirect impacts on health and social care systems^{2,3}. Currently, standard-of-care treatment is limited to pain management, physical therapy and prosthetic replacement, as no therapy capable of reversing or delaying OA progression is available. Many clinical trials have been carried out in the last years testing novel therapies in OA, yet with disappointing outcomes^{6,8}. The negative outcomes may be broken down to lack of efficiency and occurrence of severe adverse effects. There is, therefore, a necessity for the discovery of new therapeutic targets and the development of novel therapies and treatment strategies^{6,11,12,78}.

Another factor that likely precluded beneficial results in some clinical trials is that these have been carried out on unselected patient populations^{8,50,51}. OA is a very heterogeneous and multifactorial disease, with patients presenting very different clinical symptoms and phenotypes^{8,76,78}. For instance, bearing in mind that inflammation levels can vary among patients⁴⁵²⁻⁴⁵⁴, it is possible that relevant clinical effects of anti-inflammatory drugs pass unnoticed if tested on an undifferentiated patient population⁸. Hence, patient stratification based on disease phenotype and biomarker profile can improve treatment outcomes, by guiding drug development and patient selection^{8,50,51}. Furthermore, the establishment phenotypes and biomarkers for OA will not only help patient classification, but also potentiate the discovery and validation of new 'druggable' targets^{76,78}.

Last but not least, improved methods for preclinical monitoring and imaging of the effect of newly developed therapies are of utmost importance^{98,455,456}. Currently, in vitro and preclinical assessment of therapy efficiency is mainly limited to destructive and invasive techniques, such as histology and biochemical assays. Developing and validating methodologies for longitudinal monitoring of regenerative approaches and/or disease progression will improve therapy screening and facilitate translation to clinical settings⁹⁸. Furthermore, validating such methodologies for clinical use will allow a more complete and reliable follow-up of treatment outcomes.

As such, within the context of the aforementioned challenges this thesis aimed to advance the current status of cartilage repair in OA and to investigate new tools and technologies that can be used to improve OA treatment.

Antisense oligonucleotides for cartilage repair

RNA-based therapeutics have since early caused great interest in both scientific and pharma community due to their high target specificity and tailorability^{52,54}. RNA therapeutics interfere with the translational machinery, leading to decreased production

of the protein of interest. By targeting a downstream molecule of the protein of interest, a quicker and longer lasting effect is obtained as compared to small molecule or protein inhibitors, as reviewed in Chapter 2.

Considering that in OA different pathways are dysregulated and increased production of pro-inflammatory cytokines and matrix degrading enzymes is observed, it is reasonable to hypothesize these same pathways as targets for modified antisense oligonucleotides (ASOs). It has been shown that metalloproteinases (MMPs) and ADAMTSs (a disintegrin and metalloproteinase with thrombospondin motifs) 4 and 5 are the main enzymes contributing for degradation of collagen type II and aggrecan^{193,314,315}, two key components of the cartilage matrix¹¹³. Different studies have shown that inhibition of ADAMTS-4 and 5 with small molecules and antibodies led to delayed cartilage degradation in ex vivo^{315,317,318} and in vivo^{319,321} models, however no results of clinical trials have been reported so far. Small molecule inhibitors against MMPs have been tested in clinical trials, yet severe side effects were noted which were attributed to the multitude of biological processes MMPs are involved throughout the body⁶. Hence, development of more specific drugs is warranted.

In chapter 3 we show proof of concept for the use of locked nucleic acid (LNA)-modified ASOs against ADAMTS-5. An ASO sequence designed against ADAMTS-5 led to efficient gene knockdown in primary human osteoarthritic chondrocytes, with and without tumor necrosis factor alpha (TNF- α) and oncostatin M (OSM) stimulation to simulate a pro-inflammatory OA environment. Importantly, the sequence was shown to be internalized by the cells and produce silencing effect without delivery agent. Whether ADAMTS-5 is the most active aggrecanase in human osteoarthritic cartilage remains unknown. Studies have shown ADAMTS-5 to be detrimental in mice cartilage degradation³²⁰, while ADAMTS-4 was shown to be the most active in bovine cartilage explants³¹⁸. In human cartilage explants, single or combined inhibition of ADAMTS-4 and ADAMTS-5 prevented cartilage degradation³¹⁵, yet further research is warranted to determine their specific roles and contribution to aggrecan breakdown in vivo.

Cartilage diffusion is considered an essential factor that can hamper treatment outcomes of disease-modifying drugs³²⁴. Contrary to synovial lining, cartilage is an avascular tissue, hence drug delivery occurs mainly by diffusion from the synovial fluid into the matrix^{12,324}. Yet, the highly dense and negatively charged network of proteoglycans and collagens make the tissue practically impenetrable to large and/or negatively charged molecules³²⁴. It has been previously shown that smaller and positively charged molecules or nanoparticles have increased diffusion and cartilage retention profiles due to lower steric hindrance and, more importantly, due to enhanced electrostatic interactions^{266-269,324,457}. Importantly, molecule diffusion in cartilage is reported to be enhanced with degenerative changes, due to loss of proteoglycans and collagen

and matrix remodeling⁴⁵⁸⁻⁴⁶⁰. While ASOs have a net negative charge, this is likely compensated by their small size, which decreases steric hindrance within the collagen and proteoglycan mesh. In line with this, we have shown in chapter 4 that fluorescently labeled ASOs are able to penetrate into full-thickness cartilage explants and co-localized with chondrocytes. These ASOs were confirmed to be active as seen by a decrease in ADAMTS-5 expression mediated by an ASO targeting its mRNA. These results are corroborated by the work of Nakamura et al. that, albeit not showing direct miRNA-181-5p knockdown in cartilage explants treated with a targeting ASO, showed a decrease in both MMP-13 and collagen type I expression, suggesting efficient diffusion and in situ activity of the ASO²²⁷.

As discussed before, virtually any mRNA can be targeted with ASOs given appropriate sequence design and modifications, hence one can envisage tailored ASO design according to the disease phenotype and dysregulated genes in individual patients. Among the most promising ones are ASO-based strategies that either address the targets of previously developed DMOADs or that target the epigenetic changes underlying OA. Cai et al. showed efficient ASO-mediated cyclooxygenase-2 (COX-2) silencing in human chondrocytes²³¹. COX-2 has been implicated in inflammatory processes that contribute to OA progression and cartilage degradation¹³⁸. In fact, oral COX-2 inhibitors are currently used as anti-inflammatory treatment for OA, yet they carry significant risks of cardiovascular and gastrointestinal side-effects¹³⁸. Different miRNAs have also been implicated in the pathogenesis of OA^{215,220,221,227,233,237}, hence constituting suitable targets for ASO-mediated silencing. Lolli et al. demonstrated the feasibility of targeting miRNA-221, an anti-chondrogenic effector, with an LNA-modified ASO²³³. Efficient knockdown of miRNA-221 was observed in human mesenchymal stem cells (MSCs) *in vitro*. Importantly, improved endogenous cartilage repair was observed upon incorporation of an ASO-loaded fibrin gel in an osteochondral defect model implanted subcutaneously in mice. Of note, in this study only lipofectamine delivered ASOs had a significant effect on cartilage repair. Whether this was due to low cellular uptake or low concentration of the ASO remains to be clarified. MiRNA-181a-5p has also been identified as a mediator of inflammation and matrix degradation in articular cartilage²²⁰. Intra-articular injection of an LNA-modified ASO against miRNA-181a-5p led to attenuated cartilage degradation and decreased expression of catabolic markers in rats and mice²²⁷. Different OA-related molecules, including enzymes and miRNAs, have been targeted with ASOs. Whether these targets are the key players in OA remains unknown, nevertheless, these studies show important proof-of-concept for the applicability of ASO-based therapies in OA.

Given the multifactorial character of OA, ASO therapies will likely be more effective upon silencing of multiple targets. Such strategies have shown promising results in other

fields such as cancer and muscular dystrophies. Combined ASO-mediated knockdown of peptides involved in colon carcinoma, namely transforming growth factor β , amphiregulin, and CRIPTO-1, was proven to be more effective in inhibiting tumor growth in a mice xenograft model when compared to single target inhibition⁴⁶¹. A cocktail of ASOs targeting the same factors also showed improved inhibition of the proliferation of ovarian carcinoma cells as compared to single ASOs⁴⁶². Similar results were observed in an orthotopic mice model of lung carcinoma, where simultaneous administration of ASOs against multidrug resistance-associated protein (MRP1) and B-cell lymphoma 2 protein (BCL2) together with Doxorubicin lead to enhanced antitumoral activity⁴⁶³. Both MRP1 and BCL2 are known to be upregulated in lung carcinoma cells upon treatment with the Doxorubicin leading to tumor resistance⁴⁶³. Also in Duchenne Muscular Dystrophy (DMD), a genetic disorder caused by mutations in the dystrophin gene, the combination of multiple ASOs has been proposed as a promising therapeutic approach⁴⁶⁴. Mutations in the dystrophin can vary in type (i.e. deletion, duplication, and nonsense) and number, therefore application of a single ASO yields beneficial effects in a limited number of patients⁴⁶⁴. Following this rationale, a study reported the use of a cocktail of exon-skipping ASOs targeting exons 6 and 8 of the dystrophin gene in a dog model of DMD^{465,466}. Combined oligo administration led to increased dystrophin expression as compared to single administration or non-treated control. Remarkably, restoration of dystrophin expression led to improvement in clinical and behavioral parameters⁴⁶⁶.

While the first steps on antisense therapeutics in OA have been taken only recently, in other diseases these have already proved clear clinical benefit, and a number of ASO-based drugs were already approved by the Food and Drug Administration (FDA)⁴⁶⁷. As example, Formivirsene, a drug developed for treatment of cytomegalovirus (CMV) retinitis, was the first ASO approved by the FDA in 1998^{468,469}. Yet, due to development of high-activity anti-retroviral therapy, and subsequent decrease in CMV retinitis cases, the marketing and clinical application of the drug has been halted⁴⁶⁷. Recently, a splice-altering oligonucleotide was approved for the treatment of spinal muscular atrophy (SMA), a genetic disease that often leads to infant death. In numerous clinical trials, the drug lead to profound beneficial effects on infants with type I and type II SMA, reducing mortality and leading to improvements in motor function^{53,470,471}. In 2019, a one-of-a-kind “n = 1” clinical study reported the development and implementation of an ASO targeting a never seen mutation in an infant patient with neuronal ceroid lipofuscinosis 7, a fatal neurodegenerative disease⁴⁷². This was a remarkable demonstration of personalized and individualized medicine, as the authors show how ASO design can be tailored to specific and rare mutations and diseases. These successes brought an enormous pharmaceutical interest in RNA-based technologies, further endorsing their potential as drug discovery platforms and therapeutics.

Even though chemical modifications render ASOs more efficient and target specific, rapid clearance from the joint space, as for other drugs, could still be major limiting factor for prolonged therapeutic effects^{11,324}. In this regard, drug delivery platforms have the potential to improve therapeutic outcomes by providing a continuous and controlled local drug release.

Intra-articular drug delivery for osteoarthritis

Intra-articular controlled delivery of DMOADs might increase the benefit:risk ratio of drugs as compared to systemic administration by, on one hand, increasing the local concentrations of the drug and, on the other, decreasing systemic exposure and risk of side effects^{8,112}. Moreover, contrary to other forms of arthritis, OA affects usually a single joint and, therefore, the localized nature of the disease makes it suitable for intra-articular drug delivery¹¹. Depending on the type and properties of the delivery platform, it can act as i) a simple drug depot that will release the drug in a controlled manner over time or ii) actively deliver its cargo to specific cells and tissues within the joint environment. Additionally, by providing a controlled and prolonged drug retention within the joint, delivery systems also diminish patient discomfort and infection risk by decreasing the number of necessary injections¹¹².

In chapter 3 we show the applicability of a fibrin and hyaluronic acid hydrogel for incorporation of an LNA-modified ASO as an approach for simultaneous resurfacing of cartilage defects in OA and prolonged silencing of ADAMTS5. A two-gel system was established composed by a gel containing chondrocytes and ASOs and a gel only bearing chondrocytes. While the latter would mimic endogenous joint tissues, the first represented a platform for cell and ASO delivery. Ideally, the ASOs would silence ADAMTS-5 in the first gel and then diffuse to the second gel, transfect resident cells and promote efficient gene silencing. Importantly, the ASO molecules were indeed shown to efficiently diffuse into the secondary gel and transfect cells. Efficient ADAMTS-5 silencing (60-70%) was observed up to 14 days of culture in both gels with a single dose of ASO. These results indicate that in a scenario where sufficient amounts of ASO would be present in the joint, the sequence would likely diffuse into cartilage and promote gene silencing as shown in chapter 4. In this study, due to the improved trafficking properties of the ASOs it was not necessary to incorporate them in delivery vehicles that would transfect them into cells. However, this is not the case for other drugs with limited transfection capacity such as siRNAs miRNAs or growth factors⁵⁵. In these cases, if the therapeutic target is located within the cartilage matrix, drugs should be incorporated or conjugated to small (< 50 nm) and positively charged carriers, as demonstrated previously^{266-269,473}. In fact, particles bigger than 50 nm have shown limited cartilage penetration and retention profiles^{265,474,475}. Taken together, these studies highlight the ability of ASOs to diffuse

within the challenging environment of cartilage to ultimately transfect chondrocytes in situ and produce efficient gene silencing.

Even though hydrogels do not help the therapeutic molecules to transfect the cells, they can load very high concentrations of the drug and act as localized drug depot. Their tunable properties, e.g. composition, charge, functionalization or degradation profiles make them perfect controlled release systems²⁹⁹. Furthermore, as reported in chapter 3, they can act as a scaffold for cell growth and cartilage repair. In this study, fibrin and hyaluronic acid were chosen due to their biocompatible properties and widespread clinical use, in particular in the orthopedic field. Fibrin has been extensively used in orthopedic procedures as cell carrier^{336,337,476} or simply as wound sealant⁴⁷⁷, while hyaluronic acid is a natural component of synovial fluid and it has been widely explored as a drug delivery platform⁴⁷⁸. Additionally, hyaluronic acid is the major ligand for CD44⁴⁷⁹, a membrane receptor expressed in chondrocytes, which can potentiate the development of cartilage-targeting strategies^{231,480}. When it comes to drug delivery to articular cartilage, careful design and selection should take into account the type of drug, target tissue and drug release profiles. For instance, while highly charged and small nanoparticles will target cartilage tissue, less charged and bigger particles will preferentially be phagocytized by synovial cells^{324,481}. On the other hand, cartilage-penetrating nanoparticles will likely potentiate a higher therapeutic effect of nucleic acid drugs as compared to a hydrogel by enhancing cartilage penetration and cell delivery^{269,324}. An alternative strategy could be the use of hydrogels/nanoparticle composites. This modular approach allows for individual tailoring of each component, resulting in a platform with enhanced physical, chemical, and biological properties⁴⁸². While hydrogels generally provide a matrix with tissue-like properties, their high porosity leads to suboptimal fast release of the drugs⁴⁸³. On the other hand, due to their smaller size nanoparticle systems have higher in vivo clearance rates. In fact, the encapsulation of drug-loaded nanoparticles in hydrogels has showed improved and prolonged drug release profiles, as compared to drug encapsulated in the gel or nanoparticle alone^{484,485}.

Although still in its infancy, the first steps on intra-articular drug delivery in OA are being made. In 2017, the first, and so far, the only drug delivery system for pain management in OA was approved by the FDA, and it is currently being commercialized under the name of Zilretta. The poly(lactic-co-glycolic acid) based microsphere incorporating triamcinolone acetonide showed prolonged drug joint residence time, and improved pain and function scores when compared to the free drug in patients with knee OA^{246,486,487}. Even though this platform only provides pain relief and does not aim at tissue repair, such studies are pioneers in demonstrating the advantages of drug delivery systems over the free drug, and will likely pave the way for the future development of delivery systems and disease-modifying drugs in OA patients.

Target discovery, drug development and patient stratification – learning from other diseases

Currently available treatments for OA are mainly based on conservative approaches seeking symptom relief and improved joint function. Recently, focus has been given to the development of drugs with ability to slow down structural progression of OA⁶. In fact, many clinical trials have been carried out testing disease-modifying agents in OA, albeit with little success^{6,8}. Therefore, there is a need for a paradigm shift on drug development in OA. Importantly, drug development needs to be accompanied by definition of OA phenotypes and patient stratification and preceded by the establishment of novel biochemical and imaging markers^{8,5178,488}.

In chapter 5, it is shown that OSM expression correlates with hallmarks of OA in an inflammatory animal model but not in an instability-induced rodent model. Additionally, in synovial fluid of OA patients, OSM presence was associated with higher concentrations of other pro-inflammatory cytokines such as TNF- α , IL-1 α and IFN γ . While further studies are warranted to confirm the involvement and association with development of arthritis in these models, this indicates that OSM could be a potential biomarker and target for inflammatory OA phenotypes. OSM is a pro-inflammatory cytokine from the IL-6 family that has been described as an important mediator of inflammation and cartilage degradation in rheumatoid arthritis (RA)³⁷²⁻³⁷⁴. As opposed to RA, where OSM is detectable and elevated in all patients, in OA OSM is only detectable in a subset of patients^{341,372,380,381}. Interestingly, OSM has been shown to correlate with synovial markers of inflammation in RA synovial fluid, namely white blood cell count³⁷². Moreover, OSM correlated with markers of aggrecan and collagen degradation in RA but not OA patients³⁴¹, suggesting a more active role of OSM during inflammatory processes.

Several biologics targeting pro-inflammatory factors have been tested in OA patients, however without clear benefit⁶⁵⁻¹⁶⁷ and despite the very promising in vitro and preclinical work^{489,490}. Importantly, clinical trials in OA are generally performed in a general population without phenotype distinction, which can subsequently mask therapeutic efficiency in a specific subset of patients⁸. Only one clinical trial was carried in a selected patient population. In this trial, the effect of Lukitizumab, an anti-IL-1 β antibody, was evaluated in patients with knee OA and with evidence of synovitis¹⁶⁷. Here, despite selection of patients with evidence of inflammatory processes, the antibody targeting IL-1 β and IL-1 α did not lead to any improvement in pain scores or synovitis, suggesting that perhaps these cytokines do not play a major role in OA. Nevertheless, even if evidence on the benefit of anti-inflammatory therapies for OA in humans is lacking, it is clear that inflammation and inflammatory cytokines do contribute to disease progression^{452,491-493}. The success of such therapies is likely to depend on the discovery of new key players in

the inflammatory process, as well as the testing of therapies on selected patient groups. In this regard, in chapter 5 we postulate that perhaps OSM could be a suitable target for both drug development and definition of an inflammatory OA phenotype.

Knowledge on target-driven drug development and phenotype-guided patient stratification can be derived from diseases where personalized medicine and targeted therapies are more advanced and established. Cancer, for instance, is an excellent example of a disease where targeted treatment is implemented. While traditionally cancer treatment was mainly based on non-specific chemotherapy agents that would target rapidly dividing cells, currently more and more current therapies are matched to specific patient groups described and stratified by the underlying disease mechanisms and molecular signatures^{494,495}. One of the first examples of targeted therapy in cancer was the use of trastuzumab for treatment of HER2-positive metastatic breast cancer^{496,497}. Overexpression of HER2 was associated with aggressive breast cancer and with poor prognosis, and currently, HER2 is used as a predictive biomarker for the establishment of treatment strategies⁴⁹⁴. Larotrectinib, a tropomyosin receptor kinase inhibitor, has also been recently approved for cancer patients with a neurotrophic tropomyosin receptor kinase inhibitor gene fusion⁴⁹⁸. A tool that has been shown to be efficient in providing drug screening and personalized care is the organoid technology. Organoids are in vitro grown 3D structures derived from pluripotent stem cells or organ-progenitor cells that harbor and mimic the in vivo architecture and function of the organ they represent^{499,500}, which makes them very promising platforms for drug development and screening. One of the first reports on organoid-based personalized medicine was published on cystic fibrosis (CF)⁵⁰¹. After generating intestinal organoids from two patients, and observing a positive response to the CF drug ivacaftor, the treatment was then given to the patients who showed significant clinical improvements⁵⁰¹. Following these two successful cases, larger clinical trials are being carried out as follow up⁵⁰². In a similar manner, patient-specific cancer organoids are also being used for drug screening and testing⁵⁰³. Remarkably, cancer and tumor organoids maintain the genetic heterogeneity of the primary tumor, which constitutes an advantage when compared with less complex systems⁴⁹⁹. Financially, targeted therapeutics might appear less attractive to pharmaceutical companies due to a narrower patient population, and hence lower revenue. However, this might be compensated by faster and wider adoption of the drug due to superior clinical performance⁴⁹⁵.

In OA, further research is needed to successfully establish biomarkers for diagnosis, definition of phenotypes and as targets for drug development^{6,78}. It will be crucial to face OA as a multifaceted disease with multiple phenotypes and underlying disease mechanisms. Equally important will be to define patient populations according to their phenotype prior to clinical trials⁸. On this regard, several initiatives are being carried

out. For instance, the OA Biomarker Project and its follow-up consortium Progress OA are part of a two-stage strategy that has as a primary objective the validation of imaging and biochemical markers as predictive tools for OA progression⁵⁰⁴. Ultimately, the goal of this working group is to define and stratify patients, and therefore enrich clinical trials with responsive populations. Similarly, the European Society for Clinical and Economic Aspects of Osteoporosis and Osteoarthritis has set up a work group to discuss the role of magnetic resonance imaging (MRI) parameters as structural endpoints in clinical trials⁵⁰⁵. Additionally, since 2015, the APPROACH project is using an integrated bioinformatic platform to collect and process biomedical data of over 10000 OA patients, aiming at the definition of OA phenotypes and patient stratification.

Monitoring tools

In vitro and preclinical cartilage research is limited to methodologies that are generally invasive and destructive, thus not allowing longitudinal monitoring of samples and/or animals. This is an important drawback, particularly for tissue engineering and regenerative approaches where real-time monitoring of samples would provide information on the development of the constructs, matrix deposition and integration^{98,455,456}. Hence, development of new modalities and implementation of existing ones in tissue engineering research would allow for better characterization of tissue constructs overtime^{98,455}.

In chapter 6 we propose the implementation of contrast-enhanced computed tomography (CECT) for longitudinal monitoring and imaging of glycosaminoglycan (GAG) production and deposition in cartilage-engineered constructs. This method allows monitoring of the same samples over time, providing quantitative information on GAG deposition within the constructs. Additionally, the proposed technique allows for 3D imaging of GAG distribution, providing 3D “histological” images equivalent to standard histology methods. Considering that GAGs are also important constituents of other tissues, the technique proposed in this chapter would be potentially valuable for other regenerative approaches, such as intervertebral disc (IVD)^{110,449}, heart valves^{450,451}, and cornea^{447,448}.

Other methodologies such as ultrasound (US)⁴¹¹, optical imaging⁵⁰⁶, and MRI^{105,507} have also been applied to monitor tissue explants and tissue engineered constructs. US imaging originates from the difference in reflectivity to acoustic waves throughout tissue, which can then be correlated to matrix composition, density and mechanical properties⁹⁸. For instance, US imaging has been used to track cartilage matrix deposition^{106-108,410} and mineralization⁵⁰⁸ in hydrogels by measuring longitudinal changes in US attenuation. US has proved to be a cost-effective technique with high temporal resolution that allows for real-time monitoring, yet spatial resolution substantially decreases with penetration

depth and might constitute a problem for detailed imaging of larger constructs⁴¹¹. Optical imaging instead is based on the interaction (i.e. scattering, reflection) between tissues and infra-red, visible or ultraviolet light⁵⁰⁶. Although optical imaging, namely microscopy, is less suitable for large tissue constructs (> 1 mm), its high spatial resolution makes it a powerful tool for detailed imaging of cellular interactions and intracellular processes in cell monolayers or thin constructs (< 1 mm)⁵⁰⁶. Also within the optical methods, optical coherence tomography (OCT) has been used to image cartilage tissue ex vivo⁵⁰⁹ and in vivo during open knee surgery⁵¹⁰ and arthroscopic procedures⁵¹¹. Similarly to ultrasound, OCT detects differences in the refractive indexes of tissues and samples to near-infrared light⁵⁰⁶. Contrary to optical microscopy, OCT can image up to 2/3 mm in depth^{506,512}, making it suitable for imaging of larger tissue engineered constructs. While, to date, no reports exist on OCT-based in vitro imaging of cartilage engineered constructs, OCT has been used to monitor cartilage regeneration in preclinical animal models^{513,514}.

On the other hand, MRI has been used for imaging and monitoring in tissue engineering applications due to its superior soft tissue contrast and high imaging depth^{105,507}. MRI has also been used to monitor deposition of matrix components and to assess the mechanical properties of cartilage tissue-engineered constructs^{515,516}. However, to achieve high spatial resolution long scanning times are needed, which makes it incompatible with real-time and in vivo applications⁹⁸. Additionally, these studies often report the use of high field MRI scanners (3 Tesla and above) in order to achieve higher signal-to-noise ratios¹⁰⁵. Yet, high field MRI requires large facilities, and importantly, installation and maintenance costs are high when compared to other technologies, hindering its wider application in preclinical research.

All in all, implementation of these techniques in tissue engineering approaches will allow for better characterization of cell growth and tissue development, and more importantly, will facilitate standardization of tissue engineering approaches⁹⁸. Likely, the development of multimodal techniques will expedite such processes by combining the advantages of different methodologies, and by overcoming pitfalls of individual modalities⁴⁵⁶. Importantly, some of the developed techniques, specifically those not using ionizing radiation or radioactive labeling, will be important tools in future pre-clinical and clinical studies for measurement of treatment efficacy and outcome⁹⁸.

Knowledge transfer to intervertebral disc research

The work conducted in this thesis entails ASO-based therapeutic modalities and monitoring tools that could be transferred also to other degenerative cartilaginous diseases, such as disc-related chronic low back pain, a highly impairing condition and one of the most common musculoskeletal disorders worldwide¹¹⁰. The IVD, the connective tissue located between the vertebral bodies in the spine, shares many similarities with

the joint. Especially the inner nucleus pulposus (NP) is rich in proteoglycans, in fact the proteoglycan-to-collagen ratio is higher in articular cartilage⁵¹⁷. Importantly, it also has a very low regenerative capacity and it is often affected by degenerative processes similar to those occurring throughout OA in articular cartilage^{110,518}. The molecular mechanisms underlying the pathologies are similar⁵¹⁸, as are the obstacles limiting the development of more effective therapies, such as drug delivery to the disc and monitoring of disease and therapy progression. Therefore, it is hypothesized that the concepts and tools explored in this thesis could be applied to IVD research. Whether ASOs can efficiently transfect NP cells in situ remains to be studied, yet IVD degeneration could potentially be targeted with ASO-based strategies described in chapter 3 and 4. Even more so, regenerative strategies for disc repair could potentially benefit of the method described in chapter 6 for longitudinal monitoring of the deposition of proteoglycans in NP cell or organ culture employed in a preclinical setting.

Future directions and conclusions

OA is one of the most common musculoskeletal diseases worldwide, and to-date no true effective treatment is available, as pain medication and management only provide short-term solutions. Novel drug platforms, such as RNA therapeutics, may provide enhanced beneficial effects compared to small molecule inhibitors or other drug types that act at the protein level. Equally important, treatment strategies will potentially benefit from local drug administration and the use of drug delivery systems for prolonged presence of the drug and enhanced therapeutic effect at the joint level. OA needs to be approached as a multifactorial and complex disease, and as such, there will not be a “one size fits all” treatment strategy. Biomarker and phenotype definition will be crucial for drug development strategies at an early phase, and for clinical testing in selected patient populations at later stages. Finally, the development and implementation of new imaging and sensitive monitoring tools for in vitro and preclinical phases of drug development will be essential in determining the best conditions and parameters for cartilage and joint repair. As depicted in figure 1, the combination of these strategies and the crosstalk between them will be crucial for the development of effective OA therapies.

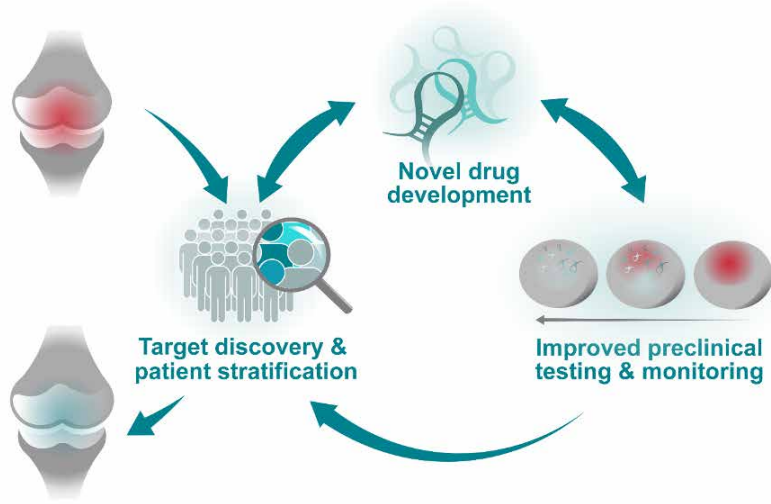
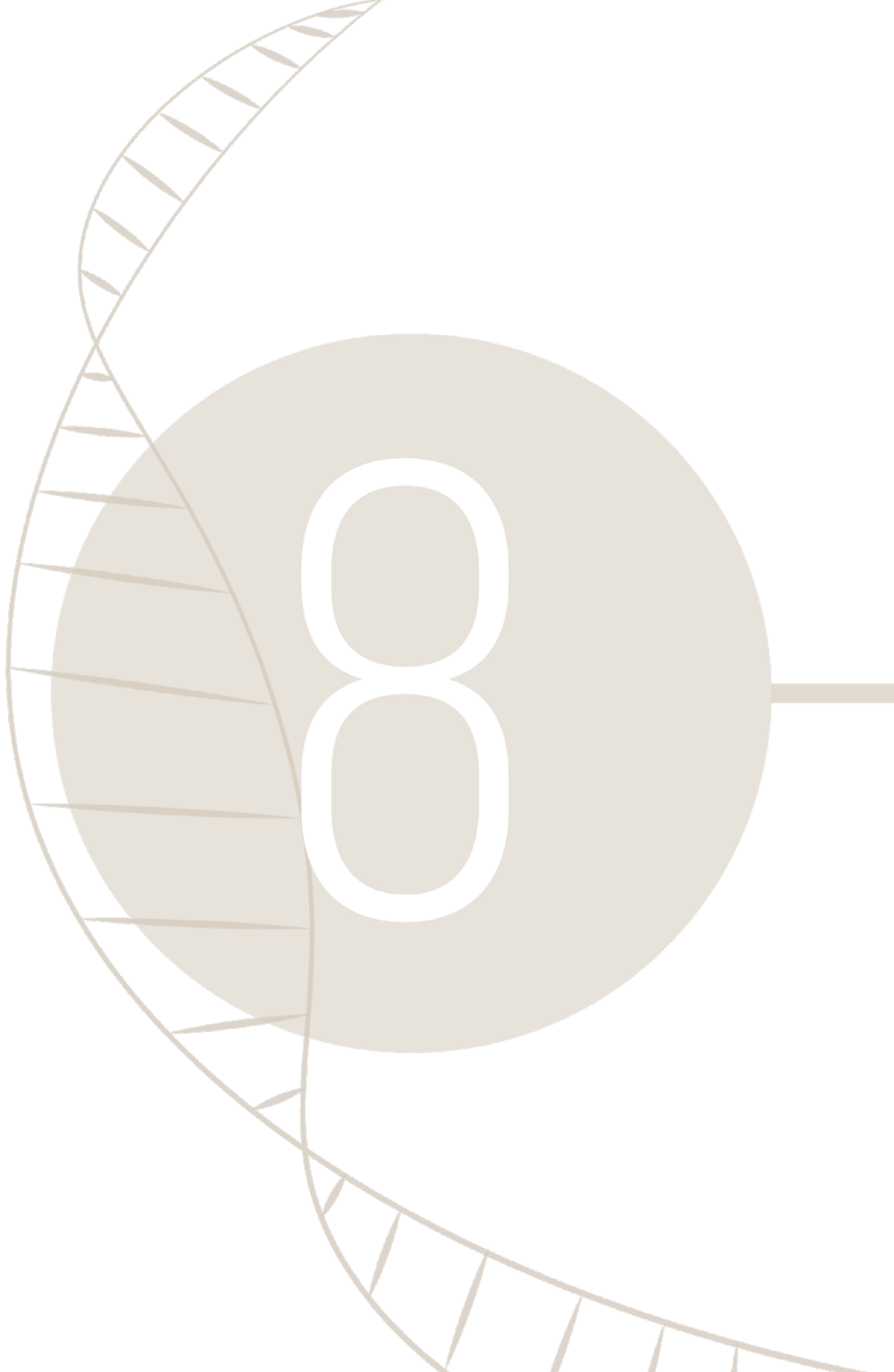


Figure 1. Tools and technologies for cartilage repair



APPENDICES

REFERENCES
NEDERLANDSE SAMENVATTING
ABBREVIATION LIST
ACKNOWLEDGMENTS
PUBLICATION LIST
CURRICULUM VITAE

REFERENCES

1. Goldring, M. B. & Goldring, S. R. Osteoarthritis. *Journal of Cellular Physiology* 213, (2007).
2. Zhang, Y. & Jordan, J. M. Epidemiology of osteoarthritis. *Clinics in Geriatric Medicine* 26, (2010).
3. Woolf, A. D. & Pfleger, B. Burden of major musculoskeletal conditions. *Bulletin of the World Health Organization* 81, (2003).
4. Lee, R. & Kean, W. F. Obesity and knee osteoarthritis. *Inflammopharmacology* 20, (2012).
5. Goldring, M. B. & Berenbaum, F. Emerging targets in osteoarthritis therapy. *Current Opinion in Pharmacology* 22, (2015).
6. Chevalier, X., Eymard, F. et al. Biologic agents in osteoarthritis: hopes and disappointments. *Nature Reviews Rheumatology* 9, (2013).
7. Salmon, J. H., Rat, A. C. et al. Economic impact of lower-limb osteoarthritis worldwide: a systematic review of cost-of-illness studies. *Osteoarthritis and Cartilage* 24, (2016).
8. Karsdal, M. A., Michaelis, M. et al. Disease-modifying treatments for osteoarthritis (DMOADs) of the knee and hip: lessons learned from failures and opportunities for the future. *Osteoarthritis and Cartilage* 24, (2016).
9. van der Kraan, P. M., Berenbaum, F. et al. Translation of clinical problems in osteoarthritis into pathophysiological research goals. *RMD Open* 2, (2016).
10. Bijlsma, J. W., Berenbaum, F. et al. Osteoarthritis: an update with relevance for clinical practice. *Lancet* 377, (2011).
11. Gerwin, N., Hops, C. et al. Intraarticular drug delivery in osteoarthritis. *Advanced Drug Delivery Reviews* 58, (2006).
12. Evans, C. H., Kraus, V. B. et al. Progress in intra-articular therapy. *Nature Reviews Rheumatology* 10, (2014).
13. Carballo, C. B., Nakagawa, Y. et al. Basic Science of Articular Cartilage. *Clinics in Sports Medicine* 36, (2017).
14. Smith, M. D. The normal synovium. *Open Rheumatology Journal* 5, (2011).
15. Levick, J. R. Microvascular architecture and exchange in synovial joints. *Microcirculation* 2, (1995).
16. Mayne, R. Cartilage collagens. What is their function, and are they involved in articular disease? *Arthritis & Rheumatism* 32, (1989).
17. Goldring, M. B. The role of the chondrocyte in osteoarthritis. *Arthritis & Rheumatology* 43, (2000).
18. Horton, W. E., Jr., Yagi, R. et al. Overview of studies comparing human normal cartilage with minimal and advanced osteoarthritic cartilage. *Clinical and Experimental Rheumatology* 23, (2005).
19. Aigner, T., Gluckert, K. et al. Activation of fibrillar collagen synthesis and phenotypic modulation of chondrocytes in early human osteoarthritic cartilage lesions. *Osteoarthritis and Cartilage* 5, (1997).
20. Bau, B., Gebhard, P. M. et al. Relative messenger RNA expression profiling of collagenases and aggrecanases in human articular chondrocytes in vivo and in vitro. *Arthritis & Rheumatism* 46, (2002).
21. Cawston, T. E. & Wilson, A. J. Understanding the role of tissue degrading enzymes and their inhibitors in development and disease. *Best Practice & Research: Clinical Rheumatology* 20, (2006).
22. Nagase, H. & Kashiwagi, M. Aggrecanases and cartilage matrix degradation. *Arthritis Research & Therapy* 5, (2003).
23. Eyre, D. Collagen of articular cartilage. *Arthritis Research & Therapy* 4, (2002).
24. Buckland-Wright, C. Subchondral bone changes in hand and knee osteoarthritis detected by radiography. *Osteoarthritis and Cartilage* 12 Suppl A, (2004).
25. Walsh, D. A., Bonnet, C. S. et al. Angiogenesis in the synovium and at the osteochondral junction in osteoarthritis. *Osteoarthritis and Cartilage* 15, (2007).
26. Intema, F., Hazewinkel, H. A. et al. In early OA, thinning of the subchondral plate is directly related to cartilage damage: results from a canine ACLT-meniscectomy model. *Osteoarthritis and Cartilage* 18, (2010).
27. Intema, F., Sniekers, Y. H. et al. Similarities and discrepancies in subchondral bone structure in two differently induced canine models of osteoarthritis. *Journal of Bone and Mineral Research* 25, (2010).
28. Xu, L., Hayashi, D. et al. Magnetic resonance imaging of subchondral bone marrow lesions in association with osteoarthritis. *Seminars in Arthritis and Rheumatism* 42, (2012).
29. Hulejova, H., Baresova, V. et al. Increased level of cytokines and matrix metalloproteinases in osteoarthritic subchondral bone. *Cytokine* 38, (2007).
30. Findlay, D. M. & Kuliwaba, J. S. Bone-cartilage crosstalk: a conversation for understanding osteoarthritis. *Bone Research* 4, (2016).
31. Goldring, M. B. & Otero, M. Inflammation in osteoarthritis. *Current Opinion in Rheumatology* 23, (2011).
32. Sellam, J. & Berenbaum, F. The role of synovitis in pathophysiology and clinical symptoms of osteo-

- arthritis. *Nature Reviews Rheumatology* 6, (2010).
33. Guilak, F., Fermor, B. et al. The role of biomechanics and inflammation in cartilage injury and repair. *Clinical Orthopaedics and Related Research*, (2004).
 34. Bigoni, M., Sacerdote, P. et al. Acute and late changes in intraarticular cytokine levels following anterior cruciate ligament injury. *Journal of Orthopaedic Research* 31, (2013).
 35. Watt, F. E., Paterson, E. et al. Acute Molecular Changes in Synovial Fluid Following Human Knee Injury: Association With Early Clinical Outcomes. *Arthritis & Rheumatology* 68, (2016).
 36. Scanzello, C. R., McKeon, B. et al. Synovial inflammation in patients undergoing arthroscopic meniscectomy: molecular characterization and relationship to symptoms. *Arthritis & Rheumatism* 63, (2011).
 37. Catterall, J. B., Stabler, T. V. et al. Changes in serum and synovial fluid biomarkers after acute injury (NCT00332254). *Arthritis Research & Therapy* 12, (2010).
 38. Ogura, T., Suzuki, M. et al. Differences in levels of inflammatory mediators in meniscal and synovial tissue of patients with meniscal lesions. *J Exp Orthop* 3, (2016).
 39. Irie, K., Uchiyama, E. et al. Intraarticular inflammatory cytokines in acute anterior cruciate ligament injured knee. *Knee* 10, (2003).
 40. Larsson, S., Englund, M. et al. Interleukin-6 and tumor necrosis factor alpha in synovial fluid are associated with progression of radiographic knee osteoarthritis in subjects with previous meniscectomy. *Osteoarthritis and Cartilage* 23, (2015).
 41. Lieberthal, J., Sambamurthy, N. et al. Inflammation in joint injury and post-traumatic osteoarthritis. *Osteoarthritis and Cartilage* 23, (2015).
 42. Lotz, M. K. & Kraus, V. B. New developments in osteoarthritis. Posttraumatic osteoarthritis: pathogenesis and pharmacological treatment options. *Arthritis Research & Therapy* 12, (2010).
 43. de Lange-Brokaar, B. J., Ioan-Facsinay, A. et al. Synovial inflammation, immune cells and their cytokines in osteoarthritis: a review. *Osteoarthritis and Cartilage* 20, (2012).
 44. Goldring, M. B., Otero, M. et al. Defining the roles of inflammatory and anabolic cytokines in cartilage metabolism. *Annals of Rheumatic Diseases* 67 Suppl 3, (2008).
 45. Marcu, K. B., Otero, M. et al. NF-kappaB signaling: multiple angles to target OA. *Curr Drug Targets* 11, (2010).
 46. Goldring, M. B., Otero, M. et al. Roles of inflammatory and anabolic cytokines in cartilage metabolism: signals and multiple effectors converge upon MMP-13 regulation in osteoarthritis. *European Cells & Materials* 21, (2011).
 47. Choi, M. C., Jo, J. et al. NF-kappaB Signaling Pathways in Osteoarthritic Cartilage Destruction. *Cells* 8, (2019).
 48. Doss, F., Menard, J. et al. Elevated IL-6 levels in the synovial fluid of osteoarthritis patients stem from plasma cells. *Scandinavian Journal of Rheumatology* 36, (2007).
 49. Bondeson, J., Blom, A. B. et al. The role of synovial macrophages and macrophage-produced mediators in driving inflammatory and destructive responses in osteoarthritis. *Arthritis & Rheumatism* 62, (2010).
 50. Karsdal, M. A., Christiansen, C. et al. Osteoarthritis--a case for personalized health care? *Osteoarthritis and Cartilage* 22, (2014).
 51. Kraus, V. B., Blanco, F. J. et al. Call for standardized definitions of osteoarthritis and risk stratification for clinical trials and clinical use. *Osteoarthritis and Cartilage* 23, (2015).
 52. Chery, J. RNA therapeutics: RNAi and antisense mechanisms and clinical applications. *Postdoc Journal* 4, (2016).
 53. Crooke, S. T., Witzum, J. L. et al. RNA-Targeted Therapeutics. *Cell Metabolism* 27, (2018).
 54. Dias, N. & Stein, C. A. Antisense oligonucleotides: basic concepts and mechanisms. *Molecular Cancer Therapeutics* 1, (2002).
 55. Dowdy, S. F. Overcoming cellular barriers for RNA therapeutics. *Nature Biotechnology* 35, (2017).
 56. Stein, C. A., Hansen, J. B. et al. Efficient gene silencing by delivery of locked nucleic acid antisense oligonucleotides, unassisted by transfection reagents. *Nucleic Acids Research* 38, (2010).
 57. Soifer, H. S., Koch, T. et al. Silencing of gene expression by gymnotic delivery of antisense oligonucleotides. *Methods in Molecular Biology* 815, (2012).
 58. Castanotto, D., Lin, M. et al. A cytoplasmic pathway for gapmer antisense oligonucleotide-mediated gene silencing in mammalian cells. *Nucleic Acids Research* 43, (2015).
 59. Crooke, S. T., Wang, S. et al. Cellular uptake and trafficking of antisense oligonucleotides. *Nature Biotechnology* 35, (2017).
 60. Stec, W. J., Zon, G. et al. Automated Solid-Phase Synthesis, Separation, and Stereochemistry of Phosphorothioate Analogs of Oligodeoxyribonucleotides. *Journal of the American Chemical Society*

106, (1984).

61. Eckstein, F. Phosphorothioates, essential components of therapeutic oligonucleotides. *Nucleic Acid Therapeutics* 24, (2014).
62. Wahlestedt, C., Salmi, P. et al. Potent and nontoxic antisense oligonucleotides containing locked nucleic acids. *Proceedings of the National Academy of Sciences of the United States of America* 97, (2000).
63. Hagedorn, P. H., Persson, R. et al. Locked nucleic acid: modality, diversity, and drug discovery. *Drug Discovery Today* 23, (2018).
64. Lundin, K. E., Hojland, T. et al. Biological activity and biotechnological aspects of locked nucleic acids. *Advances in Genetics* 82, (2013).
65. Czauderna, F., Fechtner, M. et al. Structural variations and stabilising modifications of synthetic siRNAs in mammalian cells. *Nucleic Acids Research* 31, (2003).
66. Ohrt, T., Muetze, J. et al. Intracellular localization and routing of miRNA and RNAi pathway components. *Current Topics in Medicinal Chemistry* 12, (2012).
67. Chernikov, I. V., Vlassov, V. V. et al. Current Development of siRNA Bioconjugates: From Research to the Clinic. *Frontiers in Pharmacology* 10, (2019).
68. Prakash, T. P., Allerson, C. R. et al. Positional effect of chemical modifications on short interference RNA activity in mammalian cells. *Journal of Medicinal Chemistry* 48, (2005).
69. Stahel, R. A. & Zangemeister-Witke, U. Antisense oligonucleotides for cancer therapy-an overview. *Lung Cancer* 41 Suppl 1, (2003).
70. Moreno, P. M. & Pego, A. P. Therapeutic antisense oligonucleotides against cancer: hurdling to the clinic. *Frontiers in Chemistry* 2, (2014).
71. Evers, M. M., Toonen, L. J. et al. Antisense oligonucleotides in therapy for neurodegenerative disorders. *Advanced Drug Delivery Reviews* 87, (2015).
72. Mourich, D. V. & Marshall, N. B. Antisense approaches to immune modulation for transplant and autoimmune diseases. *Current Opinion in Pharmacology* 5, (2005).
73. Tomita, N. & Morishita, R. Antisense oligonucleotides as a powerful molecular strategy for gene therapy in cardiovascular diseases. *Current Pharmaceutical Design* 10, (2004).
74. Phillips, M. I., Costales, J. et al. Antisense Therapy for Cardiovascular Diseases. *Current Pharmaceutical Design* 21, (2015).
75. Evans, C. H. Drug delivery to chondrocytes. *Osteoarthritis and Cartilage* 24, (2016).
76. Van Spij, W. E., Kubassova, O. et al. Osteoarthritis phenotypes and novel therapeutic targets. *Biochemical Pharmacology* 165, (2019).
77. Castaneda, S., Roman-Blas, J. A. et al. Osteoarthritis: a progressive disease with changing phenotypes Aetiopathogenic phenotypes to joint tissue-derived clinical manifestations. *Rheumatology* 53, (2014).
78. Lotz, M., Martel-Pelletier, J. et al. Value of biomarkers in osteoarthritis: current status and perspectives. *Annals of Rheumatic Diseases* 72, (2013).
79. Roemer, F. W., Eckstein, F. et al. The role of imaging in osteoarthritis. *Best Practice & Research: Clinical Rheumatology* 28, (2014).
80. Conaghan, P. G., Hunter, D. J. et al. Summary and recommendations of the OARSI FDA osteoarthritis Assessment of Structural Change Working Group. *Osteoarthritis and Cartilage* 19, (2011).
81. Hayashi, D., Guermazi, A. et al. MRI of osteoarthritis: the challenges of definition and quantification. *Semin Musculoskelet Radiol* 16, (2012).
82. Keen, H. I. & Conaghan, P. G. Ultrasonography in osteoarthritis. *Radiologic Clinics of North America* 47, (2009).
83. Guermazi, A., Roemer, F. W. et al. Assessment of synovitis with contrast-enhanced MRI using a whole-joint semiquantitative scoring system in people with, or at high risk of, knee osteoarthritis: the MOST study. *Annals of Rheumatic Diseases* 70, (2011).
84. Loeuille, D., Sauliere, N. et al. Comparing non-enhanced and enhanced sequences in the assessment of effusion and synovitis in knee OA: associations with clinical, macroscopic and microscopic features. *Osteoarthritis and Cartilage* 19, (2011).
85. Wu, P. T., Shao, C. J. et al. Pain in patients with equal radiographic grades of osteoarthritis in both knees: the value of gray scale ultrasound. *Osteoarthritis and Cartilage* 20, (2012).
86. Kortekaas, M. C., Kwok, W. Y. et al. In erosive hand osteoarthritis more inflammatory signs on ultrasound are found than in the rest of hand osteoarthritis. *Annals of Rheumatic Diseases* 72, (2013).
87. Roemer, F. W., Guermazi, A. et al. Prevalence of magnetic resonance imaging-defined atrophic and hypertrophic phenotypes of knee osteoarthritis in a population-based cohort. *Arthritis & Rheumatism* 64, (2012).

88. Zhu, Z., Ding, C. et al. MRI-detected osteophytes of the knee: natural history and structural correlates of change. *Arthritis Research & Therapy* 20, (2018).
89. Mathiessen, A., Slatkowsky-Christensen, B. et al. Ultrasound-detected osteophytes predict the development of radiographic and clinical features of hand osteoarthritis in the same finger joints 5 years later. *RMD Open* 3, (2017).
90. Saarakkala, S., Waris, P. et al. Diagnostic performance of knee ultrasonography for detecting degenerative changes of articular cartilage. *Osteoarthritis and Cartilage* 20, (2012).
91. Crema, M. D., Hunter, D. J. et al. Association of changes in delayed gadolinium-enhanced MRI of cartilage (dGEMRIC) with changes in cartilage thickness in the medial tibiofemoral compartment of the knee: a 2 year follow-up study using 3.0 T MRI. *Annals of Rheumatic Diseases* 73, (2014).
92. Bendele, A. M. Animal models of osteoarthritis. *Journal of Musculoskeletal & Neuronal Interactions* 1, (2001).
93. Kuyinu, E. L., Narayanan, G. et al. Animal models of osteoarthritis: classification, update, and measurement of outcomes. *Journal of Orthopaedic Surgery and Research* 11, (2016).
94. van Spil, W. E., DeGroot, J. et al. Serum and urinary biochemical markers for knee and hip-osteoarthritis: a systematic review applying the consensus BIPED criteria. *Osteoarthritis and Cartilage* 18, (2010).
95. Chung, C. & Burdick, J. A. Engineering cartilage tissue. *Advanced Drug Delivery Reviews* 60, (2008).
96. Makris, E. A., Gomoll, A. H. et al. Repair and tissue engineering techniques for articular cartilage. *Nature Reviews Rheumatology* 11, (2015).
97. Advancing tissue science and engineering: a foundation for the future. A multi-agency strategic plan. *Tissue Engineering* 13, (2007).
98. Appel, A. A., Anastasio, M. A. et al. Imaging challenges in biomaterials and tissue engineering. *Biomaterials* 34, (2013).
99. Pancrazio, J. J., Wang, F. et al. Enabling tools for tissue engineering. *Biosensors and Bioelectronics* 22, (2007).
100. Palmer, A. W., Guldberg, R. E. et al. Analysis of cartilage matrix fixed charge density and three-dimensional morphology via contrast-enhanced microcomputed tomography. *Proceedings of the National Academy of Sciences of the United States of America* 103, (2006).
101. Guldberg, R. E., Duvall, C. L. et al. 3D imaging of tissue integration with porous biomaterials. *Biomaterials* 29, (2008).
102. Potter, K., Butler, J. J. et al. Cartilage formation in a hollow fiber bioreactor studied by proton magnetic resonance microscopy. *Matrix Biology* 17, (1998).
103. Potter, K., Butler, J. J. et al. Response of engineered cartilage tissue to biochemical agents as studied by proton magnetic resonance microscopy. *Arthritis & Rheumatism* 43, (2000).
104. Chen, C. T., Fishbein, K. W. et al. Matrix fixed-charge density as determined by magnetic resonance microscopy of bioreactor-derived hyaline cartilage correlates with biochemical and biomechanical properties. *Arthritis & Rheumatism* 48, (2003).
105. Xu, H., Othman, S. F. et al. Monitoring tissue engineering using magnetic resonance imaging. *Journal of Bioscience and Bioengineering* 106, (2008).
106. Rice, M. A., Waters, K. R. et al. Ultrasound monitoring of cartilaginous matrix evolution in degradable PEG hydrogels. *Acta Biomaterialia* 5, (2009).
107. Fite, B. Z., Decaris, M. et al. Noninvasive multimodal evaluation of bioengineered cartilage constructs combining time-resolved fluorescence and ultrasound imaging. *Tissue Engineering Part C: Methods* 17, (2011).
108. Kreitz, S., Dohmen, G. et al. Nondestructive method to evaluate the collagen content of fibrin-based tissue engineered structures via ultrasound. *Tissue Engineering Part C: Methods* 17, (2011).
109. Seo, J., Shin, J. Y. et al. High-throughput approaches for screening and analysis of cell behaviors. *Biomaterials* 153, (2018).
110. Urban, J. P. & Roberts, S. Degeneration of the intervertebral disc. *Arthritis Research & Therapy* 5, (2003).
111. Blanquer, S. B., Grijpma, D. W. et al. Delivery systems for the treatment of degenerated intervertebral discs. *Advanced Drug Delivery Reviews* 84, (2015).
112. Becerra, J., Andrades, J. A. et al. Articular cartilage: structure and regeneration. *Tissue Engineering Part B: Reviews* 16, (2010).
113. Humzah, M. D. & Soames, R. W. Human Intervertebral-Disk - Structure and Function. *Anatomical Record* 220, (1988).
114. Weber, K. T., Jacobsen, T. D. et al. Developments in intervertebral disc disease research: pathophysiology, mechanobiology, and therapeutics. *Curr Rev Musculoskelet Med* 8, (2015).
115. Buckwalter, J. A. Articular cartilage: injuries and potential for healing. *Journal of Orthopaedic and*

Sports Physical Therapy 28, (1998).

116. O'Hara, B. P., Urban, J. P. et al. Influence of cyclic loading on the nutrition of articular cartilage. *Annals of Rheumatic Diseases* 49, (1990).

117. Adams, M. A. & Roughley, P. J. What is intervertebral disc degeneration, and what causes it? *Spine* 31, (2006).

118. Rajasekaran, S., Babu, J. N. et al. ISSLS prize winner: A study of diffusion in human lumbar discs: a serial magnetic resonance imaging study documenting the influence of the endplate on diffusion in normal and degenerate discs. *Spine* 29, (2004).

119. Kepler, C. K., Ponnappan, R. K. et al. The molecular basis of intervertebral disc degeneration. *The Spine Journal* 13, (2013).

120. Loeser, R. F., Goldring, S. R. et al. Osteoarthritis: a disease of the joint as an organ. *Arthritis & Rheumatism* 64, (2012).

121. Martin, J. A., Brown, T. D. et al. Chondrocyte senescence, joint loading and osteoarthritis. *Clinical Orthopaedics and Related Research*, (2004).

122. Chu, G., Shi, C. et al. Biomechanics in Annulus Fibrosus Degeneration and Regeneration. *Advances in Experimental Medicine and Biology* 1078, (2018).

123. Freemont, A. J., Peacock, T. E. et al. Nerve ingrowth into diseased intervertebral disc in chronic back pain. *Lancet* 350, (1997).

124. Podichetty, V. K. The aging spine: the role of inflammatory mediators in intervertebral disc degeneration. *Cellular and Molecular Biology (Noisy-Le-Grand, France)* 53, (2007).

125. Brown, M. F., Hukkanen, M. V. et al. Sensory and sympathetic innervation of the vertebral endplate in patients with degenerative disc disease. *Journal of Bone and Joint Surgery (British Volume)* 79, (1997).

126. Oki, S., Matsuda, Y. et al. Scanning electron microscopic observations of the vascular structure of vertebral end-plates in rabbits. *Journal of Orthopaedic Research* 12, (1994).

127. Jeon, O. H., David, N. et al. Senescent cells and osteoarthritis: a painful connection. *Journal of Clinical Investigation* 128, (2018).

128. Jeon, O. H., Kim, C. et al. Local clearance of senescent cells attenuates the development of post-traumatic osteoarthritis and creates a pro-regenerative environment. *Nature Medicine* 23, (2017).

129. Zhou, H. W., Lou, S. Q. et al. Recovery of function in osteoarthritic chondrocytes induced by p16(INK4a)-specific siRNA in vitro. *Rheumatology* 43, (2004).

130. Hochberg, M. C. Osteoarthritis year 2012 in review: clinical. *Osteoarthritis and Cartilage* 20, (2012).

131. Hochberg, M. C., Altman, R. D. et al. American College of Rheumatology 2012 recommendations for the use of nonpharmacologic and pharmacologic therapies in osteoarthritis of the hand, hip, and knee. *Arthritis Care & Research* 64, (2012).

132. Koes, B. W., van Tulder, M. W. et al. Diagnosis and treatment of low back pain. *BMJ* 332, (2006).

133. Jordan, K. M., Arden, N. K. et al. Eular recommendations: An evidence based medicine approach to knee osteoarthritis. *Annals of the Rheumatic Diseases* 62, (2003).

134. Miceli-Richard, C., Le Bars, M. et al. Paracetamol in osteoarthritis of the knee. *Annals of Rheumatic Diseases* 63, (2004).

135. Zhang, W., Moskowitz, R. W. et al. OARSI recommendations for the management of hip and knee osteoarthritis, Part II: OARSI evidence-based, expert consensus guidelines. *Osteoarthritis and Cartilage* 16, (2008).

136. Kang, M. L. & Im, G. I. Drug delivery systems for intra-articular treatment of osteoarthritis. *Expert Opinion on Drug Delivery* 11, (2014).

137. Atlas, S. J. Management of Low Back Pain: Getting From Evidence-Based Recommendations to High-Value Care. *Annals of Internal Medicine* 166, (2017).

138. Laine, L., White, W. B. et al. COX-2 selective inhibitors in the treatment of osteoarthritis. *Seminars in Arthritis and Rheumatism* 38, (2008).

139. Sostres, C., Gargallo, C. J. et al. Adverse effects of non-steroidal anti-inflammatory drugs (NSAIDs, aspirin and coxibs) on upper gastrointestinal tract. *Best Practice & Research: Clinical Gastroenterology* 24, (2010).

140. Laine, L. Gastrointestinal effects of NSAIDs and coxibs. *Journal of Pain and Symptom Management* 25, (2003).

141. Schnitzer, T. J., Ferraro, A. et al. A comprehensive review of clinical trials on the efficacy and safety of drugs for the treatment of low back pain. *Journal of Pain and Symptom Management* 28, (2004).

142. Airaksinen, O., Brox, J. I. et al. Chapter 4. European guidelines for the management of chronic nonspecific low back pain. *European Spine Journal* 15 Suppl 2, (2006).

143. van Tulder, M. W., Touray, T. et al. Muscle relaxants for nonspecific low back pain: a systematic re-

- view within the framework of the cochrane collaboration. *Spine* 28, (2003).
144. Von Korff, M. & Deyo, R. A. Potent opioids for chronic musculoskeletal pain: flying blind? *Pain* 109, (2004).
 145. Chou, R., Qaseem, A. et al. Diagnosis and treatment of low back pain: a joint clinical practice guideline from the American College of Physicians and the American Pain Society. *Annals of Internal Medicine* 147, (2007).
 146. Bellamy, N., Campbell, J. et al. Intraarticular corticosteroid for treatment of osteoarthritis of the knee. *Cochrane Database of Systematic Reviews*, (2005).
 147. Rho, M. E. & Tang, C. T. The efficacy of lumbar epidural steroid injections: transforaminal, interlaminar, and caudal approaches. *Physical Medicine and Rehabilitation Clinics of North America* 22, (2011).
 148. Adams, M. E., Lussier, A. J. et al. A risk-benefit assessment of injections of hyaluronan and its derivatives in the treatment of osteoarthritis of the knee. *Drug Safety* 23, (2000).
 149. Andia, I. & Maffulli, N. Platelet-rich plasma for managing pain and inflammation in osteoarthritis. *Nature Reviews Rheumatology* 9, (2013).
 150. O'Connell, B., Wragg, N. M. et al. The use of PRP injections in the management of knee osteoarthritis. *Cell and Tissue Research* 376, (2019).
 151. Han, Y., Huang, H. et al. Meta-analysis Comparing Platelet-Rich Plasma vs Hyaluronic Acid Injection in Patients with Knee Osteoarthritis. *Pain Medicine* 20, (2019).
 152. Bannuru, R. R., Osani, M. C. et al. OARSI guidelines for the non-surgical management of knee, hip, and polyarticular osteoarthritis. *Osteoarthritis and Cartilage* 27, (2019).
 153. Yavin, D., Casha, S. et al. Lumbar Fusion for Degenerative Disease: A Systematic Review and Meta-Analysis. *Neurosurgery* 80, (2017).
 154. Niemeyer, P., Albrecht, D. et al. Autologous chondrocyte implantation (ACI) for cartilage defects of the knee: A guideline by the working group "Clinical Tissue Regeneration" of the German Society of Orthopaedics and Trauma (DGOU). *Knee* 23, (2016).
 155. Minas, T., Gomoll, A. H. et al. Autologous chondrocyte implantation for joint preservation in patients with early osteoarthritis. *Clinical Orthopaedics and Related Research* 468, (2010).
 156. Falah, M., Nierenberg, G. et al. Treatment of articular cartilage lesions of the knee. *International Orthopaedics* 34, (2010).
 157. Tonge, D. P., Pearson, M. J. et al. The hallmarks of osteoarthritis and the potential to develop personalised disease-modifying pharmacological therapeutics. *Osteoarthritis and Cartilage* 22, (2014).
 158. Matthews, G. L. & Hunter, D. J. Emerging drugs for osteoarthritis. *Expert Opinion on Emerging Drugs* 16, (2011).
 159. Pelletier, J. P., Martel-Pelletier, J. et al. Most recent developments in strategies to reduce the progression of structural changes in osteoarthritis: today and tomorrow. *Arthritis Research & Therapy* 8, (2006).
 160. Janssen, M., Mihov, G. et al. Drugs and Polymers for Delivery Systems in OA Joints: Clinical Needs and Opportunities. *Polymers* 6, (2014).
 161. Lane, N. E., Schnitzer, T. J. et al. Tanezumab for the treatment of pain from osteoarthritis of the knee. *New England Journal of Medicine* 363, (2010).
 162. Schnitzer, T. J., Lane, N. E. et al. Long-term open-label study of tanezumab for moderate to severe osteoarthritic knee pain. *Osteoarthritis and Cartilage* 19, (2011).
 163. Birbara, C., Dabiezies, E. J., Jr. et al. Safety and efficacy of subcutaneous tanezumab in patients with knee or hip osteoarthritis. *Journal of Pain Research* 11, (2018).
 164. Schnitzer, T. J., Easton, R. et al. Effect of Tanezumab on Joint Pain, Physical Function, and Patient Global Assessment of Osteoarthritis Among Patients With Osteoarthritis of the Hip or Knee: A Randomized Clinical Trial. *JAMA* 322, (2019).
 165. Chevalier, X., Goupille, P. et al. Intraarticular injection of anakinra in osteoarthritis of the knee: a multicenter, randomized, double-blind, placebo-controlled study. *Arthritis & Rheumatism* 61, (2009).
 166. Cohen, S. B., Proudman, S. et al. A randomized, double-blind study of AMG 108 (a fully human monoclonal antibody to IL-1R1) in patients with osteoarthritis of the knee. *Arthritis Research & Therapy* 13, (2011).
 167. Fleischmann, R. M., Bliddal, H. et al. A Phase II Trial of Lutikizumab, an Anti-Interleukin-1alpha/beta Dual Variable Domain Immunoglobulin, in Knee Osteoarthritis Patients With Synovitis. *Arthritis & Rheumatology* 71, (2019).
 168. Kloppenburg, M., Peterfy, C. et al. Phase IIa, placebo-controlled, randomised study of lutikizumab, an anti-interleukin-1alpha and anti-interleukin-1beta dual variable domain immunoglobulin, in patients with erosive hand osteoarthritis. *Annals of Rheumatic Diseases* 78, (2019).

169. Cohen, S. P., Bogduk, N. et al. Randomized, double-blind, placebo-controlled, dose-response, and preclinical safety study of transforaminal epidural etanercept for the treatment of sciatica. *Anesthesiology* 110, (2009).
170. Hayashi, M., Muneta, T. et al. Intra-articular injections of bone morphogenetic protein-7 retard progression of existing cartilage degeneration. *Journal of Orthopaedic Research* 28, (2010).
171. Lohmander, L. S., Hellot, S. et al. Intraarticular sprifermin (recombinant human fibroblast growth factor 18) in knee osteoarthritis: a randomized, double-blind, placebo-controlled trial. *Arthritis & Rheumatology* 66, (2014).
172. Snijders, G. F., van den Ende, C. H. et al. The effects of doxycycline on reducing symptoms in knee osteoarthritis: results from a triple-blinded randomised controlled trial. *Annals of Rheumatic Diseases* 70, (2011).
173. Krzeski, P., Buckland-Wright, C. et al. Development of musculoskeletal toxicity without clear benefit after administration of PG-116800, a matrix metalloproteinase inhibitor, to patients with knee osteoarthritis: a randomized, 12-month, double-blind, placebo-controlled study. *Arthritis Research & Therapy* 9, (2007).
174. Helliö le Graverand, M. P., Clemmer, R. S. et al. A 2-year randomised, double-blind, placebo-controlled, multicentre study of oral selective iNOS inhibitor, cindunistat (SD-6010), in patients with symptomatic osteoarthritis of the knee. *Annals of Rheumatic Diseases* 72, (2013).
175. Yazici, Y., McAlindon, T. E. et al. A novel Wnt pathway inhibitor, SM04690, for the treatment of moderate to severe osteoarthritis of the knee: results of a 24-week, randomized, controlled, phase 1 study. *Osteoarthritis and Cartilage* 25, (2017).
176. Yazici, Y., McAlindon, T. et al. Results from a 52 Week Randomised, Double-Blind, Placebo-Controlled, Phase 2 Study of a Novel, Wnt Pathway Inhibitor (Sm04690) for Knee Osteoarthritis Treatment. *Annals of the Rheumatic Diseases* 77, (2018).
177. Karsdal, M. A., Byrjalsen, I. et al. Treatment of symptomatic knee osteoarthritis with oral salmon calcitonin: results from two phase 3 trials. *Osteoarthritis and Cartilage* 23, (2015).
178. Wang, J. Efficacy and safety of adalimumab by intra-articular injection for moderate to severe knee osteoarthritis: An open-label randomized controlled trial. *Journal of International Medical Research* 46, (2018).
179. Aitken, D., Pany, F. et al. A Randomised Double-Blind Placebo-Controlled Crossover Trial of Humira (Adalimumab) for Erosive Hand Osteoarthritis: The Humor Trial. *Osteoarthritis and Cartilage* 25, (2017).
180. Risbud, M. V. & Shapiro, I. M. Role of cytokines in intervertebral disc degeneration: pain and disc content. *Nature Reviews Rheumatology* 10, (2014).
181. Genevay, S., Stingelin, S. et al. Efficacy of etanercept in the treatment of acute, severe sciatica: a pilot study. *Annals of Rheumatic Diseases* 63, (2004).
182. Cohen, S. P., White, R. L. et al. Epidural steroids, etanercept, or saline in subacute sciatica: a multicenter, randomized trial. *Annals of Internal Medicine* 156, (2012).
183. Okoro, T., Tafazzal, S. I. et al. Tumor necrosis alpha-blocking agent (etanercept): a triple blind randomized controlled trial of its use in treatment of sciatica. *Journal of Spinal Disorders & Techniques* 23, (2010).
184. Fischer, J. A., Hueber, A. J. et al. Combined inhibition of tumor necrosis factor alpha and interleukin-17 as a therapeutic opportunity in rheumatoid arthritis: development and characterization of a novel bispecific antibody. *Arthritis & Rheumatology* 67, (2015).
185. Kamath, R. V., Simler, G. et al. Blockade of Both Il-1a and Il-1b by a Combination of Monoclonal Antibodies Prevents the Development and Reverses Established Pain in a Preclinical Model of Osteoarthritis. *Osteoarthritis and Cartilage* 20, (2012).
186. Bigg, H. The inhibition of metalloproteinases as a therapeutic target in rheumatoid arthritis and osteoarthritis. *Current Opinion in Pharmacology* 1, (2001).
187. Lewis, E. J., Bishop, J. et al. Ro 32-3555, an orally active collagenase inhibitor, prevents cartilage breakdown in vitro and in vivo. *British Journal of Pharmacology* 121, (1997).
188. Janusz, M. J., Hookfin, E. B. et al. Moderation of iodoacetate-induced experimental osteoarthritis in rats by matrix metalloproteinase inhibitors. *Osteoarthritis and Cartilage* 9, (2001).
189. Leff, R. L. Clinical trials of a stromelysin inhibitor. Osteoarthritis, matrix metalloproteinase inhibition, cartilage loss, surrogate markers, and clinical implications. *Annals of the New York Academy of Sciences* 878, (1999).
190. Dahlberg, L., Billingham, R. C. et al. Selective enhancement of collagenase-mediated cleavage of resident type II collagen in cultured osteoarthritic cartilage and arrest with a synthetic inhibitor that spares collagenase 1 (matrix metalloproteinase 1). *Arthritis & Rheumatism* 43, (2000).
191. Johnson, A. R., Pavlovsky, A. G. et al. Discovery and characterization of a novel inhibitor of matrix

metalloprotease-13 that reduces cartilage damage in vivo without joint fibroplasia side effects. *Journal of Biological Chemistry* 282, (2007).

192. Baragi, V. M., Becher, G. et al. A new class of potent matrix metalloproteinase 13 inhibitors for potential treatment of osteoarthritis: Evidence of histologic and clinical efficacy without musculoskeletal toxicity in rat models. *Arthritis & Rheumatism* 60, (2009).

193. Wang, M. N., Sampson, E. R. et al. MMP13 is a critical target gene during the progression of osteoarthritis. *Arthritis Research & Therapy* 15, (2013).

194. Siebuhr, A., Bay-Jensen, A. C. et al. The Anti-Adams-5 Nanobody (R), M6495, Protects against Cartilage Breakdown in Cartilage and Synovial Joint Tissue Explant Models. *Osteoarthritis and Cartilage* 26, (2018).

195. Sharma, N., Drobinski, P. et al. The Anti-Adams-5 Nanobody (R), M6495, Inhibits the Activation of Tlr by Adams-5-Mediated Degradation Fragments in Cartilage Explants. *Osteoarthritis and Cartilage* 27, (2019).

196. Farrell, A. J., Blake, D. R. et al. Increased concentrations of nitrite in synovial fluid and serum samples suggest increased nitric oxide synthesis in rheumatic diseases. *Annals of Rheumatic Diseases* 51, (1992).

197. Pelletier, J. P., Lascau-Coman, V. et al. Selective inhibition of inducible nitric oxide synthase in experimental osteoarthritis is associated with reduction in tissue levels of catabolic factors. *Journal of Rheumatology* 26, (1999).

198. El Hajjaji, H., Williams, J. M. et al. Treatment with calcitonin prevents the net loss of collagen, hyaluronan and proteoglycan aggregates from cartilage in the early stages of canine experimental osteoarthritis. *Osteoarthritis and Cartilage* 12, (2004).

199. Manicourt, D. H., Azria, M. et al. Oral salmon calcitonin reduces Lequesne's algofunctional index scores and decreases urinary and serum levels of biomarkers of joint metabolism in knee osteoarthritis. *Arthritis & Rheumatism* 54, (2006).

200. Karsdal, M. A., Byrjalsen, I. et al. The effect of oral salmon calcitonin delivered with 5-CNAC on bone and cartilage degradation in osteoarthritic patients: a 14-day randomized study. *Osteoarthritis and Cartilage* 18, (2010).

201. Hunter, D. J., Pike, M. C. et al. Phase 1 safety and tolerability study of BMP-7 in symptomatic knee osteoarthritis. *BMC Musculoskelet Disord* 11, (2010).

202. Chujo, T., An, H. S. et al. Effects of growth differentiation factor-5 on the intervertebral disc—in vitro bovine study and in vivo rabbit disc degeneration model study. *Spine* 31, (2006).

203. An, H. S., Takegami, K. et al. Intradiscal administration of osteogenic protein-1 increases intervertebral disc height and proteoglycan content in the nucleus pulposus in normal adolescent rabbits. *Spine* 30, (2005).

204. Masuda, K., Imai, Y. et al. Osteogenic protein-1 injection into a degenerated disc induces the restoration of disc height and structural changes in the rabbit annular puncture model. *SPINE* 31, (2006).

205. Ellsworth, J. L., Berry, J. et al. Fibroblast growth factor-18 is a trophic factor for mature chondrocytes and their progenitors. *Osteoarthritis and Cartilage* 10, (2002).

206. Moore, E. E., Bendele, A. M. et al. Fibroblast growth factor-18 stimulates chondrogenesis and cartilage repair in a rat model of injury-induced osteoarthritis. *Osteoarthritis and Cartilage* 13, (2005).

207. Evans, C. H., Gouze, J. N. et al. Osteoarthritis gene therapy. *Gene Therapy* 11, (2004).

208. Madry, H. & Cucchiari, M. Gene therapy for human osteoarthritis: principles and clinical translation. *Expert Opinion on Biological Therapy* 16, (2016).

209. Ha, C. W., Cho, J. J. et al. A Multicenter, Single-Blind, Phase IIa Clinical Trial to Evaluate the Efficacy and Safety of a Cell-Mediated Gene Therapy in Degenerative Knee Arthritis Patients. *Human Gene Therapy Clinical Development* 26, (2015).

210. Lee, M. C., Ha, C. W. et al. A placebo-controlled randomised trial to assess the effect of TGF- α 1-expressing chondrocytes in patients with arthritis of the knee. *Bone Joint J* 97-B, (2015).

211. Ghivizzani, S. C., Oligino, T. J. et al. Direct gene delivery strategies for the treatment of rheumatoid arthritis. *Drug Discovery Today* 6, (2001).

212. Sampara, P., Banala, R. R. et al. Understanding the molecular biology of intervertebral disc degeneration and potential gene therapy strategies for regeneration: a review. *Gene Therapy* 25, (2018).

213. Seki, S., Asanuma-Abe, Y. et al. Effect of small interference RNA (siRNA) for ADAMTS5 on intervertebral disc degeneration in the rabbit annular needle-puncture model. *Arthritis Research & Therapy* 11, (2009).

214. Sudo, H. & Minami, A. Caspase 3 as a therapeutic target for regulation of intervertebral disc degeneration in rabbits. *Arthritis & Rheumatism* 63, (2011).

215. Kim, D., Song, J. et al. MicroRNA-221 regulates chondrogenic differentiation through promoting proteosomal degradation of slug by targeting Mdm2. *Journal of Biological Chemistry* 285, (2010).

216. Ham, O., Song, B. W. et al. The role of microRNA-23b in the differentiation of MSC into chondrocyte by targeting protein kinase A signaling. *Biomaterials* 33, (2012).
217. Matsukawa, T., Sakai, T. et al. MicroRNA-125b regulates the expression of aggrecanase-1 (ADAMTS-4) in human osteoarthritic chondrocytes. *Arthritis Research & Therapy* 15, (2013).
218. Ning, G., Liu, X. et al. MicroRNA-92a upholds Bmp signaling by targeting noggin3 during pharyngeal cartilage formation. *Developmental Cell* 24, (2013).
219. Meng, F., Zhang, Z. et al. MicroRNA-320 regulates matrix metalloproteinase-13 expression in chondrogenesis and interleukin-1 β -induced chondrocyte responses. *Osteoarthritis and Cartilage* 24, (2016).
220. Nakamura, A., Rampersaud, Y. R. et al. Identification of microRNA-181a-5p and microRNA-4454 as mediators of facet cartilage degeneration. *JCI Insight* 1, (2016).
221. Sondag, G. R. & Haqqi, T. M. The Role of MicroRNAs and Their Targets in Osteoarthritis. *Current Rheumatology Reports* 18, (2016).
222. Vonk, L. A., Kragten, A. H. et al. Overexpression of hsa-miR-148a promotes cartilage production and inhibits cartilage degradation by osteoarthritic chondrocytes. *Osteoarthritis and Cartilage* 22, (2014).
223. Tuddenham, L., Wheeler, G. et al. The cartilage specific microRNA-140 targets histone deacetylase 4 in mouse cells. *FEBS Letters* 580, (2006).
224. Miyaki, S., Sato, T. et al. MicroRNA-140 plays dual roles in both cartilage development and homeostasis. *Genes & Development* 24, (2010).
225. Karlsen, T. A., de Souza, G. A. et al. microRNA-140 Inhibits Inflammation and Stimulates Chondrogenesis in a Model of Interleukin 1 β -induced Osteoarthritis. *Mol Ther Nucleic Acids* 5, (2016).
226. Si, H. B., Zeng, Y. et al. Intra-articular injection of microRNA-140 (miRNA-140) alleviates osteoarthritis (OA) progression by modulating extracellular matrix (ECM) homeostasis in rats. *Osteoarthritis and Cartilage* 25, (2017).
227. Nakamura, A., Rampersaud, Y. R. et al. microRNA-181a-5p antisense oligonucleotides attenuate osteoarthritis in facet and knee joints. *Annals of Rheumatic Diseases* 78, (2019).
228. Ji, M. L., Lu, J. et al. Dysregulated miR-98 Contributes to Extracellular Matrix Degradation by Targeting IL-6/STAT3 Signaling Pathway in Human Intervertebral Disc Degeneration. *Journal of Bone and Mineral Research* 31, (2016).
229. Ji, M. L., Zhang, X. J. et al. Downregulation of microRNA-193a-3p is involved in intervertebral disc degeneration by targeting MMP14. *Journal of Molecular Medicine-Jmm* 94, (2016).
230. Ji, M. L., Jiang, H. et al. Preclinical development of a microRNA-based therapy for intervertebral disc degeneration. *Nature Communications* 9, (2018).
231. Cai, Y., Lopez-Ruiz, E. et al. A hyaluronic acid-based hydrogel enabling CD44-mediated chondrocyte binding and gapmer oligonucleotide release for modulation of gene expression in osteoarthritis. *Journal of Controlled Release* 253, (2017).
232. Garcia, J. P., Stein, J. et al. Fibrin-hyaluronic acid hydrogel-based delivery of antisense oligonucleotides for ADAMTS5 inhibition in co-delivered and resident joint cells in osteoarthritis. *Journal of Controlled Release* 294, (2019).
233. Lolli, A., Sivasubramanian, K. et al. Hydrogel-based delivery of anti-miR-221 enhances cartilage regeneration by endogenous cells. *Journal of Controlled Release* 309, (2019).
234. Sun, H., Peng, G. et al. Emerging roles of long noncoding RNA in chondrogenesis, osteogenesis, and osteoarthritis. *American Journal of Translational Research* 11, (2019).
235. Ajekigbe, B., Cheung, K. et al. Identification of long non-coding RNAs expressed in knee and hip osteoarthritic cartilage. *Osteoarthritis and Cartilage* 27, (2019).
236. Cuadra, V. M. B., Gonzalez-Huerta, N. C. et al. Altered Expression of Circulating MicroRNA in Plasma of Patients with Primary Osteoarthritis and In Silico Analysis of Their Pathways. *PLoS One* 9, (2014).
237. Gibson, G. & Asahara, H. microRNAs and cartilage. *Journal of Orthopaedic Research* 31, (2013).
238. Rai, M. F., Pan, H. et al. Applications of RNA interference in the treatment of arthritis. *Translational Research: The Journal of Laboratory and Clinical Medicine* 214, (2019).
239. Asahara, H. Current Status and Strategy of microRNA Research for Cartilage Development and Osteoarthritis Pathogenesis. *J Bone Metab* 23, (2016).
240. Barroga, C., Deshmukh, V. et al. Discovery of a Small Molecule Inhibitor of the Wnt Pathway (Sm04690) as a Potential Treatment for Degenerative Disc Disease. *Osteoarthritis and Cartilage* 25, (2017).
241. Childs, B. G., Gluscevic, M. et al. Senescent cells: an emerging target for diseases of ageing. *Nature Reviews: Drug Discovery* 16, (2017).
242. van Deursen, J. M. Senolytic therapies for healthy longevity. *Science* 364, (2019).
243. Le Maitre, C. L., Freemont, A. J. et al. Accelerated cellular senescence in degenerate interverte-

bral discs: a possible role in the pathogenesis of intervertebral disc degeneration. *Arthritis Research & Therapy* 9, (2007).

244. Kumar, A., Bendele, A. M. et al. Sustained efficacy of a single intra-articular dose of FX006 in a rat model of repeated localized knee arthritis. *Osteoarthritis and Cartilage* 23, (2015).

245. Kraus, V. B., Conaghan, P. G. et al. Synovial and systemic pharmacokinetics (PK) of triamcinolone acetonide (TA) following intra-articular (IA) injection of an extended-release microsphere-based formulation (FX006) or standard crystalline suspension in patients with knee osteoarthritis (OA). *Osteoarthritis and Cartilage* 26, (2018).

246. Conaghan, P. G., Hunter, D. J. et al. Effects of a Single Intra-Articular Injection of a Microsphere Formulation of Triamcinolone Acetonide on Knee Osteoarthritis Pain: A Double-Blinded, Randomized, Placebo-Controlled, Multinational Study. *Journal of Bone and Joint Surgery-American Volume* 100, (2018).

247. NCT03529942. (<https://clinicaltrials.gov/ct2/show/NCT03529942>, 2018).

248. Rudnik-Jansen, I., Colen, S. et al. Prolonged inhibition of inflammation in osteoarthritis by triamcinolone acetonide released from a polyester amide microsphere platform. *Journal of Controlled Release* 253, (2017).

249. Rudnik-Jansen, I., Schrijver, K. et al. Intra-articular injection of triamcinolone acetonide releasing biomaterial microspheres inhibits pain and inflammation in an acute arthritis model. *Drug Delivery* 26, (2019).

250. Janssen, M., Timur, U. T. et al. Celecoxib-loaded PEA microspheres as an auto regulatory drug-delivery system after intra-articular injection. *Journal of Controlled Release* 244, (2016).

251. Tellegen, A. R., Rudnik-Jansen, I. et al. Controlled release of celecoxib inhibits inflammation, bone cysts and osteophyte formation in a preclinical model of osteoarthritis. *Drug Delivery* 25, (2018).

252. Tellegen, A. R., Rudnik-Jansen, I. et al. Intradiscal delivery of celecoxib-loaded microspheres restores intervertebral disc integrity in a preclinical canine model. *Journal of Controlled Release* 286, (2018).

253. Rudnik-Jansen, I., Tellegen, A. et al. Safety of intradiscal delivery of triamcinolone acetonide by a poly(esteramide) microsphere platform in a large animal model of intervertebral disc degeneration. *The Spine Journal* 19, (2019).

254. Ragab, A. A., Woodall, J. W. et al. A Preliminary Report on the Effects of Sustained Administration of Corticosteroid on Traumatized Disc Using the Adult Male Rat Model. *Journal of Spinal Disorders & Techniques* 22, (2009).

255. Maudens, P., Seemayer, C. A. et al. Nanocrystal-Polymer Particles: Extended Delivery Carriers for Osteoarthritis Treatment. *Small* 14, (2018).

256. Maudens, P., Seemayer, C. A. et al. Nanocrystals of a potent p38 MAPK inhibitor embedded in microparticles: Therapeutic effects in inflammatory and mechanistic murine models of osteoarthritis. *Journal of Controlled Release* 276, (2018).

257. Mwangi, T. K., Bowles, R. D. et al. Synthesis and characterization of silk fibroin microparticles for intra-articular drug delivery. *International Journal of Pharmaceutics* 485, (2015).

258. Saito, M., Takahashi, K. A. et al. Intraarticular administration of platelet-rich plasma with biodegradable gelatin hydrogel microspheres prevents osteoarthritis progression in the rabbit knee. *Clinical and Experimental Rheumatology* 27, (2009).

259. Sawamura, K., Ikeda, T. et al. Characterization of in vivo effects of platelet-rich plasma and biodegradable gelatin hydrogel microspheres on degenerated intervertebral discs. *Tissue Engineering Part A* 15, (2009).

260. Nagae, M., Ikeda, T. et al. Intervertebral disc regeneration using platelet-rich plasma and biodegradable gelatin hydrogel microspheres. *Tissue Engineering* 13, (2007).

261. Bedouet, L., Moine, L. et al. Synthesis of hydrophilic intra-articular microspheres conjugated to ibuprofen and evaluation of anti-inflammatory activity on articular explants. *International Journal of Pharmaceutics* 459, (2014).

262. Gorth, D. J., Mauck, R. L. et al. IL-1ra delivered from poly(lactic-co-glycolic acid) microspheres attenuates IL-1beta-mediated degradation of nucleus pulposus in vitro. *Arthritis Research & Therapy* 14, (2012).

263. Liang, C. Z., Li, H. et al. Dual delivery for stem cell differentiation using dexamethasone and bFGF in/on polymeric microspheres as a cell carrier for nucleus pulposus regeneration. *Journal of Materials Science-Materials in Medicine* 23, (2012).

264. Liang, C. Z., Li, H. et al. Dual release of dexamethasone and TGF-beta3 from polymeric microspheres for stem cell matrix accumulation in a rat disc degeneration model. *Acta Biomaterialia* 9, (2013).

265. Rothenfluh, D. A., Bermudez, H. et al. Biofunctional polymer nanoparticles for intra-articular targeting and retention in cartilage. *Nature Materials* 7, (2008).

266. Bajpayee, A. G., Wong, C. R. et al. Avidin as a model for charge driven transport into cartilage and drug delivery for treating early stage post-traumatic osteoarthritis. *Biomaterials* 35, (2014).

267. Bajpayee, A. G., Scheu, M. et al. Electrostatic interactions enable rapid penetration, enhanced uptake and retention of intra-articular injected avidin in rat knee joints. *Journal of Orthopaedic Research* 32, (2014).
268. Bajpayee, A. G., Quadir, M. A. et al. Charge based intra-cartilage delivery of single dose dexamethasone using Avidin nano-carriers suppresses cytokine-induced catabolism long term. *Osteoarthritis and Cartilage* 24, (2016).
269. Geiger, B. C., Wang, S. et al. Cartilage-penetrating nanocarriers improve delivery and efficacy of growth factor treatment of osteoarthritis. *Science Translational Medicine* 10, (2018).
270. Zhang, H., Yu, S. et al. Stromal cell-derived factor-1 α -encapsulated albumin/heparin nanoparticles for induced stem cell migration and intervertebral disc regeneration in vivo. *Acta Biomaterialia* 72, (2018).
271. Kedar, U., Phutane, P. et al. Advances in polymeric micelles for drug delivery and tumor targeting. *Nanomedicine: Nanotechnology, Biology, and Medicine* 6, (2010).
272. Kavanaugh, T. E., Werfel, T. A. et al. Particle-based technologies for osteoarthritis detection and therapy. *Drug Deliv Transl Res* 6, (2016).
273. Matsuzaki, T., Matsushita, T. et al. Intra-articular administration of gelatin hydrogels incorporating rapamycin-micelles reduces the development of experimental osteoarthritis in a murine model. *Biomaterials* 35, (2014).
274. Kang, M. L., Jeong, S. Y. et al. Hyaluronic Acid Hydrogel Functionalized with Self-Assembled Micelles of Amphiphilic PEGylated Kartogenin for the Treatment of Osteoarthritis. *Tissue Engineering Part A* 23, (2017).
275. Crielaard, B. J., Rijcken, C. J. et al. Glucocorticoid-loaded core-cross-linked polymeric micelles with tailorable release kinetics for targeted therapy of rheumatoid arthritis. *Angewandte Chemie, International Edition in English* 51, (2012).
276. Quan, L., Zhang, Y. et al. Nanomedicines for inflammatory arthritis: head-to-head comparison of glucocorticoid-containing polymers, micelles, and liposomes. *ACS Nano* 8, (2014).
277. Wang, Q., Jiang, J. Y. et al. Targeted delivery of low-dose dexamethasone using PCL-PEG micelles for effective treatment of rheumatoid arthritis. *Journal of Controlled Release* 230, (2016).
278. Wang, Q., Jiang, H. et al. Targeting NF- κ B signaling with polymeric hybrid micelles that co-deliver siRNA and dexamethasone for arthritis therapy. *Biomaterials* 122, (2017).
279. Wilson, D. R., Zhang, N. et al. Synthesis and evaluation of cyclosporine A-loaded polysialic acid-polycaprolactone micelles for rheumatoid arthritis. *European Journal of Pharmaceutical Sciences* 51, (2014).
280. Zhang, J. X., Yan, M. Q. et al. Local delivery of indomethacin to arthritis-bearing rats through polymeric micelles based on amphiphilic polyphosphazenes. *Pharmaceutical Research* 24, (2007).
281. Zhang, N., Xu, C. et al. Folate receptor-targeted mixed polysialic acid micelles for combating rheumatoid arthritis: in vitro and in vivo evaluation. *Drug Delivery* 25, (2018).
282. Lin, C. Y., Crowley, S. T. et al. Treatment of Intervertebral Disk Disease by the Administration of mRNA Encoding a Cartilage-Anabolic Transcription Factor. *Mol Ther Nucleic Acids* 16, (2019).
283. Feng, G., Zha, Z. et al. Sustained and Bioresponsive Two-Stage Delivery of Therapeutic miRNA via Polyplex Micelle-Loaded Injectable Hydrogels for Inhibition of Intervertebral Disc Fibrosis. *Advanced Healthcare Materials* 7, (2018).
284. Torchilin, V. P. Recent advances with liposomes as pharmaceutical carriers. *Nature Reviews Drug Discovery* 4, (2005).
285. Immordino, M. L., Dosio, F. et al. Stealth liposomes: review of the basic science, rationale, and clinical applications, existing and potential. *International Journal of Nanomedicine* 1, (2006).
286. Barenholz, Y. Doxil(R)—the first FDA-approved nano-drug: lessons learned. *Journal of Controlled Release* 160, (2012).
287. Hua, S. & Wu, S. Y. The use of lipid-based nanocarriers for targeted pain therapies. *Frontiers in Pharmacology* 4, (2013).
288. Tomita, T., Hashimoto, H. et al. In vivo direct gene transfer into articular cartilage by intraarticular injection mediated by HVJ (Sendai virus) and liposomes. *Arthritis & Rheumatism* 40, (1997).
289. Elron-Gross, I., Glucksam, Y. et al. Liposomal dexamethasone-diclofenac combinations for local osteoarthritis treatment. *International Journal of Pharmaceutics* 376, (2009).
290. Elron-Gross, I., Glucksam, Y. et al. Cyclooxygenase inhibition by diclofenac formulated in bioadhesive carriers. *Biochim Biophys Acta* 1778, (2008).
291. Dong, J., Jiang, D. et al. Intra-articular delivery of liposomal celecoxib-hyaluronate combination for the treatment of osteoarthritis in rabbit model. *International Journal of Pharmaceutics* 441, (2013).
292. Verberne, G., Schroeder, A. et al. Liposomes as potential biolubricant additives for wear reduction

- in human synovial joints. *Wear* 268, (2010).
293. Kandel, L., Dolev, Y. et al. Safety and Efficacy of Mm-li, an Intra-Articular Injection of Liposomes, in Moderate Knee Osteoarthritis. Prospective Randomized Double-Blinded Study. *Osteoarthritis and Cartilage* 22, (2014).
294. Chung, S. A., Wei, A. Q. et al. Nucleus pulposus cellular longevity by telomerase gene therapy. *Spine* 32, (2007).
295. Banala, R. R., Vemuri, S. K. et al. Efficiency of dual siRNA-mediated gene therapy for intervertebral disc degeneration (IVDD). *The Spine Journal* 19, (2019).
296. Toledano Furman, N. E., Lupu-Haber, Y. et al. Reconstructed stem cell nanoghosts: a natural tumor targeting platform. *Nano Letters* 13, (2013).
297. Gurunathan, S., Kang, M. H. et al. Review of the Isolation, Characterization, Biological Function, and Multifarious Therapeutic Approaches of Exosomes. *Cells* 8, (2019).
298. Hoare, T. R. & Kohane, D. S. Hydrogels in drug delivery: Progress and challenges. *Polymer* 49, (2008).
299. Li, J. & Mooney, D. J. Designing hydrogels for controlled drug delivery. *Nature Reviews Materials* 1, (2016).
300. Lu, H. T., Sheu, M. T. et al. Injectable hyaluronic-acid-doxycycline hydrogel therapy in experimental rabbit osteoarthritis. *BMC Vet Res* 9, (2013).
301. Pereira, C. L., Goncalves, R. M. et al. The effect of hyaluronan-based delivery of stromal cell-derived factor-1 on the recruitment of MSCs in degenerating intervertebral discs. *Biomaterials* 35, (2014).
302. Petit, A., Sandker, M. et al. Release behavior and intra-articular biocompatibility of celecoxib-loaded acetyl-capped PCLA-PEG-PCLA thermogels. *Biomaterials* 35, (2014).
303. Joshi, N., Yan, J. et al. Towards an arthritis flare-responsive drug delivery system. *Nature Communications* 9, (2018).
304. Willems, N., Yang, H. Y. et al. Biocompatibility and intradiscal application of a thermoreversible celecoxib-loaded poly-N-isopropylacrylamide MgFe-layered double hydroxide hydrogel in a canine model. *Arthritis Research & Therapy* 17, (2015).
305. Yang, H. Y., van Ee, R. J. et al. A novel injectable thermoresponsive and cytocompatible gel of poly(N-isopropylacrylamide) with layered double hydroxides facilitates siRNA delivery into chondrocytes in 3D culture. *Acta Biomaterialia* 23, (2015).
306. Lolli, A., Colella, F. et al. Targeting anti-chondrogenic factors for the stimulation of chondrogenesis: A new paradigm in cartilage repair. *Journal of Orthopaedic Research* 37, (2019).
307. Peeters, M., Detiger, S. E. et al. BMP-2 and BMP-2/7 Heterodimers Conjugated to a Fibrin/Hyaluronic Acid Hydrogel in a Large Animal Model of Mild Intervertebral Disc Degeneration. *Biores Open Access* 4, (2015).
308. Madry, H., Luyten, F. P. et al. Biological aspects of early osteoarthritis. *Knee Surg Sports Traumatol Arthrosc* 20, (2012).
309. Davies-Tuck, M. L., Wluka, A. E. et al. The natural history of cartilage defects in people with knee osteoarthritis. *Osteoarthritis and Cartilage* 16, (2008).
310. Dam, E. B., Runhaar, J. et al. Cartilage cavity-an MRI marker of cartilage lesions in knee OA with Data from CCB, OAI, and PROOF. *Magnetic Resonance in Medicine* 80, (2018).
311. Ding, C., Cicuttini, F. et al. Tibial subchondral bone size and knee cartilage defects: relevance to knee osteoarthritis. *Osteoarthritis and Cartilage* 15, (2007).
312. Hjelle, K., Solheim, E. et al. Articular cartilage defects in 1,000 knee arthroscopies. *Arthroscopy* 18, (2002).
313. Magnussen, R. A., Dunn, W. R. et al. Treatment of focal articular cartilage defects in the knee: a systematic review. *Clinical Orthopaedics and Related Research* 466, (2008).
314. Verma, P. & Dalal, K. ADAMTS-4 and ADAMTS-5: key enzymes in osteoarthritis. *Journal of Cellular Biochemistry* 112, (2011).
315. Song, R. H., Tortorella, M. D. et al. Aggrecan degradation in human articular cartilage explants is mediated by both ADAMTS-4 and ADAMTS-5. *Arthritis & Rheumatism* 56, (2007).
316. Bondeson, J., Wainwright, S. D. et al. The role of synovial macrophages and macrophage-produced cytokines in driving aggrecanases, matrix metalloproteinases, and other destructive and inflammatory responses in osteoarthritis. *Arthritis Research & Therapy* 8, (2006).
317. Deng, H., O'Keefe, H. et al. Discovery of highly potent and selective small molecule ADAMTS-5 inhibitors that inhibit human cartilage degradation via encoded library technology (ELT). *Journal of Medicinal Chemistry* 55, (2012).
318. He, Y., Zheng, Q. et al. The effect of protease inhibitors on the induction of osteoarthritis-related biomarkers in bovine full-depth cartilage explants. *PLoS One* 10, (2015).

319. Chen, P., Zhu, S. et al. The amelioration of cartilage degeneration by ADAMTS-5 inhibitor delivered in a hyaluronic acid hydrogel. *Biomaterials* 35, (2014).
320. Glasson, S. S., Askew, R. et al. Deletion of active ADAMTS5 prevents cartilage degradation in a murine model of osteoarthritis. *Nature* 434, (2005).
321. Larkin, J., Lohr, T. A. et al. Translational development of an ADAMTS-5 antibody for osteoarthritis disease modification. *Osteoarthritis and Cartilage* 23, (2015).
322. Howard, K. A. Delivery of RNA interference therapeutics using polycation-based nanoparticles. *Advanced Drug Delivery Reviews* 61, (2009).
323. Juliano, R. L., Ming, X. et al. Cellular uptake and intracellular trafficking of oligonucleotides: implications for oligonucleotide pharmacology. *Nucleic Acid Therapeutics* 24, (2014).
324. Bajpayee, A. G. & Grodzinsky, A. J. Cartilage-targeting drug delivery: can electrostatic interactions help? *Nature Reviews Rheumatology* 13, (2017).
325. Sepp-Lorenzino, L. & Ruddy, M. Challenges and opportunities for local and systemic delivery of siRNA and antisense oligonucleotides. *Clinical Pharmacology and Therapeutics* 84, (2008).
326. Zhao, X., Pan, F. et al. Controlled delivery of antisense oligonucleotides: a brief review of current strategies. *Expert Opinion on Drug Delivery* 6, (2009).
327. Domingues, M. J., Rambow, F. et al. beta-catenin inhibitor ICAT modulates the invasive motility of melanoma cells. *Cancer Research* 74, (2014).
328. Schindelin, J., Arganda-Carreras, I. et al. Fiji: an open-source platform for biological-image analysis. *Nature Methods* 9, (2012).
329. Kupcsik, L., Alini, M. et al. Epsilon-aminocaproic acid is a useful fibrin degradation inhibitor for cartilage tissue engineering. *Tissue Engineering Part A* 15, (2009).
330. Pfaffl, M. W. A new mathematical model for relative quantification in real-time RT-PCR. *Nucleic Acids Research* 29, (2001).
331. Frieden, M., Christensen, S. M. et al. Expanding the design horizon of antisense oligonucleotides with alpha-L-LNA. *Nucleic Acids Research* 31, (2003).
332. Straarup, E. M., Fisker, N. et al. Short locked nucleic acid antisense oligonucleotides potently reduce apolipoprotein B mRNA and serum cholesterol in mice and non-human primates. *Nucleic Acids Research* 38, (2010).
333. Stanton, R., Sciabola, S. et al. Chemical modification study of antisense gapmers. *Nucleic Acid Therapeutics* 22, (2012).
334. Pedersen, L., Hagedorn, P. H. et al. A Kinetic Model Explains Why Shorter and Less Affine Enzyme-recruiting Oligonucleotides Can Be More Potent. *Mol Ther Nucleic Acids* 3, (2014).
335. Muratovska, A. & Eccles, M. R. Conjugate for efficient delivery of short interfering RNA (siRNA) into mammalian cells. *FEBS Letters* 558, (2004).
336. Cortese, F., McNicholas, M. et al. Arthroscopic Delivery of Matrix-Induced Autologous Chondrocyte Implant: International Experience and Technique Recommendations. *Cartilage* 3, (2012).
337. de Windt, T. S., Vonk, L. A. et al. Allogeneic MSCs and Recycled Autologous Chondrons Mixed in a One-Stage Cartilage Cell Transplantation: A First-in-Man Trial in 35 Patients. *STEM CELLS* 35, (2017).
338. Bannuru, R. R., Natov, N. S. et al. Therapeutic trajectory of hyaluronic acid versus corticosteroids in the treatment of knee osteoarthritis: a systematic review and meta-analysis. *Arthritis & Rheumatism* 61, (2009).
339. Moreno, P. M. D., Ferreira, A. R. et al. Hydrogel-Assisted Antisense LNA Gapmer Delivery for In Situ Gene Silencing in Spinal Cord Injury. *Mol Ther Nucleic Acids* 11, (2018).
340. Wu, H., Lima, W. F. et al. Determination of the role of the human RNase H1 in the pharmacology of DNA-like antisense drugs. *Journal of Biological Chemistry* 279, (2004).
341. Manicourt, D.-H., Poilvache, P. et al. Synovial fluid levels of tumor necrosis factor β and oncostatin M correlate with levels of markers of the degradation of crosslinked collagen and cartilage aggrecan in rheumatoid arthritis but not in osteoarthritis. *Arthritis & Rheumatism* 43, (2000).
342. Ozler, K., Aktas, E. et al. Serum and knee synovial fluid matrixmetalloproteinase-13 and tumor necrosis factor-alpha levels in patients with late stage osteoarthritis. *Acta Orthopaedica et Traumatologica Turcica* 50, (2016).
343. Vincent, H. K., Percival, S. S. et al. Hyaluronic Acid (HA) Viscosupplementation on Synovial Fluid Inflammation in Knee Osteoarthritis: A Pilot Study. *Open Orthopaedics Journal* 7, (2013).
344. Dunn, S. L., Soul, J. et al. Gene expression changes in damaged osteoarthritic cartilage identify a signature of non-chondrogenic and mechanical responses. *Osteoarthritis and Cartilage* 24, (2016).
345. Wu, Z., Zheng, S. et al. E2F1 suppresses Wnt/beta-catenin activity through transactivation of beta-catenin interacting protein ICAT. *Oncogene* 30, (2011).

346. Zhu, M., Chen, M. et al. Inhibition of beta-catenin signaling in articular chondrocytes results in articular cartilage destruction. *Arthritis & Rheumatism* 58, (2008).
347. Kwapisz, A., Chojnacki, M. et al. Do gene expression changes in articular cartilage proteases of the synovial membrane correlate with expression changes of the same genes in systemic blood cells? *International Orthopaedics* 38, (2014).
348. Brophy, R. H., Sandell, L. J. et al. Traumatic and Degenerative Meniscus Tears Have Different Gene Expression Signatures. *American Journal of Sports Medicine* 45, (2017).
349. Wright, K. T., Kuiper, J. H. et al. The Absence of Detectable ADAMTS-4 (Aggrecanase-1) Activity in Synovial Fluid Is a Predictive Indicator of Autologous Chondrocyte Implantation Success. *American Journal of Sports Medicine* 45, (2017).
350. Perera, J. R., Gikas, P. D. et al. The present state of treatments for articular cartilage defects in the knee. *Annals of the Royal College of Surgeons of England* 94, (2012).
351. Devitt, B. M., Bell, S. W. et al. Surgical treatments of cartilage defects of the knee: Systematic review of randomised controlled trials. *Knee* 24, (2017).
352. Korpershoek, J. V., de Windt, T. S. et al. Cell-Based Meniscus Repair and Regeneration: At the Brink of Clinical Translation?: A Systematic Review of Preclinical Studies. *Orthopaedic Journal of Sports Medicine* 5, (2017).
353. Heraud, F., Heraud, A. et al. Apoptosis in normal and osteoarthritic human articular cartilage. *Annals of Rheumatic Diseases* 59, (2000).
354. Akkiraju, H. & Nohe, A. Role of Chondrocytes in Cartilage Formation, Progression of Osteoarthritis and Cartilage Regeneration. *J Dev Biol* 3, (2015).
355. Mobasheri, A. The future of osteoarthritis therapeutics: emerging biological therapy. *Current Rheumatology Reports* 15, (2013).
356. Dancevic, C. M. & McCulloch, D. R. Current and emerging therapeutic strategies for preventing inflammation and aggrecanase-mediated cartilage destruction in arthritis. *Arthritis Research & Therapy* 16, (2014).
357. Schiffelers, R. M., Xu, J. et al. Effects of treatment with small interfering RNA on joint inflammation in mice with collagen-induced arthritis. *Arthritis & Rheumatism* 52, (2005).
358. Bonassar, L. J., Grodzinsky, A. J. et al. The effect of dynamic compression on the response of articular cartilage to insulin-like growth factor-I. *Journal of Orthopaedic Research* 19, (2001).
359. Evans, R. C. & Quinn, T. M. Solute diffusivity correlates with mechanical properties and matrix density of compressed articular cartilage. *Archives of Biochemistry and Biophysics* 442, (2005).
360. Farndale, R. W., Buttle, D. J. et al. Improved quantitation and discrimination of sulphated glycosaminoglycans by use of dimethylmethylene blue. *Biochim Biophys Acta* 883, (1986).
361. Okada, Y., Shinmei, M. et al. Localization of matrix metalloproteinase 3 (stromelysin) in osteoarthritic cartilage and synovium. *Laboratory Investigation* 66, (1992).
362. Malda, J., de Grauw, J. C. et al. Of mice, men and elephants: the relation between articular cartilage thickness and body mass. *PLoS One* 8, (2013).
363. Yan, H., Duan, X. et al. Suppression of NF-kappaB activity via nanoparticle-based siRNA delivery alters early cartilage responses to injury. *Proceedings of the National Academy of Sciences of the United States of America* 113, (2016).
364. Wang, S., Wei, X. et al. A novel therapeutic strategy for cartilage diseases based on lipid nanoparticle-RNAi delivery system. *International Journal of Nanomedicine* 13, (2018).
365. Yan, H., Duan, X. et al. Development of a peptide-siRNA nanocomplex targeting NF- kappaB for efficient cartilage delivery. *Scientific Reports* 9, (2019).
366. Beekhuizen, M., Bastiaansen-Jenniskens, Y. M. et al. Osteoarthritic synovial tissue inhibition of proteoglycan production in human osteoarthritic knee cartilage: establishment and characterization of a long-term cartilage-synovium coculture. *Arthritis & Rheumatism* 63, (2011).
367. Dai, J., Zhou, S. et al. Bi-directional regulation of cartilage metabolism by inhibiting BET proteins-analysis of the effect of I-BET151 on human chondrocytes and murine joints. *Journal of Orthopaedic Surgery and Research* 13, (2018).
368. Zhang, E., Yan, X. et al. Aggrecanases in the human synovial fluid at different stages of osteoarthritis. *Clinical Rheumatology* 32, (2013).
369. Schue, J. R., Tawfik, O. et al. Treatment of Knee Osteoarthritis with Intraarticular Infliximab May Improve Knee Function and Reduce Synovial Infiltration by Macrophages. *Arthritis & Rheumatism* 63, (2011).
370. Richette, P., Francois, M. et al. A high interleukin 1 receptor antagonist/IL-1beta ratio occurs naturally in knee osteoarthritis. *Journal of Rheumatology* 35, (2008).
371. Simao, A. P., Almeida, T. M. et al. Soluble TNF receptors are produced at sites of inflammation and

are inversely associated with self-reported symptoms (WOMAC) in knee osteoarthritis. *Rheumatology International* 34, (2014).

372. Hui, W., Bell, M. et al. Detection of oncostatin M in synovial fluid from patients with rheumatoid arthritis. *Annals of Rheumatic Diseases* 56, (1997).

373. Cawston, T. E., Curry, V. A. et al. The role of oncostatin M in animal and human connective tissue collagen turnover and its localization within the rheumatoid joint. *Arthritis and Rheumatism* 41, (1998).

374. Fearon, U., Mullan, R. et al. Oncostatin M induces angiogenesis and cartilage degradation in rheumatoid arthritis synovial tissue and human cartilage cocultures. *Arthritis & Rheumatism* 54, (2006).

375. Hui, W., Cawston, T. E. et al. A model of inflammatory arthritis highlights a role for oncostatin M in pro-inflammatory cytokine-induced bone destruction via RANK/RANKL. *Arthritis Research & Therapy* 7, (2005).

376. Durigova, M., Roughley, P. J. et al. Mechanism of proteoglycan aggregate degradation in cartilage stimulated with oncostatin M. *Osteoarthritis and Cartilage* 16, (2008).

377. Richards, C. D. The enigmatic cytokine oncostatin m and roles in disease. *ISRN Inflamm* 2013, (2013).

378. Rowan, A. D., Hui, W. et al. Adenoviral gene transfer of interleukin-1 in combination with oncostatin M induces significant joint damage in a murine model. *American Journal of Pathology* 162, (2003).

379. Hui, W., Rowan, A. D. et al. Oncostatin M in combination with tumor necrosis factor alpha induces cartilage damage and matrix metalloproteinase expression in vitro and in vivo. *Arthritis & Rheumatism* 48, (2003).

380. Beekhuizen, M., van Osch, G. J. et al. Inhibition of oncostatin M in osteoarthritic synovial fluid enhances GAG production in osteoarthritic cartilage repair. *European Cells & Materials* 26, (2013).

381. Tsuchida, A. I., Beekhuizen, M. et al. Cytokine profiles in the joint depend on pathology, but are different between synovial fluid, cartilage tissue and cultured chondrocytes. *Arthritis Research & Therapy* 16, (2014).

382. Heymann, D. & Rousselle, A. V. gp130 Cytokine family and bone cells. *Cytokine* 12, (2000).

383. de Hooge, A. S., van de Loo, F. A. et al. Adenoviral transfer of murine oncostatin M elicits periosteal bone apposition in knee joints of mice, despite synovial inflammation and up-regulated expression of interleukin-6 and receptor activator of nuclear factor-kappa B ligand. *American Journal of Pathology* 160, (2002).

384. Walker, E. C., McGregor, N. E. et al. Oncostatin M promotes bone formation independently of resorption when signaling through leukemia inhibitory factor receptor in mice. *Journal of Clinical Investigation* 120, (2010).

385. Cross, A., Edwards, S. W. et al. Secretion of oncostatin M by neutrophils in rheumatoid arthritis. *Arthritis & Rheumatism* 50, (2004).

386. Brown, T. J., Lioubin, M. N. et al. Purification and characterization of cytostatic lymphokines produced by activated human T lymphocytes. Synergistic antiproliferative activity of transforming growth factor beta 1, interferon-gamma, and oncostatin M for human melanoma cells. *Journal of Immunology* 139, (1987).

387. Salamon, P., Shoham, N. G. et al. Human mast cells release oncostatin M on contact with activated T cells: possible biologic relevance. *Journal of Allergy and Clinical Immunology* 121, (2008).

388. Cromartie, W. J., Craddock, J. G. et al. Arthritis in rats after systemic injection of streptococcal cells or cell walls. *Journal of Experimental Medicine* 146, (1977).

389. Lampropoulou-Adamidou, K., Lelovas, P. et al. Useful animal models for the research of osteoarthritis. *European Journal of Orthopaedic Surgery & Traumatology* 24, (2014).

390. Rudnik-Jansen, I., Tellegen, A. R. et al. Local controlled release of corticosteroids extends surgically induced joint instability by inhibiting tissue healing. *British Journal of Pharmacology* 176, (2019).

391. Mankin, H. J. & Lippipello, L. Biochemical and metabolic abnormalities in articular cartilage from osteoarthritic human hips. *Journal of Bone and Joint Surgery-American Volume* 52, (1970).

392. Krenn, V., Morawietz, L. et al. Synovitis score: discrimination between chronic low-grade and high-grade synovitis. *Histopathology* 49, (2006).

393. Koo, T. K. & Li, M. Y. A Guideline of Selecting and Reporting Intraclass Correlation Coefficients for Reliability Research. *Journal of Chiropractic Medicine* 15, (2016).

394. David J. Pasta & Miriam G. Cisternas. in *SAS Conference Proceedings: SAS Users Group International* 28.

395. Wright, H. L., Moots, R. J. et al. The multifactorial role of neutrophils in rheumatoid arthritis. *Nature Reviews Rheumatology* 10, (2014).

396. Tasoglu, O., Boluk, H. et al. Is blood neutrophil-lymphocyte ratio an independent predictor of knee osteoarthritis severity? *Clinical Rheumatology* 35, (2016).

397. Walker, E. C., Johnson, R. W. et al. Murine Oncostatin M Acts via Leukemia Inhibitory Factor Recep-

tor to Phosphorylate Signal Transducer and Activator of Transcription 3 (STAT3) but Not STAT1, an Effect That Protects Bone Mass. *Journal of Biological Chemistry* 291, (2016).

398. Goldring, S. R. The effects of inflammatory arthritis on bone remodeling. *Arthritis Research & Therapy* 7, (2005).

399. Siebelt, M., Groen, H. C. et al. Increased physical activity severely induces osteoarthritic changes in knee joints with papain induced sulfate-glycosaminoglycan depleted cartilage. *Arthritis Research & Therapy* 16, (2014).

400. Moshtagh, P. R., Korthagen, N. M. et al. Early Signs of Bone and Cartilage Changes Induced by Treadmill Exercise in Rats. *JBMR Plus* 2, (2018).

401. Mantila Roosa, S. M., Liu, Y. et al. Gene expression patterns in bone following mechanical loading. *Journal of Bone and Mineral Research* 26, (2011).

402. van Lent, P. L., Blom, A. B. et al. Crucial role of synovial lining macrophages in the promotion of transforming growth factor beta-mediated osteophyte formation. *Arthritis & Rheumatism* 50, (2004).

403. Blom, A. B., van Lent, P. L. et al. Synovial lining macrophages mediate osteophyte formation during experimental osteoarthritis. *Osteoarthritis and Cartilage* 12, (2004).

404. Rudnik-Jansen, I., Woike, N. et al. Applicability of a Modified Rat Model of Acute Arthritis for Long-Term Testing of Drug Delivery Systems. *Pharmaceutics* 11, (2019).

405. Murata, K., Kanemura, N. et al. Controlling joint instability delays the degeneration of articular cartilage in a rat model. *Osteoarthritis and Cartilage* 25, (2017).

406. Marks, P. H. & Donaldson, M. L. Inflammatory cytokine profiles associated with chondral damage in the anterior cruciate ligament-deficient knee. *Arthroscopy* 21, (2005).

407. Kraus, V. B., Birmingham, J. et al. Effects of intraarticular IL-1Ra for acute anterior cruciate ligament knee injury: a randomized controlled pilot trial (NCT00332254). *Osteoarthritis and Cartilage* 20, (2012).

408. Reddy, G. K. & Enwemeka, C. S. A simplified method for the analysis of hydroxyproline in biological tissues. *Clinical Biochemistry* 29, (1996).

409. Kerckhofs, G., Stegen, S. et al. Simultaneous three-dimensional visualization of mineralized and soft skeletal tissues by a novel microCT contrast agent with polyoxometalate structure. *Biomaterials* 159, (2018).

410. Sun, Y., Responde, D. et al. Nondestructive Evaluation of Tissue Engineered Articular Cartilage Using Time-Resolved Fluorescence Spectroscopy and Ultrasound Backscatter Microscopy. *Tissue Engineering Part C: Methods* 18, (2012).

411. Deng, C. X., Hong, X. et al. Ultrasound Imaging Techniques for Spatiotemporal Characterization of Composition, Microstructure, and Mechanical Properties in Tissue Engineering. *Tissue Engineering Part B: Reviews* 22, (2016).

412. Correa, D., Somoza, R. A. et al. Nondestructive/Noninvasive Imaging Evaluation of Cellular Differentiation Progression During In Vitro Mesenchymal Stem Cell-Derived Chondrogenesis. *Tissue Engineering Part A* 24, (2018).

413. Narayanan, L. K., Thompson, T. L. et al. Label free process monitoring of 3D bioprinted engineered constructs via dielectric impedance spectroscopy. *Biofabrication* 10, (2018).

414. Lusic, H. & Grinstaff, M. W. X-ray-computed tomography contrast agents. *Chemical Reviews* 113, (2013).

415. Kokkonen, H. T., Aula, A. S. et al. Delayed Computed Tomography Arthrography of Human Knee Cartilage In Vivo. *Cartilage* 3, (2012).

416. Stewart, R. C., Bansal, P. N. et al. Contrast-enhanced CT with a high-affinity cationic contrast agent for imaging ex vivo bovine, intact ex vivo rabbit, and in vivo rabbit cartilage. *Radiology* 266, (2013).

417. Maerz, T., Newton, M. D. et al. Surface roughness and thickness analysis of contrast-enhanced articular cartilage using mesh parameterization. *Osteoarthritis and Cartilage* 24, (2016).

418. Lakin, B. A., Snyder, B. D. et al. Assessing Cartilage Biomechanical Properties: Techniques for Evaluating the Functional Performance of Cartilage in Health and Disease. *Annual Review of Biomedical Engineering* 19, (2017).

419. Lakin, B. A., Grasso, D. J. et al. Contrast enhanced CT attenuation correlates with the GAG content of bovine meniscus. *Journal of Orthopaedic Research* 31, (2013).

420. Honkanen, J. T. J., Turunen, M. J. et al. Cationic Contrast Agent Diffusion Differs Between Cartilage and Meniscus. *Annals of Biomedical Engineering* 44, (2016).

421. Oh, D. J., Lakin, B. A. et al. Contrast-enhanced CT imaging as a non-destructive tool for ex vivo examination of the biochemical content and structure of the human meniscus. *Journal of Orthopaedic Research* 35, (2017).

422. Maerz, T., Newton, M. D. et al. Three-dimensional characterization of in vivo intervertebral disc degeneration using EPIC-muCT. *Osteoarthritis and Cartilage* 22, (2014).

423. Lin, K. H. & Tang, S. Y. The Quantitative Structural and Compositional Analyses of Degenerating Intervertebral Discs Using Magnetic Resonance Imaging and Contrast-Enhanced Micro-Computed Tomography. *Annals of Biomedical Engineering* 45, (2017).
424. Newton, M. D., Hartner, S. E. et al. Contrast-enhanced μ CT of the intervertebral disc: A comparison of anionic and cationic contrast agents for biochemical and morphological characterization. *Journal of Orthopaedic Research* 35, (2017).
425. Wang, Y., Huang, Y. C. et al. Endogenous regeneration of critical-size chondral defects in immunocompromised rat xiphoid cartilage using decellularized human bone matrix scaffolds. *Tissue Engineering Part A* 18, (2012).
426. Stewart, R. C., Patwa, A. N. et al. Synthesis and Preclinical Characterization of a Cationic Iodinated Imaging Contrast Agent (CA4+) and Its Use for Quantitative Computed Tomography of Ex Vivo Human Hip Cartilage. *Journal of Medicinal Chemistry* 60, (2017).
427. Pouran, B., Arbabi, V. et al. Isolated effects of external bath osmolality, solute concentration, and electrical charge on solute transport across articular cartilage. *Medical Engineering & Physics* 38, (2016).
428. Arbabi, V., Pouran, B. et al. Multiphasic modeling of charged solute transport across articular cartilage: Application of multi-zone finite-bath model. *Journal of Biomechanics* 49, (2016).
429. Jin, L. H., Choi, B. H. et al. Nondestructive Assessment of Glycosaminoglycans in Engineered Cartilages Using Hexabrix-Enhanced Micro-Computed Tomography. *Tissue Engineering and Regenerative Medicine* 15, (2018).
430. Joshi, N. S., Bansal, P. N. et al. Effect of contrast agent charge on visualization of articular cartilage using computed tomography: exploiting electrostatic interactions for improved sensitivity. *Journal of the American Chemical Society* 131, (2009).
431. Bansal, P. N., Joshi, N. S. et al. Cationic contrast agents improve quantification of glycosaminoglycan (GAG) content by contrast enhanced CT imaging of cartilage. *Journal of Orthopaedic Research* 29, (2011).
432. Lakin, B. A., Grasso, D. J. et al. Cationic agent contrast-enhanced computed tomography imaging of cartilage correlates with the compressive modulus and coefficient of friction. *Osteoarthritis and Cartilage* 21, (2013).
433. Lakin, B. A., Patel, H. et al. Contrast-enhanced CT using a cationic contrast agent enables non-destructive assessment of the biochemical and biomechanical properties of mouse tibial plateau cartilage. *Journal of Orthopaedic Research* 34, (2016).
434. Karhula, S. S., Finnila, M. A. et al. Micro-Scale Distribution of CA4+ in Ex vivo Human Articular Cartilage Detected with Contrast-Enhanced Micro-Computed Tomography Imaging. *Frontiers in Physics* 5, (2017).
435. Pittenger, M. F., Mackay, A. M. et al. Multilineage potential of adult human mesenchymal stem cells. *Science* 284, (1999).
436. Doube, M., Klosowski, M. M. et al. BoneJ: Free and extensible bone image analysis in ImageJ. *Bone* 47, (2010).
437. Frohlich, E. The role of surface charge in cellular uptake and cytotoxicity of medical nanoparticles. *International Journal of Nanomedicine* 7, (2012).
438. Takahashi, T., Mizobuchi, H. et al. Metabolic effects of X-ray irradiation on adult human articular chondrocytes. *International Journal of Molecular Medicine* 11, (2003).
439. Margulies, B. S., Horton, J. A. et al. Effects of radiation therapy on chondrocytes in vitro. *Calcified Tissue International* 78, (2006).
440. Saintigny, Y., Cruet-Hennequart, S. et al. Impact of therapeutic irradiation on healthy articular cartilage. *Radiation Research* 183, (2015).
441. Matsumoto, T., Iwasaki, K. et al. Effects of radiation on chondrocytes in culture. *Bone* 15, (1994).
442. Cruet-Hennequart, S., Drougard, C. et al. Radiation-induced alterations of osteogenic and chondrogenic differentiation of human mesenchymal stem cells. *PLoS One* 10, (2015).
443. Jackson, A. & Gu, W. Transport Properties of Cartilaginous Tissues. *Current Rheumatology Reviews* 5, (2009).
444. Kulmala, K. A., Korhonen, R. K. et al. Diffusion coefficients of articular cartilage for different CT and MRI contrast agents. *Medical Engineering & Physics* 32, (2010).
445. Bajpayee, A. G., Scheu, M. et al. A rabbit model demonstrates the influence of cartilage thickness on intra-articular drug delivery and retention within cartilage. *Journal of Orthopaedic Research* 33, (2015).
446. Pouran, B., Arbabi, V. et al. Multi-scale imaging techniques to investigate solute transport across articular cartilage. *Journal of Biomechanics* 78, (2018).
447. Ghezzi, C. E., Rnjak-Kovacina, J. et al. Corneal tissue engineering: recent advances and future perspectives. *Tissue Engineering Part B: Reviews* 21, (2015).

448. Pacella, E., Pacella, F. et al. Glycosaminoglycans in the human cornea: age-related changes. *Ophthalmology and Eye Diseases* 7, (2015).
449. Kandel, R., Roberts, S. et al. Tissue engineering and the intervertebral disc: the challenges. *European Spine Journal* 17 Suppl 4, (2008).
450. Stephens, E. H., Chu, C. K. et al. Valve proteoglycan content and glycosaminoglycan fine structure are unique to microstructure, mechanical load and age: Relevance to an age-specific tissue-engineered heart valve. *Acta Biomaterialia* 4, (2008).
451. Sacks, M. S., Schoen, F. J. et al. Bioengineering challenges for heart valve tissue engineering. *Annual Review of Biomedical Engineering* 11, (2009).
452. Benito, M. J., Veale, D. J. et al. Synovial tissue inflammation in early and late osteoarthritis. *Annals of Rheumatic Diseases* 64, (2005).
453. Attur, M., Krasnokutsky, S. et al. Low-grade inflammation in symptomatic knee osteoarthritis: prognostic value of inflammatory plasma lipids and peripheral blood leukocyte biomarkers. *Arthritis & Rheumatology* 67, (2015).
454. Kraus, V. B., McDaniel, G. et al. Direct in vivo evidence of activated macrophages in human osteoarthritis. *Osteoarthritis and Cartilage* 24, (2016).
455. Mather, M. L., Morgan, S. P. et al. Meeting the needs of monitoring in tissue engineering. *Regenerative Medicine* 2, (2007).
456. Nam, S. Y., Ricles, L. M. et al. Imaging strategies for tissue engineering applications. *Tissue Engineering Part B: Reviews* 21, (2015).
457. Krishnan, Y., Rees, H. A. et al. Green fluorescent proteins engineered for cartilage-targeted drug delivery: Insights for transport into highly charged avascular tissues. *Biomaterials* 183, (2018).
458. Raya, J. G. Techniques and applications of in vivo diffusion imaging of articular cartilage. *Journal of Magnetic Resonance Imaging* 41, (2015).
459. Salo, E. N., Nissi, M. J. et al. Diffusion of Gd-DTPA(2)(-) into articular cartilage. *Osteoarthritis and Cartilage* 20, (2012).
460. Meder, R., de Visser, S. K. et al. Diffusion tensor imaging of articular cartilage as a measure of tissue microstructure. *Osteoarthritis and Cartilage* 14, (2006).
461. De Luca, A., Arra, C. et al. Simultaneous blockage of different EGF-like growth factors results in efficient growth inhibition of human colon carcinoma xenografts. *Oncogene* 19, (2000).
462. Casamassimi, A., De Luca, A. et al. EGF-related antisense oligonucleotides inhibit the proliferation of human ovarian carcinoma cells. *Annals of Oncology* 11, (2000).
463. Garbuzenko, O. B., Saad, M. et al. Inhibition of lung tumor growth by complex pulmonary delivery of drugs with oligonucleotides as suppressors of cellular resistance. *Proceedings of the National Academy of Sciences of the United States of America* 107, (2010).
464. Echigoya, Y. & Yokota, T. Skipping multiple exons of dystrophin transcripts using cocktail antisense oligonucleotides. *Nucleic Acid Therapeutics* 24, (2014).
465. Yokota, T., Nakamura, A. et al. Extensive and prolonged restoration of dystrophin expression with vivo-morpholino-mediated multiple exon skipping in dystrophic dogs. *Nucleic Acid Therapeutics* 22, (2012).
466. Miskew Nichols, B., Aoki, Y. et al. Multi-exon Skipping Using Cocktail Antisense Oligonucleotides in the Canine X-linked Muscular Dystrophy. *Journal of Visualized Experiments*, (2016).
467. Stein, C. A. & Castanotto, D. FDA-Approved Oligonucleotide Therapies in 2017. *Molecular Therapy* 25, (2017).
468. Vitravene Study, G. A randomized controlled clinical trial of intravitreal fomivirsen for treatment of newly diagnosed peripheral cytomegalovirus retinitis in patients with AIDS. *American Journal of Ophthalmology* 133, (2002).
469. Jabs, D. A. & Griffiths, P. D. Fomivirsen for the treatment of cytomegalovirus retinitis. *American Journal of Ophthalmology* 133, (2002).
470. Finkel, R. S., Chiriboga, C. A. et al. Treatment of infantile-onset spinal muscular atrophy with nusinersen: a phase 2, open-label, dose-escalation study. *Lancet* 388, (2016).
471. Finkel, R. S., Mercuri, E. et al. Nusinersen versus Sham Control in Infantile-Onset Spinal Muscular Atrophy. *New England Journal of Medicine* 377, (2017).
472. Kim, J., Hu, C. et al. Patient-Customized Oligonucleotide Therapy for a Rare Genetic Disease. *New England Journal of Medicine* 381, (2019).
473. Vedadghavami, A., Wagner, E. K. et al. Cartilage penetrating cationic peptide carriers for applications in drug delivery to avascular negatively charged tissues. *Acta Biomaterialia* 93, (2019).
474. Elsaid, K. A., Ferreira, L. et al. Pharmaceutical nanocarrier association with chondrocytes and cartilage explants: influence of surface modification and extracellular matrix depletion. *Osteoarthritis and*

Cartilage 21, (2013).

475. Brown, S., Pistiner, J. et al. Nanoparticle Properties for Delivery to Cartilage: The Implications of Disease State, Synovial Fluid, and Off-Target Uptake. *Molecular Pharmaceutics* 16, (2019).

476. Ronga, M., Grassi, F. A. et al. Arthroscopic autologous chondrocyte implantation for the treatment of a chondral defect in the tibial plateau of the knee. *Arthroscopy* 20, (2004).

477. Schlag, G. & Redl, H. Fibrin sealant in orthopedic surgery. *Clinical Orthopaedics and Related Research* 227, (1988).

478. Trombino, S., Servidio, C. et al. Strategies for Hyaluronic Acid-Based Hydrogel Design in Drug Delivery. *Pharmaceutics* 11, (2019).

479. Aruffo, A., Stamenkovic, I. et al. CD44 is the principal cell surface receptor for hyaluronate. *Cell* 61, (1990).

480. Ishida, O., Tanaka, Y. et al. Chondrocytes are regulated by cellular adhesion through CD44 and hyaluronic acid pathway. *Journal of Bone and Mineral Research* 12, (1997).

481. Sterner, B., Harms, M. et al. The effect of polymer size and charge of molecules on permeation through synovial membrane and accumulation in hyaline articular cartilage. *European Journal of Pharmaceutics and Biopharmaceutics* 101, (2016).

482. Gaharwar, A. K., Peppas, N. A. et al. Nanocomposite hydrogels for biomedical applications. *Biotechnology and Bioengineering* 111, (2014).

483. Gao, W., Zhang, Y. et al. Nanoparticle-Hydrogel: A Hybrid Biomaterial System for Localized Drug Delivery. *Annals of Biomedical Engineering* 44, (2016).

484. Caicco, M. J., Cooke, M. J. et al. A hydrogel composite system for sustained epi-cortical delivery of Cyclosporin A to the brain for treatment of stroke. *Journal of Controlled Release* 166, (2013).

485. Elliott Donaghue, I. & Shoichet, M. S. Controlled release of bioactive PDGF-AA from a hydrogel/nanoparticle composite. *Acta Biomaterialia* 25, (2015).

486. Langworthy, M. J., Conaghan, P. G. et al. Efficacy of Triamcinolone Acetonide Extended-Release in Participants with Unilateral Knee Osteoarthritis: A Post Hoc Analysis. *Advances in Therapy* 36, (2019).

487. Kivitz, A. J., Conaghan, P. G. et al. Rescue Analgesic Medication Use by Patients Treated with Triamcinolone Acetonide Extended-Release for Knee Osteoarthritis Pain: Pooled Analysis of Three Phase 2/3 Randomized Clinical Trials. *Pain and Therapy* 8, (2019).

488. Emery, C. A., Whittaker, J. L. et al. Establishing outcome measures in early knee osteoarthritis. *Nature Reviews Rheumatology* 15, (2019).

489. Pelletier, J. P., Caron, J. P. et al. In vivo suppression of early experimental osteoarthritis by interleukin-1 receptor antagonist using gene therapy. *Arthritis & Rheumatism* 40, (1997).

490. Caron, J. P., Fernandes, J. C. et al. Chondroprotective effect of intraarticular injections of interleukin-1 receptor antagonist in experimental osteoarthritis. Suppression of collagenase-1 expression. *Arthritis & Rheumatism* 39, (1996).

491. Ayril, X., Pickering, E. H. et al. Synovitis: a potential predictive factor of structural progression of medial tibiofemoral knee osteoarthritis -- results of a 1 year longitudinal arthroscopic study in 422 patients. *Osteoarthritis and Cartilage* 13, (2005).

492. Krasnokutsky, S., Belitskaya-Levy, I. et al. Quantitative Magnetic Resonance Imaging Evidence of Synovial Proliferation Is Associated With Radiographic Severity of Knee Osteoarthritis. *Arthritis & Rheumatism* 63, (2011).

493. Roemer, F. W., Guermazi, A. et al. Presence of MRI-detected joint effusion and synovitis increases the risk of cartilage loss in knees without osteoarthritis at 30-month follow-up: the MOST study. *Annals of the Rheumatic Diseases* 70, (2011).

494. Jorgensen, J. T. A paradigm shift in biomarker guided oncology drug development. *Annals of Translational Medicine* 7, (2019).

495. Trusheim, M. R., Berndt, E. R. et al. Stratified medicine: strategic and economic implications of combining drugs and clinical biomarkers. *Nature Reviews: Drug Discovery* 6, (2007).

496. Slamon, D. J., Clark, G. M. et al. Human breast cancer: correlation of relapse and survival with amplification of the HER-2/neu oncogene. *Science* 235, (1987).

497. Slamon, D. J., Leyland-Jones, B. et al. Use of chemotherapy plus a monoclonal antibody against HER2 for metastatic breast cancer that overexpresses HER2. *New England Journal of Medicine* 344, (2001).

498. Drilon, A., Laetsch, T. W. et al. Efficacy of Larotrectinib in TRK Fusion-Positive Cancers in Adults and Children. *New England Journal of Medicine* 378, (2018).

499. Takahashi, T. Organoids for Drug Discovery and Personalized Medicine. *Annual Review of Pharmacology and Toxicology* 59, (2019).

500. Clevers, H. C. Organoids: Avatars for Personalized Medicine. *Keio Journal of Medicine* 68, (2019).

501. Dekkers, J. F., Berkers, G. et al. Characterizing responses to CFTR-modulating drugs using rectal organoids derived from subjects with cystic fibrosis. *Science Translational Medicine* 8, (2016).
502. Bartfeld, S. & Clevers, H. Stem cell-derived organoids and their application for medical research and patient treatment. *Journal of Molecular Medicine-Jmm* 95, (2017).
503. Kondo, J. & Inoue, M. Application of Cancer Organoid Model for Drug Screening and Personalized Therapy. *Cells* 8, (2019).
504. Hunter, D. J., Nevitt, M. et al. Biomarkers for osteoarthritis: Current position and steps towards further validation. *Best Practice & Research in Clinical Rheumatology* 28, (2014).
505. Pelletier, J. P., Cooper, C. et al. What is the predictive value of MRI for the occurrence of knee replacement surgery in knee osteoarthritis? *Annals of the Rheumatic Diseases* 72, (2013).
506. Georgakoudi, I., Rice, W. L. et al. Optical spectroscopy and imaging for the noninvasive evaluation of engineered tissues. *Tissue Engineering Part B: Reviews* 14, (2008).
507. Kotecha, M., Klatt, D. et al. Monitoring cartilage tissue engineering using magnetic resonance spectroscopy, imaging, and elastography. *Tissue Engineering Part B: Reviews* 19, (2013).
508. Gudur, M., Rao, R. R. et al. Noninvasive, quantitative, spatiotemporal characterization of mineralization in three-dimensional collagen hydrogels using high-resolution spectral ultrasound imaging. *Tissue Engineering Part C: Methods* 18, (2012).
509. Herrmann, J. M., Pitris, C. et al. High resolution imaging of normal and osteoarthritic cartilage with optical coherence tomography. *Journal of Rheumatology* 26, (1999).
510. Li, X., Martin, S. et al. High-resolution optical coherence tomographic imaging of osteoarthritic cartilage during open knee surgery. *Arthritis Research & Therapy* 7, (2005).
511. Chu, C. R., Lin, D. et al. Arthroscopic microscopy of articular cartilage using optical coherence tomography. *American Journal of Sports Medicine* 32, (2004).
512. Jahr, H., Brill, N. et al. Detecting early stage osteoarthritis by optical coherence tomography? *Biomarkers* 20, (2015).
513. Han, C. W., Chu, C. R. et al. Analysis of rabbit articular cartilage repair after chondrocyte implantation using optical coherence tomography. *Osteoarthritis and Cartilage* 11, (2003).
514. Sarin, J. K., Te Moller, N. C. R. et al. Arthroscopic near infrared spectroscopy enables simultaneous quantitative evaluation of articular cartilage and subchondral bone in vivo. *Scientific Reports* 8, (2018).
515. Ramaswamy, S., Uluer, M. C. et al. Noninvasive assessment of glycosaminoglycan production in injectable tissue-engineered cartilage constructs using magnetic resonance imaging. *Tissue Engineering Part C: Methods* 14, (2008).
516. Neu, C. P., Arastu, H. F. et al. Characterization of engineered tissue construct mechanical function by magnetic resonance imaging. *Journal of Tissue Engineering and Regenerative Medicine* 3, (2009).
517. Mwale, F., Roughley, P. et al. Distinction between the extracellular matrix of the nucleus pulposus and hyaline cartilage: a requisite for tissue engineering of intervertebral disc. *European Cells & Materials* 8, (2004).
518. Rustenburg, C. M. E., Emanuel, K. S. et al. Osteoarthritis and intervertebral disc degeneration: Quite different, quite similar. *JOR Spine* 1, (2018).

NEDERLANDSE SAMENVATTING

Artrose is een van de meest veelvoorkomende aandoeningen van ons spier- en skeletstelsel en de meest voorkomende oorzaak van gewrichtsklachten. Ongeveer 15% van de wereldbevolking lijdt aan artrose. Het is een invaliderende aandoening die een diepgaande impact heeft op de kwaliteit van leven van de patiënt en daarmee op de maatschappij. Ondanks de omvang van het probleem, is er nog steeds geen effectieve behandeling beschikbaar. Daarom is het urgent om nieuwe behandelingen te ontwikkelen die gewrichtsslijtage remmen, naast behandelingen die de pijn verlichten.

In de laatste jaren zijn veel klinische onderzoeken uitgevoerd naar de werking van verschillende nieuwe biologische medicijnen voor artrose, maar de resultaten waren meestal teleurstellend. Soms kwam dit doordat de medicijnen niet effectief waren, soms door ernstige bijwerkingen. De tegenvallende effectiviteit hangt vaak samen met het feit dat medicijnen snel weer uit het gewricht verdwijnen. Bijwerkingen worden vaak gezien als een middel langdurig ingenomen moet worden. Bovendien worden dergelijke klinische studies vaak uitgevoerd zonder te kijken naar het type artrose wat de patiënt heeft, waardoor een mogelijk veelbelovend middel voor die groep patiënten niet als zodanig geïdentificeerd wordt. Er zijn dus veel hordes te nemen in de aanloop naar de ontwikkeling van een effectieve behandeling van artrose.

Daarom hebben we in dit proefschrift het artroseonderzoek van verschillende kanten benaderd en willen we duidelijk maken dat de combinatie van het vinden van nieuwe ziekteaangrijpingspunten, de ontwikkeling van nieuwe medicijnen en het ontwikkelen van nieuwe en verbeterde screeningstechnieken samen nodig zijn voor het ontwikkelen van nieuwe en effectieve behandelingen van artrose.

In **hoofdstuk 2** geven we een overzicht van de huidige en opkomende behandelopties van artrose en de recente ontwikkelingen rond materialen die ontwikkeld zijn voor lokale medicijnafgifte. Duidelijk wordt gemaakt hoe lokale afgifte medicijnen effectiever kan maken door het bewerkstelligen van een lokale langdurige hoge concentratie, terwijl bijwerkingen samenhangend met het systemisch (bv oraal of intraveneus) toedienen voorkomen worden. In lijn hiermee laten we in **hoofdstuk 3** de toepasbaarheid zien van een hydrogel voor het afgeven van chemisch gemodificeerde antisense oligonucleotiden (ASOs) die de expressie (en daarmee productie) van het kraakbeen afbrekend enzym ADAMTS5 remmen. We laten zien dat het laden van de hydrogel met ASOs tot 14 dagen een efficiënte remming van ADAMTS5 genexpressie geeft in kraakbeencellen die in dezelfde gel opgenomen zijn. Vervolgens hebben we gekeken of deze ASO ook ADAMTS5 in kraakbeen kon remmen. Kraakbeen is een heel compact weefsel door de hoge dichtheid van proteoglycanen en collageen II, waardoor diffusie van medicijnen een van de grootste bottlenecks is in medicijnafgifte in kraakbeen. Daarom onderzochten we in **hoofdstuk 4** in stukjes kraakbeenweefsel de diffusie en het vermogen van de gemodificeerde ASOs om kraakbeencellen binnen te dringen en de expressie van ADAMTS5 te remmen. Zowel de gouden standaard siRNA (small inhibitory RNA) als de ASO diffundeerde door het kraakbeenweefsel en kwam bij de cellen terecht, maar alleen de ASO gaf remming van ADAMTS5 expressie, daarmee de potentie van deze antisensetechnologie demonstrerend.

Zoals eerder genoemd, zijn er verschillende vormen van artrose, deels samenhangend met verschillende etiologie, die zich uiten in verschillende symptomen bij patiënten. Daarom zal effectieve behandeling afhangen van de te behandelen type patiënt. In **hoofdstuk 5** brengen we de expressie van oncostatin M (OSM) in kaart in twee diermodellen van gewrichtsschade, een model gebaseerd op de inductie van instabiliteit en een model gebaseerd op de inductie van ontsteking. OSM is een eiwit dat gebruikt kan worden om een onderscheid tussen types patiënten te maken. Het bleek dat in het diermodel met acute gewrichtsontsteking, maar niet in artrose geïnduceerd door instabiliteit, OSM-productie correleerde met ontstekingsparameters. Ook in de synoviale vloeistof van OA-patiënten correleerde de aanwezigheid van OSM met pro-inflammatoire cytokinen, indicatief voor een meer inflammatoir fenotype. OSM zou daarom zowel als target van behandeling kunnen dienen als biomarker voor een subset van patiënten.

Uiteindelijk beschrijven we in **hoofdstuk 6** de ontwikkeling van een kwantitatieve beeldvormingstechniek die gebruikt kan worden om in vitro kraakbeenregeneratie te volgen. Kraakbeenonderzoek wordt momenteel gekenmerkt door analytische methoden, zoals histologische en biochemische technieken, waarvoor het weefsel moet worden vernield. In dit hoofdstuk ontwikkelden we een methode gebaseerd op computed tomography (CT) die het mogelijk maakt om nondestructief de productie van proteoglycanen in in vitro weefsel over tijd te volgen. Extra voordeel van deze techniek is dat ook de ruimtelijke verdeling van proteoglycanen over het in vitro groeiende weefsel zichtbaar gemaakt kan worden, informatie die tot nog toe niet verkregen kon worden met de traditionele methoden. De ontwikkeling en toepassing van dit soort technieken zal cruciaal blijken voor het in vitro preklinisch screening en testen van nieuwe behandelingen voordat deze de kliniek bereiken.

Artrose is een van de meest voorkomende aandoeningen van ons spier- en skeletstelsel en tot op heden is er geen effectieve behandeling, waarbij pijnstilling alleen een kortetermijnoplossing is. Nieuwe soorten medicijnen, zoals die gebaseerd op RNA, hebben een meerwaarde boven de huidige "small molecule" medicijnen of andere medicijnen die op eiwitniveau interfereren. Minstens even belangrijk is het dat lokale toediening middels medicijnafgiftesystemen behandelingen effectiever zal maken door verlengde aanwezigheid van het medicijn in afdoende concentraties. Artrose moet gezien en behandeld worden als een multifactoriële ziekte, waarbij identificatie van biomarker en fenotype cruciaal zullen zijn voor de ontwikkeling van nieuwe medicijnen in een vroeg stadium en later voor de uiteindelijke behandeling in goed gedefinieerde patiëntenpopulaties. Tot slot is de ontwikkeling en toepassing van nieuwe beeldvormingstechnieken in de preklinische fase van ontwikkeling belangrijk om de beste aanpak voor gewrichtsherstel te identificeren.

ABBREVIATION LIST

μCT	Micro-computed tomography
2'-OMe	2'-O-Methyl
2'-OMOE	2'-O-methoxyethyl
3D	Three-dimensional
AC	Articular cartilage
ACI	Autologous chondrocyte implantation
ACL	Anterior cruciate ligament transection
ADAMTS	A disintegrin and metalloproteinase with thrombospondin motifs
AF	Annulus fibrosus
ASAP	Ascorbic-2-phosphate
ASOs	Antisense oligonucleotide
BCL-2	B-cell lymphoma 2 protein
bFGF	Basic fibroblast growth factor
CECT	Contrast-enhanced computed tomography
CF	Cystic fibrosis
CI	Confidence intervals
CMC	Critical micelle concentration
CMV	Cytomegalovirus
COX-2	Cyclooxygenase-2
CT	Computed tomography
CTNBP1	β-catenin interacting protein 1
DMD	Duchenne muscular dystrophy
DMEM	Dulbecco's modified eagle's medium
DMMB	1,9-dimethylmethylene blue
DMOADs	Disease-modifying drugs for OA
ECM	Extracellular matrix
EDTA	Ethylenediaminetetraacetic acid
F	Fibrin
FBS	Fetal bovine serum
FDA	Food and drug administration
FJ	Facet joint
FSC	Forward scatter
GAG	Glycosaminoglycan
GAPDH	Glyceraldehyde 3-phosphate dehydrogenase
GDF-5	Growth and differentiation factor-5
GI	Gastrointestinal
HA	Hyaluronic acid
HAS	Human serum albumin
hTERT	Human telomerase reverse transcriptase
ICC	Intra-class correlation coefficient
IGF-1	Insulin-like growth factor 1
IHC	Immunohistochemistry
IL	Interleukin
IL-1Ra	IL-1 receptor antagonist
ITS-X	Insulin-transferrin-selenium-ethanolamine
IVD	Intervertebral disc
IVDD	Intervertebral disc degeneration
LDH	Lactate dehydrogenase
LNAs	Locked nucleic acids

MACI	Matrix-assisted ACI
miRNAs	Micro RNAs
MMPs	Metalloproteinases
MRI	Magnetic resonance imaging
mRNA	messenger RNA
MRP-1	Multidrug resistance-associated protein
MSCs	Mesenchymal stromal cells
NGF	Nerve growth factor
NO	Nitric oxide
NP	Nucleus pulposus
NSAIDs	Non-steroidal anti-inflammatory drugs
OA	Osteoarthritis
OCT	Optical coherence tomography
OSM	Oncostatin M
PAMAM	Polyamidoamine
PBS	Phosphate buffer saline
PEA	Polyester amide
PEG	Poly(ethylene-glycol)
PGPS	Peptidoglycan-polysaccharide
pHPMAmLacn	Poly(N-(2-hydroxypropyl)methacrylamide-lactate)
PLA	Poly(lactic) acid
PLGA	Poly(lactic-co-glycolic acid)
PRP	Platelet-rich plasma
PS	Phosphorothioate
qPCR	Real-time PCR
RA	Rheumatoid arthritis
RNA	Ribonucleic acid
RPL19	Ribosomal protein L19
SDF-1 α	Stromal cell-derived factor-1 alpha
SDHA	Succinate dehydrogenase complex subunit A
siRNAs	Small interfering RNAs
SMA	Spinal muscular atrophy
SSC	Side scatter
TAA	Triamcinolone acetonide
TCP	Tricalcium phosphate
TIMPs	Tissue inhibitors of metalloproteinases
TNF- α	Tumour necrosis factor alpha
TRAP	Tartrate-resistant acid phosphatase
US	Ultrasound

ACKNOWLEDGMENTS

During the last 5 years, many were the people that I cross paths with, and that in way or another made my PhD experience one that I am proud of. To all of you, thank you!

Promotion team

My promotors, Prof. dr. Cumhuri Oner and Prof. dr. Marianna Tryfonidou, thank you for the support over these years and the useful and essential feedback on the manuscripts and thesis. Marianna, it is really impressive that although being quite busy you put an enormous effort into teaching and training your students. I still remember that back in 2015 you were the one teaching me how to do immunohistochemistry. It was a pleasure to collaborate with you all these years, and looking forward for what's to come!

Dear Laura, first of all, thank you for giving me the opportunity to be a PhD student with you, and specially to be part of the TargetCare consortium. You have been an incredible supervisor and, above all, an excellent mentor over these 5 years. I am really grateful for all the great scientific discussions we had, the challenges you put me up to, and more importantly, the freedom you gave me during my PhD. I am happy that you would (almost) always support and let me explore my new (but not necessarily bright) research ideas. Last but not least, besides being an excellent scientist and supervisor, you can see your students beyond the lab coat and you do care about their well-being! Won't forget how surprised I was when you lent me your car only two weeks after meeting me (that was risky).

Colleagues & Friends

I would like to thank all my colleagues at the Department of Orthopedics and RMCU, and some of you in particular:

First of all, I would like to thank our lab technicians Mattie, Inge and Anneloes for keeping the lab running smoothly. Mattie, I think my PhD would have taken 2 or 3 years longer if you were not at the Orthopedics. I could always count on you to help me find my way around the lab, and I am pretty sure you never replied "I don't know" to any of my (many) questions or requests. I told you once I could use your problem-solving skills in my personal life. It would make things much easier!

Brenda, can't thank you enough for your bureaucratic superpowers and the numerous times you helped me throughout the years.

Imke, I am sorry for you. Laura labeled both of us as Ms. and Mr. Chaos, however, I do think that compared to me you have a tiny level of OCD. I am sorry for the day I tried to feed you codfish, I still have nightmares with the face you did after biting it (it hurts!). Jokes apart, it was a blast working with you: you are smart, creative, super fun and you do like your snacks. We drunk together, we laughed together, but for some reason I'm happy we never sang together! I wish you all the best in Denmark with your super family, Mariusz, Aleks and Julian. I do hope we can one day share a lab bench again (perhaps one with less specimens in formalin)!

Lizette, thank you for the collaboration and friendship in the last years, and for sharing

my frustrations on the OSM project. I'm impressed on how super efficient you are, and your troubleshoot capacity is off the charts (really!). I like it how you are always up for a good laugh or to discuss the last T-bone steak or Rib-eye we had. I am super happy you joined the iPSpine project! Behdad, it was great to have you as an office mate, and the project we built together was definitely one of the most interesting during my PhD. I am happy we had the chance to become friends over the years, but above all, thanks for being my personal (and infinite) source of saffron and pistachio! Mylene, we didn't really cross paths at the beginning of the PhD, but you did make a difference at the end! I really enjoyed our climbing sessions where we would discuss ideas and (more often) frustrations. I also became almost proficient at understanding your sarcasm and irony. Hope we get to do a climbing trip soon, but before let's practice those (super scary) falls. Jie, what an impact you made in the last year of my PhD. While I thought I would be teaching you stuff and showing you around, I was the one learning the most: from the most famous Chinese alcoholic beverages to the Chinese political system. And guess what? I became a fan of Chinese cuisine, specially of those cola wings (yes, chicken wings with coca cola). I find it impressive on how you can always remain so calm and relaxed even though things don't always go as planned. Iris, I still remember how out of place I felt when you brought us to one of those nights at Stairway to Heaven! Had a lot of fun in those Macumba parties, but I still believe Mama Africa tops it up, easily! Alessia, thank you for the company on those long working nights and weekends in the Hubrecht, and for sharing those unhealthy amounts of delivery sushi. I had tons of fun during our baby-steps in climbing and bouldering. Those moments did leave beautiful memories and made the first years of the PhD and of living in Utrecht happier!

The Sox9 crew. Koen, Chella, Maaïke and Prof. Croes, remember that house we rented in Davos, where the size of the room was proportional to the size of the person sleeping there? That was fun!

Dear colleagues of the Orthopedics department: Saber (what's up?), Miguel, Riccardo, Susanna, Yang, Flor, Iris O., Paweena, Margo, Joost, Margot, Jasmijn, Anita, Serafim, Irina, Barbara, Jaqueline, Kelly, Luuk, Maddie, Nada and all RMCU colleagues. Thank you for welcoming me, for all the scientific input and fruitful discussions, chats over coffee, and the borrels we had over the years.

Thank you to all the colleagues at the veterinary department, Alberto, Frank, Saskia, Frances, Anna and Michelle for all the interesting discussions and feedback during the cartilage meetings.

A big-up to the students I supervised over the years: Jeroen, Miguel, Tulu and Valerie. Thank you for the dedication and hard work. Wish you all the best!

The TargetCaRe team: Andrea, Bernardo, Bradley, Fabio, Federico, Florian, Jacopo, Letizia, Luana, Lucia, Mimmo, Serdar, Sonja, Yunpeng. It was a pleasure to share my PhD with you! I had so much fun meeting you in different parts of the world during TargetCaRe meetings or conferences, and especially those after-dinner moments. Mimmo and Lucia I had a lot of fun having you in Utrecht and working with you. We did not only do a lot of fun science, but we also became movie-makers, wow! Lucia, I can say with great certainty

that you are the most proficient chemist at trypsinizing cells. Mimmo, I won't forget one of my most memorable life stories happened when I was on my way to meet you in Tel Aviv! What a weird situation! Thank you for all the amazing guanciale and 'nduja you provided the last years, or the cheese that almost got confiscated in an Israeli airport! Thank you to all the PI's integrating TargetCaRe, namely Gerjo, for putting this consortium together and for the amazing scientific discussions, new ideas and troubleshooting during our meetings.

I would also like to thank some other people I had the chance to share some projects since 2015. Luca, thanks for the tips and tricks you gave me on making a reporter cell lines! Lies, it was a pleasure to meet you and to work on a little project together, and specially discussing about the best restaurants in Utrecht.

Friends

My Garlicanos, or Oreganos! Elena! Wow, where to start! It is difficult to admit but you might be one of the most patient and understanding persons I have met. Somehow you managed to host me in your house for almost 3 months while I was writing my thesis, and that is a feat not everybody would be up to! You would not care much about my weird mood swings, and you would always have a beautiful smile to give back! Carlo, I think we are soulmates when it comes to food! It's amazing how you are always up for spontaneous (often very tight) food plans, like going for mozzarella in Amsterdam (then replaced by some Lebanese tapas), followed by the best apple pie at Winkel 43, and a climbing session after that. The romantic way you describe dishes and recipes: I would pay for a podcast on this! Pleeeeeeaaase, include me in the plans once you open that restaurant in Tuscany! I promise my Italian will be better once I'm back from Italy!

All the Vibes group! Cyril, this hurricane of moods and emotions. I just checked and you haven't left a WhatsApp group in quite some months, I see an improvement. Jokes apart, during my PhD I could always count on you for a little sport session (swimming, biking, climbing, you name it). More importantly, I could always bother you for some wise words! PS: you still owe me a visit to the KLM lounge. Italy did not count. Luisa, *bellezza de mio cuore, sono molto felici di averti nella mia vita* – and that's how far I can go without translator. I would say you are most likely the 2nd best at doing the awkward facing dog, but there is room for improvement. However, to train, you have to come back from your sabbatical year in Italy! Martina, my dear spinach, I'm impressed how fast and efficient we were in organizing the climbing trip to that place "that cannot be named". Although it did not happen, I am pretty sure we will have plenty of time to go on climbing trips, what about combining a catamaran and Kalymnos next year? I am also very glad you were a constant presence on our runs during lockdown! With you I can freely express my musical taste without being judged! Isi, warms my heart knowing you are now capable of tying your shoe laces, and that I am partially responsible for that! Lisa, you probably have the best dance moves in Utrecht, period. Deji, I am always surprised on how you are in a constant party mood. Had a lot of fun going to summer festivals with you, specially that Encore in Amsterdam! H elene, I still cannot believe you hired a food-truck for your birthday!

Thanks to the LN house: Alex, Magda, Aisha, Anna, Anne, Casper, Matteo, Tom, Mirthe, Stefano, Saskia, Soraya. Thank you for all the brunches, lunches and dinners that we shared, those crazy parties when half of Utrecht would come into the house, or those lazy Sundays watching TV in the living room. I won't forget how welcomed I felt as soon as I stepped in number 74 of Lange Nieuwstraat, or how you organized a birthday party 3 days after meeting me! Lange Nieuwstraat was definitely a second home and family for me.

Michele, I have to say I was sad when you had to move abroad for your PhD. Although now I realize that the fact that we don't live in the same city has most likely increased our life expectancy by many years. We did spend some amazing time in Italy, Netherlands, Austria, Portugal and Spain, where will the next one be?

Ciccio, the first (and perhaps the craziest) person I've met in the Netherlands: still remember the first beer we had at Lebowski 5 years ago. Had so much fun with you, especially when I joined you and Vic in Filicudi. That became my new threshold for a wedding! If I ever marry it will be on an island!

Francesca, we have been spending time together over the last years, but only during the lockdown I have realized how important you were and the peace of mind you would give me. Cannot say I am happy that you would distract me so many times while I was trying to work during the lockdown, but you did make the last months a lot more fun!

Thank you to my Portuguese family in Utrecht. Aida e Alexandre, obrigado por acolherem um (quase) estranho em vossa casa na chegada a Utrecht! Bem, no final de contas parece que tivemos que sair de Portugal para a seleção ser campeã da Europa. Obrigado por todas as churrascadas, tainadas, mariscadas e outras -adas que serviram para matar algumas saudades do Tugal ao longo dos anos. E muitos parabéns aos dois pelo Vicente. Não podia ser um "tio" mais babado!

I big shout-out to my friends from back home! João Martins, ainda estou a espera que me visites aqui na Holanda ahahah! Agradeço-te por sempre poder contar contigo para umas boas sessões de peer-revieweig! Ana, um muito obrigado pelos pequenos catch-ups ao longo dos anos, e pelo teu contributo nesta tese (Yes, Ana is a scientific illustrator and she is quite good, ana@anasilvillustrations.com).

Um obrigado ao Tasco! Tudo começou no longínquo ano de 2010 em que um grupo de pós-adolescentes se foi conhecendo nas imediações da FCUP. Tendo a Torrinha como quartel general, as relações de colegas de curso, catalizadas por apropriadas doses de receita e sangria, foram-se transformando em sólidas amizades ao longo do tempo. Quase 10 anos depois, relembro com carinho os tempos de faculdade, e espero ansiosamente para o próximo reencontro, acompanhado com, hopefully, uma bela francesinha. Um bem haja!

Family

To my siblings, and paranymphs, Inês e Luís. Um dos aspectos mais difíceis de sair de Portugal foi de facto passar menos tempo com vocês. Tão difícil que, aparentemente, alguém teve que vir viver para a Holanda, por duas vezes. Tenho muito orgulho nos adultos que os dois se tornaram, cada um com os seus sonhos e grandes ambições pessoais. Voltar a casa tem outro sabor quando posso passar algum tempo com vocês, seja a passear na marginal ou a simplesmente a ver Netflix com a Inês. Obrigado Luís pelo trabalho fabuloso com a capa e o layout da tese. Tenho a certeza que a nossa relação não vai mudar em nada ao longo dos anos, a não ser quando for para discutir quem fica com o quadro do Bando JLL.

Finalmente devo um agradecimento especial aos meus pais, Carlos e Maria (mais conhecidos por Sr. Ministro e Dona Mariazinha), pelo apoio incondicional desde 5 de Setembro de 1992. É de louvar que para vocês o sucesso pessoal e profissional dos vossos filhos sempre foi a prioridade. Esta será uma das principais razões para hoje estar onde estou. Apesar de já não ter um colchão no meu quarto, voltar a Esposende e a nossa casa é sempre um recarregar de baterias. Papá e mamã, seja na Holanda ou no outro lado do mundo, sempre vos levarei no coração.

PUBLICATION LIST

Included in this thesis:

J. P. Garcia*, F. Colella*, M. Sorbona*, A. Lolli, B. Antunes, D. D'Atri, F.P.Y. Barré, J. Oieni, L. Vainieri, L. Zerrillo, S. Capar, S. Haecckel, Y. Cai, L. B. Creemers. Drug delivery in intervertebral disc degeneration and osteoarthritis: selecting the optimal platform for the delivery of disease-modifying agents. Under revision

J. P. Garcia, L. Utomo, I. Rudnik-Jansen, N. P. A. Zuithoff, A. Krouwels, G. van Osch, L. B. Creemers. Association between oncostatin M expression and inflammatory phenotype in experimental arthritis models and osteoarthritis patients. Submitted

J. P. Garcia, A. Longoni, D. Gawlitta, A. Rosenberg, M. W. Grinstaff, J. Toyras, H. Weinans, L. B. Creemers, B. Pouran. Contrast Enhanced Computed Tomography for Real-time Quantification of Glycosaminoglycans in Cartilage Tissue Engineered Constructs. *Acta Biomaterialia*, 2019, 100, 202-212

J. P. Garcia, J. Stein, Y. Cai, F. Riemers, E. Wexselblatt, J. Wengel, M. Tryfonidou, A. Yayon, K. A. Howard, L. B. Creemers Fibrin-hyaluronic acid hydrogel-based delivery of antisense oligonucleotides for ADAMTS5 inhibition in co-delivered and resident joint cells in osteoarthritis. *Journal of Controlled Release*, 2018, 294, 247–258

Not included in this thesis:

D. D'Atri, L. Zerrillo, **J.P. Garcia**, J. Oieni, S. Zaharan, T. Bronshtein, T. Schomann, A. Chan, L.J. Cruz L.B. Creemers, M. Machluff. Nanoghosts: Mesenchymal Stem Cells derived nanoparticles as a novel approach for cartilage regeneration. Submitted

L. Zerrillo, M. R. Gigliobianco, D. D'Atri, **J.P. Garcia**, F. Baldazzi, Y. Ridwan; A. Chan, L. B. Creemers, R. Censi, P. Di Martino, L.J. Cruz. Poly (lactic-co-glycolic acid) nanoparticles decorated with hyaluronic acid improve site specificity and drug dose delivery in osteoarthritis nanotherapy. Submitted

I. Otto, P. Capendale, **J. P. Garcia**, M. de Ruijter, R. van Doremalen, M. Castilho, T. Lawson, M. Grinstaff, C. Breugem, M. Kon, R. Levato, J. Malda. Biofabrication of a shape-stable auricular structure for the reconstruction of ear deformities. Submitted

F.P.Y. Barré, M.R.L. Paine, B. Flinders, A.J. Trevitt, P.D. Kelly, R. Ait-Belkacem, **J. P. Garcia**, L.B. Creemers, J. Stauber, R.J. Vreeken, B. Cillero-Pastor, S.R. Ellis, R.M.A. Heeren. Enhanced Sensitivity Using MALDI Imaging Coupled with Laser Postionization (MALDI-2) for Pharmaceutical Research. *Analytical Chemistry*, 2019, 91, 10840-10848

V. Leiro, **J. P. Garcia**, P. M. D. Moreno, A. P. Spencer, M. Fernandez-Villamarin, R. Riguera, E. Fernandez-Megia, A.P. Pêgo. Biodegradable PEG–dendritic block copolymers: synthesis and biofunctionality assessment as vectors of siRNA. *Journal of Materials Chemistry B*, 2017, 5, 4901–4917

F. Barre, B. Flinders, **J. P. Garcia**, L. H. S. Huizing, T. Porta, L. B. Creemers, R. M. A. Heeren, B. Cillero-Pastor. Derivatization Strategies for the Detection of Triamcinolone Acetonide in Cartilage by Using Matrix-Assisted Laser Desorption/Ionization Mass Spectrometry Imaging. *Analytical Chemistry*, 2016, 88, 12051–12059

V. Leiro, **J. P. Garcia**, H. Tomas, A.P. Pego. The present and the future of degradable dendrimers and derivatives in theranostics. *Bioconjugate Chemistry*, 2015, 26, 1182–1197

CURRICULUM VITAE



João Pedro Marques Garcia was born on September 5th 1992 in Viana do Castelo, Portugal. He graduated from high school in 2010 and in the same year he moved to Porto to start his bachelor studies in Biochemistry at the Faculty of Sciences at the University of Porto. In 2013, he moved to Stockholm, Sweden, as part of an Erasmus Exchange Program where conducted an internship at the Department of Biochemistry and Biophysics at the Stockholm University. After graduation, he moved back to Porto and enrolled in 2-year master program in Biomedical Engineering at the Faculty of Engineering at the University of Porto. During his master studies, he completed a 1.5 year internship at the Instituto Nacional de Engenharia Biomédica (INEB) under supervision of Prof. dr. Ana Paula Pêgo and dr. Victoria Leiro. During this period, he worked on the development and validation of biodegradable dendrimers as delivery systems for siRNA.

In August 2015, he moved to The Netherlands to pursue a PhD degree in Regenerative Medicine at the Department of Orthopedics at the University Medical Centre Utrecht under supervision of Prof. D Chumur Oner, Prof. Marianna Tryfonidou and dr. Laura Creemers. His PhD project was part of the TargetCaRe consortium (H2020 ITN), an European project aiming at the development of drug delivery platforms for treatment of Osteoarthritis and intervertebral disc degeneration. Among other projects, he focused on the development of antisense oligonucleotides as therapeutics for Osteoarthritis and the validation of contrast-enhanced tomography for imaging of cartilage engineered constructs. The results of his PhD project are presented and discussed in this thesis.

Since May 2019, he is appointed as a junior researcher at the Department of Orthopedics. He is currently working within the iPSpine consortium (H2020), specifically on setting up and validating culture systems to test regenerative therapies for intervertebral disc degeneration.

